Universidade de Aveiro Departamento de Química
2013

FRANCISCO MIGUEL RIBEIRO CARDONA

SÍNTESE DE NOVOS LIGANDOS Aβ PARA DIAGNÓSTICO DA DOENÇA DE ALZHEIMER

SYNTHESIS OF NEW Aβ-LIGANDS USEFUL IN DIAGNOSIS OF ALZHEIMER'S DISEASE

Universidade de Aveiro Departamento de Química
2013

FRANCISCO MIGUEL RIBEIRO CARDONA

SÍNTESE DE NOVOS LIGANDOS Aβ PARA DIAGNÓSTICO DA DOENÇA DE ALZHEIMER

SYNTHESIS OF NEW Aβ-LIGANDS USEFUL IN DIAGNOSIS OF ALZHEIMER'S DISEASE

Tese apresentada à Universidade de Aveiro para cumprimento dos requisitos necessários à obtenção do grau de Doutor em Química, realizada sob a orientação científica do Doutor Artur Silva, Professor Catedrático do Departamento de Química da Universidade de Aveiro e do Doutor Francesco Nicotra, Professor Catedrático do Departamento de Biotecnologia e Biociência da Universidade de Milão-Bicocca.

Apoio financeiro do POPH – QREN.

PROGRAMA OPERACIONAL POTENCIAL HUMANO

Apoio financeiro da FCT e do FSE no âmbito do III Quadro Comunitário de Apoio.

FCT
Fundação para a Ciência e a Tecnologia

UNIÃO EUROPEIA
Fundo Social Europeu

o júri

presidente

Prof. Doutor Vasile Staicu
professor catedrático do Departamento de Matemática da Universidade de Aveiro

Prof. Doutor Francesco Nicotra
professor catedrático do Departamento de Biotecnologia e Biociência da Universidade de Milão-Bicocca

Prof. Doutor Carlos Alberto Mateus Afonso
professor catedrático da Faculdade de Farmácia da Universidade de Lisboa

Prof. Doutor Artur Manuel Soares da Silva
professor catedrático do Departamento de Química da Universidade de Aveiro

Prof. Doutora Amélia Pilar Rauter
professora associada com agregação da Faculdade de Ciências da Universidade de Lisboa

Prof. Doutora Barbara La Ferla
investigadora auxiliar do Departamento de Biotecnologia e Biociência da Universidade de Milão-Bicocca

Prof. Doutora Cristina Airoldi
investigadora auxiliar do Departamento de Biotecnologia e Biociência da Universidade de Milão-Bicocca

palavras-chave

Doença de Alzheimer, barreira hematoencefálica, péptido beta-amilóide, glúcidos, fluoróforos, reacção de Michael-Dieckmann, reacção de Diels-Alder

resumo

A doença de Alzheimer é uma doença crónica neurodegenerativa e uma das formas mais comuns de demência. Está associada à perda de memória, declínio cognitivo, incapacidade física e comportamental, e, em última análise, pode levar à morte. A doença de Alzheimer é uma doença complexa, ocorrendo na maioria dos casos esporadicamente, sendo a idade o principal fator de risco. A produção e acumulação do péptido beta-amilóide no sistema nervoso central é um facto importante no desenvolvimento da doença de Alzheimer.

O principal objetivo deste projeto consiste na síntese de ligandos beta-amilóide, de compostos fluoróforos e transportadores de fármacos através da barreira hematoencefálica para o diagnóstico e tratamento da doença de Alzheimer. Serão sintetizados diversos ligandos do péptido beta-amilóide e estudada a capacidade destes compostos interatuarem com as placas beta-amilóides através de espectroscopia de ressonância magnética nuclear. Será também realizado um estudo de otimização do composto líder. Já foram identificados muitos compostos naturais e sintéticos capazes de interagir com o péptido beta-amilóide, entre eles um conjunto de pequenas moléculas nas quais se constata que a parte aromática possui um papel importante na inibição da sua agregação, nomeadamente compostos hetero-aromáticos policíclicos, tais como as tetraciclinas. Porém as tetraciclinas apresentam instabilidade química, baixa solubilidade em água e possuem atividade antibacteriana, a qual é neste contexto indesejada. De modo a ultrapassar estas limitações, um dos objectivos deste trabalho é sintetizar compostos análogos de tetraciclinas, possuindo uma estrutura policíclica com uma melhor estabilidade química e solubilidade em água e possivelmente não possuindo atividade antibacteriana, mas conservando a capacidade de interação com o péptido beta-amilóide. As tetraciclinas possuem em comum um quarto ciclo sem carácter aromático e possuindo diferentes grupos funcionais. Com este projeto pretende-se sintetizar derivados nos quais este quarto ciclo é constiuído por uma entidade glucídica, portanto, possuindo diferentes posições funcionalizáveis ou criar derivados nos quais se irá acrescentar ou diminuir o número de anéis fundidos. De modo a criar um potencial fármaco, estas moléculas deverão também possuir as corretas propriedades físico-químicas. A entidade glucídica, não estando diretamente envolvida na interação com o péptido beta-amilóide, assegura possíveis derivatizações, tais como a conjugação a outras entidades moleculares (nanopartículas, suportes poliméricos, etc.) e a funcionalização com outros grupos funcionais capazes de modularem as propriedades lipofílicas e hidrofílicas. Estes compostos só serão úteis se atravessarem a barreira hematoencefálica e serem de algum modo detetados para fins de diagnóstico.

keywords

Alzheimer’s disease, blood brain barrier, amyloid-beta peptide, carbohydrates, fluorophores, Michael-Dieckmann annulation, Diels-Alder reaction

abstract

Alzheimer’s disease is a chronic progressive neurodegenerative disease and is the most common form of dementia (estimated 50–60% of all cases), associated with loss of memory (in particular episodic memory), cognitive decline, and behavioural and physical disability, ultimately leading to death. Alzheimer’s disease is a complex disease, mostly occurring sporadically with no apparent inheritance and being the age the main risk factor. The production and accumulation of amyloid-beta peptide in the central nervous system is a key event in the development of Alzheimer’s disease.

This project is devoted to the synthesis of amyloid-beta ligands, fluorophores and blood brain barrier-transporters for diagnosis and therapy of Alzheimer’s disease. Different amyloid-beta ligands will be synthesized and their ability to interact with amyloid-beta plaques will be studied with nuclear magnetic resonance techniques and a process of lead optimization will be performed. Many natural and synthetic compounds able to interact as amyloid-beta ligands have been identified. Among them, a set of small molecules in which aromatic moieties seem to play a key role to inhibit amyloid-beta aggregation, in particular heteroaromatic polycyclic compounds such as tetracyclines. Nevertheless tetracyclines suffer from chemical instability, low water solubility and possess, in this contest, undesired anti-bacterial activity. In order to overcome these limitations, one of our goals is to synthesize tetracyclines analogues bearing a polycyclic structure with improved chemical stability and water solubility, possibly lacking antibacterial activity but conserving the ability to interact with amyloid-beta peptides. Known tetracyclines have in common a fourth cycle without an aromatic character and with different functionalisations. We aim to synthesize derivatives in which this cycle is represented by a sugar moiety, thus bearing different derivatisable positions or create derivatives in which we will increase or decrease the number of fused rings. In order to generate a potential drug-tool candidate, these molecules should also possess the correct chemical-physical characteristics. The glycidic moiety, not being directly involved in the binding, it assures further possible derivatizations, such as conjugation to others molecular entities (nanoparticles, polymeric supports, etc.), and functionalization with chemical groups able to modulate the hydro/lipophilicity. In order to be useful such compounds should perform their action within the brain, therefore they have to be able to cross the blood brain barrier, and to be somehow detected for diagnostic purposes.

CONTENTS

FIGURES LIST

Tables List

ABREVIATIONS

2-D	two-dimensional (also 2D)
9-BBN	9-borabicyclo[3.3.1]nonane
AA	amyloid A
Ac	acetyl
AD	Alzheimer's disease
AIBN	2,2'-azobisisobutyronitrile
AICD	amyloid precursor protein intracellular domain
AL	amyloid light chain
ALS	amyotrophic lateral sclerosis
APOE	apolipoprotein E
APP	amyloid precursor protein
APP/AβPP	amyloid-beta precursor protein
ATTR	amyloidosis-transthyretin
ATTP	transthyretin related heriditary amyloidosis
Aβ	amyloid-beta peptide
Aβ40, Aβ(1–40)	amyloid-beta pepetide 40
Aβ42, Aβ(1–42)	amyloid-beta peptide 42
BACE1	beta-secretase 1
BBB	blood brain barrier
Bn	benzyl
BOC, boc	*tert*-butoxycarbonyl
BTSFA	*N*,*O*-bis(trimethylsilyl)trifluoroacetamide
calcd	calculated
CaMKII	calcium-calmodulin protein kinase
CAN	Cerium (IV) ammonium nitrate
cat	catalytic
Cdk5	cyclin-dependent kinase 5
Chol	cholesterol
CNS	central nervous system
COSY	$^{1}H/^{1}H$ correlation spectroscopy
CQ	clioquinol
CSA	camphorsulfonic acid
CSF	cerebrospinal fluid
d	doublet
Da	Dalton
DA	Diels-Alder
DCC	*N*,*N'*-dicyclohexylcarbodiimide
DCM	dichloromethane
dd	double of doublet
ddd	double doublet of doublets
ddt	double doublet of triplets
DDQ	2,3-dichloro-5,6-dicyano-1,4-benzoquinone

DIBAL-H	diisobutylaluminum hydride
DIC	*N*,*N*'-diisopropylcarbodiimide
DIPEA	*N*,*N*-diisopropylethylamine
DLS	dynamic light scattering
DMAP	4-(*N*,*N*-dimethylamino)pyridine
DMF	*N*,*N*-dimethylformamide
DMP	2,2-dimethoxypropane
DMSO	dimethyl sulfoxide
DPPC	1,2-dipalmitoyl-*sn*-glycero-3-phosphocholine
e.g.	for example
Equiv.	equivalent
ESI	electrospray ionization
EWG	electron withdrawing group
Fc	fragment crystallizable
FGI	functional group interconversion
Glc	glucose
GSH	glutathione
GSK-3β	glycogen synthase kinase 3
GSSG	oxidized glutathione
HBTU	*O*-benzotriazole-*N*,*N*,*N'*,*N'*-tetramethyl-uronium-hexafluoro phosphate
HD	Huntington's disease
HSQC	$^{1}H/^{13}C$ heteronuclear single quantum coherente spectroscopy
i-Pr	isopropyl
J	coupling constant (in NMR spectroscopy)
LDA	lithium diisopropylamide
logP	logarithm of partition coefficient
m	multiplet
m/z	mass-to-charge ratio (mass spectrometry)
M+	parent molecular ion
MAPK	mitogen-activated protein kinase
MARK	microtubule affinity-regulating kinase
MCI	mield cognitive impariment
MD	molecular dynamics
MDB	microtubule-binding main domain
Me	methyl
MHz	megahertz
Mix	mixing time
MLV	multilamellar vesicle (liposome)
MM	molecular mechanics
Mol, mol	mole(s)
MRI	magnetic resonance imaging
Ms	methanesulfonyl
MW	Molecular weight
NBS	*N*-bromosuccinimide
NFT	neurofibrillary tangle(s)
NGF	nerve growth factor
NMO	*N*-methylmorpholine-*N*-oxide

NMR	nuclear magnetic resonance
NOE	nuclear Overhauser effect
NOESY	$^{1}H/^{1}H$ nuclear Overhauser effect spectroscopy
Np	Nanoparticle(s)
Ns	number of scans
NSAID	non-steroidal anti-inflammatory drug
ºC	degrees celsius
oQDMS	*ortho*-quinodimethanes
PBS	phosphate buffered saline
PD	Parkinson's disease
Pd	palladium
PDFT	proline density functional theory
PdI	polydispersity index
PE	endothelial permeability
PEG	polyethylene glycol
PES	potential energy surface
PET	positron emission tomography
PHFs	paired helical filaments
PKA	protein kinase a
PMB	*p*-methoxybenzyl
ppm	part per million
PS1	protein preselin 1
PS2	protein preselin 2
Py	pyridine
RCM	ring closing metathesis
RNS	reactive nitrogen species
ROS	reactive oxygen species
rt/r.t.	room temperature
s	singlet
SAA	serum amyloid A protein
SAR	structure-activity relationship
SCA	spinocerebellar ataxia
SOD	superoxide dismutase
STD	saturation transfer difference
SUV	small unilamellar vesicle (liposome)
sym-Collidine	2,4,6-trimethylpyridine
TBAF	tetra-*N*-butylammonium fluoride
TC	tetracycline(s)
TEA	triethylamine
TEER	trans-endothelial-electrical resistance
TEM	transmission electron spray microscopy
TES	triethylsilane
TFA	trifluoroacetic acid
TFAA	trifluoroacetic anhydride
Tg	transgenic
THF	tetrahydrofuran
ThT	thioflavin

TLC	thin layer chromatography
TMOF	trimethyl orthoformate
TMSOTf	trimethylsilyl trifluoromethanesulfonate
tr-NOESY	transferred nuclear Overhauser effect spectroscopy
TRR	transthyretin
TS	transition state
TSE	transmissible spongiform encephalopathie(s)
Water-LOGSY	water-ligand observed via gradient spectroscopy
$[\alpha]$	specific rotation
α	observed optical rotation in degrees
δ	chemical shift in parts per milion donwfield from tetramethylsilane
ζ-potential	zeta-potential

Chapter 1
State of the art

1. State of the art

It was in 1906 that Alois Alzheimer first presented at a scientific meeting a case of progressive dementia in a 51 years old patient. Postmortem analysis revealed two pathologies, namely, senile plaques and neurofibrillary tangles. In 1910 Emil Kraeplin, Alzheimer's mentor, named this disease after its discover. [1]

1.1. Protein misfolding and human disease

The correct activity of a network of thousands of proteins is fundamental to ensure that cells and organisms function properly. The function of a protein depends on its three-dimensional structure, which is determined by its amino acids sequence. Chaperone proteins supervise protein folding in order that, in most cases, mistakes are avoided and malfunctioning proteins are removed. Nevertheless, under certain circumstances a protein or a specific peptide fails to adopt or remain in its native functional conformational state leading to a broad range of human diseases. These pathological conditions are generally referred as protein misfolding diseases. Evidence is accumulated that protein misfolding and aggregation is the most likely cause of various neurological and systemic diseases.[2-4]

They include pathological states in which impairment in the folding efficiency of a given protein results in a quantity reduction of the protein available to play its normal role. This reduction may occur as the result of one of several post translational processes, such as an increase probability of degradation via the quality control system of the endoplasmic reticulum, as in the case of cystic fibrosis, or the improper trafficking of a protein, as seen in early-onset emphysema. Althought the largest group of misfolding diseases is associated with the conversion of specific peptides or proteins from their soluble functional states ultimately into highly organized fibrillar aggregates. These structures are generally described as amyloid fibrils or plaques when they accumulate extracellularly, but the term "intracellular inclusions" has been suggested as more appropriate when fibrils morphologically and structurally related to extracellular amyloid form inside the cell. It is also becoming clear that fibrillar species with amyloid characteristics can have a number of biological functions in living organisms, provided they are formed under controlled conditions.[3]

Pathogenic amyloid formation can lead to a wide range of protein misfolding diseases known as amyloidosis, these diseases include:

a. systemic amyloidoses in which deposits may occur in any part of the body, such as: amyloid light-chain (AL), amyloidosis due to the accumulation of immunoglobulin light chain amyloid fibrils; amyloid A (AA), or reactive systemic amyloidosis resulting from deposits of catabolic products of the serum amyloid A protein (SAA); transthyretin-related hereditary amyloidosis **(**ATTR) due to transthyretin (TTR) accumulation;

b. amyloidosis in which a single organ is affected — possibly including pancreatic accumulation of islet amyloid polypeptide in type 2 diabetes.

c. many protein-misfolding diseases affect the nervous system. Interestingly, certain proteins specifically aggregate and are toxic in the central nervous system (CNS) despite the fact that they are ubiquitously expressed. These neurodegenerative diseases include (Table 1.1)[3]:
   - Alzheimer's disease (AD);
   - Parkinson's disease (PD);
   - Huntington's disease (HD) (and related polyglutamine disorders including several forms of spinocerebellar ataxia or SCA);
   - transmissible spongiform encephalopathies (TSEs), (also known as prion disorders, include Creutzfeldt–Jakob disease, fatal familial insomnia, Gerstmann–Straussler syndrome, bovine spongiform encephalopathy and scrapie);
   - amyotrophic lateral sclerosis (ALS).

Table 1.1: Clinical and pathological features of neurodegenerative diseases.

Disease	Clinical features	Protein involved	Affected regions of the brain
Alzheimer's	Progressive dementia	Amyloid-β and tau	Hippocampus, cerebral cortex
Parkinson's	Movement disorder	α-Synuclein	Substantia nigra, hypothalamus
Huntington's	Dementia, motor and psychiatric problems	Huntungtin	Striatum, cerebral cortex
Amyotrophic lateral sclorosis	Movement disorder	Superoxide dismutase	Motor cortex, brainstem
Transmissible spongiform encephalopathies	Dementia, ataxia, psychiatric problems or insomnia	Prion protein	Various regions depending on the disease

Until recently, it was considered impossible to find a common molecular mechanism among this group of diseases. However, despite their obvious differences in clinical symptoms and disease progression, these disorders share some common features: most of them (except HD and SCA) have both sporadic and inherited origins, while all of them appear later in life (usually after the fourth or fifth decade), and their pathology is characterized by neuronal loss and synaptic abnormalities.

The hallmark feature of conformational disorders is that a particular protein can fold into a stable alternative conformation, which in most cases results in its aggregation and accumulation in tissues as fibrillar deposits. These deposits have some similar morphological, structural and staining characteristics (Figure 1.1),[3] but it is likely that different protein deposits may also have distinct biochemical or biological features, particularly depending on whether the aggregates accumulate intra- or extracellularly.[3,5]

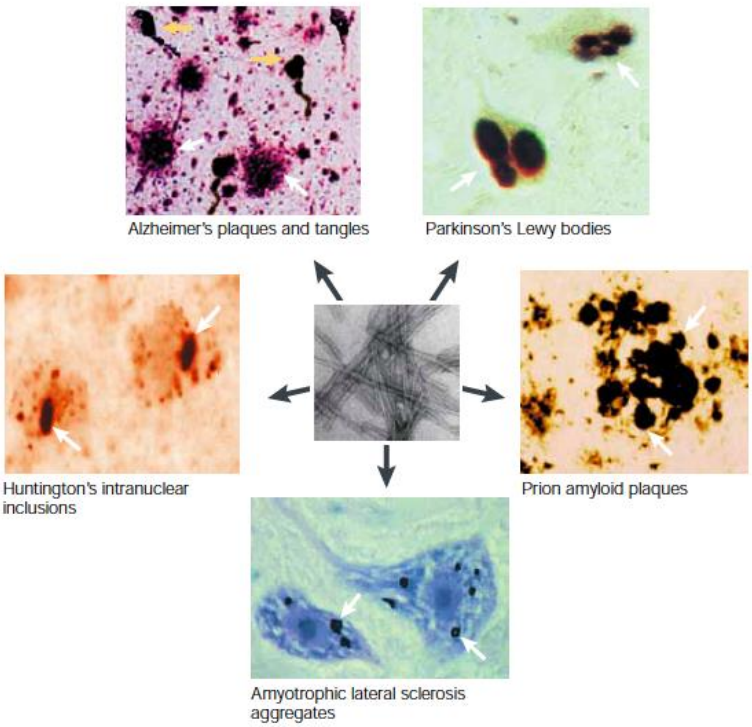

Figure 1.1: Aggregates staining in neurodegenerative diseases.

1.2. The Alzheimer's disease

AD is a chronic progressive neurodegenerative disease and is the most common form of dementia (estimated 50−60% of all cases) associated with loss of memory (in particular episodic memory), cognitive decline, and behavioral and physical disability, ultimately leading to death. AD is a complex disease, mostly occurring sporadically with no apparent inheritance and being the age the main risk factor. The perceived complexity of AD implies that the disease has a broad clinical spectrum aggravated by a plurality of genetic and environmental factors and is affected by many genes of small but cumulative significance. Exogenous risk factors include: brain trauma, smoking, obesity, diabetes, hypertension, cholesterol, elevated homocysteine levels (hyperhomocysteinemia) and exogenous metal exposure, including lead, mercury, and aluminum.

Genetic risk factors are now known to cause AD in rare cases, most notably due to mutations in amyloid precursor protein (APP) or presenilin, which is a constituent of the γ-secretase enzyme complex that degrades APP into amyloid-beta peptide (Aβ) giving rise to familial AD, and due to isoforms of the cholesterol transporter apolipoprotein E (APOE), APOE4.[6] Humans possess three common *APOE* alleles: *APOE2*, *APOE3* and *APOE4.* The possession of an *APOE4* allele can bring forward considerably the age of disease onset, *APOE3* can be considered to be neutral, and *APOE2* is thought to be protective. How the different APOE proteins mediate their effects in AD is not known.[7]

The disease is pathological characterized by the presence of extracellular senile plaques, which consists of a core of Aβ, and intracellular neurofibrillary tangles (NFTs), as well as the selective loss of neurons and synaptic connections. NFTs are composed of paired helical filaments (PHFs) that consist of aggregation of hyperphosphorylated tau protein (Figure 1.2),[8] associated with the microtubule protein, whereas Aβ is rich in senile plaques. The causes that induce the above pathological characteristics are poorly known at present.[9,10]

Although debated until now, according to the so-called amyloid hypothesis, tangles are considered only a secondary event in the disease progression, being a consequence of the formation of Aβ plaques.[9]

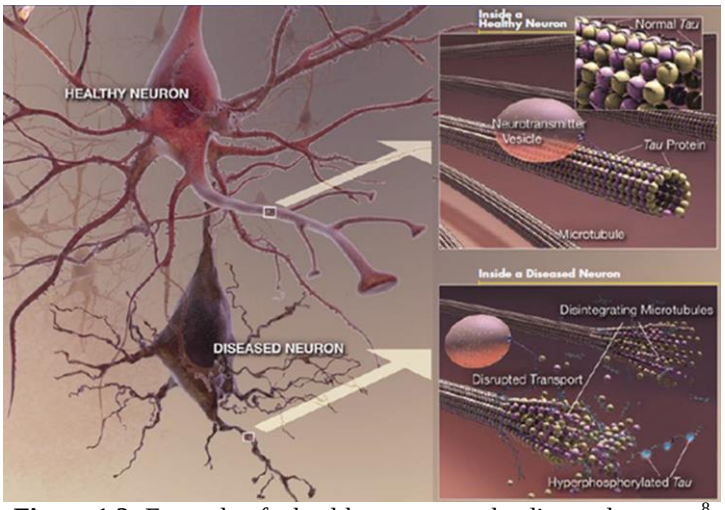

Figure 1.2: Example of a healthy neuron and a diseased neuron.[8]

While the etiology of AD remains unclear, there is an increase of the genetic evidence that altered cellular processing of APP is a causative factor in many cases. However, citoxicity of Aβ is not only due to the ability to form fibrillar aggregates in the extracellular environment, but also to the presence of soluble Aβ oligomers into the intracellular environment. Both forms or their intermediates, produce different damages to cell membrane and different organelles inducing alteration of physiological biochemical pathways and leading to oxidative stress, inflammation and, at the end, to cell death. [9]

The two main disease mechanisms-based approaches, which have been studied for more than 10 years, are based on the involvement of the two proteins – Aβ and tau .[11]

1.2.1. Aβ

The production and accumulation of Aβ in the CNS are key events in the development of AD. Levels of Aβ in the brain are regulated by the activity of enzymes involved in its production, degradation and clearance.[12]

Aβ is present in the brain of healthy humans throughout life and the mere presence of Aβ does not imply neuropathy. In contrast, when neuronal injury appears, the aggregation of physiologically secreted soluble Aβ into oligomers and large Aβ fibrils is currently considered to be a crucial event in AD onset. The main question remains, why the Aβ, which normally circulates in soluble form in the cerebrospinal fluid (CSF) and in plasma,

becomes prone to aggregate, forming highly toxic oligomers and protofibrils and mature fibrils accumulating in plaques.[9]

Aβ derive from proteolysis of the large transmembrane protein amyloid–beta percursor protein (AβPP) (Figure 1.3),[6] which is a type I integral membrane glycoprotein (abundantly expressed in the brain) produced in three predominant forms, 695, 751 or 770 amino acids.[12]

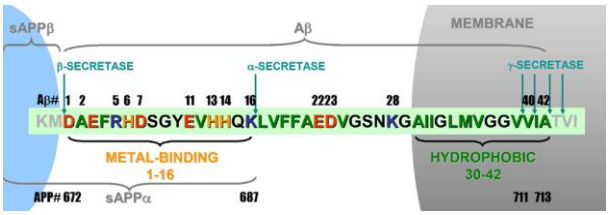

Figure 1.3: The Aβ sequence within APP and the main secretase cleavage positions.

The Aβ is derived through endoproteolytic processing of AβPP by sequencial enzymatic actions of alpha-site APP cleaving enzyme α-secretase, denominated the nonamyloidogenic pathway and beta-site APP-cleaving enzyme (BACE-1), a β–secretase, and γ-secretase, a protein complex with presenilin 1 at its catalytic core, corresponding to the amyloidogenic process (Figure 1.4).[13]

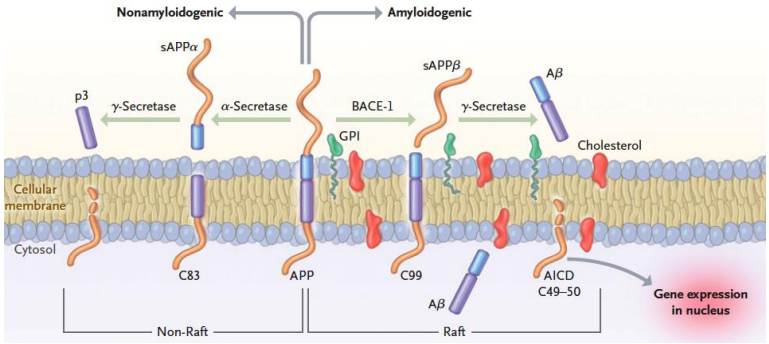

Figure 1.4: Processing of amyloid precursor protein.

In the α-secretase pathway, α-secretase cleaves in the middle of the amyloid-β region to release a large soluble APP-fragment, sAPPα. The carboxy (C)-terminal C83 peptide is metabolized to p3 by γ-secretase. In the amyloid-forming β-secretase pathway, β-secretase releases a large soluble fragment, sAPPβ. The C-terminal C99 peptide is then cleaved by γ-secretase at several positions, leading to the formation of amyloid-β40 (Aβ40) and the

pathogenic amyloid-β42 Aβ(1-42) in the extracellular space. γ-Secretase cleavage also releases the APP intracellular domain (AICD), which could have a role in transcriptional regulation. The soluble Aβ tends to aggregate.[11]

The C-terminal 12 amino acid residues of the Aβ are hydrophobic and confer to the peptide the ability to self-aggregate and polymerise into amyloid fibrils. The term β of Aβ indicates, indeed, its propensity to form partial β-plated sheet structures once it aggregates into amyloid fibrils.[9]

Depending on the exact point of cleavage by γ-secretase, three principal forms of Aβ, comprising 39, 40, and 42 amino acid residues, respectively, are produced. The relative amount of Aβ(1-42) is particularly important because it has more tendency to oligomerize and form amyloid fibrils with respect to the shorter peptides.[9]

Aβ production is a normal process but in a small number of individuals an imbalance between production, clearance, and aggregation of peptides causes Aβ to accumulate, and this excess may be the initiating factor in AD. This idea, called the "amyloid cascade hypothesis", is based on studies of genetic forms of AD, and evidence that Aβ(1–42) is toxic to cells.[13] A number of studies have confirmed that Aβ(1–42) is the more neurotoxic form of Aβ. It has been shown that Aβ(1–40) and Aβ(1–42) possess different biochemical properties, and Aβ(1–42) is considered to be the major etiologic agent in the pathogenesis of AD due to its aggressive aggregation or oligomerization properties (Figure 1.5).[14] The mutations associated with inherited forms of AD provide strong evidence that the aggregation of Aβ(1–42) is a causative factor in the etiology of AD because the mutations increase the relative amount of Aβ(1–42).[15,16]

a) *b)*

Figure 1.5: "Typical" Aβ-fibril morphology by transmission electron microscopy (TEM), obtained from incubated 50 μM solutions of (a) Aβ(1-40) and (b) Aβ(1-42).

1.2.2. Tau

NFTs are filamentous inclusions in pyramidal neurons that occur in AD and other neurodegenerative disorders named tauopathies. The number of NFTs is a pathologic marker of the severity of AD. The major component of the tangles is an abnormally hyperphosphorylated and aggregated form of tau. Normally an abundant soluble protein in axons, tau promotes assembly and stability of microtubules, and self-associates into paired helical filament structures. Enzymes that add and those that remove phosphate residues regulate the extent of tau phosphorylation.[13]

The microtubule-binding main domain (MDB) of tau (Figure 1.6),[13] is formed by repeated sequences (R1-R4). Normal phosphorylation of tau occurs on serine (S; inset, above horizontal bar) and threonine (T; inset, below horizontal bar) residues, numbered according to their position in the full tau sequence. When followed by proline (P), these amino acids are phosphorylated by glycogen synthase kinase 3 (GSK-3β), cyclin-dependent kinase (cdk5), and its activator subunit p25, or mitogen-activated protein kinase (MAPK). Nonproline-directed kinases — Akt, Fyn, protein kinase A (PKA), calcium–calmodulin protein kinase 2 (CaMKII), and microtubule affinity-regulating kinase (MARK) — are also shown. KXGS (denoting lysine, an unknown or other amino acid, glycine, and serine) is a target motif. Hyperphosphorylated sites specific to paired helical filament tau in AD tend to flank the MBD. Tau binding promotes microtubule assembly and stability. Excessive kinase, reduced phosphatase activities, or both cause hyperphosphorylated tau to detach and self-aggregate and this causes the destabilization of microtubules.[13]

It is commonly accepted that blocking tau pathology could have therapeutic benefit, even though tau pathology might be downstream from amyloid in the pathogenic cascade. In general, tau has received much less attention from the pharmaceutical industry than amyloid, because of both fundamental and practical concerns. At the fundamental level, the amyloid cascade hypothesis (Figure 1.7)[14] indicates that tau pathology might be too far downstream in the cascade. However, more importantly, tractable targets in the pathway from tau to tangle formation remain to be identified. Tau kinases have been proposed as targets, but the role of tau phosphorylation and of specific kinases in tangle formation is not completely understood.[13]

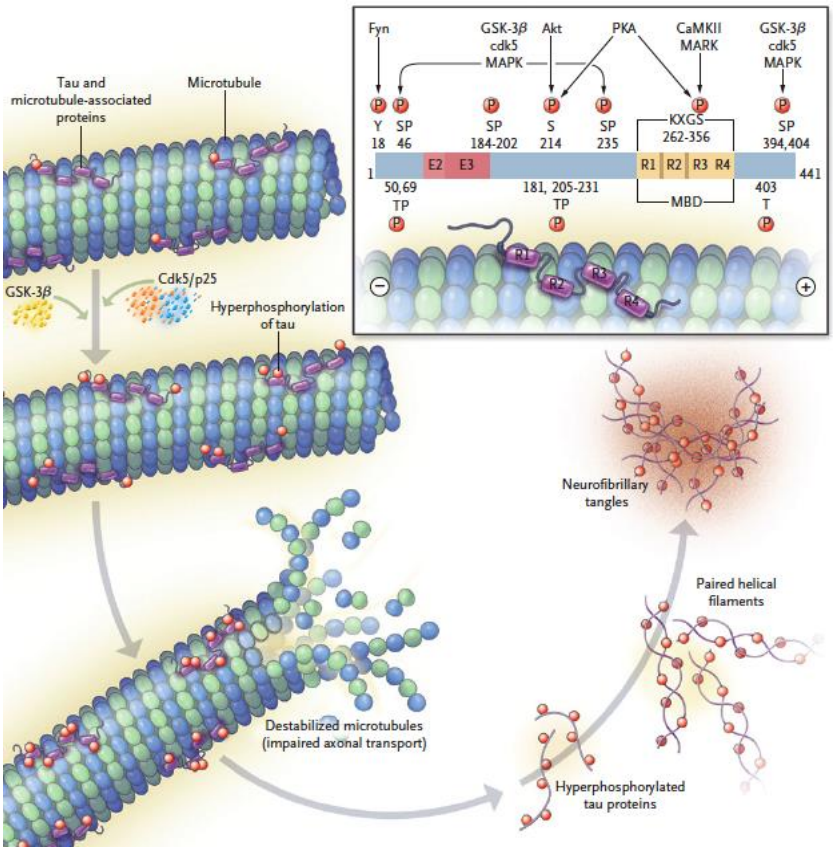

Figure 1.6: Tau structure and function.

Also, well-characterized mouse models of tangle formation have only recently become available. Although there are several lines of evidence that CDK5 could have a crucial role in tangle formation, the generation of highly specific tau kinase inhibitor drugs that are suitable for the chronic treatment of AD is likely to represent a considerable challenge.[13]

1.3. Alzheimer's disease pathogenesis

During the past decade, three main hypotheses on the pathogenesis of AD have emerged that focus on different features of the disease and are in some extent seen as competing: the amyloid cascade hypothesis, the metal ion hypothesis, and the oxidative stress hypothesis.[6,7]

a. The amyloid cascade hypothesis states that impaired balance between Aβ production and clearance is the main cause of AD and that amyloids are the main neurotoxic substances in AD. Consequently, this hypothesis favors treatments that inhibit Aβ production or enhance Aβ clearance in the AD brain.

b. The metal ion hypothesis states that the underlying cause of AD is impaired metal homeostasis, in particular of Zn, Cu, and Fe, with Aβ imbalance being a consequence of this. This hypothesis favors treatments such as chelators that address the metal ion imbalances supposedly causing amyloid accumulation.

c. The oxidative stress hypothesis claims that age-enhanced or genetically and environmentally enhanced oxidative stress results in accumulated gene defects and declining mitochondrial function. This subsequently leads to neurological disorders, either gradually or when reaching a critical threshold that initiates apoptosis in neurons. Apoptosis occurs in a wide range of neurological disorders and by a range of pathways that can be triggered, for example, by lesions, misfolded proteins, oxidative stress, excitotoxicity, or Ca^{2+} dyshomeostasis.[6,7]

1.3.1. The amyloid cascade hypothesis

The amyloid cascade hypothesis for AD has been very influential in the research conducted both in academia and in the pharmaceutical industry. This hypothesis synthesises histopathological and genetic information, and claims that the deposition of Aβ in the brain parenchyma initiates a sequence of events that ultimately lead to AD dementia.[7]

The "amyloid cascade hypothesis" (Figure 1.7)[14] is initiated by the generation of Aβ42. In familial early onset AD, Aβ42 is overproduced owing to pathogenic mutations. In sporadic AD, various factors can contribute to an increased load of Aβ42 oligomers and aggregates. Aβ oligomers might directly injure the synapses and neurites of brain neurons, in addition to activating microglia and astrocytes.[11,14]

Preventing Aβ aggregation is therapeutically attractive because this process is believed to be an exclusive pathological event, and compounds targeting this mechanism are more likely to have a better safety profile compared to some other approaches currently being followed. In addition although soluble oligomers can be on a pathway to Aβ fibrils and ultimately amyloid plaque.[15]

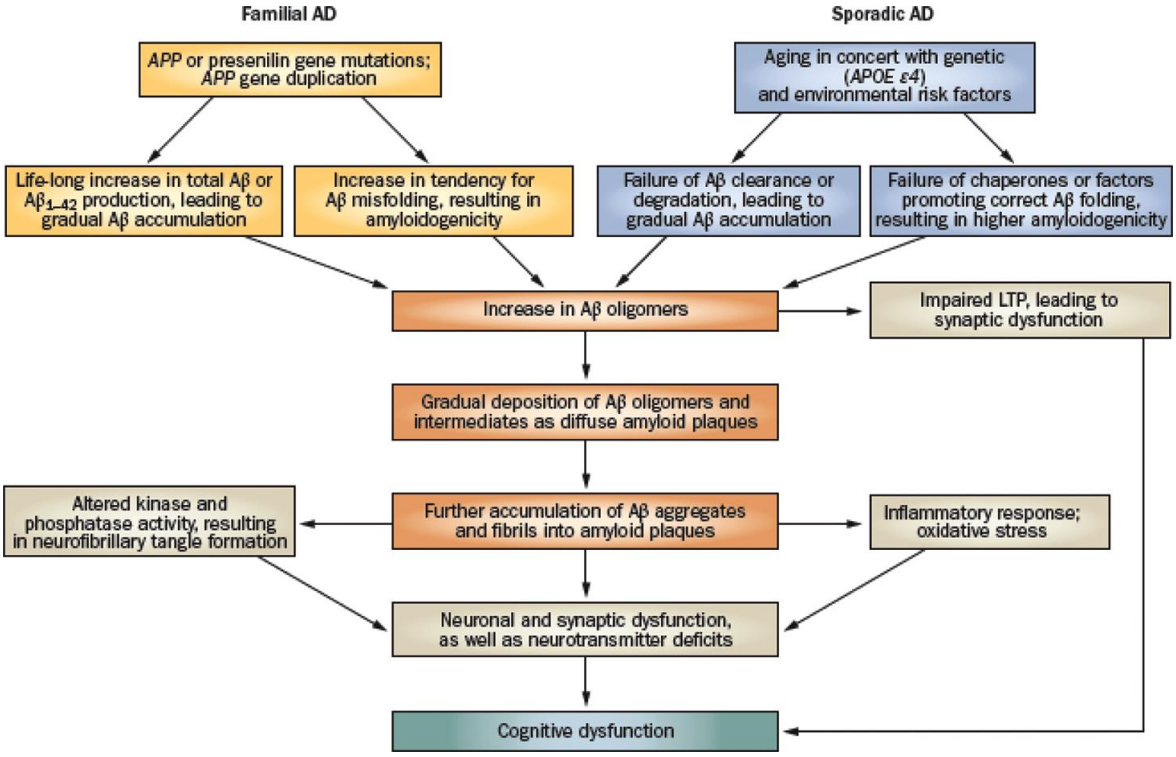

Figure 1.7: The amyloid cascade hypothesis.

A simplified scheme of the Aβ aggregation pathways that generate toxic assemblies is showed in Figure 1.8.[17] Once Aβ is stabilized as its monomeric form or as non-toxic oligomeric forms, these species might be expected to be cleared by normal pathways.[15]

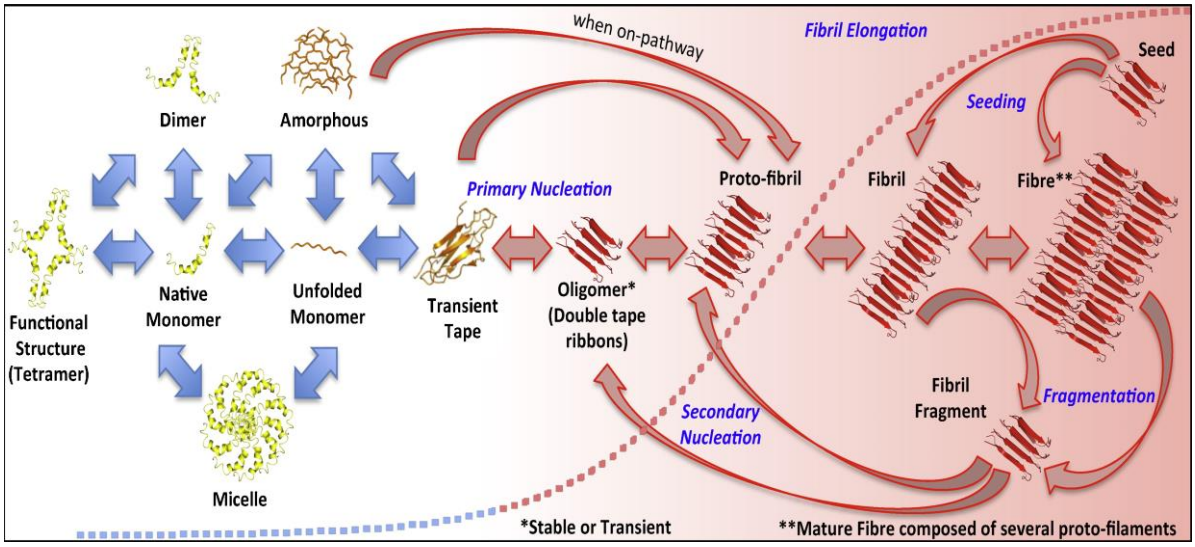

Figure 1.8: Aβ aggregation pathways.

1.3.2. The metal ion hypothesis

The brain is a specialized organ that requires metal ions for a number of important cellular processes. Therefore, the brain contains a relatively high concentration of a number of transition metals, such as Fe, Zn, and Cu. They take part in the neuronal activity within the synapses [Zn(II) in particular] and ensure the function of various metalloproteins (cytochrome C-oxidase, Cu/Zn superoxyde dismutase...). A breakdown of these mechanisms, or absorption of metals with no known biological function, alter the ionic balance and can result in a disease state, including several neurodegenerative disorders as AD.[18] Many studies have shown that the most important biometals, i.e., copper, zinc, and iron as well as nonphysiological aluminium are involved in AD. They are suggested to have two distinct roles in the pathophysiology of AD, namelly aggregation of Aβ peptide, and production of reactive oxygen species induced by Aβ.[19]

The metal hypothesis of AD asserts that the interactions between metal ions and Aβ, as well as abnormal metal ion homeostasis, are connected with AD neuropathogenesis.[20-23] Based on this hypothesis, disruption of metal-Aβ interactions *via* metal chelation therapy has been proposed in order to reduce neurotoxicity of metal-Aβ species and restore metal ion homeostasis in the brain.[20] However, in order to be used as potential drugs in the treatment of neurodegenerative diseases, chelators must have particular properties. They must have a low molecular weight, be poorly or not charged to favor blood-brain-barrier (BBB) crossing and stable. They must selectively target certain metal ions, because a strong non-specific chelation would result in a general depletion of metal ions, including those of metalloenzymes, which are essential. Once the chelator is in the brain, the molecule must be able to complex the metal ions present in excess in the aggregated proteins so as to allow their dissolution and elimination. Finally, successful treatment with any chelator requires low toxicity and minimum side effects of the drug itself. To date, several metal chelators have been used as agents for metal ion chelation therapy in AD (Figure 1.9).[19]

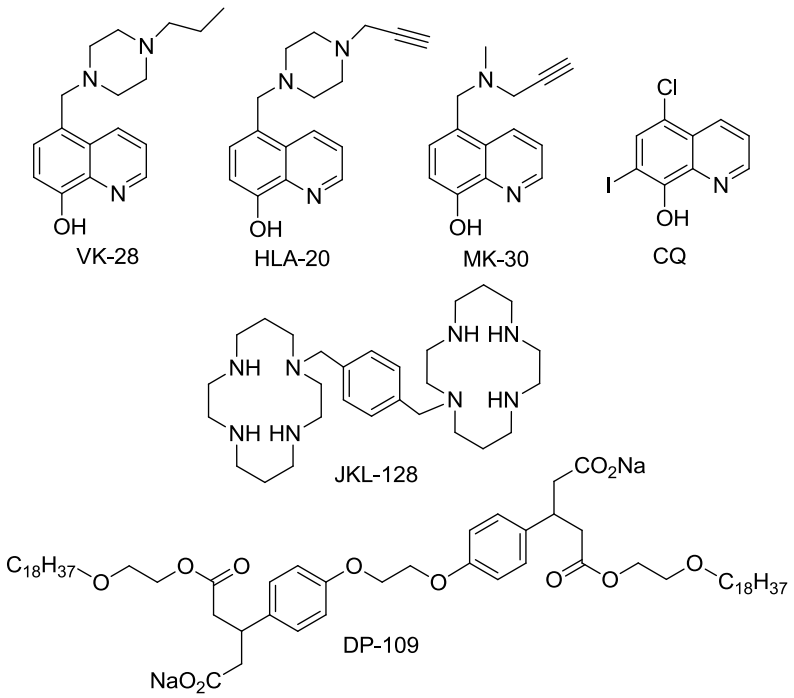

Figure 1.9: Examples of metal chelators used as agents for metal chelation therapy.

Among the few chelators tested so far, clioquinol (CQ) was the first to reach the pilot phase II clinical trial, which demonstrates the applicability of this exogenous metal chelator. Whilst the use of CQ has been suspended in AD research, a new and promising oxine based analogue PBT2 is presently under development, which clearly indicates that this strategy will be favored. Combining antioxidant activity and binding functionality into a single drug would broaden the chances of success in AD therapy.[19]

1.3.3. The oxidative stress hypothesis

Oxidative stress is caused by an imbalance in the pro-oxidant/antioxidant systems and might cause reversible and/or irreversible modifications on sensitive proteins leading to structural, functional and stability modulations. Protein modifications such as carbonylation, nitration and protein–protein cross-linking are generally associated with loss of function and may lead to either the unfolding and degradation of the damaged proteins, or aggregation leading to accumulation as cytoplasmic inclusions, as observed in age-related neurodegenerative disorders.[24-27]

The oxidative hypothesis, postulates that the age-related accumulation of reactive oxygen species (ROS) or reactive nitrogen species (RNS) results in damage to the major

components of cells: nucleus, mitochondrial DNA, membranes, and cytoplasmic proteins. The imbalance between the generation of free radicals and ROS or RNS may be involved in the pathogenesis of AD, since brain tissue has multiple potential sources of ROS and a large oxidative capacity, but its ability to combat oxidative stress is limited.[25,28-30]

Glutathione (GSH) is a well-known antioxidant that is synthesized in the cell cytoplasm and is present in higher concentrations in the mitochondrial matrix. Because most oxidized GSH (GSSG) forms are under oxidative stress, several different enzymes are necessary to reduce GSSG to maintain the GSH/GSSG ratio. Under severe conditions of oxidative stress, cells are not able to maintain the appropriate GSH/GSSG ratio, causing an accumulation of GSSG and resulting in protein modifications. The level of GSSG is a key factor in determining neuronal susceptibility to ROS or RNS mediated neuronal injury.[31,32]

It is estimated that approximately 1−3% of all normal O_2 is converted into ROS in mammals, due to inefficiencies of the electron transport chain, and this ROS production can be enhanced if mitochondria are not working optimally due to hypoxic or hyperoxic or other stress-related conditions.[33] ROS that escape the organisms' antioxidant defenses then oxidatively modify nearby proteins and lipids, sometimes rendering them less stable or functional, or nucleic acids of the DNA, leading to mutations.[34]

The RNS are primarily derived from nitric oxide radical, which is produced by nitric oxide synthase and serves signaling and immune defense roles in the healthy organism, in the form of peroxynitrite. When peroxynitrite is overproduced due to reduced proficiency of superoxide dismutase (SOD), it reacts with bicarbonates to generate carbonate radicals but will also react readily with heme proteins and sulfur and selenium groups of relevance to metal homeostasis and oxidative stress control.[35]

Metal ions play key roles in both ROS and RNS as ligands, and both copper an iron produce hydroxyl radical in solvent exposed cellular environments, notably via variations of the simplest form of the Fenton reaction:[6,36]

$$Fe^{3+} + H_2O_2 \longrightarrow Fe^{2+} + HOO^{\bullet} + H^+$$

$$Fe^{2+} + H_2O_2 \longrightarrow Fe^{3+} + HO^- + HO^{\bullet}$$

$$Cu^{+} + H_2O_2 \longrightarrow Cu^{2+} + HO^- + HO^{\bullet}$$

The Fenton chemistry unites metal ion dyshomeostasis, which shifts balance from bound to free metal ions, with oxidative stress pathogenesis, which is predominantly aggravated by free Cu and Fe. Thereby, in the absence of direct toxicity of soluble Cu(II)−Aβ oligomers, disturbed metal homeostasis resulting in increased concentrations of free intracellular metal ions that will itself generate ROS that could lead to oxidative stress. Consequently, the two hypotheses are intimately related via a vast number of Cu-, Zn-, and Fe-containing proteins involved in oxidative stress modulation.[37,38]

1.4. Intervention strategies for Alzheimer's disease

Researchers in AD are moving forward with the development of treatments that target the known neuropathologic hallmarks of the illness (Table 1.2)[5], the amyloid plaques and tau-based neurofibrillary tangles.[39]

Table 1.2: Summary of therapeutic strategies for protein aggregation diseases.

Approach	*Therapy*	*Expected effect*	*Current status*
Inhibition of amyloid formation	γ-Secretase inhibitors and modulators	Reduced carboxy-terminal cleavage of APP to form Aβ40 or Aβ42	Phase II and III clinical trials
	β-Secretase inhibitors	Reduced amino-terminal of Aβ-containing aggregates	Phase I clinical trials
Promotion of amyloid clearance	Aβ immunotherapy	Enhanced clearance of Aβ containing aggregates	Phase II and III clinical trials
	Prion immunotherapy	Enhanced clearance of PrPSc-containing aggregates; prevention of the invasion of prions into neurons	Preclinical
Inhibition of amyloid aggregation	Scyllo-inositol	Prevention of the formation of higher-order aggregates	Phase II clinical trials
	Tafamidis	Stabilization of the native state of transthyretin	Phase II and III clinical trials

1.4.1. Targeting Aβ production

The accumulation of Aβ has been postulated as being the earliest factor in the development of AD. The only known genetic forms of the illness are caused by mutations in Aβ or the enzymes that are involved in its formation.[39]

Steady state levels of Aβ monomers are controlled by its rates of production and degradation. Above a certain critical concentration Aβ monomers can self-associate to form dimers, trimers and larger oligomers (Figure 1.10).[40] Consequently, inhibition of Aβ production (Figure 1.10*(1)*) or stimulation of Aβ degradation (Figure 1.10*(2)*) should decrease or prevent formation of oligomers and then amyloid fibrils. Certain proteases can degrade both Aβ monomers and polymers, so stimulation of such enzymes would serve to lower Aβ monomer levels and hence reduce again the formation of oligomers while also facilitating removal of pre-existing Aβ polymers.[40]

Small molecules or biologics that bind to and stabilize Aβ monomers (Figure 1.10*(3)*) should prevent oligomerization and allow for the natural removal of monomers by the brain's degradative machinery. Similarly, agents capable of disrupting pre-formed oligomers (Figure 1.10*(4)*) should reduce the concentration of toxic oligomers. [40]

Small molecules or antibodies capable of binding to a variety of Aβ assemblies (Figure 1.10*(5)*) could neutralize both small and large Aβ assemblies and facilitate their elimination.[40]

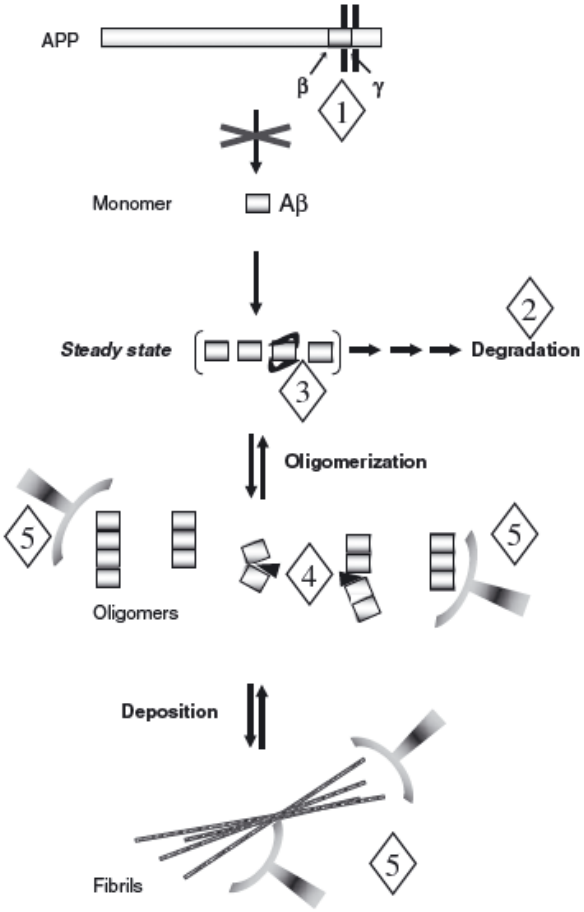

Figure 1.10: Strategies for targeting neurotoxic Aβ oligomers.

Thereby, five strategies to reduce Aβ production have been proposed: immunotherapy, inhibition of β-secretase, inhibition of γ-secretase, stimulation of α-secretase and inhibition of Aβ aggregation.

1.4.1.1 Immunotherapy targeted to reduce Aβ

Anti-amyloid immunotherapy for AD has received considerable attention following the publication of the Elan Corporation's paper, that reported amyloid pathology reduction in an APP transgenic mouse model after vaccination with aggregated Aβ42.[41]

Over the last years, Aβ immunotheraphy has emerged from preclinical studies in transgenic mouse models of AD to enter clinical trials in humans (Table 1.3 and 1.4).[41] At least 13 different Aβ immunotherapies are in clinical trials worldwide.

Table 1.3: Examples of ongoing clinical trials of passive Aβ immunotherapies.

Therapy	***Sponsors***	***Antibody***	***Phase and number of trials***	***Estimated patient enrollment***	***Primary outcome measures***
Bapineuzumab (AAB-001)*	Elan; Wyeth; JANSSEN Alzheimer Immunotherapy	Anti-Aβ amino terminal MAb	III; one trial	1,350	Safety and efficacy
Bapineuzumab (AAB-001)*	Elan; Wyeth; JANSSEN Alzheimer Immunotherapy	Anti-Aβ amino terminal MAb	III; five trials	4,650	Cognition and global function
Solanezumab (LY2062430)	Eli Lilly	Anti-Aβ mid-region MAb	III; two trials	2,000	Cognition and global function

Table 1.4: Examples of ongoing clinical trials of active Aβ immunotherapies.

Therapy	***Sponsors***	***Vaccine***	***Phase and number of trials***	***Estimated patient enrollment***	***Primary outcome measures***
ACC001	Elan; Weyth	Aβ amino-terminal conjugate	II; three trials	360	Safety, tolerability and treatment-related adverse effects
V950	Merck	Aβ amino-terminal peptides conjugated to ISCO-MATRIX	I; one trial	124	Safety and tolerability

Several types of immunotheraphy for AD are under investigation; presently there are three different approaches to generate antibodies directed against Aβ. The first strategy involves active-immunization with full length Aβ, which contains 42 amino acids (Figure 1.11*(a)*).[42] After injection, the peptide uptaken by antigen-presenting cells, and fragments of the peptide are presented to T-cells. Subsequently, various B cells that can recognize epitopes on Aβ42 are engaged and proliferate. These eventually produce anti-Aβ antibodies. It is thought that these antibodies are key to effecting the reduction in pathogenic Aβ that has been seen in a number of APP transgenic mouse models after Aβ42 immunization.[42]

The second type of active-immunization approach involves the administration of small fragments of Aβ conjugated to an unrelated carrier protein (Figure 1.11*(b)*).[42] This immunoconjugate approach is similar to the first strategy with the exception that the T-cells are stimulated by the carrier protein rather than by the Aβ fragment (which lacks T-cell epitopes). This approach also yields a strong antibody response to a region of the Aβ.[42]

The third strategy envolves the administration of anti-Aβ antibodies directly (Figure 1.11*(c)*).[42] This approach does not require any type of immunological response from the

host and then has the potential to be useful in individuals that might not otherwise generate an immune response to Aβ administration.[42]

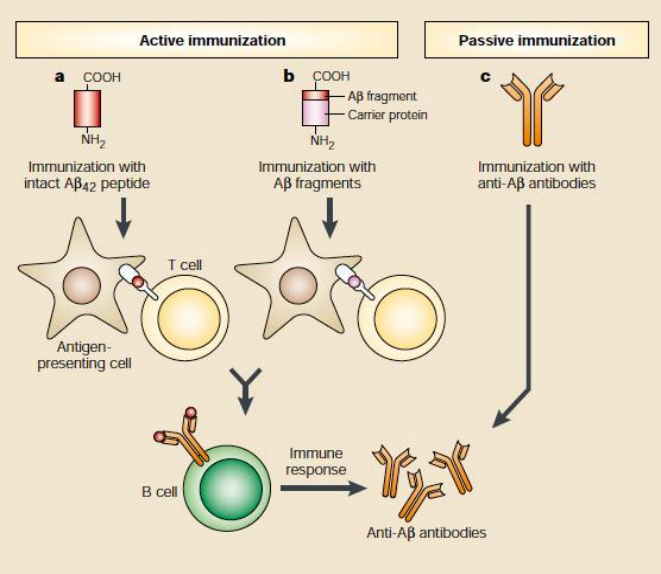

Figure 1.11: Strategies for Aβ immunotherapy.

Active vs passive Aβ immunization

Both active and passive Aβ immunotherapies have their advantages and disadvantges. Active Aβ immunotherapies have the potential to be more cost-effective and long-lasting than passive immunization, which requires monthly infusions of costly humanized monoclonal antibodies. Active therapies might have additional benefits. One study has reported that Aβ vaccination in non-human primates led to an increase in the production of cross-reactive, potentially protective Aβ auto-antibodies. Such antibodies are typically lower in patients with AD than in age-matched healthy individuals, therefore, boosting the levels of these proteins might be beneficial.[41]

In some cases, a passive Aβ immunotherapy might be beneficial. Vaccination usually involves delivery of a strong adjuvant to boost antibody production. Such adjuvants could potentially induce an undesirable immune response, especially in elderly individuals in whom proinflammatory cytokines are already above normal levels. Another problem for active therapies is that if an adverse event does occur, the immune response to the active vaccine can be difficult to stop quickly. Passive Aβ immunotherapies, on the other hand,

can be stopped at any time. Another advantage to the passive therapeutic approach is the use of antibodies that are specific for a particular Aβ conformation or species thought to be most toxic, thereby avoiding removal of all Aβ from the brain. Although one disadvantage of this approach is the potential for patients to eventually develop neutralizing antibodies against the passive therapy.[41]

1.4.1.2 Mechanism of Aβ clearence

Several mechanisms could explain how antibodies directed at Aβ promote the clearance of this peptide *in vivo*. When anti-Aβ antibodies form complexes with Aβ, the fragment crystallizable region (Fc) portion of the antibodies might bind the Fc receptor on microglia, inducing phagocytosis of these complexes. This mechanism would require that anti-Aβ antibodies cross the BBB and bind Aβ within the CNS. Some evidences have been reported to support this mechanism, although, two studies showed that Fc-mediated phagocytosis is not required for immunotherapy-induced Aβ clearance.[41]

In an alternative mechanism, anti-Aβ antibodies in the blood might cause a shift in the concentration gradient of Aβ across the BBB, thus resulting in an increase in Aβ efflux from the brain to the periphery. Aβ antibodies might bind and remove small Aβ aggregates, therefore neutralizing the effects of toxic Aβ species on synapses. These proposed mechanisms of Aβ clearance by immunotherapy are not mutually exclusive and might be disease stage-dependent.[41]

In the future, Aβ immunotherapy might be an effective treatment for preventing AD. Imaging and biomarkers have improved dramatically over the past years, increasing the probability of identifying at-risk individuals before clinical symptons onset and allowing the Aβ immunotherapy response to be monitored. If given early, before AD pathogenesis is well underway, Aβ immunization might be able to prevent aggregation of neurotoxic forms of Aβ, thereby preventing downstream effects, such as synaptic dysfunction, neuronal damage and cognitive impairment.[41]

1.4.1.3 Secretase inhibitors targeted to reduce Aβ

While anti-Aβ antibodies target the amyloid cascade at the level of Aβ aggregation and accumulation, the inhibitors of secretases approach the amyloid cascade at its root, namely, production of Aβ. This could be the "cleanest" approach which would remove all the monomeric Aβ and subsquent oligomers and aggregates. Therefore, pharmacological inhibition of the enzymes responsible for Aβ formation (γ-secretase and β-secretase) is a prime strategy for blocking Aβ production.[5,43]

The potential problem with secretase inhibitors is the physiological function of secretases. Both cleave a number of additional substrates and the inhibition of these other cleavages can limit the clinical utility of inhibitors. This limitation is very clear for γ-secretase inhibitors, but it is also a potential threat for β-secretase inhibitors.[43]

a) γ-secretase

The γ-secretase complex consists of four proteins, the catalytic activity of which is thought to be mediated by the presenilin 1 (PS1) and PS2 proteins. The γ-secretase complex is responsible for the carboxy-terminal cleavage of APP to produce Aβ40 or Aβ42. Potent small-molecule inhibitors of γ-secretase can dramatically reduce Aβ40 and Aβ42 production. The primary caveat to targeting γ-secretase for AD therapeutics is that APP is not the only substrate of γ-secretase. The disadvantage of this is that potent γ-secretase inhibitors have serious gastrointestinal and immunological side effects.[5]

As a result of this drawback, the field has shifted towards the development of γ-secretase modulators. These compounds either selectively inhibit γ-secretase cleavage of APP, or alter γ-secretase cleavage to favor Aβ40 production rather than Aβ42. The less abundant 42 amino acid isoform of Aβ, Aβ42, seems to be more strictly associated with the development of amyloid pathology than its counterpart Aβ40.[5]

Drugs that modulate γ-secretase activity in this manner include non-steroidal anti-inflammatory drugs (NSAIDs), such as ibuprofen and compounds that interact with ATP-binding motif PS1 near the γ-secretase active site.[5]

One such γ-secretase-modulating compound, the NSAID (*R*)-flurbiprofen (also known as tarenflurbil), effectively reduced amyloid plaque formation and rescued memory deficits in APP-transgenic mice. However, (*R*)-flurbiprofen failed to enhance cognitive performance of patients with AD in phase III clinical trials and has been abandoned as a potential therapy.

The compound screening approach may identify additional promising small-molecule γ-secretase modulators, and other compounds may be more successful than (*R*)-flurbiprofen in human trials, for example, semagacestat from Lilly and Elan is currently in phase III trials.

b) β-secretase

The amino-terminal cleavage of APP to form both Aβ40 and Aβ42 results from β-secretase activity. After the discovery that β-secretase cleavage of APP seemed to be due to the activity of a single aspartic protease, β-secretase 1 (BACE1; also known as memapsin 2 and ASP2), there was much interest in the possibility of targeting β-secretase for the treatment of AD.[5]

Inhibition of BACE1 activity can block the production of Aβ, prevent the development of amyloid pathology in the brain and rescue AD-related memory deficits in mice. Althought, despite nearly a decade has passed since the initial identification of BACE1 as the β-secretase, researchers still continue to struggle with the development of effective BACE1 inhibitors that are active in the CNS.[5]

The large BACE1 active site requires the identification of large compounds for potent BACE1 inhibition that also readily penetrate the BBB and are reasonably stable, but the slow progress of the BACE1 inhibitor field is a testament to the fact that such molecules are relatively rare.[5]

1.4.1.4 Inhibition of Aβ aggregation

Preventing Aβ aggregation is therapeutically attractive because this process is believed to be an exclusive pathological event, and compounds targeting this mechanism are more

likely to have a better safety profile compared to some other approaches currently being adopted.[15]

The strategy of inhibiting Aβ aggregation using small molecules is principally attractive, considering their lower cost and easier administration compared to antibodies. This approach is, however, complicated by several potential obstacles. Preventing Aβ aggregation either by blocking intermolecular interactions necessary for polymerization, or by stabilising the "native" structure of Aβ would potentially stop the pathogenic process before any toxic species could be formed. However, since there is no consensus as to what aggregates are the most toxic, finding out what step on the aggregation pathway to target is an unresolved key issue. The structural flexible nature of soluble, monomeric Aβ, and possibly also of Aβ oligomers, probably makes it difficult to find ligands that bind strongly to one particular structure.[44]

A large number of diverse compounds, including peptides and small organic molecules, have been shown to interfere with Aβ aggregation *in vitro*. Early studies concentrated on finding molecules that would prevent fibril formation, since the fibrils were believed to be the causative agent. However, when the idea of toxic oligomers appeared, other compounds that could inhibit aggregation into early stages were presented.

Examples of compounds identified as inhibitors of aggregation, regardless the mode of action, include congo red, polyphenols, nicotine, rifampicin, tetracyclines, curcumin, scyllo-inositol, and peptide-based inhibitors (Figure 1.12).[44] Molecules capable of disrupting pre-formed oligomers have not come to clinical trials.

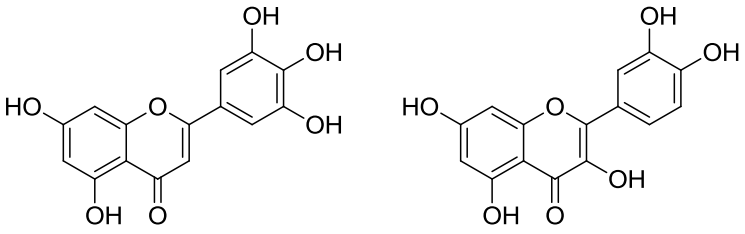

Figure 1.12: Structures of myrcetin, quercetin. ***(cont.)***

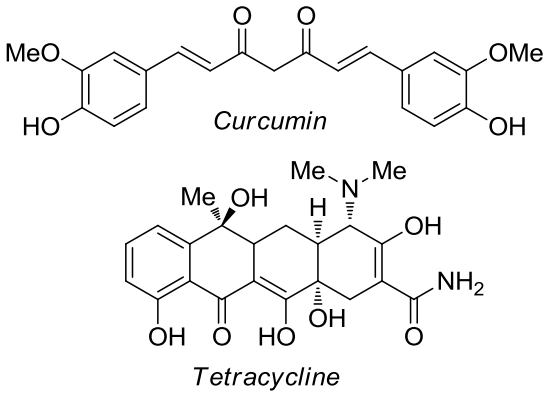

Figure 1.12: ***(cont.)*** Structures of curcumin and tetracycline.

1.4.2. Targeting Tau

Accumulation of hyperphosphorylated tau as paired helical filaments within NFTs and in neuritic processes is the intracellular hallmark of AD pathogenesis. Both genetic and animal modeling studies closely link abnormal tau metabolism to neuronal dysfunction and death. Some investigators have proposed that tau pathology appears independently of Aβ pathology, and that AD, at least in some circumstances, may represent a convergence of two distinct pathological processes – an Aβ amyloidosis and a taupathy rather than a linear cascade in which the Aβ amyloidosis drives the thaupathy.[45]

The relative scarcity of tau therapeutics can be attributed to:

- the uncertainty regarding the relationship between specific alterations in tau and induction of neurodegeneration;

- scarcity of clearly defined druggable targets that directly modulate tau in a way that should be protective from neurodegeneration.

Despite these uncertainties, there are some strategies that may be promising in a near future, such as targeting tau production, altering tau aggregation, altering tau phosphorylation and tau immunotherapy.[45]

1.4.2.1 Targeting tau production

Even though the exact neurotoxic species of tau has not been definitively identified, decreasing tau synthesis or a specific tau isoform is proposed to decrease the probability that tau will aggregate into a neurotoxic species. Therapeutics targeting tau production

remains in the conceptual stage, though some preclinical studies do provide proof of concept that lowering tau production can have a beneficial disease modifying effect.[45]

1.4.2.2 Altering tau aggregation

Even if a large number of tau aggregation inhibitors have been identified, these compounds are only effective *in vitro*, no proof of concept study has shown them capable of inhibiting tau aggregation *in vivo*. Nevertheless, the concept that a small molecule inhibitor could block aggregation of multiple proteins involved in neurodegeneration is intriguing. Future results studying the effect of these compounds in animal models are awaited.[45]

1.4.2.3 Altering tau phosphorylation

Tau contains multiple phosphorylation sites and phosphorylation seems to control the binding affinity for microtubules. Increased phosphorylation of the tau protein from an average of two to three phosphates in normal brain to an average of nine phosphates per molecules is seen in AD. Hyperphosphorylated, abnormally folded tau or tau aggregates may exert direct toxic effects on neurons. It is still debated whether phosphorylation of tau drives aggregation, results in toxicity, or is a consequence of aggregate formation. In any case, the link between phosphorylation and tau pathology has provided the impulse to examine the role of kinase inhibitors as potential therapeutics targeting tau.[45]

1.4.2.4 Tau immunotherapy

Antibodies targeting the pathological conformers of tau might clear or suppress tau pathology. Though theoretically attractive, there are concerns that antibodies are not optimal agents for targeting intraneuronal proteins. Additionally, the lack of clarity regarding which conformer of tau should be targeted remains a concern.[45]

In conclusion, all these premises strongly suggest a possible approach to AD, relying on brain Aβ as a target for therapy of the disease. This goal could be pursued either seeking an interaction with Aβ plaques, or through an interaction with soluble circulating Aβ, preventing amyloidogenesis.

In addition, several experimental evidences suggest that Aβ in the blood is in equilibrium with soluble Aβ in the brain, through the BBB. It can be predicted that this equilibrium may be shifted towards the circulating Aβ pool, whether peripheral molecules specifically interacting with Aβ are inducing its sequestration, eventually withdrawing brain Aβ and leading to plaque disappearance. Therefore, circulating Aβ is also a potential candidate target for the therapy of AD.

1.5. Nanoparticles for drug delivery through blood brain barrier

The number of drugs developed for treatment of CNS disorders has been growing constantly, however, only a few new drugs acting on the CNS enter the market.[46] There is a lack of potential new pharmaceutical entities, thus at present for many neurological disorders no satisfactory treatment exists. This group of diseases includes AD, PD, HD, ALS, lysosomal storage diseases, HIV infection of the brain, brain tumors, and CNS intoxications, for instance, with organophosphorous compounds. Drugs that are intended to act in the CNS can be administered systemically, if they have the ability to circumvent the BBB, or have to be introduced directly in the CNS by invasive methods, if such circumvention is limited. The BBB is essential for the maintenance of the unique neuroparenchymal environment but represents an invincible obstacle for a multiplicity of therapeutically important drugs.[47,48]

A variety of novel strategies have been proposed to improve the permeability of drugs into the CNS, including BBB disruption, alternative routes to CNS drug delivery, chemical drug delivery, biological drug delivery. One of the possibilities to deliver drugs to the brain is the employment of nanoparticles (NPs).[49] NPs can act as carriers for several classes of drugs, such as anticancer agents, antihypertensive, immunomodulators, and hormones, and macromolecules, such as nucleic acids, proteins, peptides, and antibodies.[48]

The mechanism of passive diffusion of the molecule across the BBB is dependent on its structural and physicochemical properties, such as molecular size, charge, hydrogen bonding potential, and lipophilicity. Besides compounds essential for brain homeostasis, such as amino acids, hexoses, neuropeptides, and proteins, which are transported into the brain via specific carriers, only small lipophilic molecules of less than 500 Da are able to cross this complex barrier.[50-52]

The strategies employed for enhancement the drug concentrations in the brain can be classified as invasive or non-invasive:

- The invasive methods include the temporary increase of the BBB permeability (e.g. by the osmotic disruption), the direct intraventricular or intracerebral infusion of the agent, or the intracerebral implantation of depot formulations for a controlled-release of the drug, such as the GLIADEL® Wafer (polifeprosan 20 with carmustine implant) indicated for patients with newly-diagnosed or recurrent high-grade malignant glioma in addition to radiation and/or surgery. As expected, all invasive techniques are associated with a high risk of complications, such as intracranial infections or brain edema. These procedures are also rather expensive and demand long reconvalescence periods.[48,53]

- The non-invasive strategies for brain delivery include modification of the drug molecules using chemical (i.e. synthesis of prodrugs) or biochemical approaches (i.e. conjugation with specific antibodies), as well as the employment of the olfactory route. However, in the latter case the quantities of drugs in olfactory lobes do not exceed nanomolar levels with bioavailabilities ranging from 0.01% to 0.1%. In addition, inhibition of the efflux transporters as well as the delivery via endogenous transporters such as the carrier-mediated transport system for glucose or amino acids are possible approaches to enhance brain delivery.[48,51,54]

A promising way to deliver drugs to the targets within the CNS is the employment of colloidal carriers, in particular, biodegradable polymeric NPs. As shown by a number of studies, surface modification of the NPs enables their entry into the brain after intravenous administration via receptor-mediated pathways. Another important advantage of this technology is that it does not require any modification of the drug molecule for the brain

delivery, which is achieved by masking the unfavorable physicochemical characteristics of the incorporated molecule.[48]

Drugs or other groups may be dissolved into the NPs, entrapped, encapsulated and/or adsorbed or attached. The aim in using NPs is to increase the specificity towards cells or tissues, to improve the bioavailability of drugs by increasing their diffusion through biological membranes and/or to protect them against enzyme inactivation.[49]

The field of nanoparticle drug technology is not yet well developed in AD research but NPs are promising candidates in the investigation of AD, because they are capable of: [55]

- opening tight juntions;
- crossing the BBB;
- high drug loading capacities;
- targeting towards mutagenic proteins of AD.

1.5.1. Liposomes

First described in the late sixties, liposomes are one of the first NP platforms to be applied in medicine. Today, there are more than a dozen of formulations approved for clinical use, with many more in clinical and preclinical development. Liposomal drug formulations typically improve the pharmacokinetics and biodistribution of a drug.[56]

A liposome is a tiny bubble (vesicle), made out of the same material as a cell membrane. Liposomes can be filled with drugs, and used to deliver drugs for cancer and other diseases. Membranes are usually made of phospholipids, which are molecules that have a head group and a tail group. The head is attracted to water, and the tail, which is made of a long hydrocarbon chain, is repelled by water. In nature, phospholipids are found in stable membranes composed of two layers (a bilayer). A liposome can be formed at a variety of sizes as uni-lamellar or multi-lamellar construction, and its name relates to its structural building blocks, phospholipids, and not to its size.[57]

The lipid bilayer closes in on itself due to interactions between water molecules and the hydrophobic phosphate groups of the phospholipids. This process of liposome formation is spontaneous because the amphiphilic phospholipids self-associate into bilayers. Drug loading into liposomes can be achieved through:[58]

(i) liposome formation in an aqueous solution saturated with soluble drug;
(ii) the use of organic solvents and solvent exchange mechanisms;
(iii) the use of lipophilic drugs;
(iv) pH gradient methods.

Liposomes have been considered for brain targeting in several pathologies through both intracerebral and intravenous administrations. An enhanced transport of liposome-encapsulated drugs has been observed in several reported studies (Table 1.5).

Table 1.5: Examples of liposomes used as brain drug delivery during CNS diseases.

Molecule tested	*Liposome type*	*CNS disease*
CM-Dil	PEG-liposomes coupled with transferrin	Ischemia
Doxorubicin	Pegylated liposomes (commercial formulation Caelyx®)	Brain tumor
IFN-b gene plasmid	Cationic liposomes	Brain tumor

Most of the studies have focused on tumor therapies to deliver doxorubicin and other antineoplastic agents with the aid of either cationic or pegylated liposomes (i.e. liposomes sterically stabilized by a coating of PEG).[59]

The generation of NPs properly loaded with antiamyloidogenic ligands, which could be concentrated at the brain surface and/or able to cross the BBB, represents a novel promising therapeutic approach.[60,61]

Chapter 2
Objectives

2. Objectives

The aim of this project is the preparation of innovative amyloid-beta peptide (Aβ) ligands, which could be used for the generation of nanoparticles (NPs) suitables for diagnosis and therapy of Alzheimer's disease (AD) (Figure 2.1).

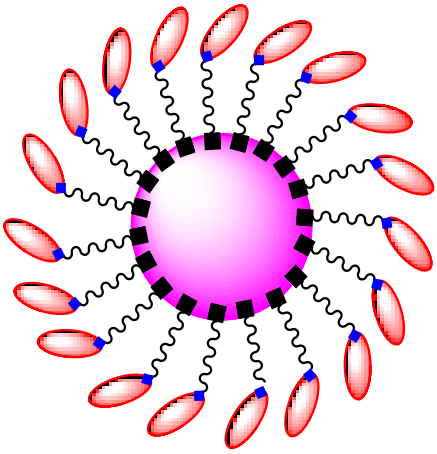

1) Aβ ligands: preparation of Aβ ligands functionalized monomers and eventual modification of Aβ ligands for chemical ligation

2) Nuclear magnetic ressonance screening experiments

3) Functionalization of Aβ ligands: conjugation of Aβ ligands to contrast agents/fluorophore and liposomes.

Figure 2.1: Strategy for functionalization of NPs or liposomes.

Many natural and synthetic compounds able to interact as Aβ ligands have been identified. Among them, we have paid attention to a set of small molecules in which aromatic moieties seem to play a key role. Unfortunately, many of these compounds lack solubility, chemical stability and/or show pharmacological activities not directly correlated to AD. Therefore, the correct therapeutic evaluation of these molecules towards AD cannot be performed in a straightforward manner.

Since Aβ are concentrated inside the brain or within the brain surface, the identified compounds must be concentrated near the blood brain barrier (BBB), for the interaction with circulating Aβ, and have the ability to cross this barrier, for the interaction with Aβ or plaques inside the brain.

The present project will be organized in the following steps:

2.1. Preparation of Aβ ligands

Different classes of putative ligands will be selected among the small molecules able to inhibit Aβ aggregation, in particular we will focus on heteroaromatic polycyclic compounds such as tetracyclines (TCs). Among the different class of compounds with reported ability to interact with Aβ, TCs are particularly attractive and are very versatile molecules, in some cases their structure-activity-relationship (SAR) are knowned, especially against bacteria. In other diverse fields of research, such as neurology, oncology and virology the activity of the tetracyclines (TCs) are being discovered.[62]

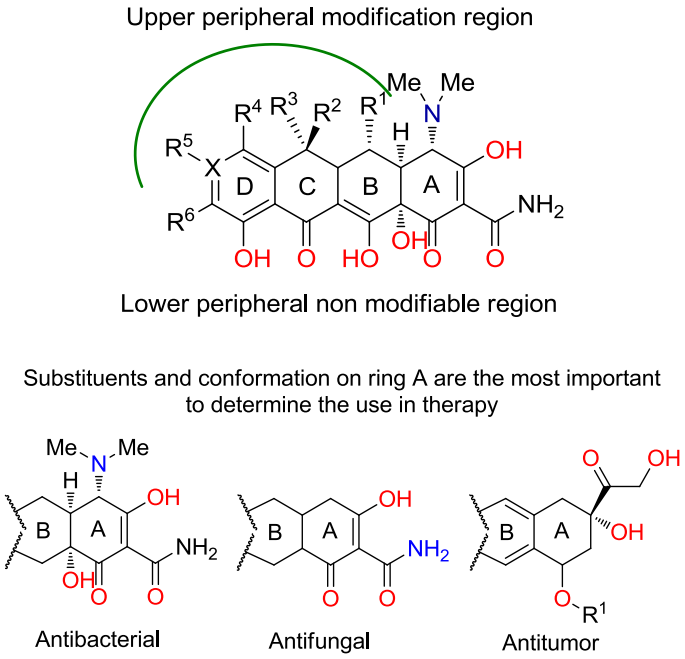

Figure 2.2: Tetracyclines drugs.

Example of therapeutic uses of TCs:

- Antibacterial resistance;[63]
- Target toward inflammation;[64]
- Neurology: Huntington's disease (HD), Parkinson's disease (PD), AD and Prion diseases;[65-69]
- Antiviral and Anticancer.[70]

Nevertheless TCs suffer from chemical instability, low water solubility and possess, in this contest, undesired anti-bacterial activity.[71,72]

In order to overcome these limitations, one of our goals is to synthesize TCs analogues bearing a polycyclic structure with improved chemical stability and water solubility, possibly lacking antibacterial activity but conserving the ability to interact with Aβ . We will start with the synthesis of a new class of potential Aβ ligands based on a structure resembling that of TCs. Known that TCs have in common a fourth cycle without an aromatic character and with different functionalization's, we aim to synthesize derivatives in which this cycle is represented by a sugar moiety, thus bearing different derivatisable positions or create derivatives in which we will increase or decrease the number of fused rings, but also bearing a sugar moiety.

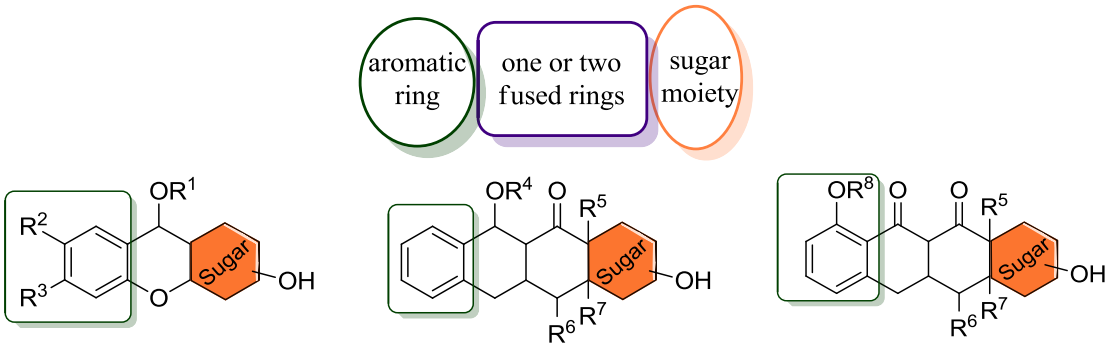

Figure 2.3: Synthetic scope.

We propose two different synthetic approaches:

2.1.1. Synthesis of glycofused tricyclic derivatives

- Exploit hetero Diels-Alder (DA) reactions, using carbohydrates moieties as dienophiles, for example glycals.

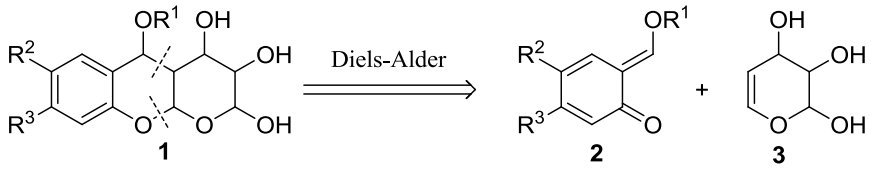

Scheme 2.1

The retrosynthetic approach idealized for compound **1** is showed in Schemes 2.1 and 2.2. We thought in a hetero-DA reaction of 2-hydroxybenzaldehyde derivatives **9** with the sugar diene derivative **2**. This kind of sugar derivatives containing a double bond, designated as "dehydro sugars", are versatile building blocks for the synthesis of glycosides and other natural products. Of the unsaturated sugars, these with the double

bound between C-1 and C-2 are referred to as glycals. Their utility laws in the unique reactivity of the cyclic enol ether, with the ring oxygen influencing the regioselectivity of reactions and the nature and orientation of the ring substituents, contributing to the overall reactivity and stereochemical outcomes of the reactions.[73]

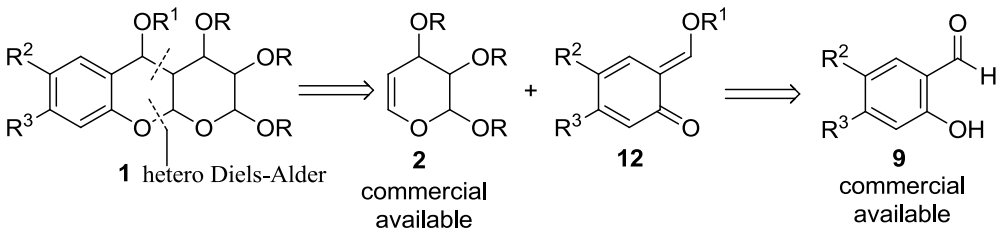

Scheme 2.2

2.1.2. Synthesis of glycofused tetracyclic derivatives

- Synthesis of new sugar bicyclic scaffolds (compounds **6** and **10**) to be employed in tandem Michael-Dieckmann reactions or in DA reactions to synthesize tetracyclic derivatives.

To be able to achieve our aims in the most excellent way, it is necessary to find the best synthetic pathways, and for that, we have hypothesised some retrosynthetic approaches. Our synthetic analysis of tetracyclic compounds **4**, **7**, **9** and **11** is described in Scheme 2.3. The target molecules **4** and **9** could be made using a tandem Michael-Dieckamn reaction of compound **5** with compounds **6** or **10,** respectively, whereas **7** and **11** could be realized by DA reaction of diene **8** with dienophiles **6** or **10,** respectively.

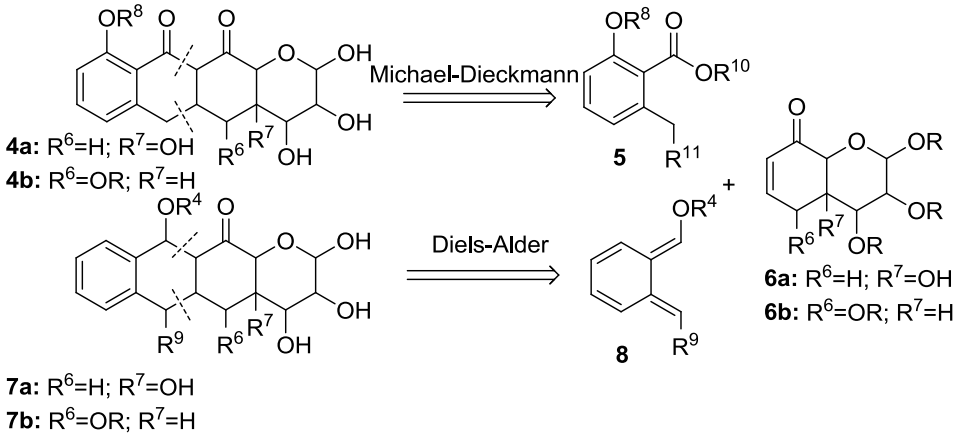

Scheme 2.3

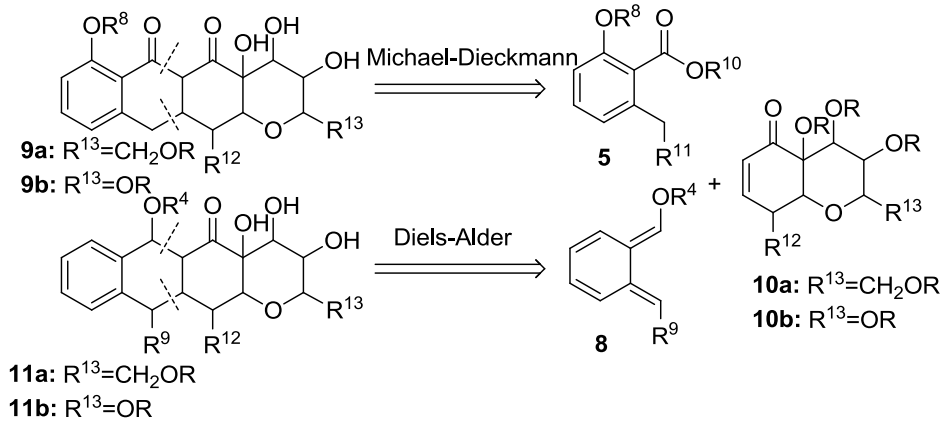

Scheme 2.3 (cont.)

Intermediate **5** could be obtained by esterification of acid **13**, which in turn could be synthesized from nitro compound **14**, by hydrolysis of a diazonium salt or by oxidation of dimethylanisole derivative **15**.

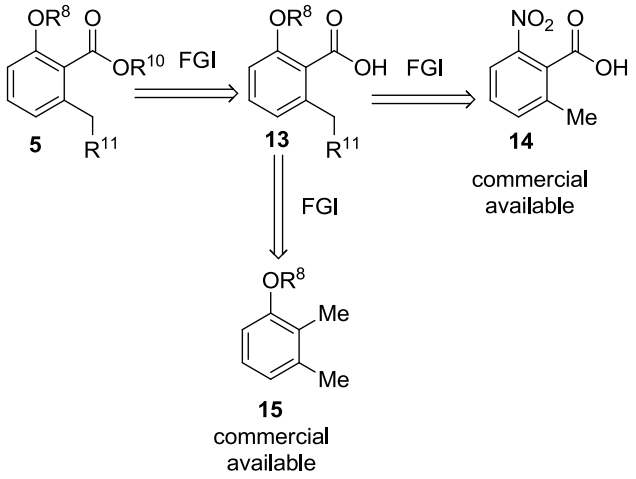

Scheme 2.4

ortho-Quinodimethane **8**, is a potent reactive intermediate, reported in literature,[74-77] which could be synthesize from commercial available 2'-bromoacetophenone.

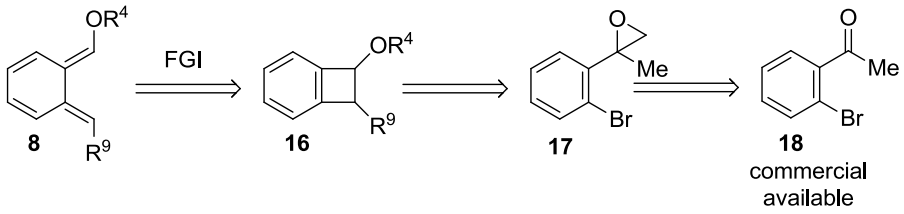

Scheme 2.5

The synthetic route developed for compound **6a** is depicted in the retrosynthetic Scheme 2.6. Our analysis began with the straightforward functional group interconversion (FGI) to generate compound **19**. From here, a double bond disconnection revelead the intermediate **20**, which could be obtained from Grignard reaction of **21** with vinyl magnesium bromide. Taking advantage of another FGI we would obtain compound **22**. This intermediate could be synthesized from ketone **23**, by another Grignard reaction. In both Grignard reactions we expect good diastereoselectivity. The reason is that magnesium can chelate with electronegative atoms in α-position to the carbonyl group and the carbonyl group itself (Figure 2.4). The stereoselectivity is likely to be high if a cyclic transition state is involved, and chelation involves just such transition state.

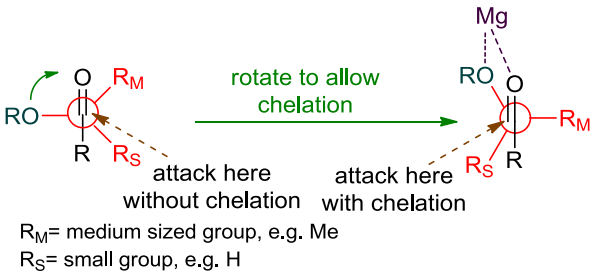

Figure 2.4: Chelation model for carbonyls groups' alkylation with electronegative atoms in α-position.

We planned to construct intermediate **23** by oxidation and using different protecting groups, i.e., taking advantage from orthogonality of compound **24**, which could be readily obtained from commercial available glycopyranoside **25**.

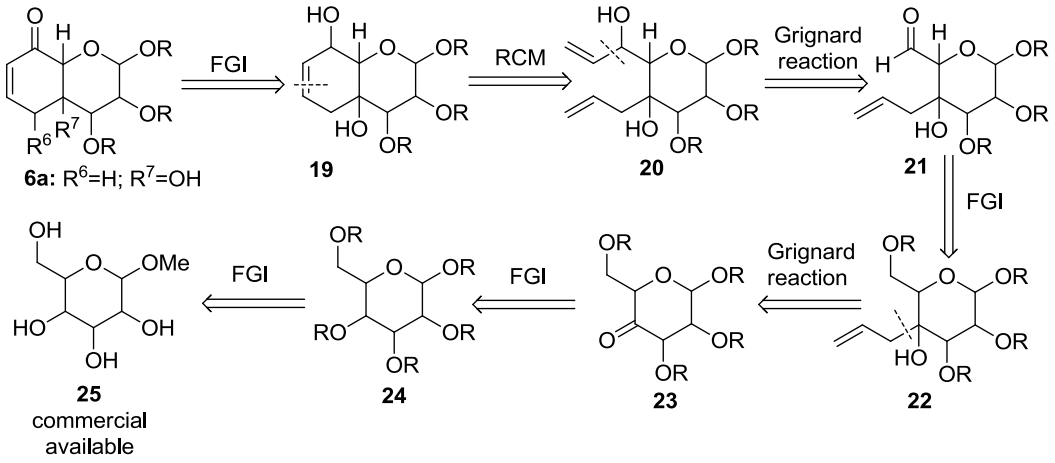

Scheme 2.6

The formation of bicyclic compound **6b** is presented in Scheme 2.7. This compound could be achived by ring closing metathesis (RCM) and FGI of compound **27**. The requisite compound **27** would be derived from compound **30**, which in turn could be constructed by hydroboration of intermediate **31**, obtained by a Wittig reaction of compound **23**. Ketone **23** could be prepared from the known glucose derivative **25**, by simple functional group manipulation and functional group interconversion.

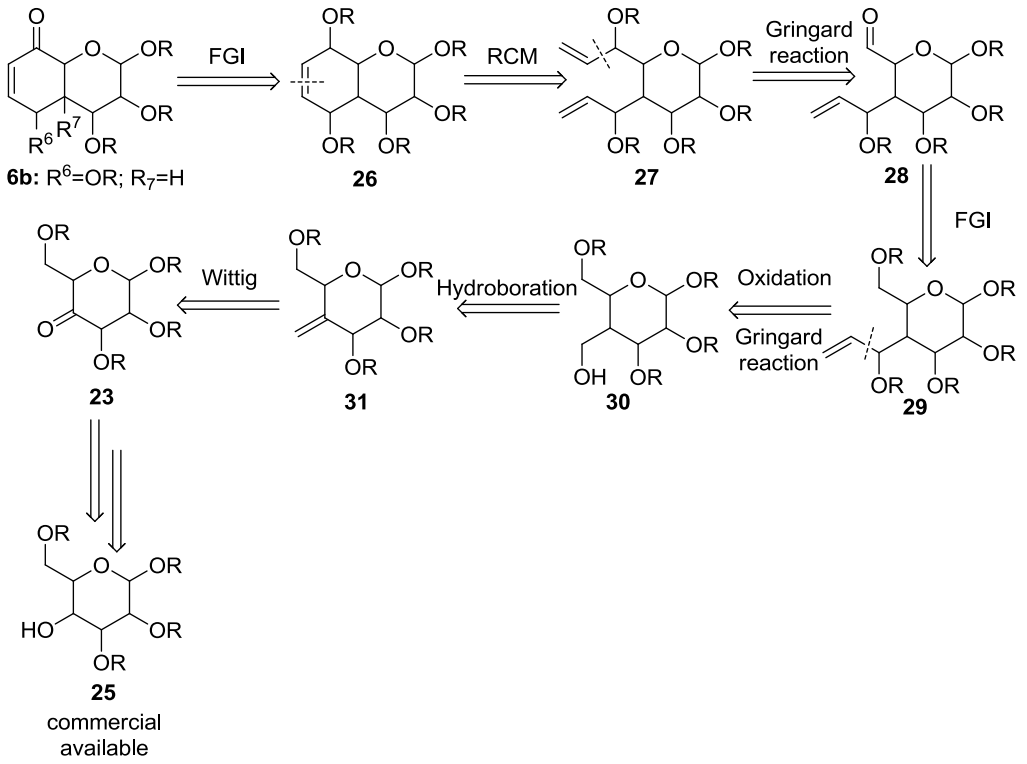

Scheme 2.7

Scheme 2.8 shows, in retrosynthetic format, the key carbon-carbon bond disconnections and FGI employed to devise the synthetic strategy towards compound **10a**. This compound could be obtained from an allylic oxidation of compound **32**, which in turn could be synthesised from RCM of **33**, in the presence of Grubbs second generation catalyst. Precursor **33** could be prepared in diastereoselective manner by a Grignard reaction with ketone **34**, whose origin was traced back to compound **35**, through oxidation of the free hydroxyl group. Intermediate **35** could then be converted retrosynthetically to commercial available glycopyranoside **25** through a Sakurai reaction,[78] followed by iodo cyclization and a β–elimination.

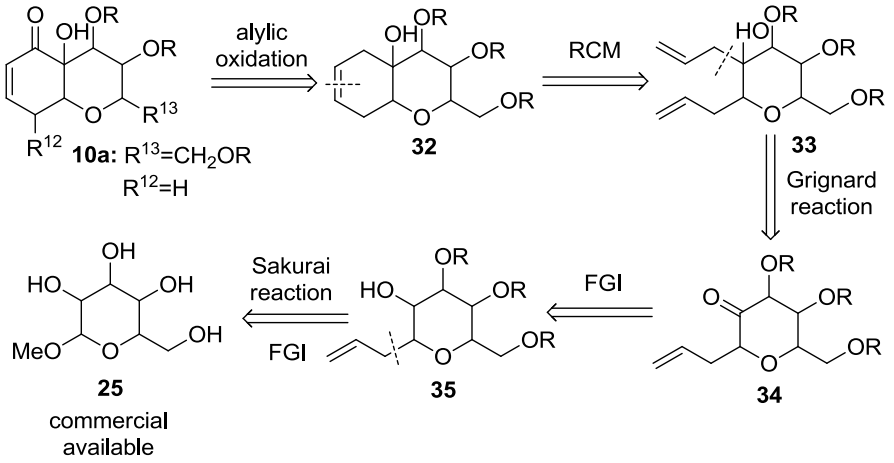

Scheme 2.8

Finally, intermediate **10b** could be obtained by RCM of **37** followed by Grignard reaction of **38**. We planned to construct intermediate **41** by dihydroxylation of the key intermediate **31**.

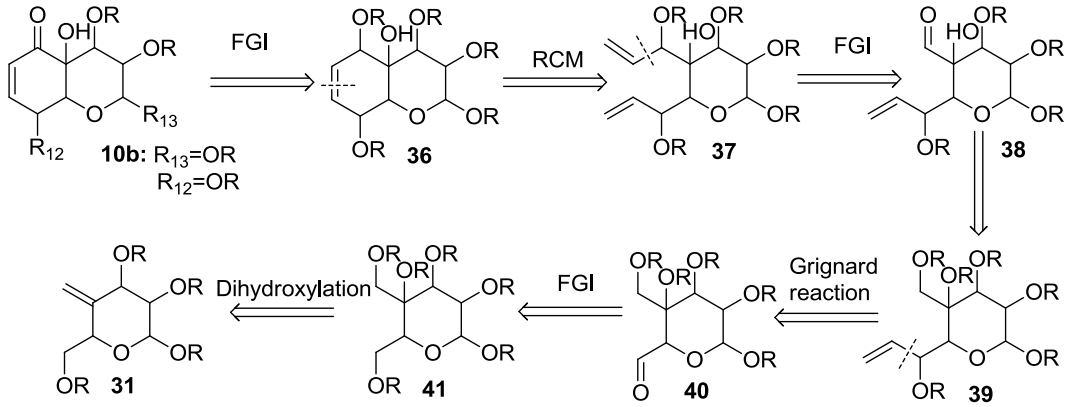

Scheme 2.9

2.2. Nuclear magnetic ressonance screening experiments

Selected compounds will be screened for their affinity towards Aβ, using solution nuclear magnetic ressonance (NMR) experiments that have the ability to probe at atomic resolution the molecular interaction between ligands and receptors. Specifically, saturation transfer difference (STD) and transferred nuclear Overhauser effect spectroscopy (tr-NOESY), will be used to screen Aβ oligomer, fibril, plaque binders and Aβ aggregation inhibitors.

2.2.1. Saturation transfer difference spectroscopy

STD-NMR spectroscopy is one of the most powerful NMR techniques for detection and characterization of receptor–ligand interactions in solution. If the irradiation conditions are adequately chosen, it is possible to saturate very efficiently only protons of the protein, but not those of the ligand. In this situation, if binding occurs, magnetization from the receptor protons will be transferred to ligand protons that are close in space in the bound state (Figure 2.5).

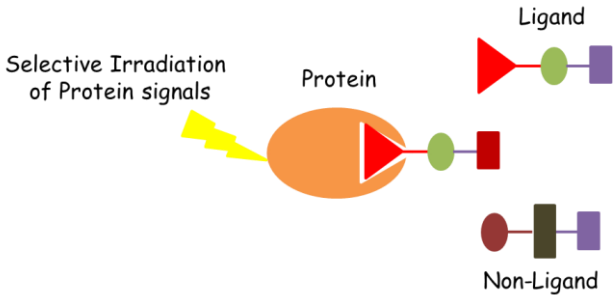

Figure 2.5: Schematic representation of STD-NMR experiment.

These experiments will allow to map the interactions highlighting the functional groups involved and their correct reciprocal orientation and distance. The results will allow designing more efficient ligands. This part of the project will focus on the design, on the based NMR data, and synthesis of small libraries of selected natural ligand derivatives and the evaluation of their real ability to bind Aβ. In case of positive results and improved binding with respect to the parent compounds, these derivatives will be used themselves to produce functionalised liposomes.

2.2.2. Transferred nuclear Overhauser effect spectroscopy

tr-NOESY is used to probe the conformation of a ligand while bound to its macromolecular receptor. It is primarily applied to systems for which exchange is fast, so that ligand protons show a single resonance peak averaged over the free and bound states.[79]

Fast exchange generally corresponds to $K_D > 10^{-6}$ M. The tr-NOESY method uses excess ligand (typical ligand:receptor site ratios range from 10 to 50), so that the resonance line shapes resemble those of the unbound ligand in solution, but the cross relaxation measured from the NOE spectrum is predominantly determined by internuclear distances within the ligand in the bound state.[79,80]

For a small molecule, the cross-peaks in the tr-NOESY spectrum have the opposite sign to the diagonal peaks, but in the presence of a receptor, the cross-peaks for the interacting compounds will change sign and become negative, due to the change in their effective rotational correlation time. The analysis of these negative cross-peaks provides information on the bound geometry of the ligand (Figure 2.6).[81]

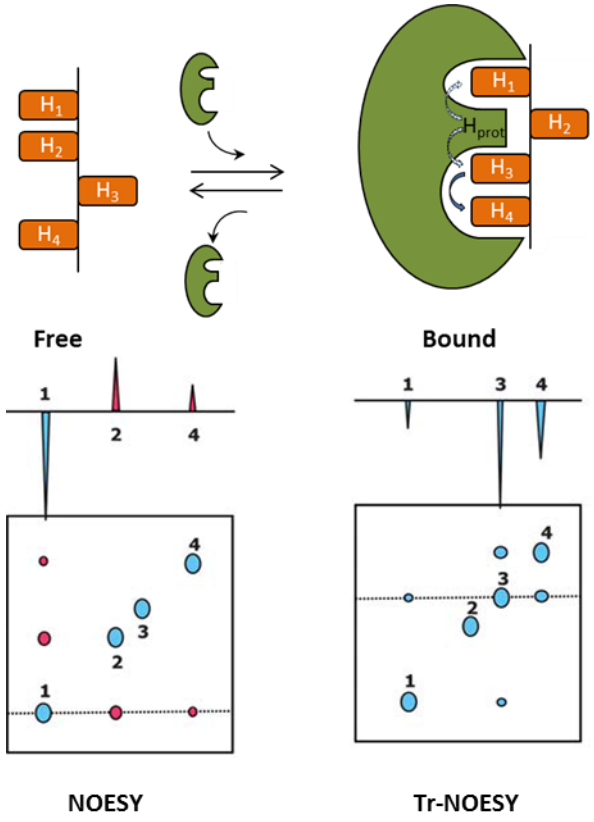

Figure 2.6: Schematic representation of the tr-NOESY experiment.

2.3. Functionalisation of Aβ ligands

Aβ ligands will be linked to liposomes exploiting the following strategy:

- Linker/spacer will be conjugated to Aβ ligands for subsequent functionalisation of liposomes.

Very few ligands are suitable as such to be linked to a spacer polyethylene glycol (PEG) or to be directly attached to a liposome, so in these cases the ligands have to be opportunely

modified with the introduction of a group suitable for ligation. Besides the traditional carboxylic acid/amine conjugation, exploiting the peptide synthesis procedures, chemoselective-coupling procedures will be performed involving an azido group and a triple bond to generate a triazole, belonging to very efficient reactions termed “click chemistry”.

The chemistry developed and optimized for the conjugation of Aβ ligands to liposomes will then be exploited to link also a contrast agents/fluorophore, useful as diagnostic tool, and/or a BBB transporter. The latest will allow the generation of liposomes able to pass the BBB with more efficacies with respect to the non-derivatized compounds.

Chapter 3
Results and discussion

3. Results and discussion

In this section is described the synthetic achievements of this project, as mentioned early, one of our goals is to synthesize tetracyclines (TCs) analogues bearing a polycyclic structure, possibly lacking antibacterial activity, with improved chemical stability and water solubility but conserving the ability to interact with amyloid beta peptides (Aβ). This tetracyclic structure will be glycofused, thus bearing different derivatisable positions; the number of fused rings will be changed, but likewise bearing a sugar moiety.

3.1. Synthesis of glycofused tricyclic derivatives

a) Exploit hetero-Diels-Alder (hetero-DA) reactions, using carbohydrate moieties as dienophiles, for example glycals.

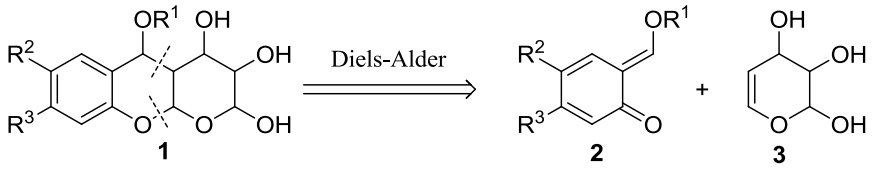

Scheme 3.1

The Diels-Alder (DA) reaction is arguably one of the most powerful reactions in the arsenal of the synthetic organic chemistry. By varying the nature of the diene and dienophile, many different types of carbocyclic structures can be built up. Nevertheless, the presence of electron-withdrawing groups in the dienophile and electron-releasing groups in the diene or *vice-versa* can drastically accelerate the process.[82]

The use of carbohydrate derivatives containing a double bond in DA reactions are versatile building blocks to be used in organic synthesis and they have been extensively used in

hetero-DA reactions. Based on the retrosynthetic analysis was need to use a 1,2-anhydro sugars as dienophiles.

The employed synthetic strategy exploits the reaction between *o*-hydroxybenzaldehydes and glycals using a catalytic amount of scandium triflate in the presence of trimethyl orthoformate (TMOF), as described by Yadav et al.[83] In order to verify the influence of the various parts of the molecule on the interaction with the Aβ, we generated a small library of glyco-fused benzopyran compounds, using differently substituted *o*-hydroxybenzaldehydes and employing both glucal (**50**) and galactal (**49**). In all cases, we obtained *cis*-fused pyrano[3,2-*b*]benzopyran (21–91% yield), but in contrast to previous reports,[83] the reaction afforded a variable ratio of separable mixtures of two diastereoisomers at C5 (Scheme 3.2, Table 3.1).

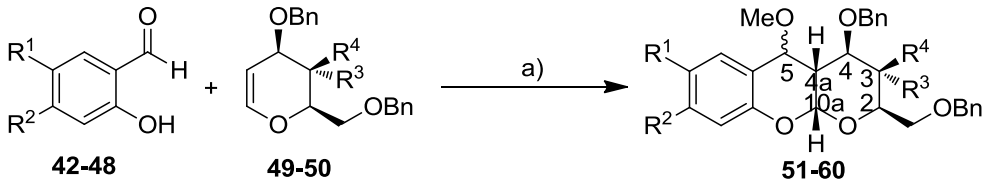

Scheme 3.2. *reagents and conditions:* a) $Sc(OTf)_3$ (3% mol), TMOF (2.5 equiv.), CH_2Cl_2, rt.

Table 3.1: Protected *cis*-fused glyco benzopyrans.

o-hydroxy benzaldehyde	D-glycal	Protected products	C5 *R/S* (yield%)
42 R^1,R^2= H,H	**49**	**51** R^1,R^2,R^3,R^4= H,H,H,OBn	92/8 (59%)
43 R^1,R^2= NO_2,H	**49**	**52** R^1,R^2,R^3,R^4= NO_2,H,H,OBn	100/0 (40%)
44 R^1,R^2= OBn,H	**49**	**53** R^1,R^2,R^3,R^4= OBn,H,H,OBn	100/0(35%)
45 R^1,R^2= OMe,H	**49**	**54** R^1,R^2,R^3,R^4= OMe,H,H,OBn	85/15 (73%)
46 R^1,R^2= CH_3,H	**49**	**55** R^1,R^2,R^3,R^4= CH_3,H,H,OBn	95/5 (91%)
47 R^1,R^2= H, OMe	**49**	**56** R^1,R^2,R^3,R^4= H,OMe,H,OBn	53/47 (64%)
48 R^1,R^2= H,CH_3	**49**	**57** R^1,R^2,R^3,R^4= H,CH_3,H,OBn	100/0 (45%)
46 R^1,R^2= CH_3,H	**50**	**58** R^1,R^2,R^3,R^4= CH_3,H,OBn,H	100/0 (66%)
47 R^1,R^2= H, OMe	**50**	**59** R^1,R^2,R^3,R^4= H,OMe,OBn,H	100/0 (37%)
48 R^1,R^2= H,CH_3	**50**	**60** R^1,R^2,R^3,R^4= H, CH_3, OBn,H	100/0 (21%)

The reaction may proceed through the formation of *o*-quinone methides generated *in situ* from salicylaldehydes and TMOF as shown in Scheme 3.3.

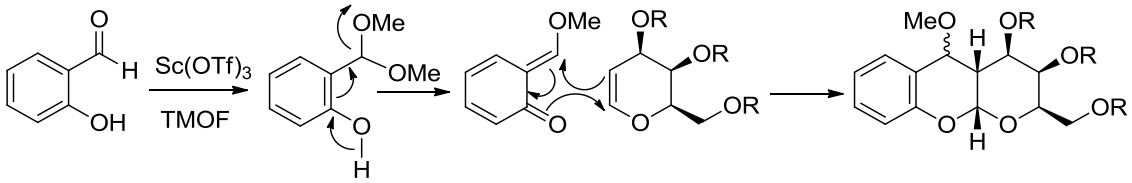

Scheme 3.3

The major isomer was then deprotected by hydrogenolysis to afford the final compounds **61**–**70** (Scheme 3.4, Table 3.2).

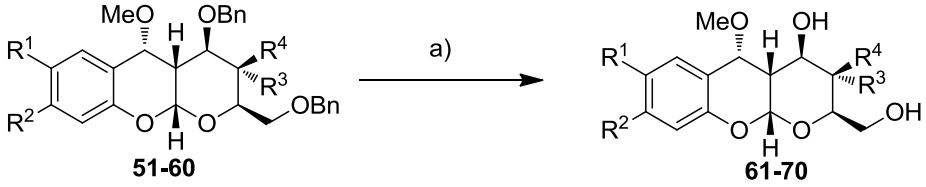

Scheme 3.4. *reagents and conditions:* a) H_2, $Pd(OH)_2$ (5% mol), AcOEt:MeOH (1:1), rt

Table 3.2: Deprotected *cis*-fused glyco benzopyrans.

Protected products	Deprotected compounds C5-*R* (yield%)
51 R^1,R^2,R^3,R^4= H,H,H,OBn	**61** R^1,R^2,R^3,R^4= H,H,H,OH (97%)
52 R^1,R^2,R^3,R^4= NO_2,H,H,OBn	**62** R^1,R^2,R^3,R^4= NH_2,H,H,OH (94%)
53 R^1,R^2,R^3,R^4= OBn,H,H,OBn	**63** R^1,R^2,R^3,R^4= OH,H,H,OH (100%)
54 R^1,R^2,R^3,R^4= OMe,H,H,OBn	**64** R^1,R^2,R^3,R^4= OMe,H,H,OH (96%)
55 R^1,R^2,R^3,R^4= CH_3,H,H,OBn	**65** R^1,R^2,R^3,R^4= CH_3,H,H,OH (95%)
56 R^1,R^2,R^3,R^4= H,OMe,H,OBn	**66** R^1,R^2,R^3,R^4= H,OMe,H,OH (97%)
57 R^1,R^2,R^3,R^4= H,CH_3,H,OBn	**67** R^1,R^2,R^3,R^4= H,CH_3,H,OH (97%)
58 R^1,R^2,R^3,R^4= CH_3,H,OBn,H	**68** R^1,R^2,R^3,R^4= CH_3,H,OH,H (98%)
59 R^1,R^2,R^3,R^4= H,OMe,OBn,H	**69** R^1,R^2,R^3,R^4= H,OMe,OH,H (97%)
60 R^1,R^2,R^3,R^4= H, CH_3, OBn,H	**70** R^1,R^2,R^3,R^4= H, CH_3, OH,H (98%)

Compound **56** was chosen as an example to describe the structural charatcterization of these type of compounds. From ^{1}H NMR spectrum (Figure 3.1) we found that $J_{H\text{-}4a\text{-}H\text{-}5}$ is 4.4 Hz for compound **56** (C5-*S*) and 2.2 Hz for compound **56** (C5-*R*)**,** and $J_{H\text{-}4a\text{-}H\text{-}10a}$ is 2.9 Hz for compound **56** (C5-*S*) and 3.3 Hz for compound **56** (C5-*R*)**,** we can confirm that also in this molecule (C5-*R*) H-4a and H-10a are *cis* related.

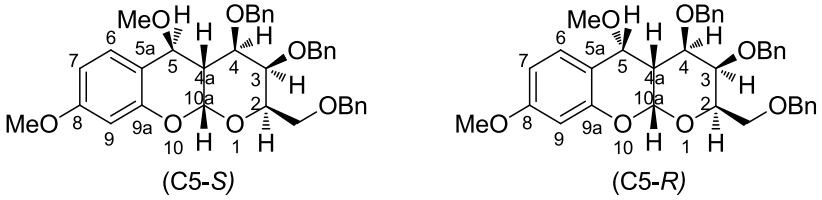

Scheme 3.5

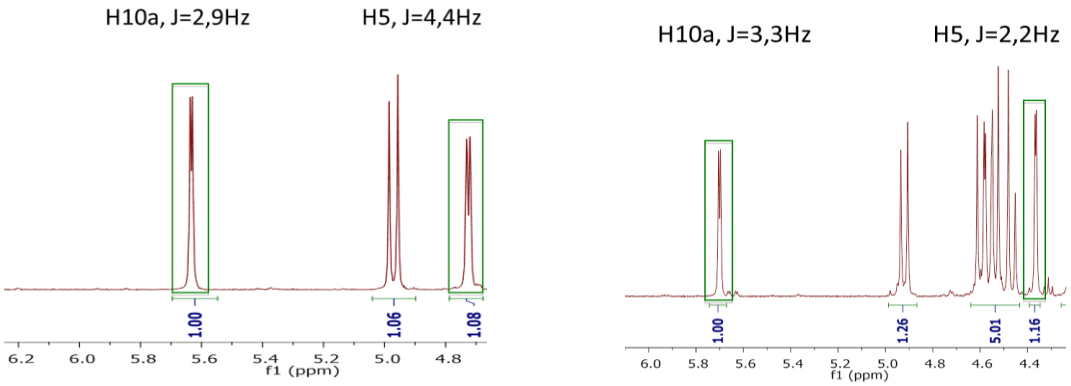

Figure 3.1: ^{1}H NMR spectrum (400 MHz, $CDCl_3$) of compounds **56** (C5-*S*) and (C5-*R*).

To confirm that the tricyclic is *cis*-fused was performed a two-dimensional nuclear Overhauser effect spectroscopy (2D-NOESY) experiment of compound **56** (C5-*R*) (Figure 3.2). The presence of nuclear Overhauser effect (NOE) contacts was observed between H-10a and H-5, H-10a and H-4a, while H-4 showed correlations with H-3 and H-2. Absence of a cross-peak between H-10a and H-4 shows that they are in opposite sides. These experimental evidences indicate that the stereochemistry indicated in the structure of compoumd **56** is the correct one.

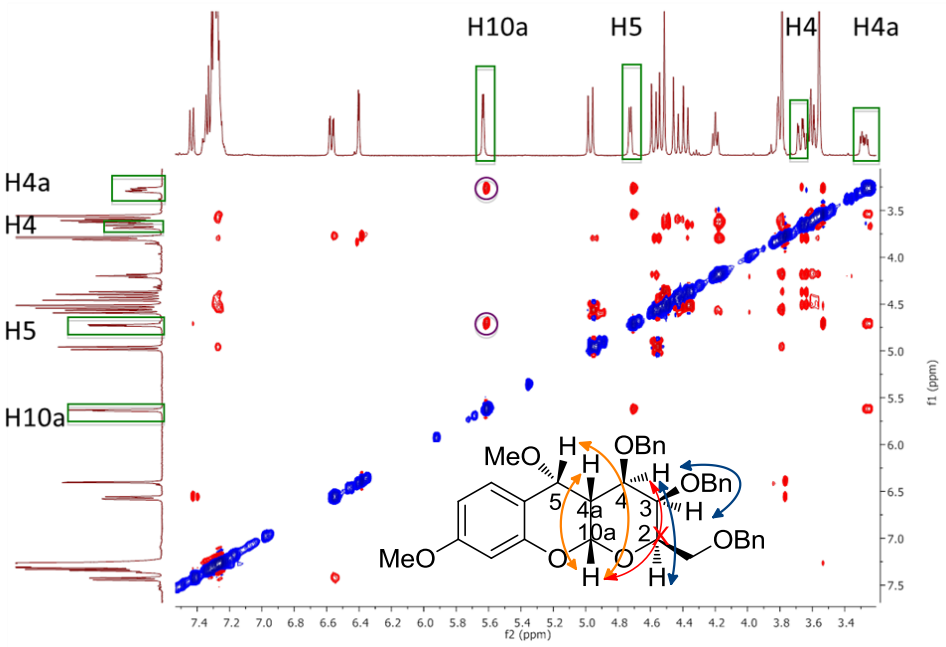

Figure 3.2: 2D-NOESY spectrum (400 MHz, $CDCl_3$) of compound **56** (C5-*R*).

3.1.1. STD and tr-NOESY NMR experiments

From the molecular recognition perspective, very recently, it was employed saturation transfer difference-nuclear magnetic ressonance (STD-NMR) experiments to characterize the interaction of tetracycline and thioflavin T (ThT) with Aβ(1-40) and Aβ(1-42) .[67,84,85]

Thus, the same methodology has been applied herein to check the effect of benzopyran derivatives of the debenzylated compounds **61-70**, on the Aβ(1-42) oligomer recognition process. In particular, the interaction studies with the amyloid peptide Aβ(1-42) were carried out by using STD and transferred nuclear Overhauser effect spectroscopy (tr-NOESY) NMR experiments.

STD-NMR experiments were performed using ligand:peptide 20:1 mixtures dissolved in deuterated phosphate buffer saline (PBS), pH=7.4, 25°C. Each mixture was analyzed irradiating the sample at -1.0 ppm to achieve the selective saturation of some aliphatic resonances of Aβ oligomers. The presence of NMR signals of the test molecule in the STD spectra is a non ambiguous demonstration of the existence of interaction. Conversely, the absence of NMR resonances in the STD spectra indicates that the employed molecule is not an Aβ ligand. In all cases, several NMR resonances of compounds **61-70** appeared in the corresponding STD spectra recorded in the presence of Aβ oligomers (Figure 3.3 and 3.4), thus showing their ability to recognize and bind Aβ(1-42) , with the notable exception of compound **62**, whose signals are absent (Figure 3.3B).

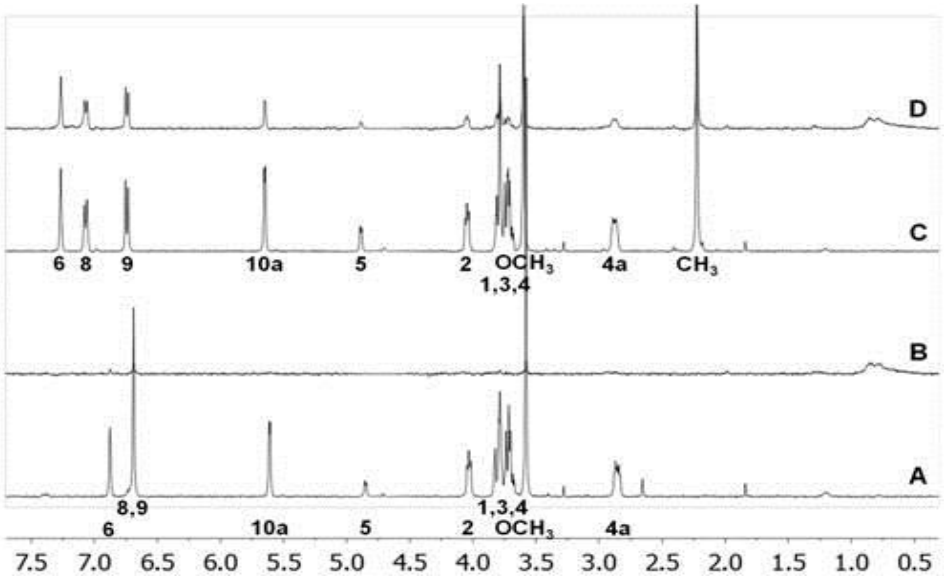

Figure 3.3: Comparison between STD experiments acquired in the presence of compound **62** and **65**. ^{1}H (A and C) and 1D-STD (B and D) spectra recorded on Aβ:ligand mixtures dissolved in deuterated PBS, pH=7.5 at 25°C and containing Aβ(1-42) (80 mM) and a test molecule (1.6 mM) (A and B, compound **62**; C and D, compound **65**). ^{1}H NMR spectra were acquired with 64 scans, 1D-STD NMR spectra with 512 scans and 2 s of saturation time.

Additional tr-NOESY experiments acquired on the same ligand:peptide mixtures supported these results. The change in the sign of the cross-peaks of the test molecule, from positive (blue color), in the absence of Aβ(1-42), to negative (red color) in presence of Aβ(1-42) , reflects an increase of its effective rotational motion correlation time, and supports its binding to a large molecular entity, here represented by the Aβ oligomers.[85]

In agreement with the STD results, all tr-NOESY spectra of compounds **61-70** acquired in the presence of Aβ(1-42) showed the key change, from positive to negative, of the

corresponding cross-peak signs, except for compound **62.** In this case, the NOE cross--peaks remained positive, indicating that this molecule does not bind to Aβ(1-42) in a significant manner (Figure 3.5).

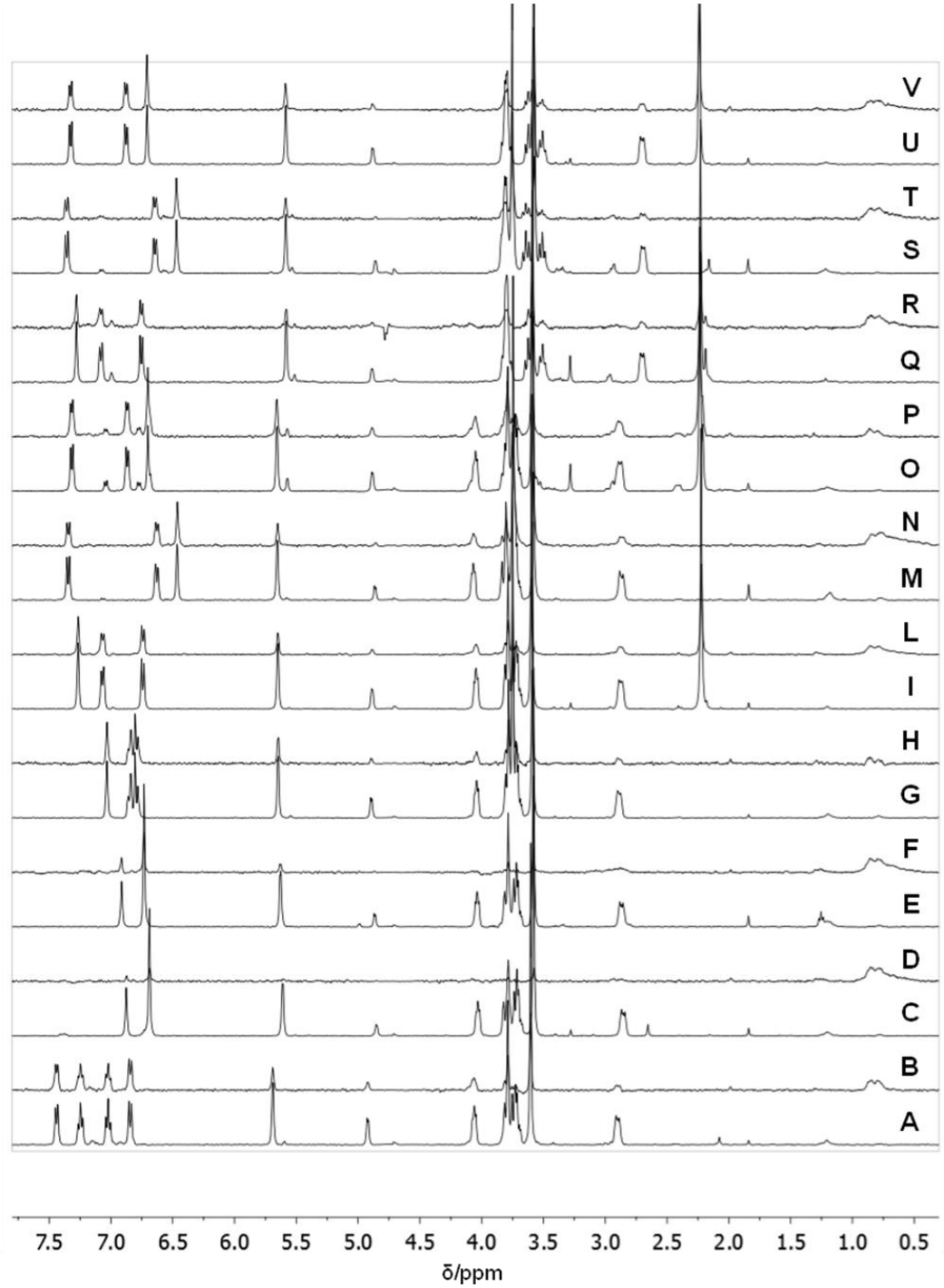

Figure 3.4: ^{1}H NMR spectra (A, C, E, G, I, M, O, Q, S and U) and 1D-STD NMR spectra (B, D, F, H, L, N, P, R, T and V) of mixtures dissolved in deuterated PBS, pH=7.5 at 25°C containing Aβ(1-42) (80 μM) and a test molecule (1.6 mM) (A and B, compound **61**; C and D, compound **62**; E and F, compound **63**; G and H, compound **64**; I and L compound **65**; M and N, compound **66**; O and P, compound **67**; Q and R, compound **68**; S and T, compound **69** e U and V, compound **70**). ^{1}H NMR spectra were acquired with 64 scans, 1D-STD spectra with 512 scans and 2 s of saturation time.

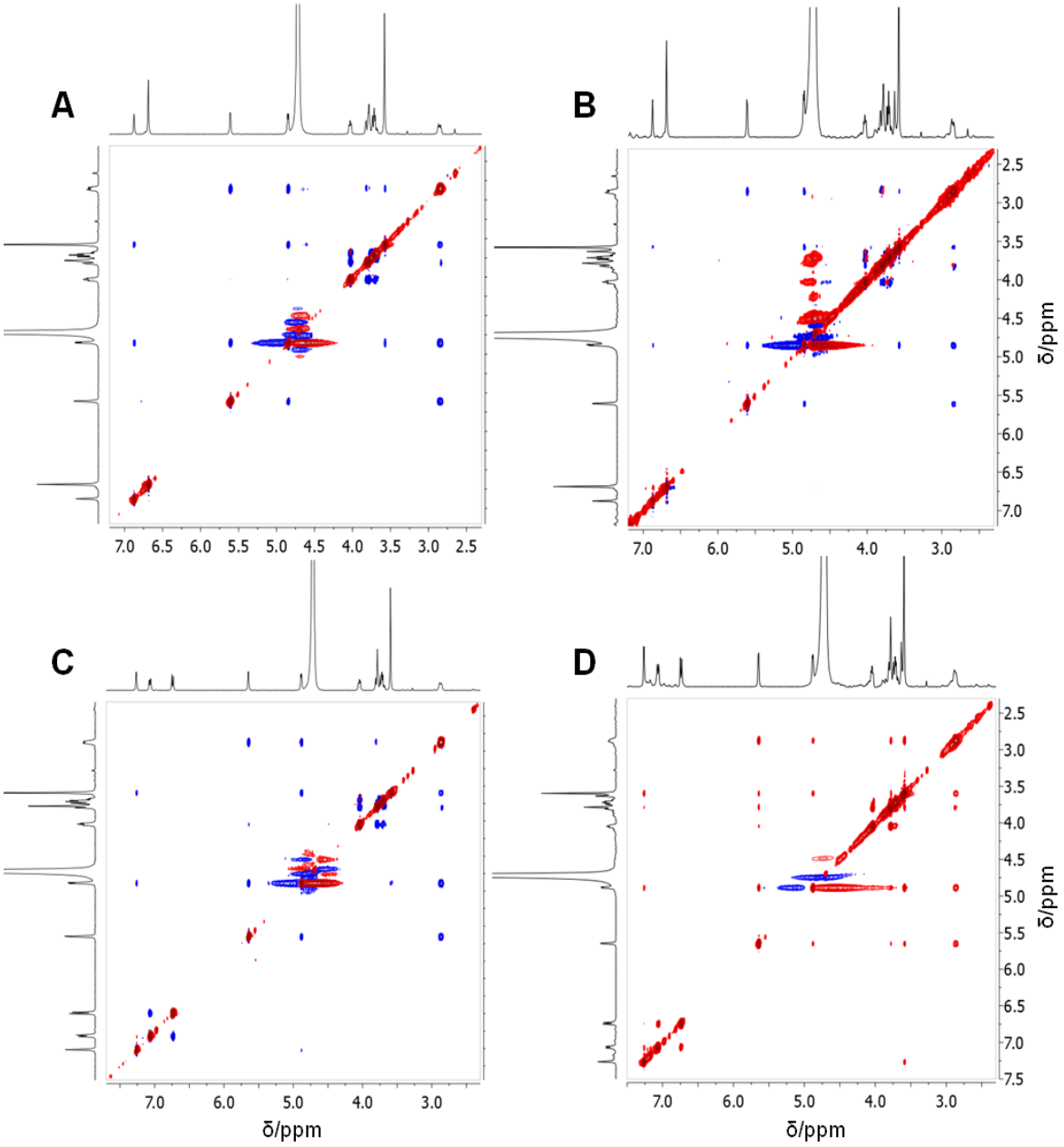

Figure 3.5: 2D-NOESY spectra of compounds **62** (A) e **65** (C) dissolved in deuterated PBS, pH=7.5, 25°C, mixing time 0.9 s. tr-NOESY of mixture containing Aβ(1-42) (80 μM) and compound **62** (B) or compound **65** (D) dissolved in deuterated PBS, pH=7.5, 25°C, mixing time 0.3 s. Positive cross-peak are blue, negative ones red.

Since the STD intensity is proportional to the ligand binding affinity for the molecular target,[85] we exploited competitive STD experiments to rank the affinity of compounds **61-70** for the peptide. Due to extensive resonance overlapping, the acquisition of competitive STD spectra on a unique mixture containing all the molecules was not feasible. Hence, we performed three different competitive experiments of the different molecules in the presence of Aβ(1-42) oligomers. Thus, separate experiments for mixtures containing the

D-galactose derivatives (**61**-**67**), the D-glucose analogues (**68**-**70**), or "the best ligands" identified from the two previous screenings (**65** and **70**) were performed.

In the first and second competitive experiments, we measured the STD effect on H-6, and in the third experiment on H-10a (see Scheme 3.5). For each molecule, the fractional STD effect was calculated as $(I-I_0)/I_0$, where I is the intensity of the monitored signal in the STD spectrum and I_0 is the intensity of the same signal in a reference spectrum. Compounds **65** and **68** showed the same affinity for Aβ(1-42) , as their H-10a signals presented equal intensities. Hence, to compare the data obtained in the different competitive experiments, the fractional STD effects of **65** and **68** were set equal to 1 and, therefore, the relative intensities for the other molecules were calculated. The results are summarized in Figure 3.6.

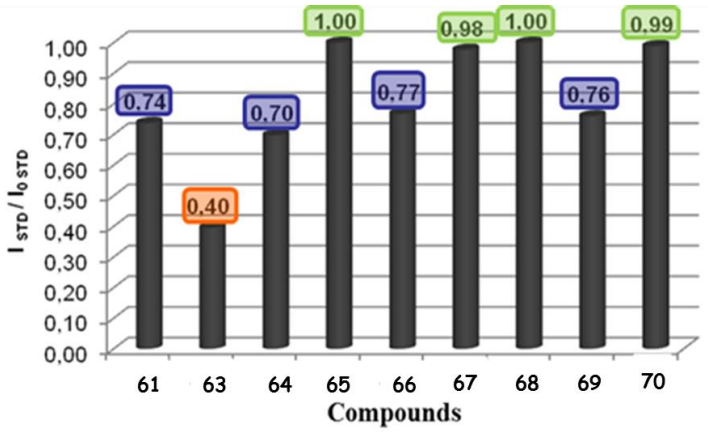

Figure 3.6: Fractional STD effects calculated for compounds **61**, **63**, **64**, **65**, **66**, **67**, **68**, **69** and **70**. These values are proportional to compounds affinity for Aβ(1-42) oligomers.

Thus, **65**, **67**, **68** and **70**, whose aromatic rings are substituted with a methyl group, are the ligands with the highest affinities for Aβ oligomers, followed by **64**, **66** and **69**, which present a *O*-methyl group as substituent, and by **61**, with no aromatic substituent. These molecules display fractional STD effects higher than 70%. Finally, **63**, with a hydroxyl group at position 7, has the lowest affinity. These data, together with the absence of binding of **62** (with an amine substituent) to Aβ oligomers, clearly indicate that the lower the polarity of the substituents on the aromatic ring, the greater the compound affinity for Aβ(1-42) . Moreover, the position of substituents on the aromatic ring (position 7 or 8), as well as the nature of the saccharide entity, are not relevant, as supported by the evidence

that compounds **65**, **67**, **68** and **70** showed equal binding affinity, and the same applies for compounds **64**, **66** and **69**.

These findings are in full agreement with the STD-based epitope-mapping, recorded with five different saturation times (0.5, 1.2, 2.0, 3.0, 5.0 s) (Figure 3.7). According to the STD relative intensities, the region of the ligand mainly involved in the interaction with Aβ (the binding epitope) is the aromatic ring, while protons of the saccharide portion showed the least intense STD signals. These evidences explain why the stereochemistry of sugar carbons does not influence the binding affinity, while the polarity of the aromatic substituents, as previously stated, plays a crucial role in the interaction.

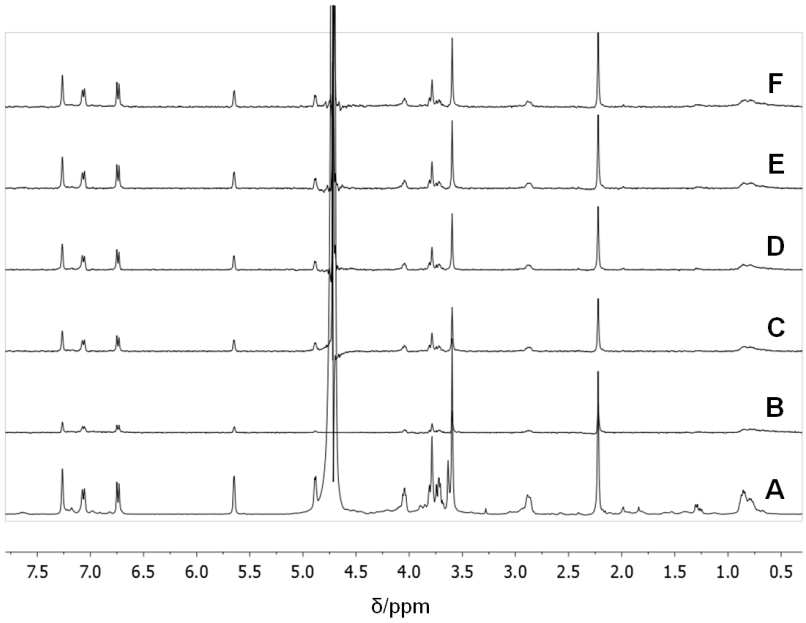

Figure 3.7: A) ^{1}H NMR spectrum of the mixture containing Aβ(1-42) (80 μM) and compound **65** (1.6 mM) in PBS, pH=7.5, 25°C; B-F**)** STD-NMR spectra of the same mixture acquired with different saturation times. (B 0.5 s; C 1,2 s; D 2,0 s; E 3,0 s; F 5,0 s).

3.1.2. Conformational analysis: molecular dynamics and molecular mechanics simulations

In order to be sure that the observed difference in the binding ability was only due to the polarity of the substituent and not to a different molecular conformation induced by the substituent itself, we carried out a conformational analysis. This analysis was performed using molecular mechanics (MM) and molecular dynamics (MD) simulations. Calculations were performed by using MM3*14 force field, as implemented in the MacroModel program (Maestro Suite). After a first run of minimizations, a conformational search was

performed for each molecule. The conformation with the lowest energy was selected, minimized and submitted to MD simulations. 100 structures were sampled and further minimized. According to the modelling data, compounds **61-70** present the same conformation. The 30 conformations with the lowest energy found for compound **61-70** are reported in Figure 3.8.

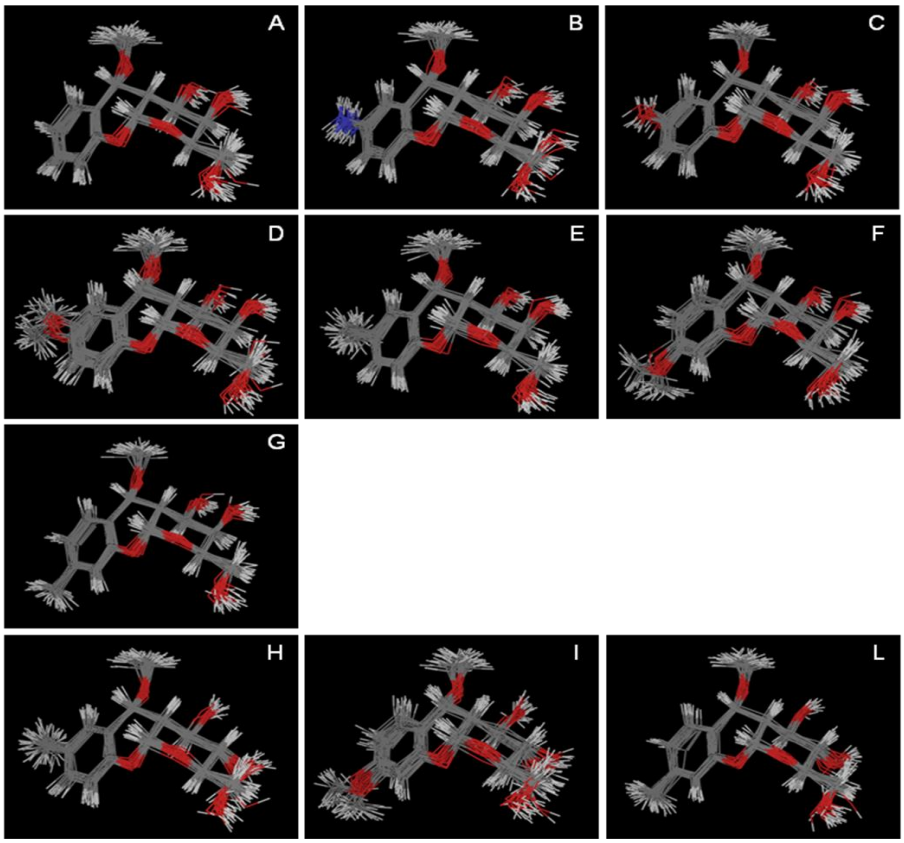

Figure 3.8: Superimposition of the 30 structures with the lowest energy calculated through MD simulations in water, 298K; A, compound **61**; B, compound **62**; C, compound **63** ; D, compound **64**; E, compound **65**; F, compound **66**; G, compound **67**; H, compound **68**; I, compound **69**; L, compound **70**.

The values of the key proton-proton distances H2-H3, H2-H4, H3-H4, H4a-H10a, H4a-H5 and H5-H10a as well as the values of the dihedral angle H2-C2-C3-H3, H3-C3-C4-H4, H4a-C4a-C10a-H10a and H4a-C4a-C5-H5 were monitored during the MD. All compounds showed the same values of H2-H4, H4a-H5, H4a-H10a, and H5-H10a distances (Figure 3.9), and of the dihedral angles H4a-C4a-C10a-H10a (average value θ=62°) and H4a-C4a-C5-H5 (average value θ=-53°), which are the diagnostic parameters to identify molecule conformation. On the other hand, on the basis of the distances H2-H3 and H3-H4 and the dihedral angles H2-C2-C3-H3 and H3-C3-C4-H4, molecules **61-70** could be clustered into two groups (**61-67**, with average θH2-C2-C3-H3=-60°, θH3-C3-C4-H4=60° and **68-70**,

with average θH2-C2-C3-H3=-180°, average θH3-C3-C4-H4=180°), depending on C3 stereochemistry (Figure 3.9). From these results was concluded that the differences in affinity for Aβ(1-42) are due to the nature of the substituent on the aromatic ring and are not a consequence of conformational differences

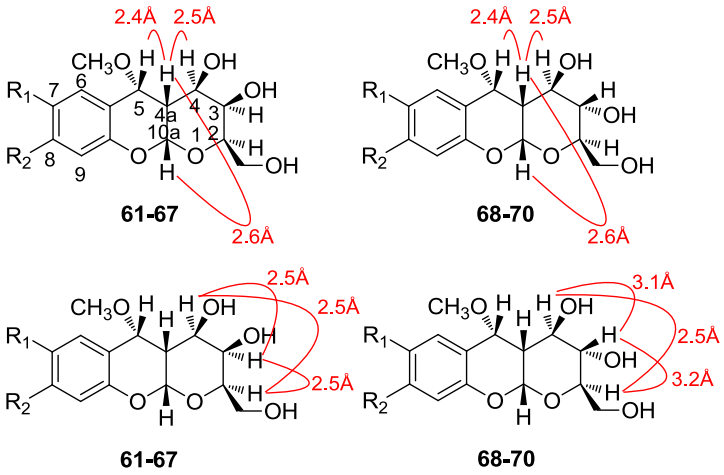

Figure 3.9: Average values for H2-H3, H2-H4, H3-H4, H4a-H10a and H5-H10a interproton distances. Concerning H2-H3 and H3-H4, compounds **61-70** can be clustered into two groups (bottom).

3.1.3. Functionalisation of glycofused tricyclic derivatives: generation of fluorescent-lipophilic derivatives

The *cis*-glyco fused benzopyran compounds described above as new Aβ ligands, present key interesting features that make them attractive for the development of potential diagnostic and/or therapeutic tools. For these purposes the Aβ binding ability is a fundamental characteristic but, as such, is not sufficient, in order to generate a potential drug-tool candidate, the molecules should also possess the correct physical-chemical characteristics. The glycidic moiety, not being directly involved in the binding assures further possible derivatizations, such as conjugation to other molecular entities [nanoparticles (NPs), polymeric supports, etc.], and functionalization with chemical groups able to modulate the hydro/lipophilicity. In order to be useful such compounds should perform their action within the brain, therefore they have to be able to cross the blood-brain-barrier (BBB), and to be somehow detected for diagnostic purposes.

3.1.3.1 Synthesis of fluorescent glycofused tricyclic compounds

The scope of this part of the project consists in the synthesis of fluorescent tricyclic derivatives to verify the ability of the test compounds to pass through the BBB, using spetrofluorimetric techniques (Figure 3.10), and to be used as diagnostic tools to detect the presence of Aβ oligomers/plaques.

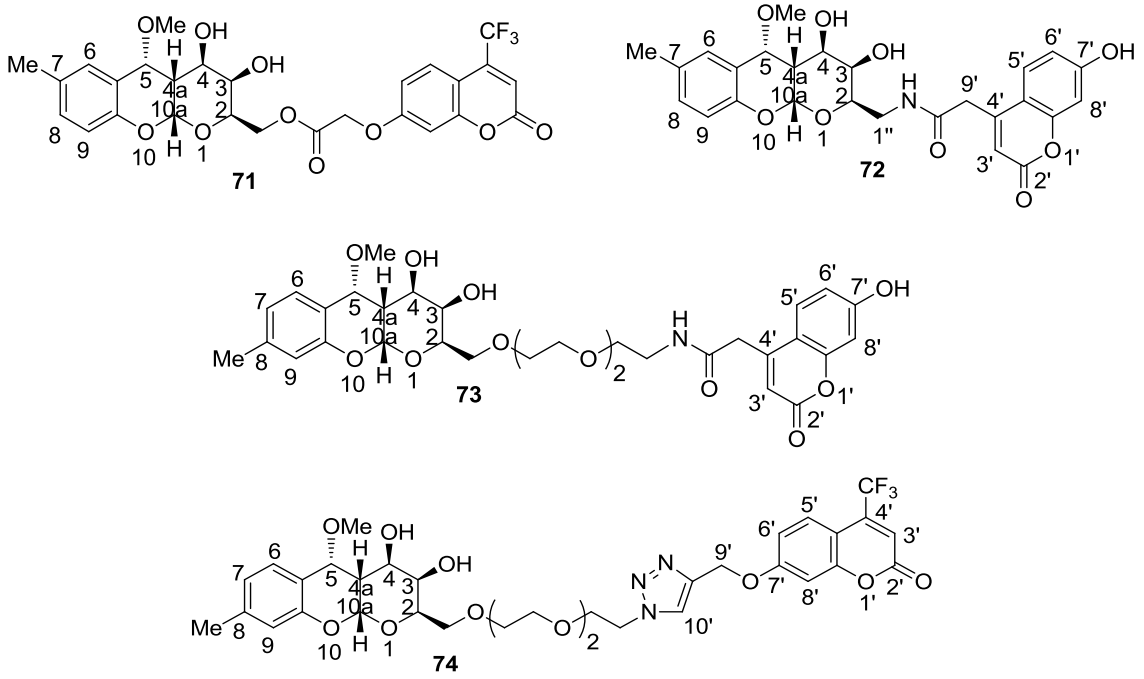

Figure 3.10: Fluorescent derivatives of Aβ-peptides ligands (**71**-**74**).

The choice of the fluorophore was done in order to modulate the hydrophilic properties of the molecule maintaining the molecular weight low enough for a diffusion mechanism, since we knew from previous experiments that the hydrophilicity of our derivative was too high to assure the permeation through the BBB.

As fluorophore we selected coumarin derivatives (Figure 3.11), due to its relatively small dimension with respect to other commonly used fluorescent entities such as rhodamine and fluorescein. In this way we wanted to limit as much as possible the possible interference of the fluorophore in the ligand binding, which in any case should be assessed. Moreover, coumarin has a lipophilic character and its conjugation to the tricyclic compound would modulate the solubity affording the correct logP value to the derivative.

For the conjugation we exploited the primary hydroxyl group of the glycidic moiety, since, as expected, previous binding studies of section 3.1.1. confirmed that the sugar moiety was

not or very poorly involved in the binding with the Aβ, and this hydroxyl group can be selectively functionalised.

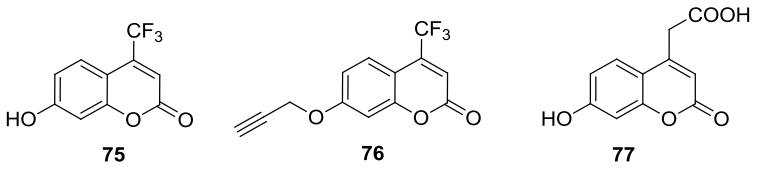

Figure 3.11: Coumarin derivatives.

Our first approach was focused on the direct conjugation of the fluorophore to the Aβ ligand. Among the previously identified ligands, compounds bearing the methyl substituent at position C7 and/or C8 of the aromatic ring showed the best binding properties, thus compounds **65** and **67** were used in this section. For the synthesis of compound **71** (Scheme 3.6), ligand **65** was regioselectively acylated with bromoacetyl bromide at low temperature (-45°C) affording compound **78**, that was reacted with coumarin derivative **75** in basic conditions ($CsCO_3$) to afford the final product **71** with a 37%, not optimized, overall yield.

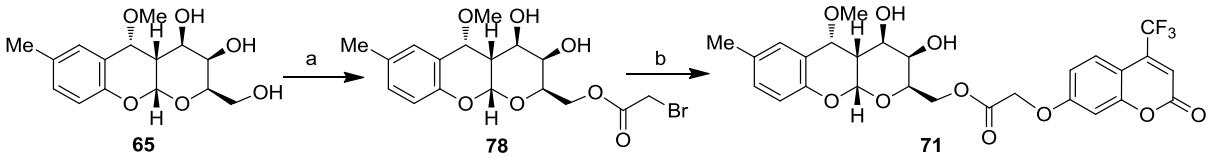

Scheme 3.6. *reagents and conditions:* **a)** $BrCH_2COBr$ (1.3 equiv.), dry DMF, *sym*-collidine (1.4 equiv.), -45°C, 40 min., 54%; **b) 75** (1.5 equiv.), $CsCO_3$ (1.1 equiv.), dry DMF, rt, 1 h, 37%.

For the synthesis of compound **72** (Scheme 3.7), the primary hydroxyl was first converted to the corresponding amine **81**, by a tosylation (TsCl, dry Py) reaction followed by a nucleophilic azide substitution (NaN_3, dry DMF) and final reduction (H_2, Pd-Lindlar, MeOH). Compound **81** was then coupled with coumarin derivative **77,** using standard coupling conditions (DIC, HBTU, DIPEA, dry DMF) affording the final product **72.**

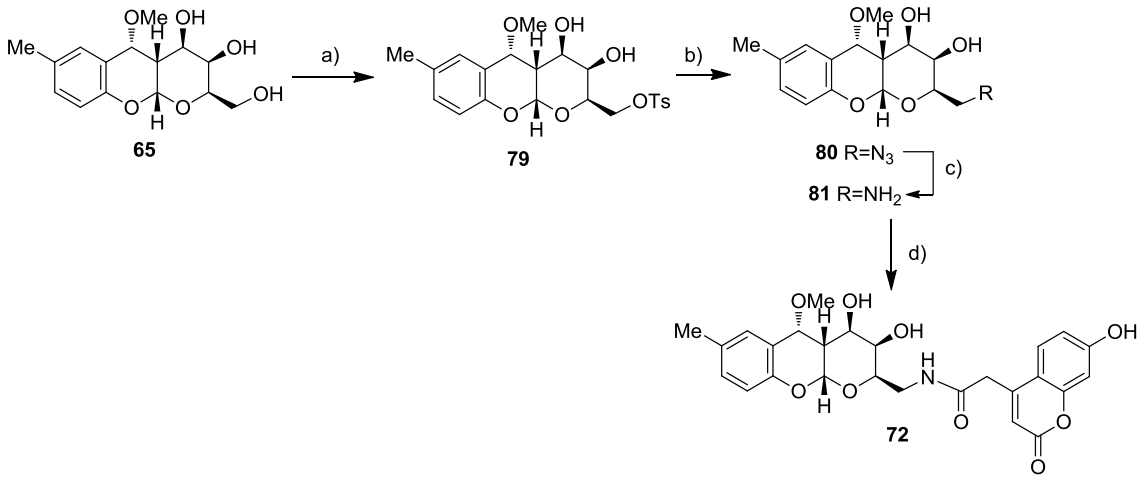

Scheme 3.7. *reagents and conditons*: **a)** TsCl (1.1 equiv.), DMAP (cat.), dry Py, 0°C-rt, 12 h, 98%; **b)** NaN_3 (7.0 equiv.), dry DMF, 100°C, 12 h, 60%; **c)** H_2, Pd-Lindlar, MeOH, rt, 1 h; d) **77** (1.2 equiv.), DIC (1.5 equiv.), HBTU (1.5 equiv.), DIPEA (3.0 equiv.), dry DMF, rt, 47% (over two steps).

^{1}H NMR spectrum of compound **72** (Figure 3.12) shows a doublet for proton H-5' at δ 7.59 ppm with a *J* = 8.8 Hz, and analysis of 2D-COSY NMR shows only vicinal coupling with H-6' at δ 6.76 ppm. For the coumarin scaffold we can also see from ^{1}H NMR, a singlet at δ 6.16 ppm corresponding to H-3' proton and proton H-8' that appears between δ 6.68 – 6.58 ppm. The protons C<u>H$_2$</u>CONH- appear between δ 3.81 – 3.71 ppm. In relation to the tryciclic part, H-10a appears as a doublet at δ 5.54 ppm showing only vicinal coupling with H-4a, *J* = 2.8Hz, confirming that these protons are *cis* related.

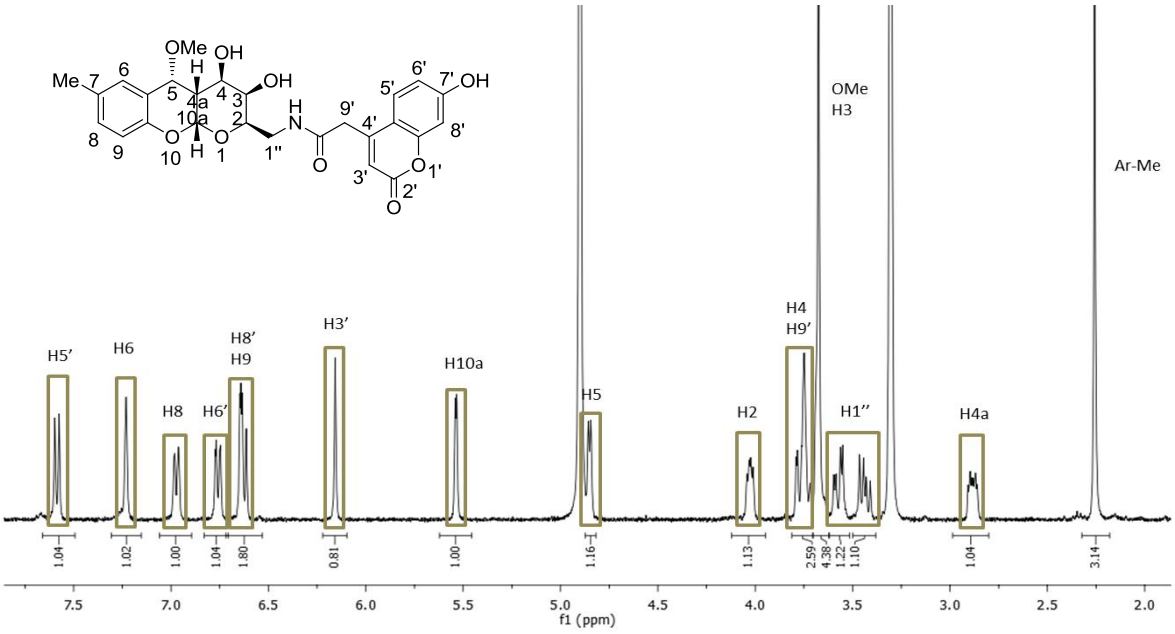

Figure 3.12: ^{1}H NMR spectrum (400 MHz, CD_3OD) of compound **72**.

In order to verify the influence of the fluorophore on the binding properties to Aβ, STD--NMR experiments were carried out on both compounds. Unfortunately, compound **71** resulted chemically unstable, as it hydrolyzed immediately after dissolution in aqueous buffer (data not shown), probably because of the presence of the ether linkage in α to the ester group.

Conversely, compound **72** resulted stable to hydrolysis and, in order to verify the influence of the fluorophore on the binding properties to Aβ, its interaction with Aβ(1-42) was investigated by STD-NMR experiments.[67,84-88]

NMR binding studies were carried out employing the same methodology previously described.[61] In particular, compounds **72** ability to interact with Aβ(1-42) oligomers was assessed by STD-NMR spectroscopy. STD-NMR experiments were performed using a ligand:peptide 10:1 mixture dissolved in deuterated PBS, pH=7.4, 37°C. The mixture was analyzed irradiating the sample at -1.0 ppm to achieve the selective saturation of some aliphatic resonances of Aβ oligomers. In general, the presence of NMR signals of the test molecule in the STD spectrum is a clear demonstration of the existence of interaction (Figure 3.13).

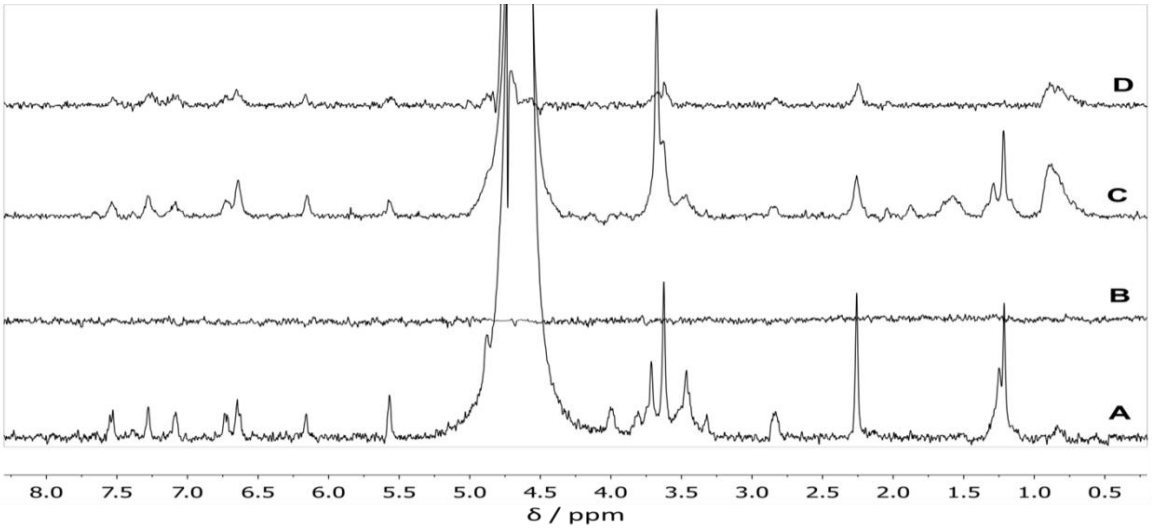

Figure 3.13: A) ^{1}H NMR spectrum of the compound **72** (0.5 mM) in PBS, pH=7.4, 37°C; B) Blank STD-NMR spectrum of compound **72** acquired with a saturation time of 3.0 s and 2304 scans; C) ^{1}H NMR spectrum of the mixture containing the peptide Aβ(1-42) (50 μM) and compound **72** (0.5 mM) in PBS, pH=7.4, 37°C; D) STD-NMR spectrum acquired on the same mixture with a saturation time of 3.0 s and 2304 scans.

STD experiments evidenced the binding ability of compound **72**, even if its STD signals were rather low in intensity, probably due to solubility problems in physiological

conditions. The poor quality of STD spectrum prevented the possibility to obtain a detailed epitope mapping and the acquisition of further NMR interaction experiments. In order to overcome the limitations encountered for derivatives **71** and **72**, we planned to introduce a triethylene glycol spacer between the ligand and the fluorophore. This should increase both water solubility and chemical stability, avoiding the liable α-oxy ester group.

For the preparation of this second set of derivatives we used Aβ ligand **67** (Scheme 3.8) that in our previous section showed the same binding properties of compound **65**, and a more straightforward preparation from commercially available reagents. Secondary hydroxyls were protected with an isopropylidene group (DMP, dry CH_3CN, CSA) and the free primary hydroxyl was reacted with triethylene derivative **83** (NaH, dry DMF), to afford intermediate compound **84**. Removal of the protecting group (*p*-TsOH, H_2O:CH_3CN [0.5:1.5 / (v:v)] afforded derivative **85** bearing an azido functionality at the end of the triethylene moiety. For the synthesis of compound **73** the azido group was reduced (H_2, Pd-Lindlar, MeOH) and the resulting amine **86** was coupled with coumarin derivative **77** (DIC, HBTU, DIPEA, dry DMF), while for the preparation of compound **74** the azido group was exploited in a chemoselective click cycloaddition reaction [$CuSO_4$•$5H_2O$, sodium ascorbate, *t*-BuOH:THF(1/1:v/v)] with the alkyne coumarin derivative **76**, obtained from **75** through propargylation of the phenolic OH group(Scheme 3.8). ^{1}H NMR spectrum of compound **74** shows the characteristic signal correspondig to the triazole proton H-10' at δ 8.26 ppm as a singlet, while ^{13}C NMR spectrum shows the characteristic lactone signal at δ 162.3 ppm. ^{19}F spectrum shows a singlet at δ -62.2 ppm.

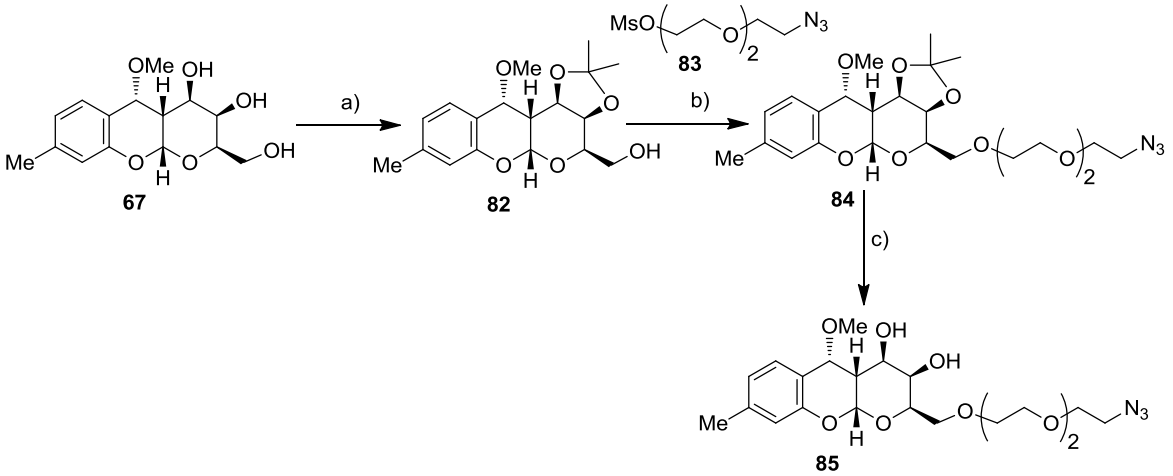

Scheme 3.8. *reagents and conditions:* a) DMP (4.0 equiv.), CSA (1% mmol), dry CH_3CN, rt, 1 h, 60%; b) **83** (2.0 equiv.), NaH 60% (1.5 equiv.), dry DMF, 100ºC, 12 h, 75%; c) *p*-TsOH (0.01 equiv.), H_2O:CH_3CN (0.5/1.5:v/v), rt, 30 min., 90%; ***(cont.)***

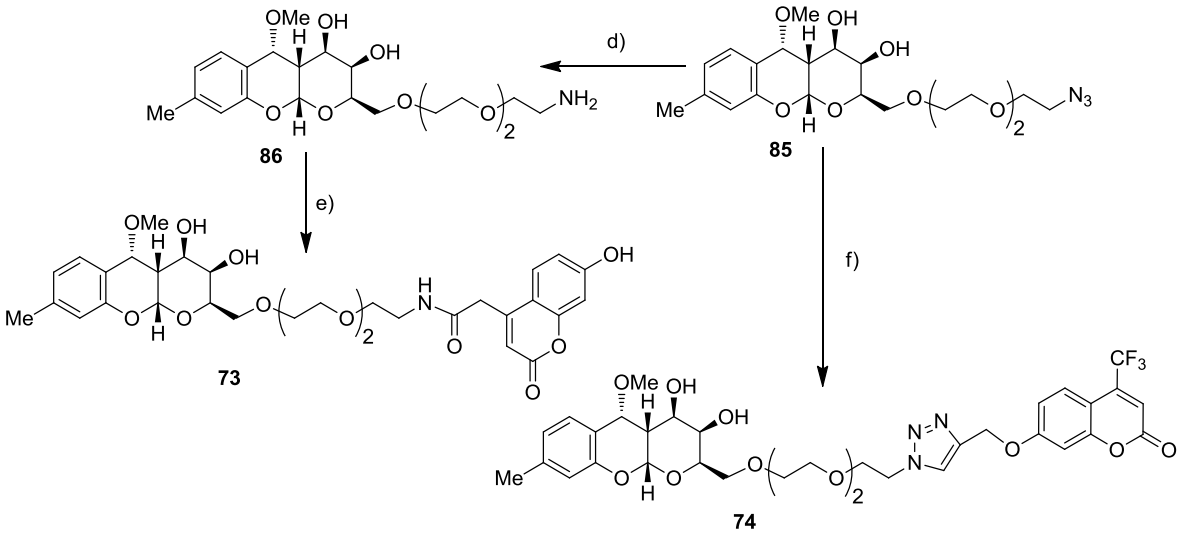

Scheme 3.8. ***(cont.)*** *reagents and conditions:* **d)** H_2, Pd-Lindlar, MeOH, r.t, 1 h, 90%; **e) 77** (1.2 equiv.), DIC (1.5 equiv.), HBTU (1.5 equiv.), DIPEA (3.0 equiv.), dry DMF, rt, 12 h, 20%; **f) 76** (1.2 equiv.), $CuSO_4.5H_2O$ (0.15 equiv.), sodium ascorbate (0.30 equiv.), *t*-BuOH:THF(1/1:v/v), rt, 12 h, 55%.

As expected, the solubility of compound **73** in water allowed to perform both STD and tr-NOESY NMR experiments to verify its ability to interact with Aβ oligomers. Both the techniques were applied on a sample containing Aβ(1-42) and compound **73** dissolved in deuterated PBS, pH=7.4, 25°C at the final concentrations of 80 µM and 0.5 mM respectively. Figure 3.14 reports the STD spectra recorded with five different saturation times (D 3 s; E 2 s; F 1.2 s; G 0.7 s; H 0.3 s).

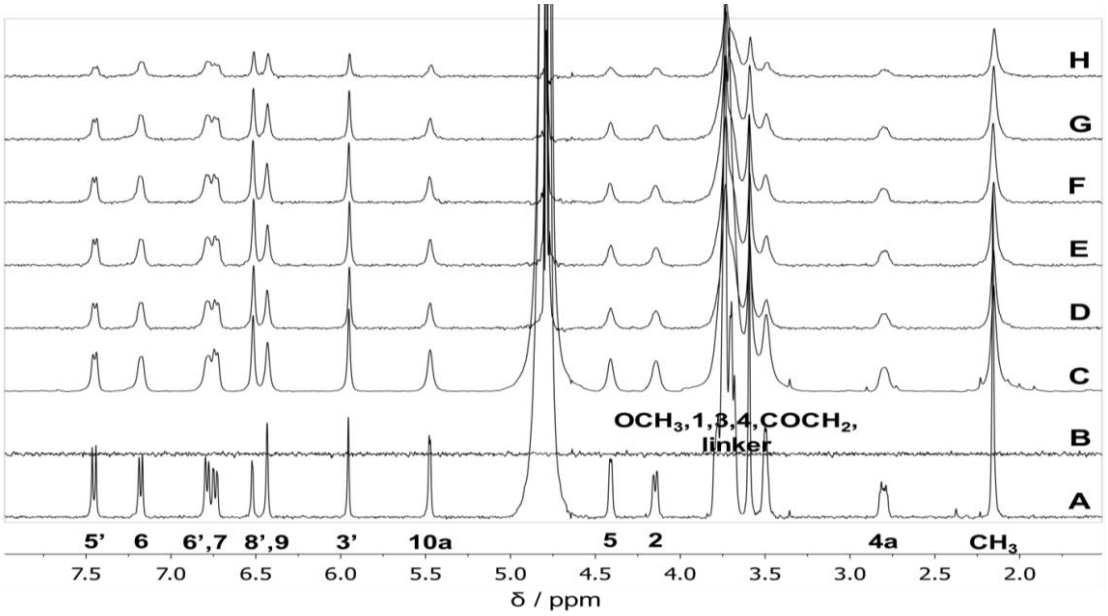

Figure 3.14: A) ^{1}H NMR spectrum of a solution of compound **73** (0.5 mM) in PBS; B) Blank STD-NMR spectrum of the same solution acquired with 3.0 s of saturation time; C) ^{1}H NMR spectrum of the mixture containing Aβ(1-42) (80 µM) and compound **73** (0.5 mM) in PBS, pH=7.5, 25°C; D-H STD-NMR spectra of the same mixture acquired with different saturation times. (D 3.0 s; E 2.0 s; F 1.2 s; G 0.7 s; H 0.3 s).

STD spectra clearly demonstrated compounds' **73** ability to recognize and bind Aβ oligomers. The existence of interaction was also supported by the broadening of molecule **73** resonances when the molecule was dissolved in the presence of the peptide (compare spectra A and C, Figure 3.14). This broadening reflects a decrease in proton relaxation times due to the formation of a receptor-ligand complex.

To map the ligand binding epitope, the STD spectrum acquired with a saturation time of 0.3 s was analysed in order to minimize the effect of relaxation on STD intensities.[89]

Figure 3.15 reports schematically the fractional STD effect for some ligand protons (or groups of protons), calculated as $(I_0 - I)/I_0*100$, where I is the intensity of the monitored signal in the STD spectrum and I_0 is the intensity of the same signal in a reference spectrum. The region of the ligand presenting the higher fractional STD effect (value around 40%), is the aromatic ring of the tricycle, thus resulting the ligand structural moiety mainly involved in the interaction with Aβ, in agreement with data obtained for the non-functionalized ligand.[90]

The coumarin moiety also participates to the interactions, but its contribution is less significant.

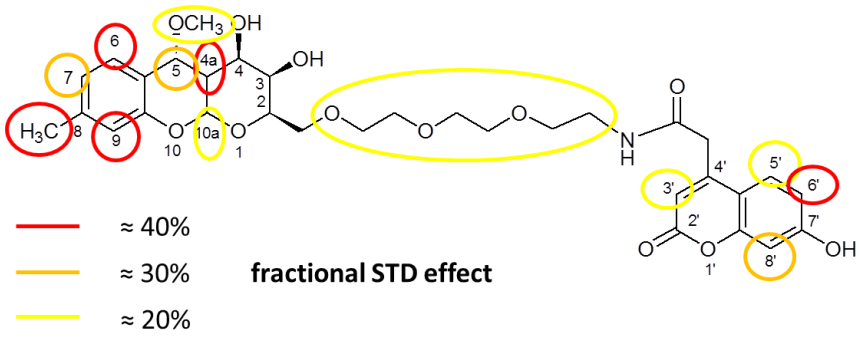

Figure 3.15: Fractional STD effects calculated for different protons of compounds **73**.

The binding was further assessed by tr-NOESY experiments. A blank NOESY spectrum of compound **73** was recorded in the absence of the Aβ(1-42) (Figure 3.16A). An inversion of the sign of the NOESY cross-peaks of the molecule was observed between both spectra, passing from positive (red color), in the absence of Aβ(1-42), to negative (blue color) in the presence of Aβ(1-42) (Figure 3.16B). This change is due to an increase of the effective

rotational motion correlation time of the molecule in the presence of the Aβ oligomers, that demonstrated the existence of a binding between the small molecule and Aβ aggregates.[91]

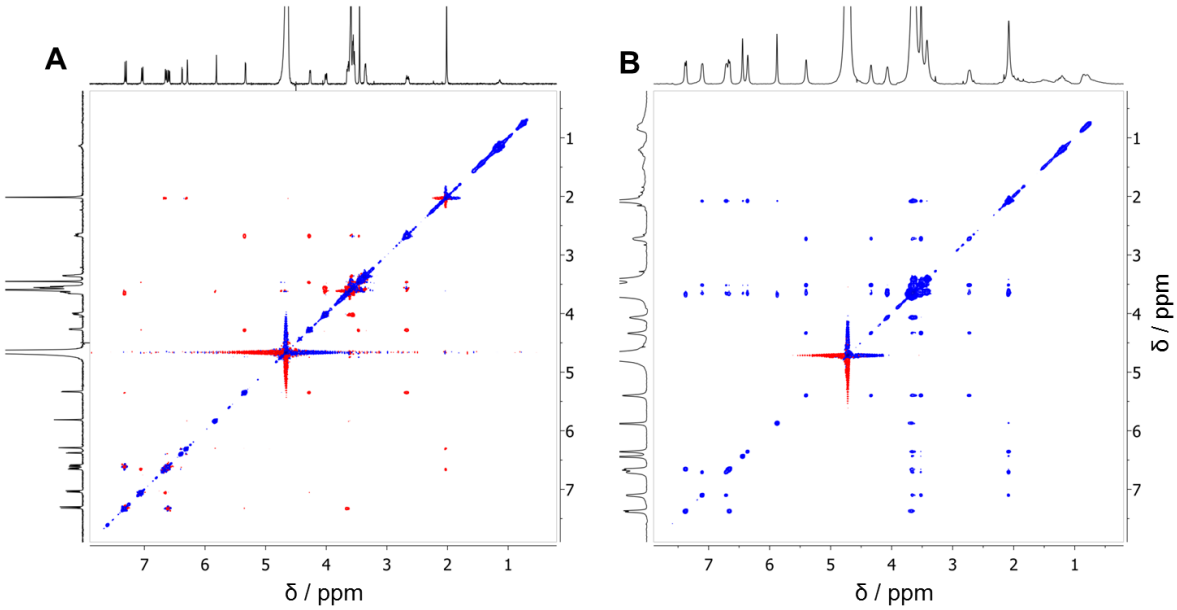

Figure 3.16: (A) 2D-NOESY spectrum of compound **73** dissolved in deuterated PBS, pH=7.5, 25°C, mixing time 0.9 s; (B) tr-NOESY of mixture containing Aβ(1-42) (80 µM) and compound **73** (0.5 mM) dissolved in deuterated PBS, pH=7.5, 25°C, mixing time 0.3 s. Positive cross-peaks are red, negative ones blue.

The solubility of compound **74** in aqueous buffer was very poor. In particular, NMR binding experiments were performed on a sample containing the test molecule at a concentration of 0.5 mM in PBS, pH=7.5, 25°C, to which 5% of d_6-DMSO was added to promote its dissolution. Aβ(1-42) was added at a final concentration of 80 µM. In these conditions we obtained an STD spectrum of low quality (Figure 3.17A-4), but sufficient to assess the existence of interaction with Aβ(1-42). The binding was further supported by the significant broadening of compound **74** ^{1}H Aβ(1-42) peptide (Figure 3.17A-3).

In addition, we could exploit the presence of the CF_3 substituent on the coumarin moiety, as a dramatic change also in its line width can be observed when the ^{19}F NMR spectrum of the molecule alone (Figure 3.17B-1) is compared with the corresponding spectrum acquired on the ligand:receptor mixture (Figure 3.17B-2).

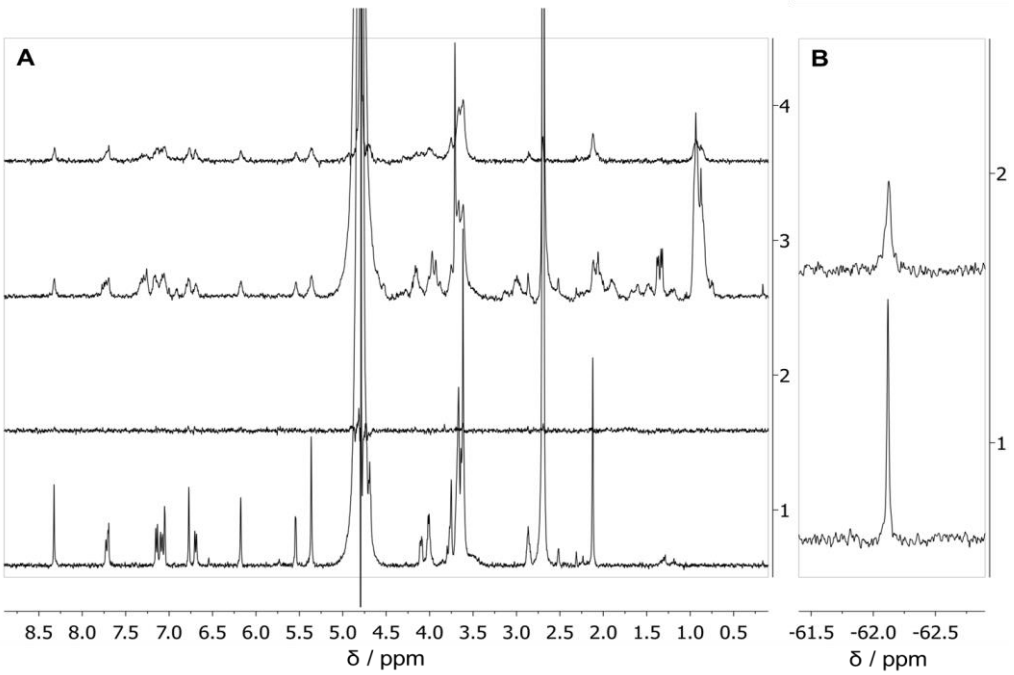

Figure 3.17: A-1) ^{1}H NMR spectrum of the compound **74** (0.5 mM); **A-2)** blank STD-NMR spectrum of compound **74** acquired with a saturation time of 2.0 s and 5200 scans; **A-3)** ^{1}H NMR spectrum of the mixture containing the peptide Aβ(1-42) (80 μM) and compound **74** (0.5 mM); **A-4)** STD-NMR spectrum acquired on the same mixture with a saturation time of 2.0 s and 5200 scans. **B)** ^{19}F NMR spectra of compound **74** dissolved in the absence (1) or in the presence (2) of Aβ oligomers. Samples were dissolved in PBS, pH=7.5, 25°C, adding 5% of d_6-DMSO.

3.1.3.2 Transport experiments to the brain: in vitro experiments

The ability to pass the BBB was evaluated using *in vitro* experiments with a BBB model, in collaboration with the Department of Experimental Medicine, University of Milano–Bicocca. Currently available *in vitro* models for BBB allow to evaluate quickly and in a reproducible way the predictive *in vivo* permeability of compounds and drugs under development.

The development of a cell culture system that mimics an *in vivo* BBB requires endothelial cells to be cultured on microporous supports. hCMEC/D3 cells (passages 25-35) were seeded on 12-well Transwell® inserts coated with type I collagen in a density of 5x104 cells/cm^2 and cultured with 0.5 mL and 1 mL of culture medium in the upper and in the lower chamber, respectively as previously described.[92]

Cells were treated with compound **73** when the trans-endothelial-electrical resistance (TEER) value was found to be the highest. The functional properties of monolayers were assessed by measuring the endothelial permeability of sucrose (between 0-180 min) as

described in literature.[89] 0.5 mL of 9.4 and 94 µM solution of compound **73** were added to the upper chamber and incubated between 0 and 180 min. After these periods of incubation, the fluorescence in the upper and lower chambers was measured (λex = 280 nm) to calculate the endothelial permeability (PE) across the cell monolayers, taking account of the passage of compound **73** through the filter without cells.[89] Each experiment was performed at least in triplicate. All the transport studies have been replicated in the presence of a paracellular marker [^{14}C]-sucrose, in order to monitor potential toxic effects on the BBB exhibited by compound **73**.

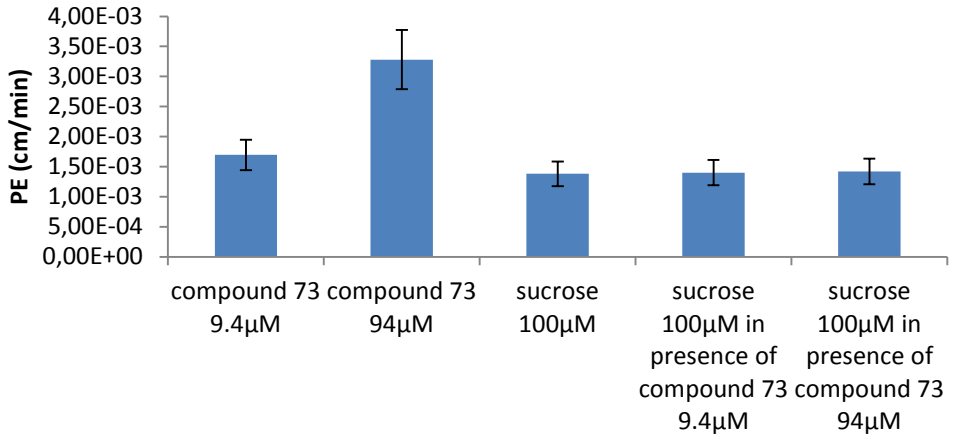

Figure 3.18: PE values of compound **73** 9.4 and 94 µM across the cell monolayers and PE values of sucrose 100 µM alone and in presence of compound **73**.

The Aβ ligand compound **73** does not affect the tightness of the hCMEC/D3 cell monolayer, since the TEER value and the permeability of [^{14}C]-sucrose did not change, within the experimental error (<3%), after hCMEC/D3 incubation with compound **73** (PE sucrose=1.38±0.1x10^{-3} cm/min and in presence of curcumin derivative, PE sucrose= 1.40±0.1x10^{-3} cm/min). hCMEC/D3 cells, grown on transwell membrane inserts, were incubated with fluorescent Aβ ligand compound **73** on day 12, when the maximal TEER value was registered (68±8 Ω·cm^2). Transport of [^{14}C]-sucrose was measured, with PE values of 1.38±0.2x10^{-3} cm/min in agreement with the values reported in literature.[93]

Different amounts of compound **73** were added in the upper compartment and amount in the lower compartment has been measured over time at 0, 60 and 180 min. The PE of fluorescent Aβ ligand compound **73** across the cell monolayers was 3.03±1.19x10^{-3} cm/min and 1.69±0.59x10^{-3} cm/min and these values are strictly correlated to the administered amount within the upper compartment respectively 94.0 µM vs

9.4 μM. The PE of compound **73** were closer of those of the transcellular marker propranolol, a reference point in term of lypophilic compound which can permeate the BBB.[93]

3.1.3.3 Staining

The ability of compound **73** to bind amyloid deposits was tested in brain sections from Tg CRND8 mice. This test was done in collaboration with Department of Molecular Biochemistry and Pharmacology, Mario Negri Institute for Pharmacological Research. Tg CRND8 mice carry a human APP with double mutations and accumulate Aβ deposits in brain parenchyma and at cerebrovascular level. Cryostatic sections of 20 μm were obtained from fresh tissue, mounted on gelatin coated microscope slides and used for a staining assay. Solutions of EtOH:H_2O 50:50 (v/v) of test compound were layered on tissue sections. Fluorescent sections were viewed using fluoromicroscope equipped with FITC and DAPI filters. ThT at 3 μM was used as a reference. The test compound **73** was able to label amyloid plaques and vascular walls at a concentration of 6 μM, obtaining a result comparable to thioflavin (ThT) staining. These results suggested that tested compound **73** is able to recognize the β-pleated sheet structure of amyloid fibrils similarly to ThT and without being involved in apecific binding to tissue preparations (Figure 3.19).

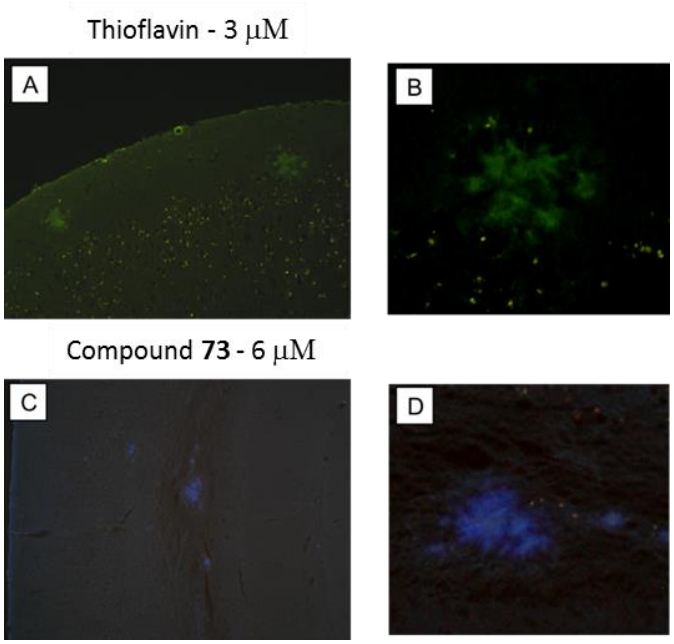

Figure 3.19: Brain sections of Tg CRND8 mice incubated with ThT (A-B) at 3 μM and compound **73** (C-D) at 6 μM. Fluorescent sections were viewed using fluoromicroscope FITC for ThT staining and DAPI for compound staining.

In conclusion, in this section we demonstrate through NMR experiments the preserved ability of derivatives **73** and **74** to bind Aβ, moreover, fluorescence mesurements carried out with compound **73** indicate that its favorable physical–chemical properties, in terms of balanced hydrophylicity/lipophylicity, allow these compounds to permeate through the BBB, most probably exploiting a diffusion mechanism, and to stain amyloid plaques. These properties, taken together, suggest that these compounds could be very promising candidates for possible future applications both in the therapy and in the diagnosis of AD.

3.1.3.4 Synthesis of a tricyclic derivative for the assembly of liposomes

As previously discussed, NPs represent a promising tool for the delivery of drugs and/or contrast agents, in particular, properly functionalised NPs may be used for the delivery to the brain. For this reason we planned to generate nanoliposomes functionalised with our Aβ ligands.

In order to fulfill the aim of this topic we designed and synthesised a derivative of the tricyclic product **65** bearing a PEG-cyclooctyne functionality (Scheme 3.9 and 3.10). The use of cyclooctyne has been recently reported by Bertozzi and co-workers.[94] The choice fell on the cyclooctyne moiety for two main reasons: firstly because the liposomes adopted in the project are properly functionalized with an azido group that will chemoselectively react with the alkyne, secondly because the tensioned cyclooctyne entity allows to carry out the reaction without the use of the Cu(I) catalyst, which renders the product purification very difficult.[95-97]

According to literature,[98] bicyclic compound **88** was synthesized from commercial available cycloheptene **87**. Silver perchlorate was then used to carry out the electrocyclic ring-opening of **88** to the *trans*-allylic cation, which was captured with tetraethylene glycol affording (*E*)-bromocyclooctene **89**. The ^{1}H NMR spectrum of **89** clearly shows a signal at 6.18 ppm characteristic of the vinylic proton. Cyclooctyne PEG **90** was obtained in dry *i*-PrOH at rt using *t*-BuOK as the base (Scheme 3.9). ^{13}C NMR spectrum of **90** shows the characteristic C≡C signals at 100.5 and 92.8 ppm. Mesylation of cyclooctyne PEG **90** with MsCl in dry CH_2Cl_2 followed by a substitution reaction with potassium thioacetate in dry

DMF afford thioester **92**, which was subject to reduction with $LiAlH_4$ affording the correspondent thiol **93** (Scheme 3.9).

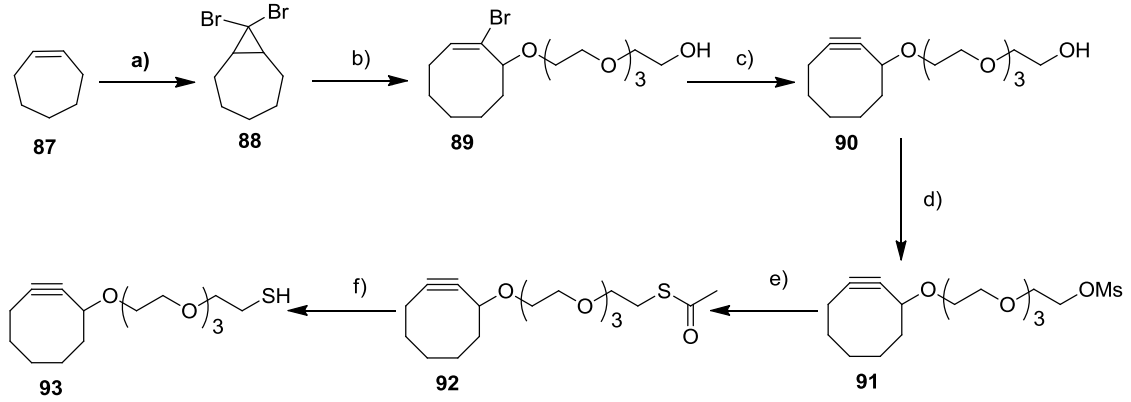

Scheme 3.9. *reagents and conditions:* a) $CHBr_3$ (1.0 equiv.), *t*-BuOK (1.15 equiv.), dry pentane, 0ºC, 6 h; b) tetraethylene glycol (30.0 equiv.) $AgClO_4$ (3.0 equiv.), dry toluene, dry pyridine, 4 h, reflux, 54% (2 steps); c) *t*-BuOK (2.5 equiv.), dry *i*-PrOH, 60 h, rt, 84%; d) MsCl (1.2 equiv.), Et_3N (1.5 equiv.), dry CH_2Cl_2, 0ºC-rt, 3 h; e) potassium thioacetate (2.1 equiv.), dry DMF, rt, 2h, 74% (over 2 steps); f) $LiAlH_4$ (5.0 equiv.), dry THF, 0ºC, 15 min.

Compound 65 was first selectively bromoacetylated[99] at the primary hydroxyl group, to give intermediate 78 (55 %). Treatment of the latter with the crude thiol 93 in dry DMF afforded compound 94 (77 %) (Scheme 3.10). The ^{1}H NMR spectrum of 94 shows a signal at δ 3.35 ppm corresponding to C=OC<u>H</u>$_2$S, while ^{13}C NMR spectrum of 94 shows the characteristic C≡C signals at δ 100.2 and δ 93.1 ppm, and the O<u>C</u>O signal at δ 170.6 ppm.

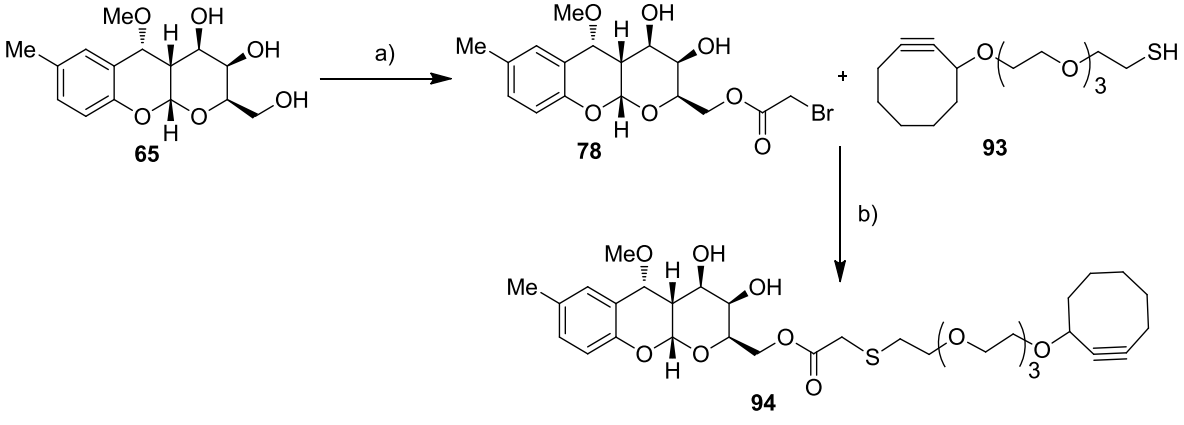

Scheme 3.10. *reagents and conditions:* a) bromoacetyl bromide (1.3 equiv.), *sym*-collidine (1.4 equiv.), dry DMF, -45ºC, 40 min., 55%; b) $CsCO_3$ (1.1 equiv.), thiol **93** (1.5 equiv.), rt, 40 min., 77%.

3.1.3.5 Generation of liposomes

In collaboration with Dr. S. Mourtas from the group of Professor S. Antimisiaris of the Laboratory of Pharmaceutical Technology, University of Patras, Greece (UPAT), functionalized liposomes were obtained by simply reacting the liposome bearing the azido-PEG-lipid **95** and the glycofused tricyclic-PEG-cyclooctyne derivative **94** in PBS buffer/DMSO.

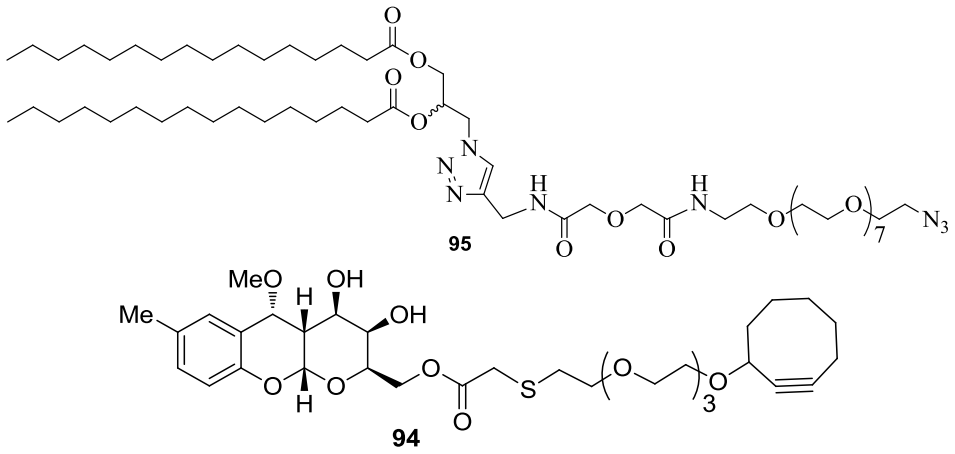

Figure 3.20: Azido-PEG-lipid and glycofused tryciclic-PEG-cyclooctyne.

Liposome preparation

The thin film method was used for multilamellar liposome (MLV-range from 500 to 10,000 nm) preparation. Probe sonication was used in order to prepare unilamellar small liposomes (SUV) approximately 50-100 nm. Calcein encapsulated liposomes were prepared in order to measure liposome integrity, control liposomes without **94** or **94** decorated liposomes. Liposome dispersions were purified from non-encapsulated calcein by column chromatography.

For the case of liposomes with lipid-peg-N_3 **95**, the latter was incorporated in liposome membrane in 5% and 20% (half of the azido groups should be on the outer surface of liposomes and half inside) during thin film formation. This means that final liposomes will have 2.5% or 10% of lipids with an azide group available to react with cyclooctyne moieties. It was found that reaction of **94** with SUV liposomes **96** (Scheme 3.11) results in moderate yields with available N_3-groups.

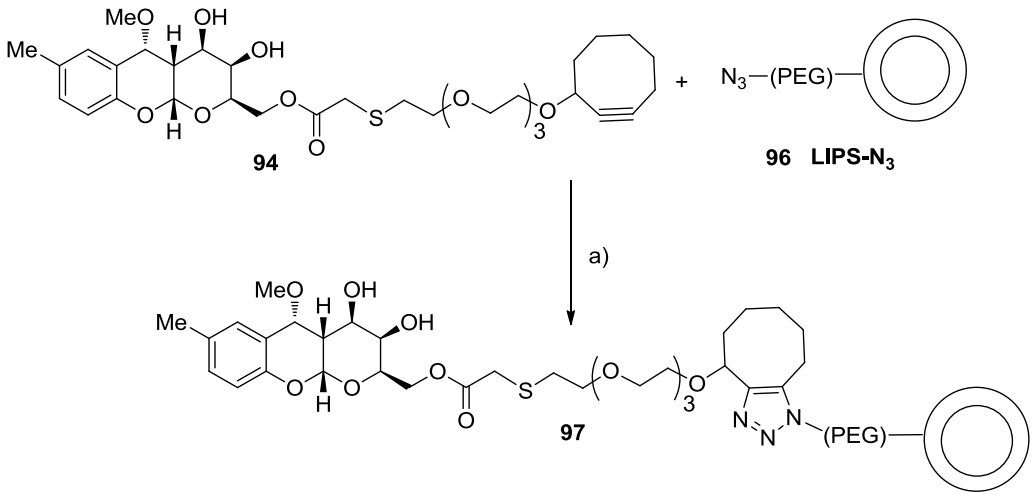

Scheme 3.11. *reagents and conditions:* a) PBS pH=7.4, 32ºC, 48h, 58%.

In this synthesis different reaction conditions, especially different lipid ratios were considered and the reaction was monitored at different times. The lipid concentration is measured by the Stewart method and shows the total lipid concentration of the prepared liposomes (Stewart method measures mostly phospholipids).

Time of reaction	Lipid concentration
6h	2.5 mg/mL
6h	10 mg/mL
24h	2.5 mg/mL
24h	10 mg/mL
48h	2.5 mg/mL
48h	10 mg/mL

The reaction product was identified using ESI-MS, while the liposome reaction efficiency was monitored using ^{1}H-NMR on decorated liposomes **97**. After purification by dialysis to remove all unreacted ligand, liposomes were dissolved in methanol and a selected peek integrated. In particular we were interested in evaluating the percentage of azido group reaction. To do this we identified a peek belonging to the azido linker which integration we set equal to 1, and quantified the reaction integrating the formation of the new peak, which was correlated to the proton signal from the glycofused tricyclic (Figure 3.21)

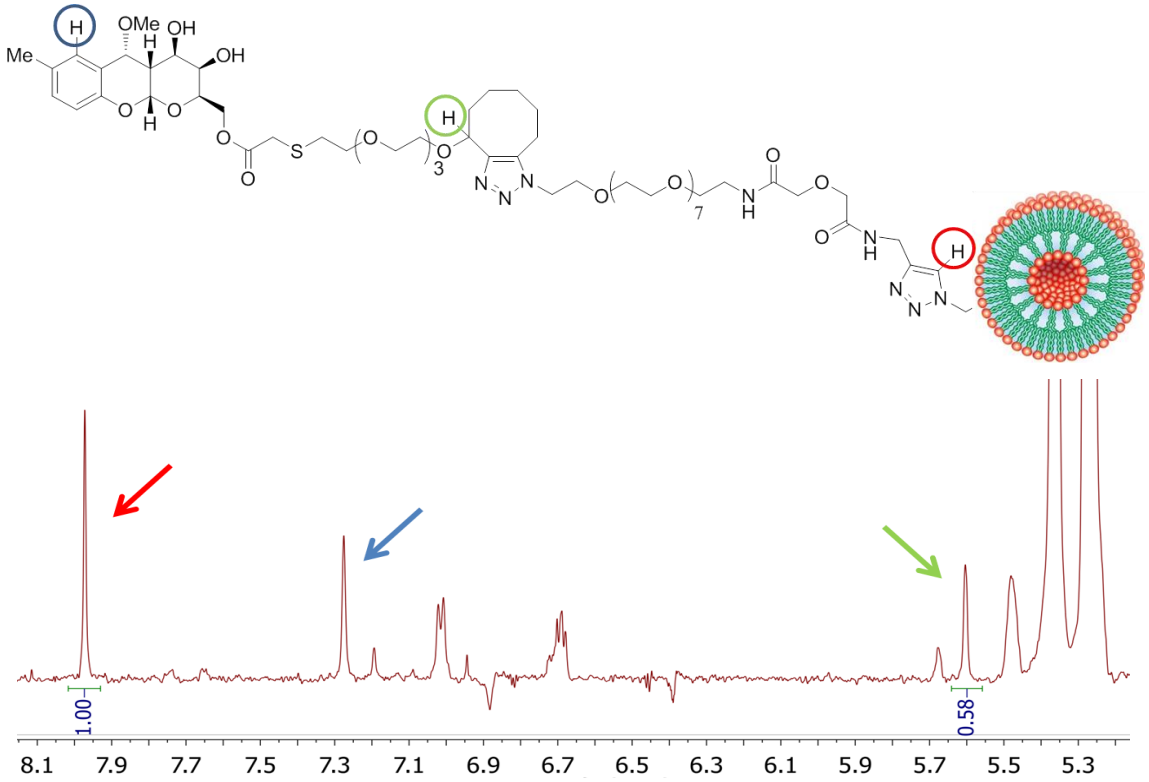

Figure 3.21: ^{1}H NMR **q**uantification of azido group reaction with glycofused tricyclic derivative **94**.

Best results correspond to 58% azido conversion at 48 h 10 mg/mL lipid concentration (Figure 3.22).

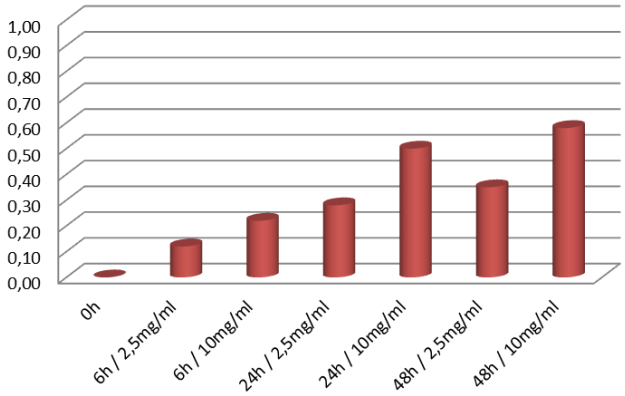

Figure 3.22: Quantification of azido group reaction with glycofused tricyclic derivative **94**..

Liposome compositions

(96 Before click reaction):
1,2-dipalmitoyl-sn-glycero-3-phosphocholine/Cholesterol DPPC/Chol (1:1)
Lipid-Peg1000-OMe (4 mol%)
Lipid-Peg-N_3 (5 mol%)

(97 After click reaction):
DPPC/Chol (1:1)
Lipid-Peg1000-OMe (4 mol%)
Lipid-Peg-N_3 ***96*** *(2.5 mol % not reacted)*
*Lipid-**97** (2.5 mol %)*

Liposome control:
DPPC/Chol (1:1)
Lipid-Peg1000-OMe (9 mol%)

Liposome characterization

Decorated (2.5%) liposomes **97** were characterized by dynamic light scattering (DLS) (Malvern Nano-ZS, Malvern Instrument, UK) at 25°C at 175° angle for size distribution, polydispersity index (PdI) and zeta-potential (Table 3.3). According to these findings, the mean diameter of the decorated (2.5%) liposomes **97** during storage at 4ºC was stable at least for a period of 7 days. Some evidence of liposome aggregation was seen after 16 days of storage (PdI≈0.35). However, bath sonication for a few minutes (1-5 min) of liposome **97**, leads to their complete disaggregation (PdI≈0.17).

Table 3.3: Characterization of decorated liposome **97** [DPPC/Chol (1:1) + 4% DSPE-PEG1000-OMe + 2,5% **95** + 2,5% **97**].

storage period (days)	Liposome treatment	Diameter (nm)	PdI	z-potential (mV)
0	-	153.9 ± 0.4	0.22	-2.64 ± 0.064
1	-	157.3 ± 1.8	0.31	-2.54 ± 0.044
7	-	148.8 ± 2.2	0.24	-2.37 ± 0.141
16	-	155.6 ± 1.8	0.35	-2.45 ± 0.021
21	sonication	127.12± 0.17	0.17	-2.52 ± 0.034

Calcein release from vesicles was used in order to measure SUV-liposome integrity. Thus liposomes **97** and the corresponding control liposomes (without **94**) were incubated in presence of serum proteins (at 37°C for 48 h). The results are presented in Figure 3.23.

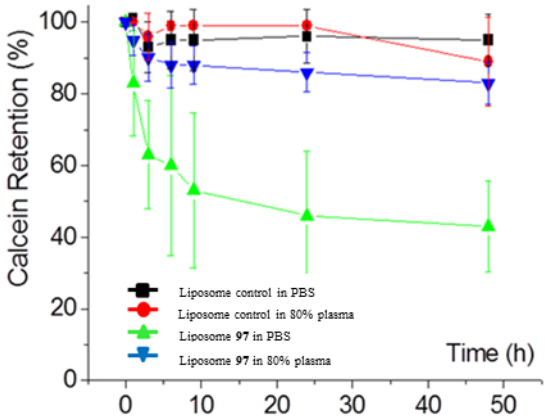

Figure 3.23: Liposome integrity.

As can be seen, although decorated liposomes **97** seem unstable during incubation at 37°C, these are very stable in presence of plasma proteins, even after 48 hours of incubation, indicating that these liposomes can be used for further *in vivo* experiments.

The use of DSPE-PEG2000-OMe instead of DSPE-PEG1000-OMe at the same percentage (8% in both cases), did not affect size stability even after prolonged storage according to the following results (Table 3.4).

Table 3.4: Characterization of decorated liposome **97** [DPPC/Chol (1:1) + 8% DSPE-PEG2000-OMe + 10% **95** + 10% **97**].

Storage period (days)	Liposome treatment	Diameter (nm)	PdI	z-potential (mV)
1	-	174.8 ± 0.07	0.199	-2.50 ± 0.034
8	-	178.7 ± 0.141	0.213	-1.71 ± 0.454
11	-	191.4 ± 1.202	0.268	-1.96 ± 0.134
15	sonication	204.6 ± 1.626	0.309	-1.78 ± 0.346

Some aggregation is seen at 15 days. Normally (like in Table 3.3) the liposomes will be disaggregated after a few probe sonication (1-5 min), but we will keep the experiment for 15 more days and then sonicate.

A novel, very simple method, was developed in order to covalently attach a tricyclic derivative **94** on liposome surfaces. Such attachment may increase the binding affinity for Aβ, due to multivalency, and/or allow the preparation of dual decorated NPs. The synthesized decorated nanoliposomes **97**, demonstrated high size stability at 4^{o}C and high integrity (retention of encapsulated calcein) at 37^{o}C in the presence of plasma proteins, revealing either possible interactions of decorated nanoliposome **97** with plasma serum proteins, preventing the usual action of plasma proteins on nanoliposomes, or approach difficulties of proteins on the decorated **97** nanoliposome surface.

3.1.3.6 Decorated liposomes NMR binding studies

Previously were described STD-NMR interactions studies on glyco fused tricyclic derivatives, with or whithout functionalization with a lipophilic entitie. The same methodology has been applied herein to check the effect of decorated lipsome **97** on the Aβ(1-42) oligomer recognition process. In particular, the interaction studies with the Aβ(1-42) were carried out using Water-Ligand Observed via Gradient Spectroscopy (Water-LOGSY) experiment. In a Water-LOGSY experiment, the NMR resonance of the water is selectively excited and the magnetization is allowed to be transferred by NOE to all other protons. The water magnetization is transferred by NOE to the protein and from there to the ligand (spin-diffusion). In this experiment, the resonances of non-binding compounds

appear with opposite sign and tend to be weaker than those of the interacting ligand. The ligand is used in very large excess over the protein so that the protein is not observable in the NMR spectrum.[100,101]

Water-LOGSY experiments were performed using ligand:peptide 20:1 mixtures dissolved in deuterated PBS, pH=7.4, 25°C. In the water-LOGSY experiments acquired in the presence of Aβ, was observed the presence of tricyclic aromatic signals, which are absent in the corresponding spectra of the lyposome preparation alone, meaning that there is interaction between the tricycle on the liposome surface and Aβ (Figure 3.25).

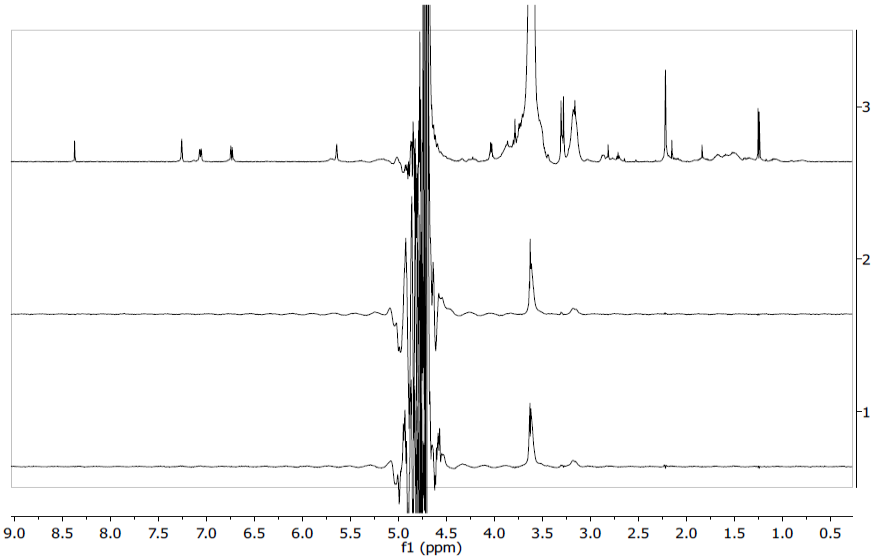

Figure 3.24: Decorated liposomes **97**, PBS, pH=7.4, 25ºC: ^{1}H NMR spectrum (3); water-LOGSY NMR spectrum with 1.2 s mixing time (2); water-LOGSY NMR spectrum with 1.6 s mixing time (1).

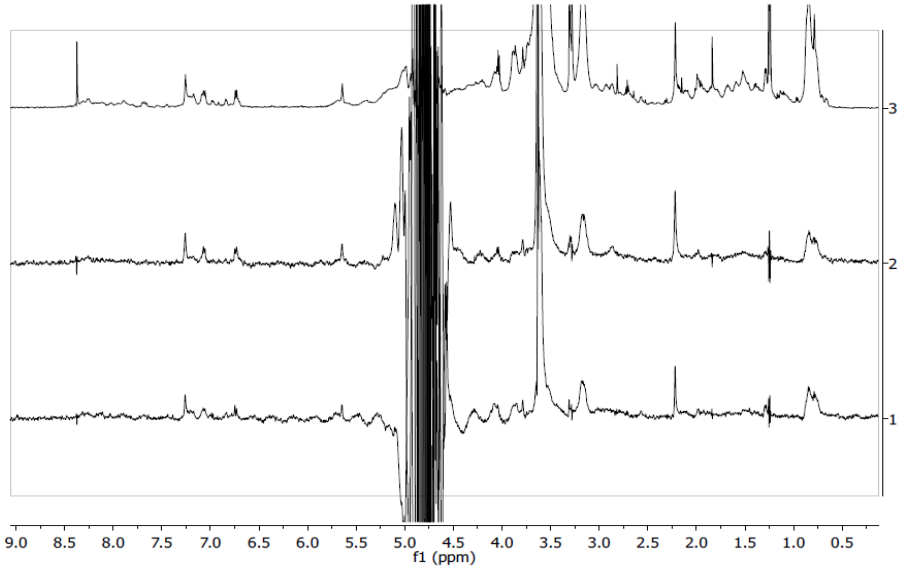

Figure 3.25: Aβ(1-42) 80 μM with decorated liposomes **97**, PBS, pH=7.4, 25ºC: ^{1}H NMR spectrum (3); water-LOGSY NMR spectrum with 1.2 s mixing time (2); water-LOGSY NMR spectrum with 1.6 s mixing time (1).

3.2. Synthesis of glycofused tetracyclic derivatives

The scope of this section is to develop synthetic procedures that will allow the generation of tetracyclic glucofused compounds. Many natural and synthetic compounds of biological interest bear a linear fused tetracyclic structure, part of which displays an aromatic character. Among them tetracyclines (TCs) and anthracyclines constitute two families of compounds that have found wide application in pharmaceutical field. Anthracyclines are glycoconjugated molecules that constitute a family of natural compounds in which the aglycon is characterized by a tetracyclic system with a skeleton of 7,8,9,10-tetrahydrotetracene-5,12-quinone, the anthracyclinone.[102,103,104] They differ in the aglycone and in a wide array of attached sugar residues. The high scientific and industrial interest in anthracyclines arise from their remarkable pharmaceutical properties. Their significant activity in the treatment of solid tumors, as well as acute mieloblastic leukemia, made them among the most widely used anticancer drugs and the most intensively studied natural products over the past 50 years.[103,105] TCs are a group of structurally related antibiotics, discovered in the late 1940s. The basic chemical structure, which characterizes in general all TCs is represented by the naphthacene carboxamide nucleus, composed of four linear fused hexamerous rings A, B, C and D. Chemical modifications of natural structures and synthesis of new compounds produced a number of novel tetracyclines, including minocycline and doxycycline, which are the more common semi-synthetic clinical antibiotics.[106] More recently the anti-amyloidogenic activity of TCs was described and curiously, these old class of antibiotics which was almost abandoned because of the development of resistant bacterial strains, are currently involved in more than 130 clinical trials, non-related to their antimicrobial activity.[106]

This section will center on the development of synthetic methods for the generation of glycofused linear tetracyclic systems, analogues of the upper mentioned tetracyclic compounds that may find similar pharmacological applications. The introduction of the glycofused moiety has the purpose to improve physical-chemical properties, allowing for example the modulation of the solubility characteristics, as well as to constitute a derivatisable moiety that may allow the conjugation of the compound to other entities (NPs, contrast agents, other drugs, etc.) for the generation of novel diagnostic and/or therapeutic tools.

In particular, as described in the previous sections, being particularly interested in the identification of novel Aβ ligands, this section will focus on the synthesis of small molecules with a heteroaromatic polycyclic structure which resemble TCs (Figure 3.26). These compounds maintain the aromatic feature which is present in a wide range of small molecules able to interact with Aβ and which seems to be crucial for the binding ability,[67,86] and at the same time, possess a glycofused entity which confers them ideal water solubility properties.

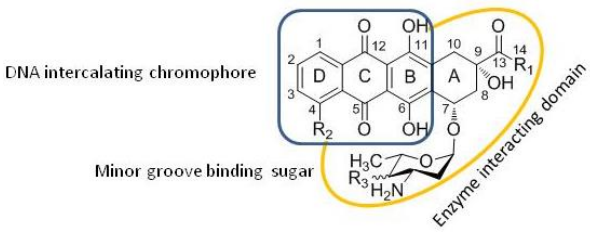

Anthracyclines

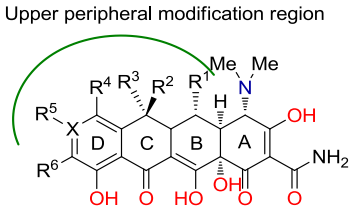

Tetracyclines

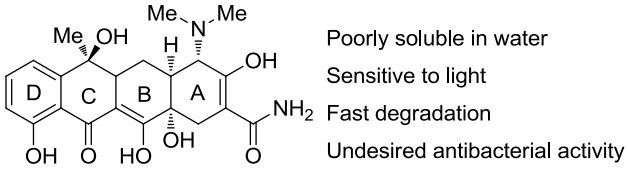

Tetracycline

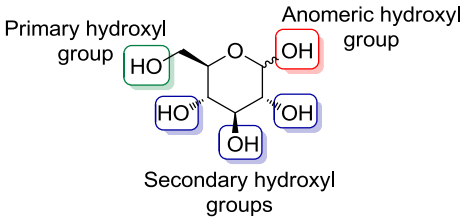

Carbohydrate moiety (e.g. D-Glucose)

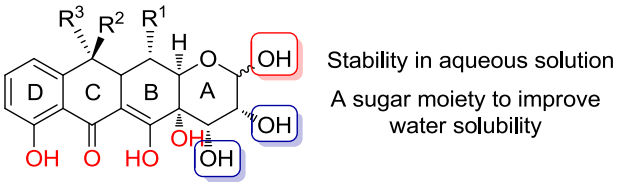

Figure 3.26: Glycofused tetracyclic structure.

The strategy it's aimed to obtain new tetracyclic glycofused compounds starting from new glycidic scaffolds (**6** and **10**) that could be used in a tandem Michael-Dieckmann reaction (Scheme 3.12).

- Synthesis of a new sugar scaffolds to be employed in tandem Michael-Dieckmann reactions or in DA reactions to synthesize new tetracyclic derivatives.

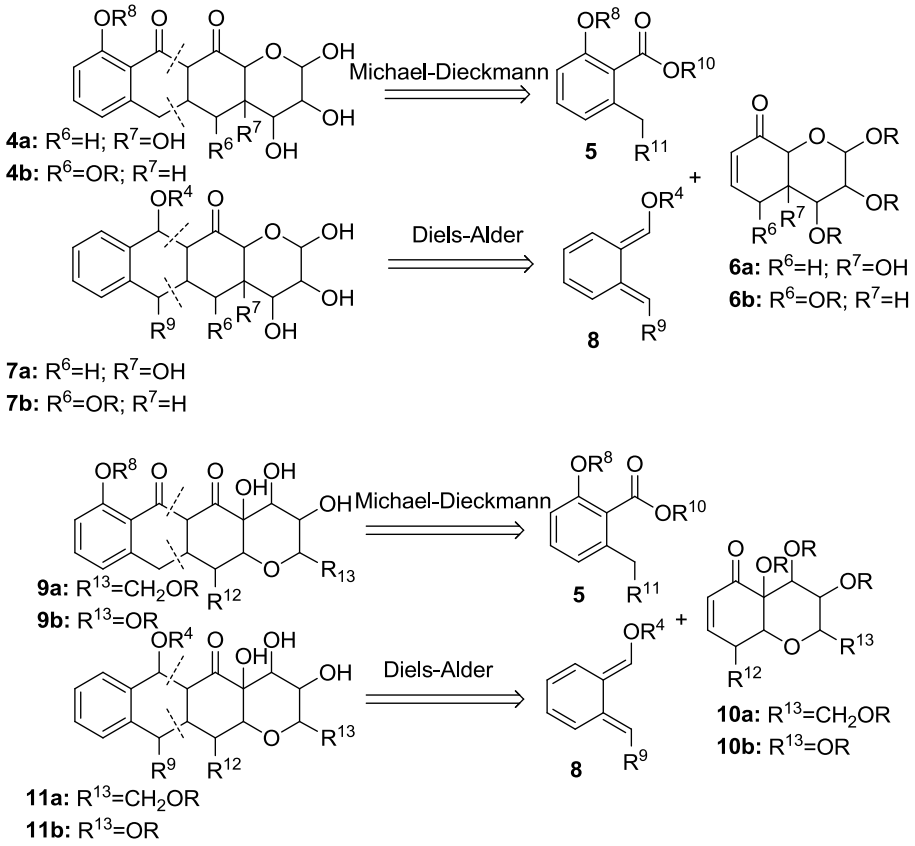

Scheme 3.12

3.2.1. Synthesis of the glycofused bicyclic scafffold 6a and 6b

The synthesis of a suitable Michael acceptor such as **6a** according to the retrosynthetic analysis is depicted in Scheme 3.13. Methyl α-D-glucopyranoside **98** is conveniently protected in position 4 and 6 as a *p*-methoxybenzylidene acetal **99**. Orthogonally protection of compound **99** with benzyl bromide and selective opening of the *p*-methoxybenzylidene affords compound **101**.[107] Swern oxidation of the free hydroxyl group of **101** leads to ketone **102**.[108] Alkylation with allyl magnesium bromide affords compound **103**, with a 60% yield (over 2 steps), the absolute configuration was determined by NMR experiments.

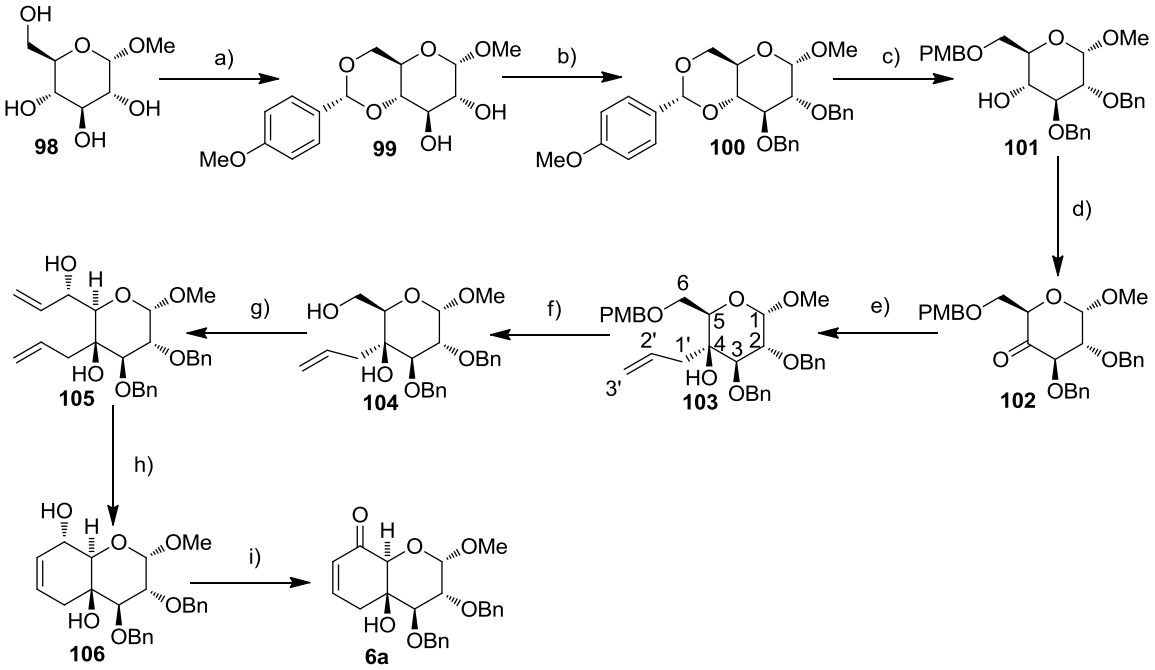

Scheme 3.13. *reagents and conditions:* a) anisaldehyde dimethylacetal (1.2 equiv.), CSA (0.01 equiv.), dry DMF, 60ºC, 2 h, 75%; b) BnBr (3.0 equiv.), NaH (3.0 equiv.), dry DMF, rt, 1 h, 96%; c) $NaCNBH_3$ (5.0 equiv.), TFA (10.0 equiv.), 3Å MS, dry DMF, rt, 12 h, 87%; d) $(COCl)_2$ (4.0 equiv.), dry DMSO (8.0 equiv.), dry Et_3N (10.0 equiv.), -78ºC, 2 h; e) allylmagnesium bromide 1M Et_2O (3.0 equiv.), dry THF, -78ºC, 3 h, 60% (over 2 steps); f) CAN (5.0 equiv.), H_2O, CH_3CN, rt, 20 min., 72%; g) i. $(COCl)_2$ (4.0 equiv.), dry DMSO (8.0 equiv.), dry Et_3N (10.0 equiv.), -78ºC, 2 h; ii. vinylmagnesium bromide 1M THF (12.0 equiv.), dry THF,-78ºC, 4 h, 45% (over two steps); h) Hoveyda-Grubbs catalyst 2nd generation (5% weight), dry CH_2Cl_2, 40ºC, 1 h, 89%; i) MnO_2 activated (7.0 equiv.), EtOAc, reflux, 2 h, 91%.

^{1}H NMR spectrum of compound **103** (Figure 3.27) clearly shows a signal between δ 5.84 - 5.57 ppm characteristic of the allylic proton H-2', which couples with H-3' at δ 4.86 ppm, and H-1a' and H-1b' at δ 2.66 and δ 2.34 ppm, corresponding all of them to the allylic system. H-1 signal appears at δ 4.75 ppm as a doublet with J = 3.4 Hz, indicating that H-1 being couple only with H-2. From 2D-COSY, H-2 couples with H-3 at δ 4.00 ppm.

The 2D-NOESY spectrum of compound **103** is shown in Figure 3.28, where a weak NOE effect can be observed between H-3 and H-1', and absence of a NOE effect between H-2 and H-1'.

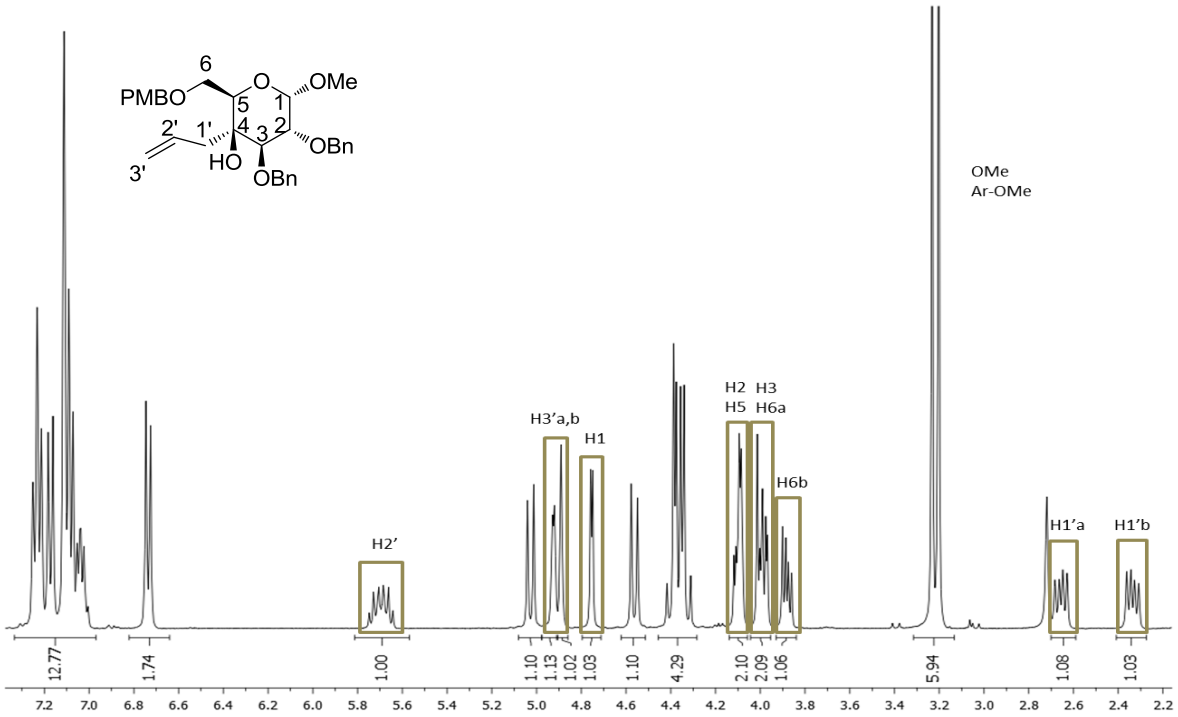

Figure 3.27: ^{1}H NMR spectrum (400 MHz, $CDCl_3$) of compound **103**.

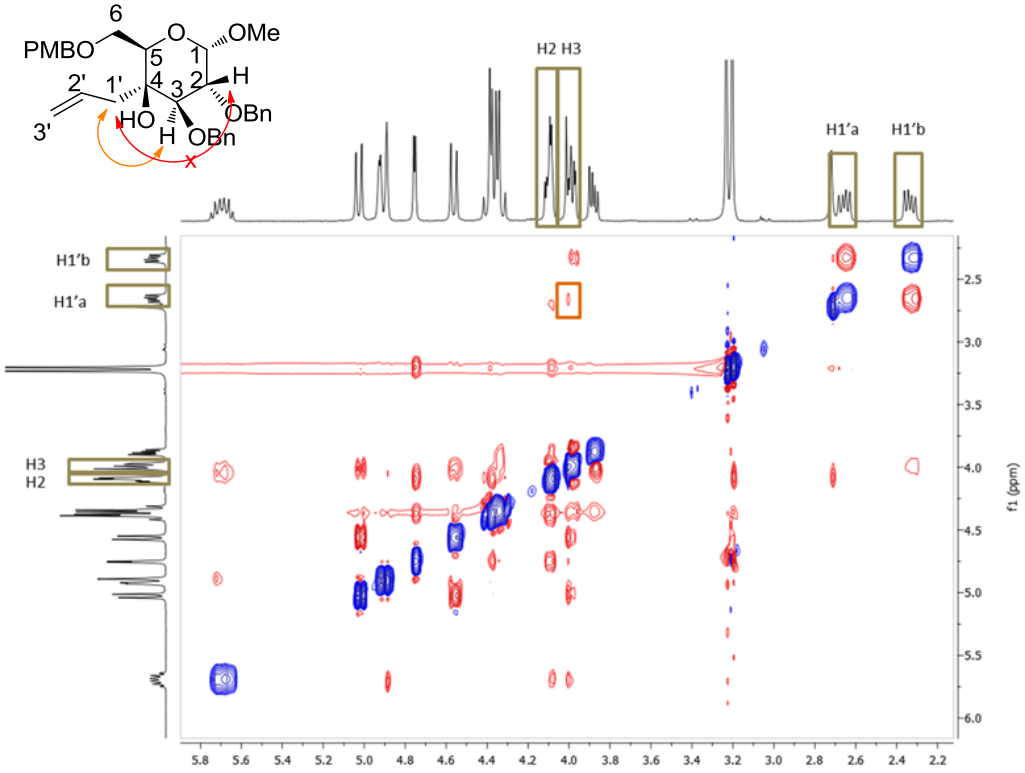

Figure 3.28: 2D-NOESY spectrum (400 MHz, $CDCl_3$) of compound **103**.

The stereoselectivity of this reaction can be ascribed to the formation of a Cram chelated intermediate in which the magnesium ion coordinates the carbonyl group and the benzylic oxygen. This has been explained for similar systems by chelation of the magnesium atom of the Grignard reagent with the C-4 carbonyl oxygen and the C-3 oxygen atom. The chelated oxo sugar assumes a $^4C_1$ conformation (Figure 3.29), and equatorial attack of the nucleophile dominates over the sterically hindered axial attack.[109]

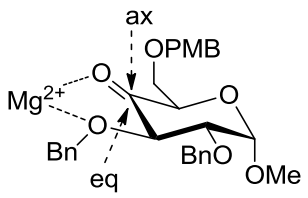

Figure 3.29: Cram chelate model for compound **102**.

Compound **104** was obtained by selective deprotection of primary hydroxyl group of **103** using cerium (IV) ammonium nitrate (CAN).[110] Swern oxidation of the alcohol **104** led to the formation of an aldehyde, which upon treatment with vinylmagnesium bromide in THF at -78°C afforded allylic alcohol **105** as a single diastereomer, which could be isolated in 45% yield (over 2 steps). Ring closing metathesis (RCM) of diene **105** using Hoveyda-Grubbs catalyst 2nd generation afforded compound **106**. The ^{1}H NMR spectrum of the bicyclic product **106**, isolated in 89% yield, was used to establish the stereochemistry of the new chiral center formed in the Grignard reaction used to produce **105**. The observation of a vicinal coupling between H-7 and H-7a (J = 8.5 Hz), confirmed the antiperiplanar orientation of these two protons. Finally oxidation of allylic alchohol **106** affords α,β-unsaturated ketone **6a** in 91% yield. ^{13}C NMR spectrum of **6a** shows the characteristic C=O signal at δ 193.6 ppm.

^{1}H NMR spectrum of compound **106** (Figure 3.30) shows a doublet for proton H-7a at δ 3.61 ppm with a J = 8.5Hz, due to the coupling with H-7 and indicating their *trans*-diaxial relationship. Proton H-3 appear at δ 3.71 ppm as a doublet with a J = 9.5 Hz, indicating the expected *trans*-diaxial orientation with respect to H-2. The signal corresponding to H-2 appear at δ 3.92 ppm as a double doublet with J = 9.5, 3.5 Hz. The presence of only two olefinic protons H-6 and H-5 between δ 5.70 - 5.58 ppm confirmed the formation of the expected cyclized product. The allylic protons H-4appear at δ 2.38 and 2.08 ppm respectively

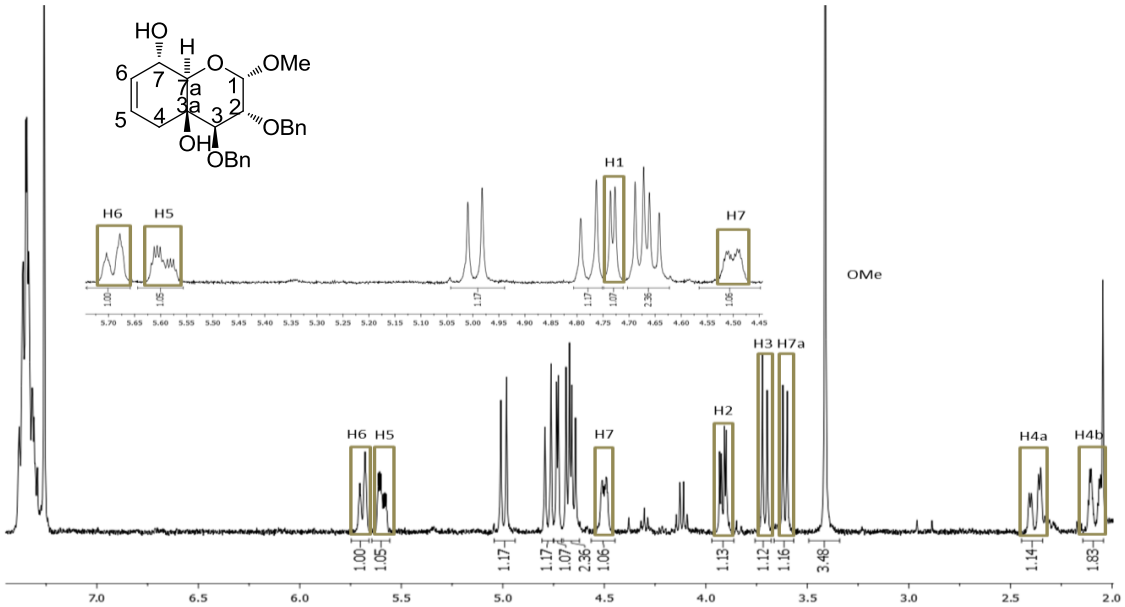

Figure 3.30: ^{1}H NMR spectrum (400 MHz, $CDCl_3$) of compound **106.**

The synthesis of compound **6b** (Scheme 3.14) took advantage of the already know aldehyde **110** that was prepared from the known ketone **102** via a sliglithly modified literature procedure. This transformation requires Wittig methylenation of **102** to give olefin **107** and hydroboration using BH_3•Me_2S to afford a separable mixture in 4:3 ratio, corresponding to the boron placed on the less substituted carbon and the other bearing the boron atom placed on the more substituted carbon. A more hindred borane like 9-BBN, which could favourable the formation of the desired product was tried; unfortunately 9-BBN didn't react with olefin **107**. This could be due to steric hindrance of the substrate. The resulting alkylborane was treated with hydrogen peroxide in the second step. This process replaces the B-C bonds with HO-C bonds, affording compound **108** in 49% yield. Oxidation of compound **108** affords the corresponding aldehyde **110** in 98% yield, which upon treatment with vinylmagnesium bromide in THF at -78°C afforded alcohol **111** as single diastereomer, which could be isolated in 84% yield.

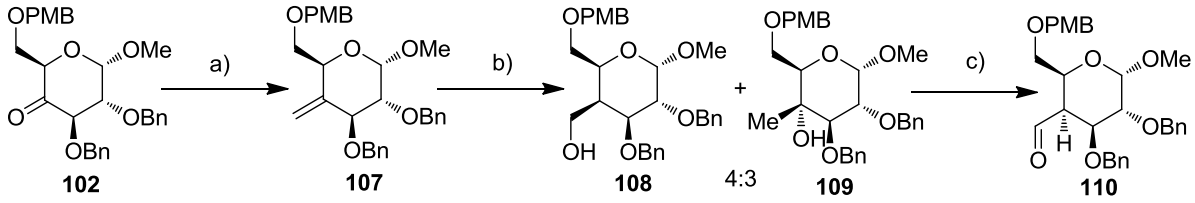

Scheme 3.14. *reagents and conditions:* a) methyl phenylphosphonium bromide (7.0 equiv.), BuLi (6.5 equiv.), dry THF, -78ºC, 12 h, 80%; b) BH_3•Me_2S (1.25 equiv.), NaOH, H_2O_2 30%, dry THF, rt, 12 h, 49%; c) $(COCl)_2$ (4.0 equiv.), dry DMSO (8.0 equiv.), dry Et_3N (10.0 equiv.), dry CH_2Cl_2, -78ºC, 2 h, 98%; ***(cont.)***

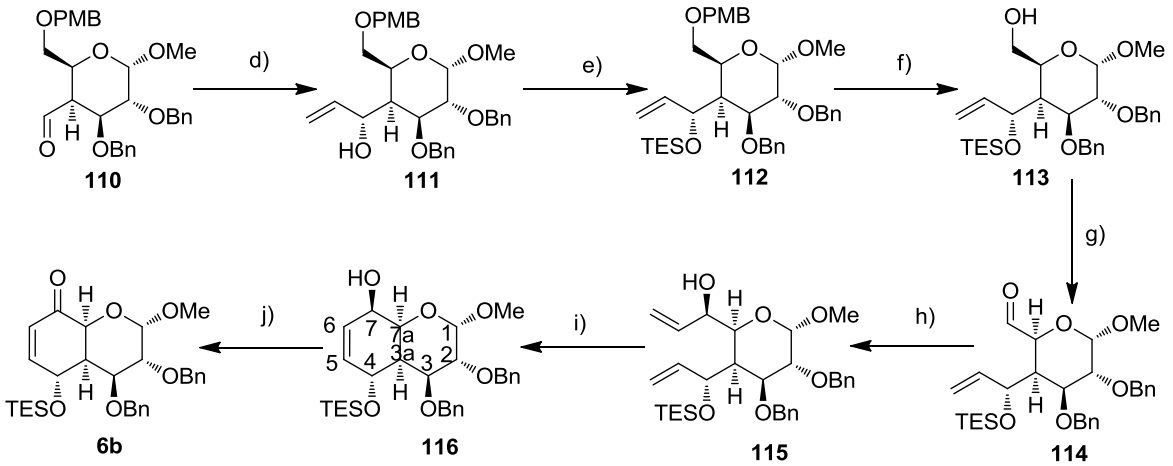

Scheme 3.14. ***(cont.)*** *reagents and conditions:* d) vinylmagnesium bromide 1M THF (2.5 equiv.), dry THF, -78ºC, 90 min., 84%; e) TESCl (1.5 equiv.), imidazole (2.0 equiv.), dry DMF, 60ºC, 1 h, 85%; f) DDQ (1.4 equiv.), CH_2Cl_2/H_20 (20:1), 0ºC, 3 h, 87%; g) $(COCl)_2$ (4.0 equiv.), dry DMSO (8.0 equiv.), dry Et_3N (10.0 equiv.), dry CH_2Cl_2, -78ºC, 2 h; h) vinylmagnesium bromide 1M THF (2.5 equiv.), dry THF, -78ºC, 90 min., 69% (over 2 steps); i) Hoveyda-Grubbs catalyst 2nd generation (5% weight), dry CH_2Cl_2, 40ºC, 2 h, 84%; j) MnO_2 activated (7.0 equiv.), EtOAc, reflux, 2 h, 70%.

Protection of the allyl alcohol **111** with TESCl followed by selectively removal of *p*-methoxybenzyl protection group using 2,3-dichloro-5,6-dicyano-1,4-benzoquinone (DDQ), results in primary alcohol **113** that was then smoothly oxidized under Swern conditions leading to aldehyde **114**. Treatment of **114** with vinylmagnesium bromide gave rise to the allylic alcohol **115**, as a single diastereomer, in 69% (over 2 steps) yield. RCM of diene **115** using Hoveyda-Grubbs catalyst 2nd generation afforded compound **116**, isolated in 84% yield, that was oxidized with MnO_2 to give de desired product **6b** in 70% yield.

The ^{1}H NMR spectrum (Figure 3.31) of the bicyclic product **116** and the corresponding 2D-NOESY (Figure 3.32) were used to establish the stereochemistry of the new stereocenters formed in the Grignard reactions used to produce **111** and **115**. The observation of a small vicinal coupling in ^{1}H NMR between H-7 and H-7a confirmed the *cis* orientation of these two protons.

The double doublet corresponding to proton H-2 at δ 3.71 ppm (J = 9.1, 3.7 Hz) has a NOE cross-peak found in the 2D-NOESY experiment with a double doublet matching to proton H-4 at δ 4.39 ppm (J = 6.3 Hz), which allow to determining the right stereochemistry of that assymetric carbon as being the one depicted in Figure 3.31. Another evidence is the absence of cross-peaks between proton H-4 and proton H-3 δ 3.94 ppm.

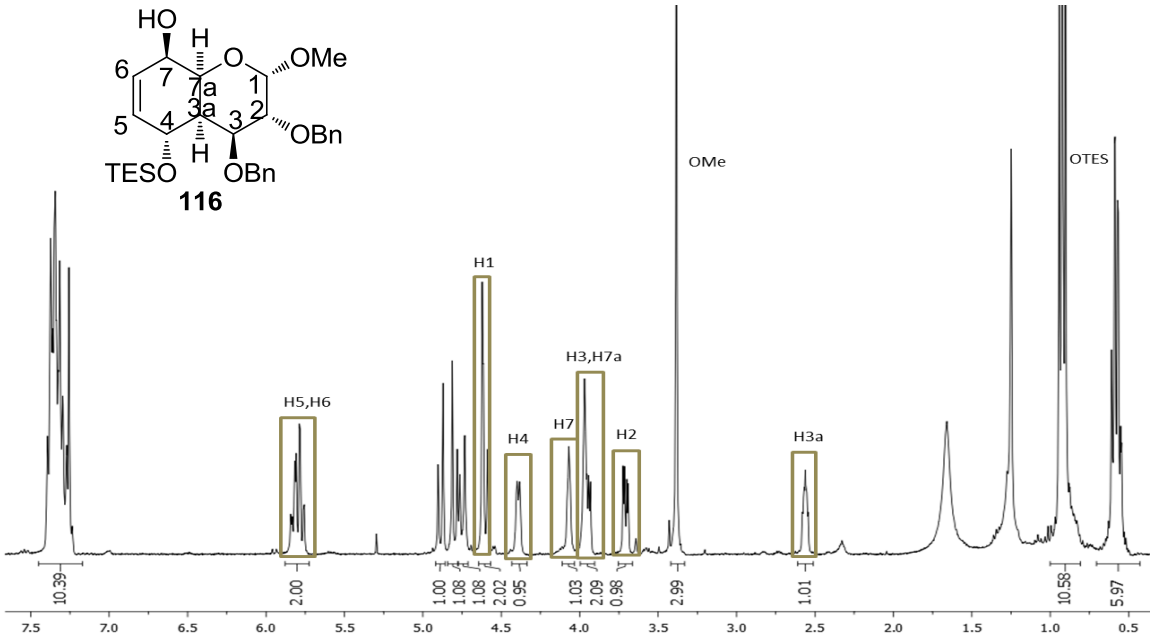

Figure 3.31: ^{1}H NMR spectrum (400 MHz, $CDCl_3$), T=19ºC, of compound **116**.

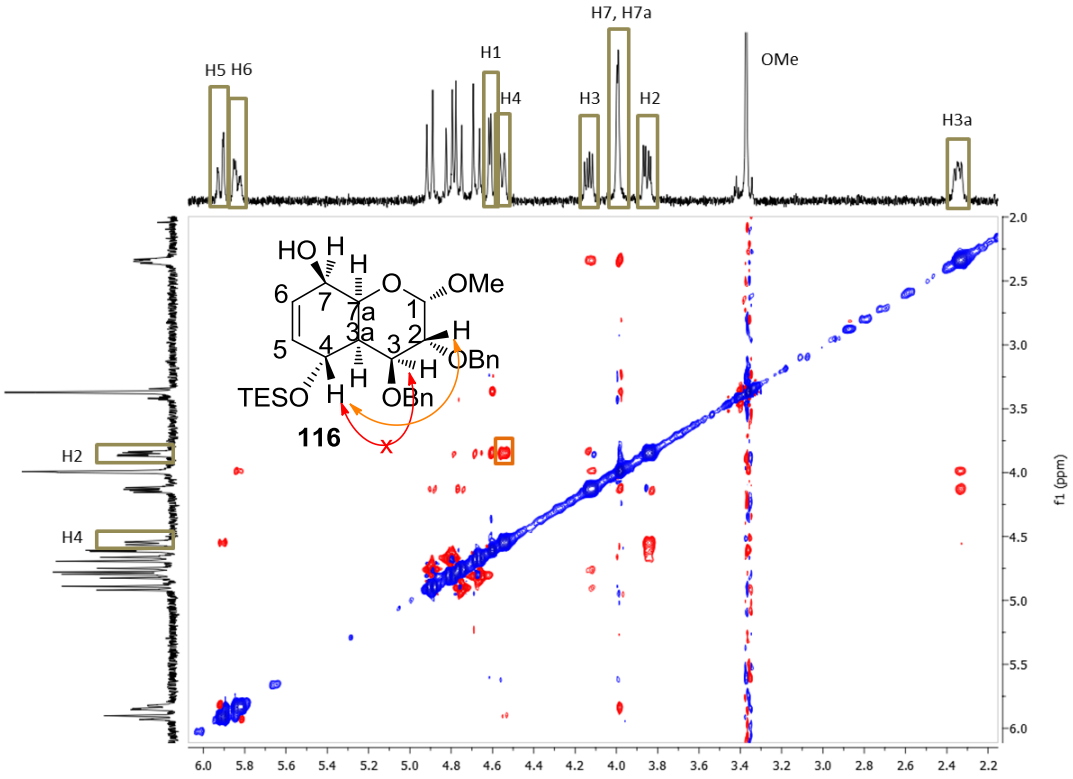

Figure 3.32: 2D-NOESY spectrum (400 MHz, $CDCl_3$), T=25ºC, of compound **116.**

3.2.2. Synthesis of glycofused bicyclic scafffold 10a and 10b

The synthesis of scaffold **10a** starts from α-allyl-*C*-glucoside **117** which can be easily obtained by a Sakurai reaction[111] from methyl α-D-glucopyranoside **98**. Benzylation of **117**, followed by selective debenzilation of C-2 hydroxyl group using a well established iodocyclization reaction followed by reductive elimination (I_2, then Zn and AcOH) afforded derivative **120**.[112] This selective deprotection was exploited for the introduction of a second double bond (Scheme 3.15). Oxidation of alcohol **120** afforded the corresponding ketone **121**, which was subject to a Grignard reaction with allylmagnesium bromide in toluene:CH_2Cl_2 (2:1)[113] affording a separable mixture of tertiary alchohols **122a** and **122b** (68:32 ratio, 85%), in favor of the D-manno configured isomer **122a**, (the absolute configuration was determined by NMR experiments). RCM of **122a** using a second-generation Grubb's catalyst (5% weight) at 40°C in CH_2Cl_2 afforded the expected cyclized product **123** in 88% yield. The presence of only two olefinic protons at δ 5.53 ppm and δ 5.49 ppm as two broad singlets for these two protons in its ^{1}H NMR spectrum confirmed the formation of the expected cyclized product. Debenzylation of **123** with BCl_3 at -78ºC in CH_2Cl_2 produce bicyclic product **124**, which was then acetylated affording compound **125** in 80% yield. Allylic oxidation of **125** was achieved using commercially available manganese(III) acetate dihydrate as the catalyst and TBHP as the cooxidant at room temperature.[114] 3Å molecular sieves were added to remove the trace amount of water. After 48 h the α,β-unsaturated compound **10a** was obtained in 52% yield. ^{13}C NMR spectrum of **10a** shows the characteristic C=O signal at δ 196.4 ppm.

The major diene **122a** has the allyl group at C-2 equatorially oriented. Its ^{1}H NMR spectrum showed a clean doublet at δ 3.60 with J = 7.8 Hz, indicating that proton H-3 couples only with H-4 and thus must be *trans*-diaxial to each other. Proton H-1a'' appeared as a double doublet at δ 2.74 ppm with J = 14.6, 5.6 Hz, and proton H-2'' appeared as a multiplet at δ 6.12–5.68 ppm. The 2D-NOESY spectrum for the derivative **122a** (Figure 3.33) showed a cross-peak between H-3 and H-1a'', H-1b'', and of H-1a' and H-1b'. Also evident is the absence of a cross-peak between proton H-4 and protons H-1a'' and H-1b''. Likewise, the structure of the minor compound **122b** was established on the basis of its spectral data.

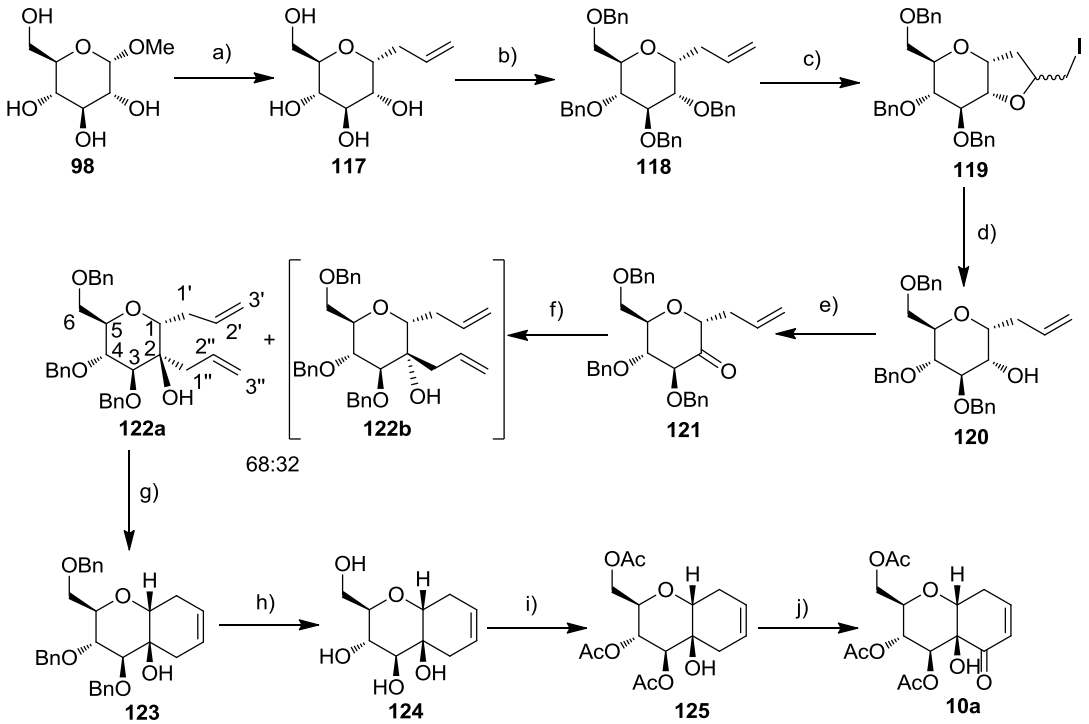

Scheme 3.15. *reagents and conditions:* a) BTSTFA (3.0 equiv.), $AllSi(CH_3)_3$ (2.0 equiv.), TMSOTf (0.5 equiv.), dry CH_3CN, 60ºC–rt, 12 h, 75%; b) BnBr (5.0 equiv.), NaH 60% (5.0 equiv.), dry DMF, rt, 12 h, 80%; c) I_2 (5.0 equiv.), dry CH_2Cl_2, rt, 90 min.; d) Zn (10.0 equiv.), AcOH glacial (2.0 equiv.), Et_2O:MeOH (1:1), 3 h, rt, 74% (over 2 steps); e) $(COCl)_2$ (4.0 equiv.), dry DMSO (8.0 equiv.), dry Et_3N (10.0 equiv.), dry CH_2Cl_2, -78ºC, 2 h, 89%; f) allylmagnesium bromide 1M Et_2O (2.5 equiv.), dry toluene:CH_2Cl_2 (2:1), -78ºC, 3 h, 85%; g) Hoveyda-Grubbs catalyst 2nd generation (5% weight), dry CH_2Cl_2, 40ºC, 90 min., 88%; h) BCl_3 (12.0 equiv.), dry CH_2Cl_2, -78ºC–rt, 12 h, 71%; i) Ac_2O (10.0 equiv.), DMAP (cat.), dry Py, rt, 80%; j) *t*-BuOOH 6.0M decane (5.2 equiv.), $Mn_3(OAc)_9 \cdot 2H_2O$ (0.1 equiv.), 3Å MS, dry EtOAc, 48 h, 52%.

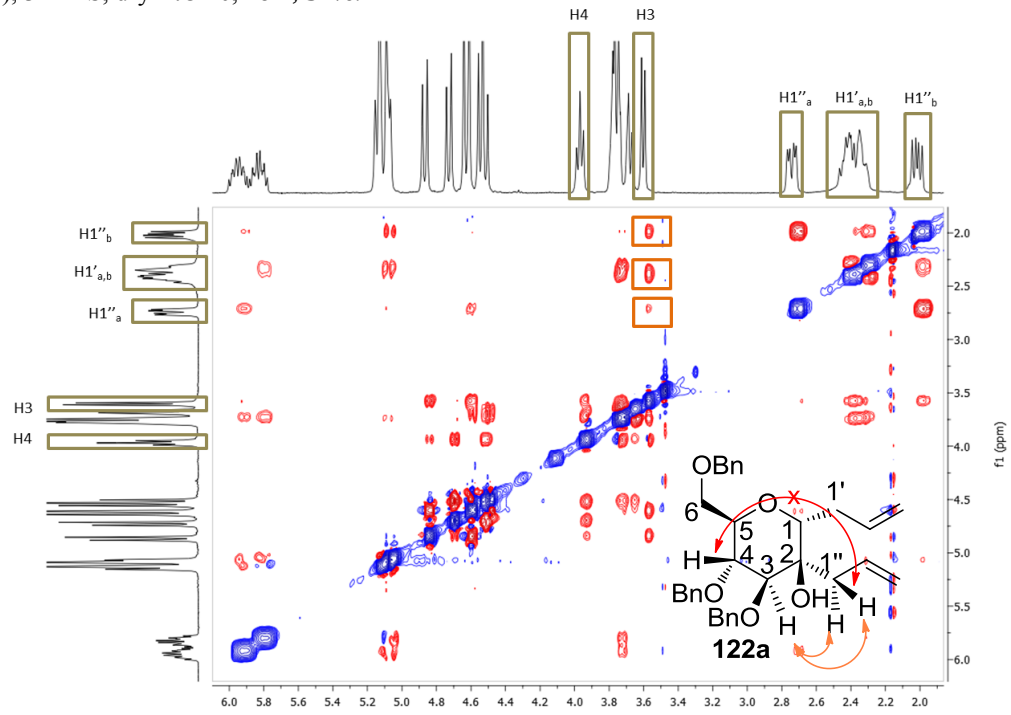

Figure 3.33: 2D-NOESY (400 MHz, $CDCl_3$) of compound **122a**.

For the synthesis of Michael acceptor **10b** (Scheme 3.16), *O*-methyl-α-D-glucopyranoside was transformed into compound **107** according to know procedures.[115] Dihydroxylation of **107** with OsO_4/*N*-methylmorpholine *N*-oxide (NMO) led exclusively to α-face attack furnishing derivative **126.**[116] Protection of the free hydroxyl groups with acetone dimethylacetal affords compound **127** in 77% yield (over 2 steps). Selective cleavage of PMB group, provides compound **128** which was oxidized to the corresponding aldehyde **129**, and subject to a Grignard reaction with vinylmagnesium bromide in THF affording allylic alchohol **130**, in 80% yield (over 2 steps), as a single diastereoisomer. ^{1}H NMR spectrum showed a clean doublet at δ 3.44 ppm with J = 4.3 Hz indicating that proton H-5 couples only with H-6 and thus must be on the same side. Allyl alcholol **130** was subsequently benzylated with PMBBr affording the derivative **131** in 80% yield (Scheme 3.16). Cleavage of isopropylidene group forms compound **132** in quantitative yield. To achieve the final bicyclic product **10b** it will be necessary to oxidize the primary alcohol of compound **132**, followed by alkylation of the corresponding aldehyde with vinylmagnesium bromide to the resultant allylic alcohol. RCM of **133** followed by allylic oxidation with MnO_2 will originate the desired product **10b**.

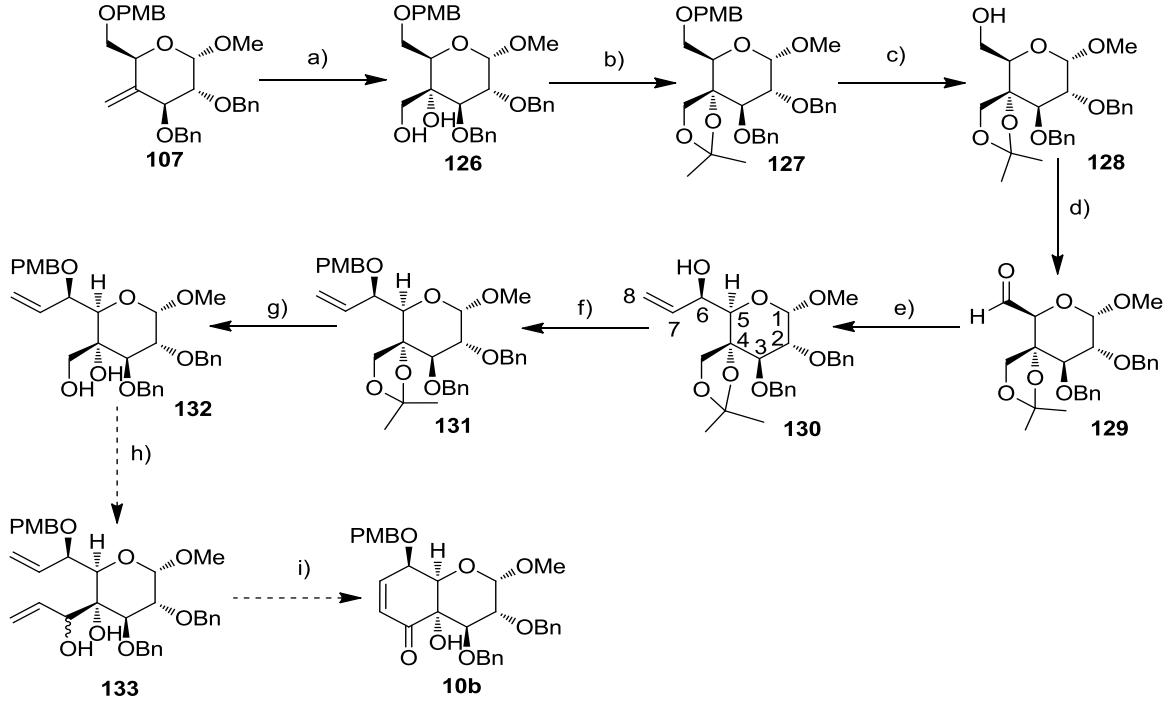

Scheme 3.16. *reagents and conditions:* a) OsO_4 0.076 M in *t*-BuOH (0.05 equiv.), NMO (2.1 equiv.), H_2O:THF (0.5:1.5), rt, 90 min.; b) 2,2-dimethoxypropane (4.0 equiv.), CSA (0.1 equiv.), dry Et_3N (4.0 equiv.), dry CH_3CN, rt, 20 min., 77% (over 2 steps); c) CAN (5.0 equiv.), H_2O, CH_3CN, rt, 20 min., 82%; d) Dess-Martin (1.5 equiv.), CH_2Cl_2, rt, 30 min.; e) vinylmagnesium bromide 1M THF (2.5 equiv.), dry THF, -78ºC, 1 h, 80% (over 2 steps); f) PMBBr (1.2 equiv.), NaH (1.2 equiv.), dry DMF, 60ºC, 1 h, 80% ; g) AcOH 60%, THF, 60ºC, 6 h, 100%.

The 2D-NOESY spectrum of product **127** was used to establish the correct stereochemistry of the dihydroxylation reaction of compound **107**. A cross-peak between H-2 and H-1'a, and between H-1'b and H-6b (Figure 3.34) confirmed the introduction of the C-4 OH from the α face.

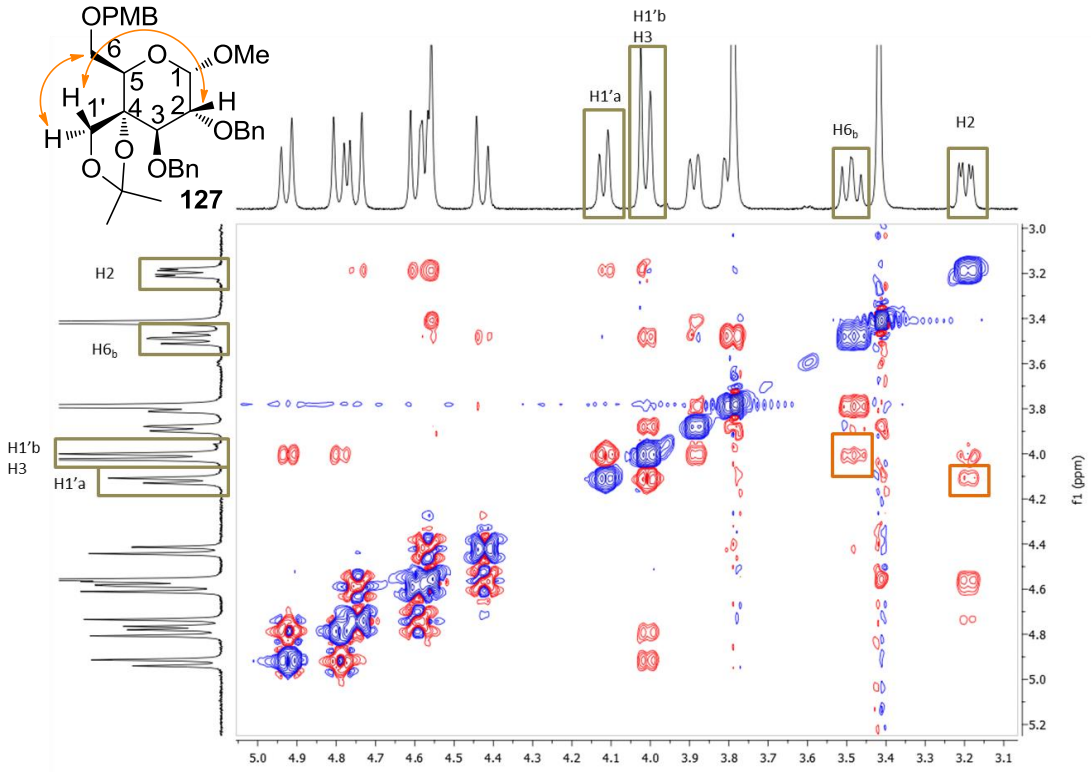

Figure 3.34: 2D-NOESY spectrum (400 MHz, $CDCl_3$) of compound **127**.

Within this section were developed three different synthetic procedures for the synthesis of bicyclic glycofused scaffolds **6a**, **6b** and **10a**. In relation to compound **10b**, we weren't able to reach the desired scaffold due to fact of having reached the end of time for this PhD project. Bicyclic glycofused compounds **6a**, **6b** and **10a** were synthesized in a straightforward manner (Figure 3.35). These compounds will be used to synthesize the corresponding tetracyclic derivatives, taking advantage of the α,β-unsaturated ketones, that can be used as Michael acceptors for the Michael-Dieckmann annulation or as dienophiles for the DA reaction.

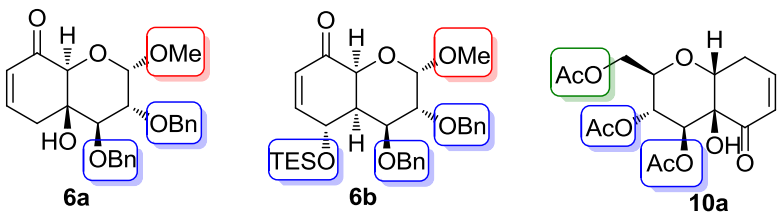

Figure 3.35: Synthesized glycofused bicyclic compounds **6a**, **6b**, **10a**.

3.2.3. Synthesis of the Michael donors

The condensation of *o*-toluate anions (e.g. precursor **5**) with various Michael acceptors (e.g. compound **6a**) represents an useful and well established protocol for the synthesis of polycyclic natural products. An absolute requirement for the toluate is the presence of a substituent (usually OR) at the R^2 position (Scheme 3.17).

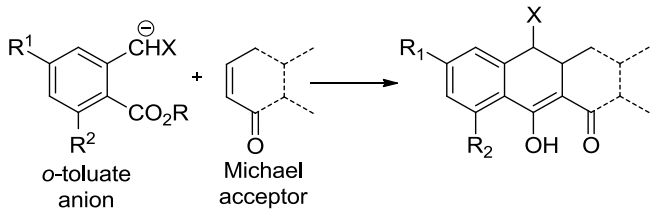

Scheme 3.17

Without it, rapid dimerization of the anion ($X=R^2=H$) takes place. The scope and limitations of this attractive annulation were established by the pioneering research of Hauser, Staunton, and Weinreb.[107,117,118] Additional methoxy groups were tolerated (e.g., $R^1=R^2=$ OMe, X=H) and the ester could be varied (R=Me, Et, Ph).[119]

Herein is described the synthesis of two analogs for precursor **5**. The first precursor, compound **137** (Scheme 3.18), was prepared from the commercially available nitro compound **134** in five steps. Therefore, compound **135** was transformed to phenol **136** via hydrogenation followed by diazotization.[120] Compound **136** was then treated with diazomethane in ether to yield the corresponding methyl ester **137**.[121,122] It is noteworthy that the phenolic hydroxyl group remains unaffected during the etherification with diazomethane, which is probably due to strong intramolecular hydrogen bonding. Phenol **137** was then protected with Boc anhydride to provide methyl ether **138**.[123] Compound **138**, on bromination with *N*-bromosuccinimide (NBS) in the presence of a catalytic amount of 2,2'-azobisisobutyronitrile (AIBN) yielded **139** in 62% yield.

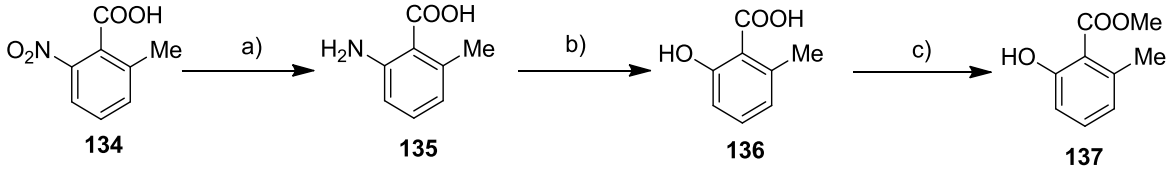

134 **135** **136** **137**

Scheme 3.18. *reagents and conditions:* **a)** Pd/C, H_2, MeOH, rt, 12 h; **b)** $NaNO_2$ (1.1 equiv.), 10% H_2SO_4 in water, -5ºC to 70ºC, 2 h, 81% (over 2 steps); **c)** CH_2N_2/diethyl ether, 0ºC, 2 h, 96%; ***(cont.)***

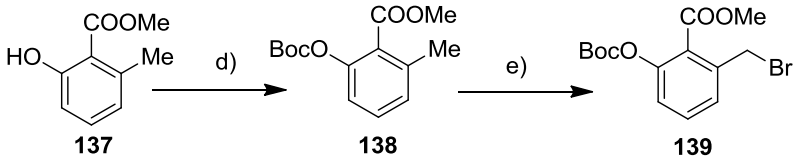

Scheme 3.18 ***(cont.)*** *reagents and conditions:* **d)** Boc_2O (1.02 equiv.), DMAP (0.05 equiv.), hexane, rt, 2 h, 75%; **e)** NBS (1.1 equiv.), AIBN (cat.), CCl_4, 2.5h, 62%.

The second *o*-toluate anion precursor **143** was synthesized as depicted in Scheme 3.19 in 3 steps, starting from 2,3-dimethylanisole.[124,125] Commercial available 2,3-dimethylanisole **140** was selectively oxidized to the corresponding aldehyde **141** by copper(II) sulfate pentahydrate and potassium peroxydisulfate, followed by oxidation to the corresponding carboxylic acid **142** using sulfamic acid in water/THF. Subsequent esterification afford phenyl ester **143** in 54% overall yield.

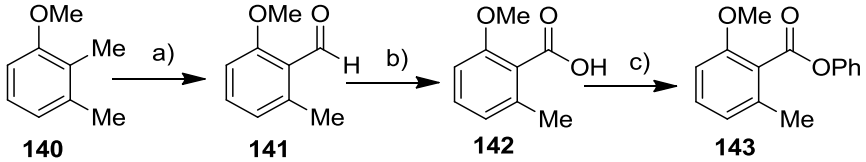

Scheme 3.19. *reagents and conditions:* a) $CuSO_4 \cdot 5H_2O$ (1.02 equiv.), $K_2S_2O_8$ (3.18 equiv.), CH_3CN/H_2O (1:1), 75ºC, 1 h, 85%; b) H_2NSO_3H (1.34 equiv.), $NaClO_4$ (1.3 equiv.), H_2O/THF (2:1), rt, 1 h, 70%; c) $(COCl)_2$ (4.0 equiv.), PhOH (2.0 equiv.), DMAP (2.0 equiv.), dry DMF, dry CH_2Cl_2, rt, 24 h, 91%.

3.2.4. Synthesis of benzocyclobutenol precursor

Benzocyclobutenols are important in natural product syntheses since undergo ring opening to the reactive *ortho*-quinodimethanes (oQDMS) **8** which readily undergo inter- and intramolecular DA reactions. oQDMs have been extensively studied over the last 40 years in order to design intra- and intermolecular DA reactions for synthesizing target complex molecules, including steroids, alkaloids, and anthracyclines.[126-129] As *cis*-dienes, oQDMs have a remarkable DA reactivity and are often used as building blocks in the syntheses of cyclic organic compounds.

Here is describe the synthesis of benzocyclobutenol **147**, present in literature (Scheme 3.20).[130] Epoxide **145** was prepared by reaction of sulfur ylide, generated from the corresponding sulfonium salt with 2'-bromoacetophenone **144**. Epoxide **145** was then converted in intermediate benzocyclobutenol **146**, using $MgBr_2 \bullet Et_2O$ and BuLi at -78ºC in dry THF. Finally protection of the secondary hydroxyl group in compound **146** as silyl ether, give the desired product **147** in 54% yield.

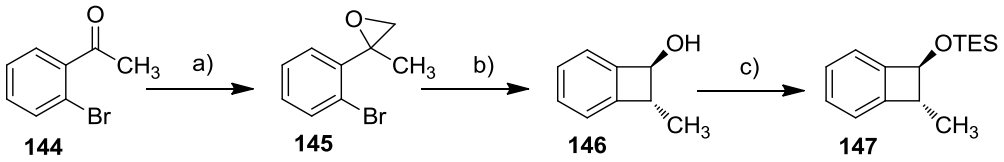

Scheme 3.20. reagents and conditions: a) trimethylsulfoxonium iodide (1.3 equiv.), NaH (1.3 equiv.), dry DMSO, 48 h, rt, 86%; b) $MgBr_2$•Et_2O (2.0 equiv.), BuLi 1.6M (1.1 equiv.), dry THF, -78ºC, 60%; c) TESOTf (1.3 equiv.), dry Et_3N (1.5 equiv.), dry CH_2Cl_2, rt, 30 min. 54%.

The 2D-NOESY spectrum of product **147** (Figure 3.36) shows the respective cross-peak between C*H*-OR and C*H*$_3$.

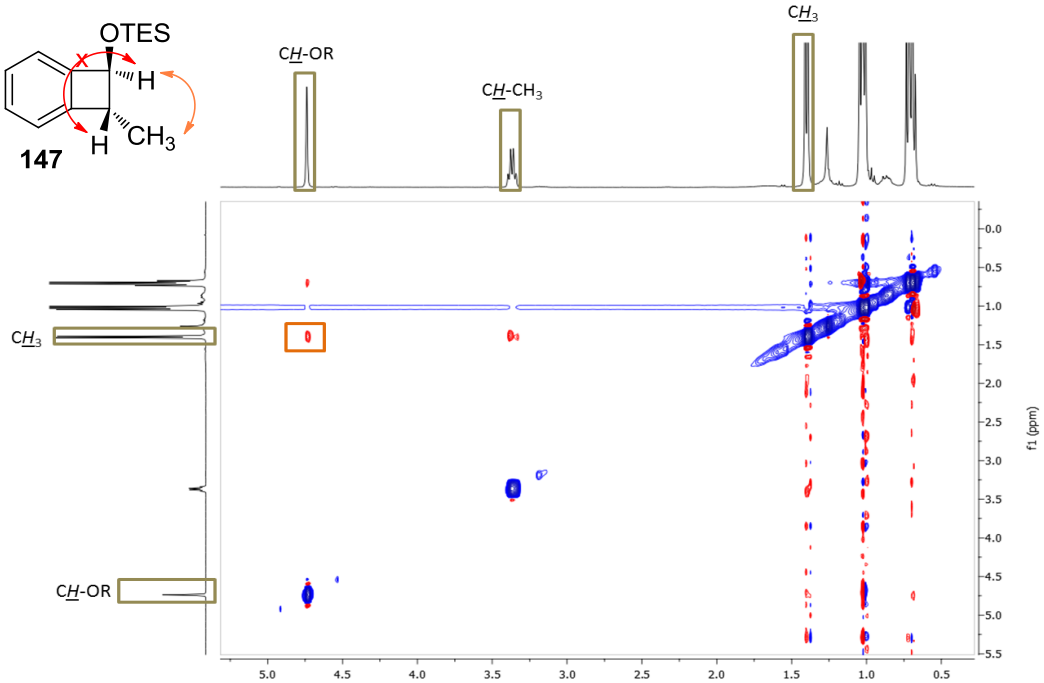

Figure 3.36: 2D-NOESY spectrum (400 MHz, $CDCl_3$) of compound **147.**

3.2.5. Michael-Dieckmann reaction approach

Michael-Dieckmann cyclization reaction[121,127,128] of compound **139**, which will form the *o*-toluate anion once reated with a strong base as BuLi, with the Michael acceptor **6a** provided the formation of compound **148** instead of the desired glycofused tetracyclic, as depicted in Scheme 3.21.

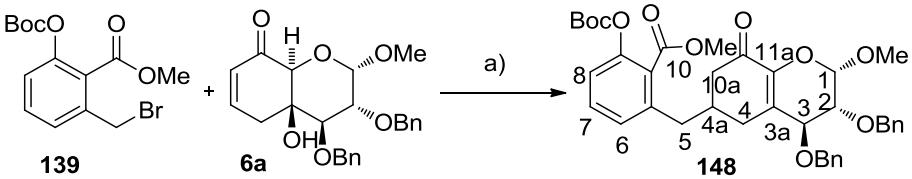

Scheme 3.21. *reagents and conditions:* a) **139** (3.0 equiv.), BuLi 1.6 M (8.0 equiv.), dry THF, -78ºC-rt, 12 h, 52%.

This might be due to the fact that the methyl ester present in the aromatic ring of compound **139** is not a good leaving group and also to the fact that compound **6a** has a hydroxyl group in anti-periplanar position to the proton in α to a carbonyl group which favors the elimination product. ^{1}H NMR spectrum of compound **148** (Figure 3.37) shows a doublet at δ 4.86 ppm (*J* = 2.3 Hz) characteristic of anomeric proton H-1, which couples with H-2, a double doublet at δ 3.82 ppm (*J* = 8.0, 2.3 Hz).

From 2D-COSY, H-3 appears at δ 4.24 ppm as a doublet (*J* = 8.0 Hz) coupling only with H-2. H-10a appears at δ 2.55 ppm as a double doublet (*J* = 16.1, 2.6 Hz) and the other H-10a at δ 2.26 ppm also as a double doublet (*J* = 16.1, 11.4 Hz), both coupling each other and with H-4a at δ 2.38 ppm, that appears as a broad multiplet. H-5 potons appear between δ 2.80–2.64 ppm as a multiplet due to the coupling with only H-4a. The H-7 appears at δ 7.22 ppm, H-8 at δ 7.10 ppm as a doublet (*J* = 8.0 Hz) and H-6 at δ 7.02 ppm also as a doublet (*J* = 7.6 Hz). ^{13}C NMR spectrum cleary shows a peak at δ 192.9 ppm corresponding to the carbonyl group of the α,β-unsaturated ketone moiety and at δ 166.7 ppm belonging to the carbonyl carbon of the ester group.

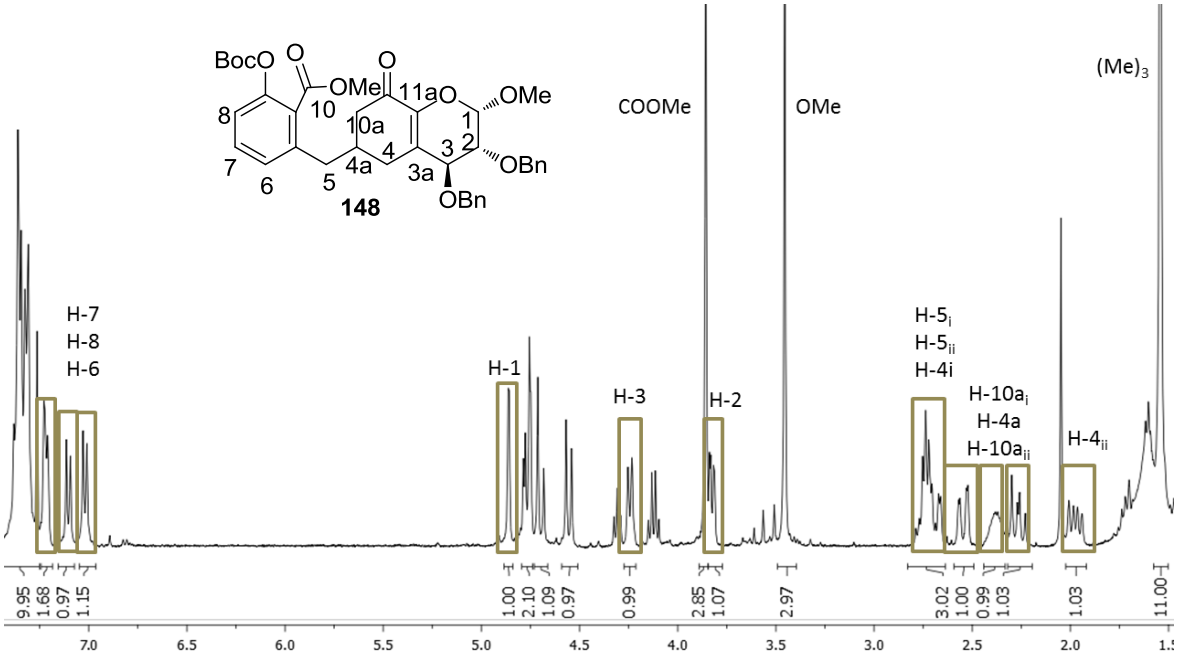

Figure 3.37: ^{1}H NMR spectrum (400 MHz, $CDCl_3$), T=19ºC, of compound **148**.

This constrains lead to the development of a new synthetic route for the Michael acceptor **6b** as showed in Scheme 3.14, as well as for the *o*-tuloate anion precursor (Scheme 3.19).

The tandem Michael-Dieckmann was carried out by the deprotonation of **143** with LDA in the presence of lithium bromide in THF at -78 °C followed by the addition of enone **6b**, yielding the crude intermediate **149** (not optimized). Unfortunely, it was not manageable to purify this product and perform an acurate characterization.

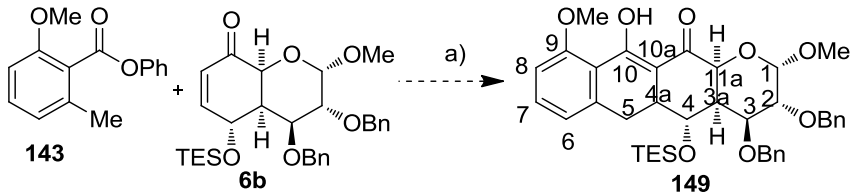

Scheme 3.22. *reagents and conditions:* a) *i*-Pr_2NH (3 equiv.), BuLi 1.6 M (2.8 equiv.), **143** (3.1 equiv.), dry THF, -78ºC, 12 h.

Nevertheless ^1H NMR spectrum for the crude product shows a clean triplet at δ 4.21 ppm with J = 6.2 Hz indicating that proton H-4 couples with other two protons, H-4a and H-3a. Protons H-5 appeared as a broad signal between δ 2.38-2.27 ppm and from 2D-COSY it only couples with H-4a.

3.2.6. Diels-Alder reaction approach

The Diels-Alder reaction is considered to be one of the most powerful and reliable synthetic strategy to achieve structural and stereochemical complexity. This is testified to by its many applications in total synthesis.[131] It occupies a position of particular importance in the resource of the synthetic organic chemist providing the possibility to generate six-membered-rings with high regio- and stereoselectivity, leading to the creation of four continuous stereogenic centers in one synthetic operation.[132]

The reaction is stereospecifically *syn* (suprafacial) for both the diene and dienophile, *endo*-products are stereoselectively preferred over *exo* isomers and 1,2-disubstituted products are regioselectively preferred over 1,3-disubstituted isomers.[132,133]

Herein is described the synthesis for the dienophile **155** (Scheme 3.23). Taking advantage of previously synthesized compound **6a**, an improvement of the overall yield was done by methylation of the tertiary hydroxyl group of compound **103**, affording compound **150** in 92% yield. Selective deprotection of primary hydroxyl group of **150** using CAN, afforded compound **151** in 82% yield. Selective oxidation of the primary hydroxyl group of compound **151** with Dess-Martin leds to aldehyde **152**. Alkylation with vinylmagnesium

bromide afforded compound **153**, with an yield of 94% in a separable mixture of diastereomers (*R*:*S* 62:38) (the absolute configuration was determined by NMR experiments). This mixture was subject to RCM using Hoveyda-Grubbs catalyst 2nd generation affording compounds **154**, which where oxidized to produce the α,β-unsaturated ketone **155** in 95% yield. These changes resulted in an improvement in the overall yield from 10% up to 22%. ^{1}H NMR spectrum showed the presence of only two olefinic protons H-5 [δ 6.68 ppm (ddd, *J* = 10.1, 5.9, 2.1 Hz)] and H-6 [δ 6.06 ppm (dd, *J* = 10.1, 3.1 Hz)].^{13}C NMR spectrum of **155** shows the characteristic C=O signal at δ 193.8 ppm confirming the formation of the expected product.

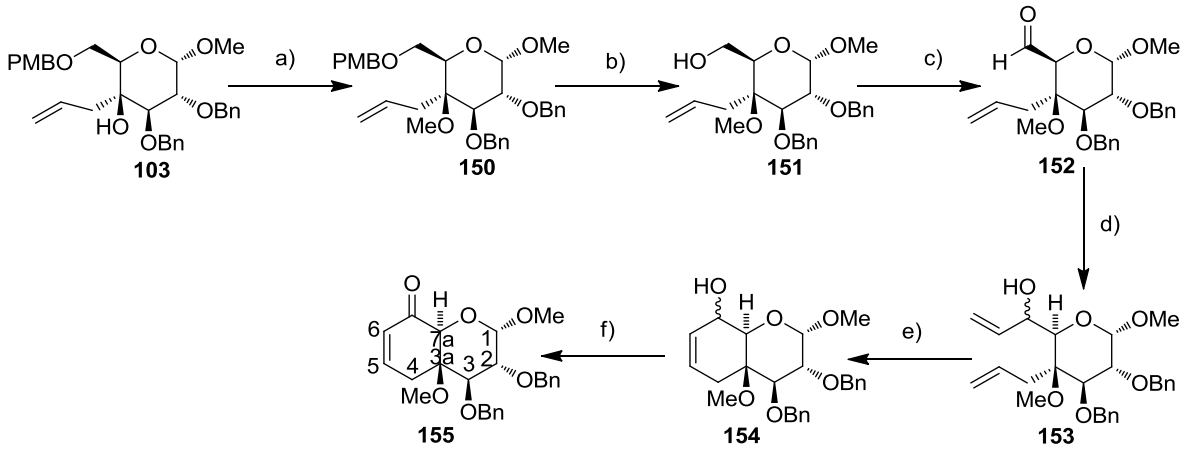

Scheme 3.23. *reagents and conditions:* a) MeI (1.2 equiv.), NaH (2.0), dry DMF, rt, 2 h, 92%; b) CAN, H_2O, CH_3CN, rt, 20 min., 82%; c) Dess-Martin, CH_2Cl_2, rt, 1 h, 89%; d) vinylmagnesium bromide 1M THF (2.5 equiv.), dry THF, -78ºC, 1 h, 94%; e) Hoveyda-Grubbs catalyst 2nd generation (5% weight), dry CH_2Cl_2, 40ºC, 2 h, 97%; f) MnO_2 activated (7.0 equiv.), EtOAc, reflux, 2 h, 95%.

Benzocyclobutenol **147** in 1,2-dichlorobenzene at 160ºC generates intermediate oQDM **156**, which readily undergo DA reaction with dienophile **155**, producing glycofused tetracyclic compound **157** in 74% yield, and traceless amount of the other diastereomer.

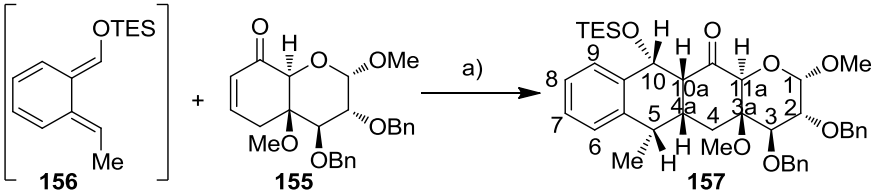

Scheme 3.24. *reagents and condtions:* 1,2-dichlorobenzene, 160ºC, 90 min., 74%.

The stereochemistry of the new stereocenters for compound **157** formed in the DA reaction was determined by ^{1}H NMR and 2D-NOESY spectrum. ^{1}H NMR spectrum showed H-10a at δ 3.21 ppm as a broad triplet with *J* = 8.2 Hz. The 2D-NOESY experiment (Figure 3.38)

of the tetracyclic compound **157** showed a cross-peak between H-5 and H-4a, H-5 and H-10a, and H-5 and H-10, thus all these protons are on the same side. Absence of a cross-peak between H-10a and H-11a is consistent with the *anti*-conformation of these protons. Finally ^{13}C NMR spectrum of **157** shows the characteristic C=O signal at δ 203.3 ppm.

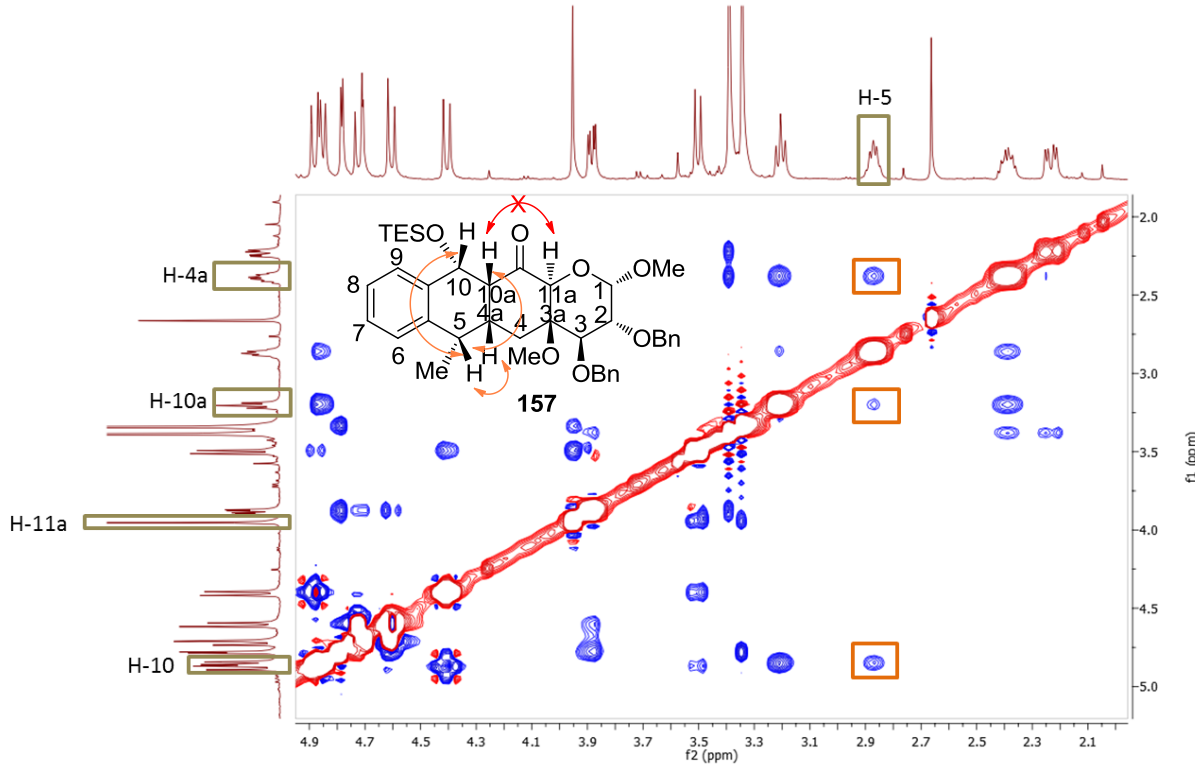

Figure 3.38: 2D-NOESY (400 MHz, $CDCl_3$) of compound **157**.

Silyl ether cleavage from glycofused tetracyclic **157**, revealed to be tricky (Scheme 3.25). The deprotection of silyl ethers is usually carried out with tetrabutylammonium fluoride (TBAF), aqueous acid, aqueous HF–CH_3CN or various Lewis acids. Many other methods have also been reported including catalytic transfer hydrogenation using Pd as catalyst, reductive cleavage by diisobutylaluminium hydride (DIBAL-H) and oxidative cleavage by DDQ. [134,135] Tetracyclic **157** possesses a leaving group (R-OMe) in *anti*-periplanar position to a hydrogen in α-position to a carbonyl group. Thus using basic conditions will engage the formation of elimination products, which were confirmed using TBAF in dry THF that formed a separable mixture of two elimination products (Scheme 3.25 *c)*). Thus, the cleavage of this silyl ether must be done in neutral conditions. Two procedures were tried, one using a solution of H_2O:THF:AcOH and TBAF, and the other using $NaIO_4$ in THF:H_2O, both procedures revealed not be effective (Scheme 3.25 *a)* and *b)*). The last procedure that was tried was the catalytic transfer hydrogenolysis using Pd as catalyst.[136]

This procedure led to the cleavage of benzyl ethers, but unfortunately triethylsilyl ether remained untouched (Scheme 3.25 *d)*).

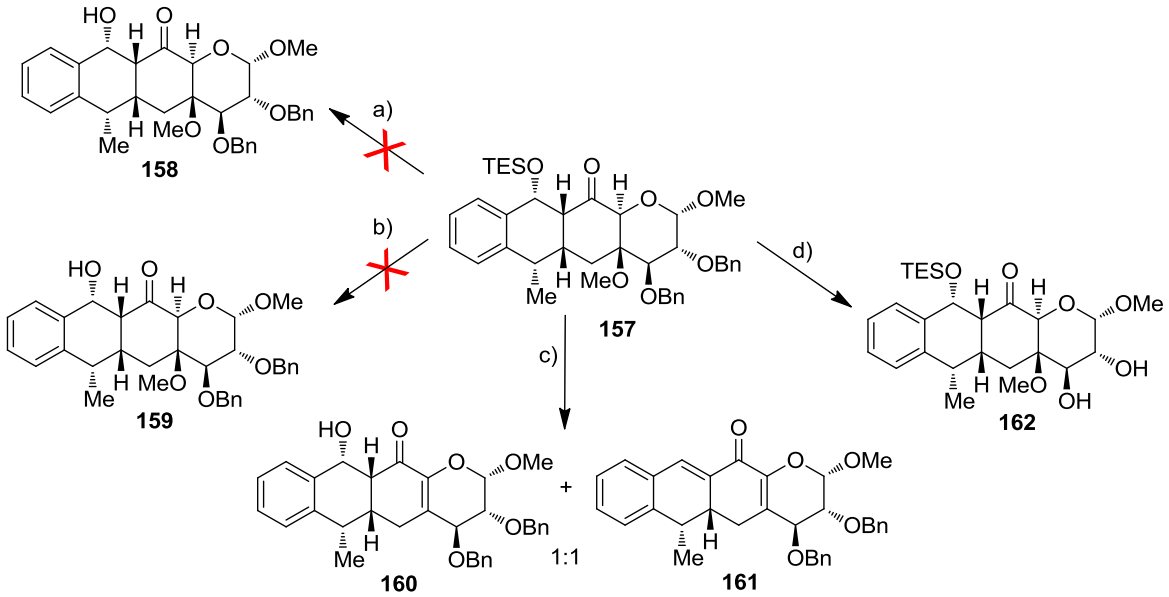

Scheme 3.25: *reagents and conditions:* a) H_2O:HOAc:THF (3:5:11), TBAF 1M in THF (0.8 equiv.), rt, 2 h; b) $NaIO_4$ (6.0 equiv.), THF:H_2O (4:1); c) TBAF 1.0M in THF (1.1 equiv.), dry THF, 5ºC, 1 h, 75% (overall yield); d) Pd/C (10%), H_2, EtOAc:MeOH (1:9), AcOH, rt, 24h.

Within this section were described different procedures to accomplish the formation of glycofused tetracyclic structures. Michael-Dieckmann annulation gave promising results that will be improved for the subsequent synthesis of the desired products. Concerning DA approach, it was synthesized a glycofused tetracyclic structure **157**, unfortunatley deprotection of group OTES revealed to be complicated. Protective group manipulation of diene **147** will be attempt. It was also synthesized promising glycofused bicyclic structures **6a**, **6b** and **10a** that could be used for the synthesis of natural compounds.

Chapter 4
Conclusions and future perspectives

4. Conclusions and future perspectives

4.1. Conclusions

This very last section summarises the scientific results of the research done in the framework of this PhD dissertation. At the same time provides some outlooks for further continuation of this research.

Glycofused tricyclic compounds

Synthesis of a small library of glycofused tricyclic compounds was accomplished and their interaction with amyloid-beta peptide (Aβ)(1-42) evaluated by saturation transfer difference - nuclear magnetic resonance (STD-NMR) experiments. Several NMR of compounds **61-70** appeared in the STD spectra recorded in the presence of Aβ oligomers, showing their ability to recognize and bind Aβ(1-42) , with the notable exception of compound **62**, whose signals are absent. In agreement with the STD results, all 2D transferred nuclear Overhauser effect spectroscopy (tr-NOESY) spectra of compounds **61-70** acquired in the presence of Aβ(1-42) showed the key change, from positive to negative, of the corresponding cross-peak signs, except for compound **62**. According to the STD relative intensities, the region of the ligand mainly involved in the interaction with Aβ(1-42) (the binding epitope) is the aromatic ring, while protons of the saccharide portion showed the least intense STD signals. These evidences explain why the stereochemistry of sugar carbons does not influence the binding affinity, while the polarity of the aromatic substituents, as previously stated, plays a crucial role in the interaction.

Fluorescent derivative **73** was synthesized, in order to perform blood brain barrier (BBB) passage studies. Fluorescency measurements carried out with this compound indicate that its favorable physical–chemical properties, in terms of balanced hydrophylicity/ lipophylicity, allow this compound to permeate through the BBB, most probably exploiting a diffusion mechanism, and to stain amyloid plaques.

STD spectra of nanoliposomes functionalised with our Aβ ligands also clearly demonstrate their ability to recognize and bind Aβ(1-42).

These properties, taken together, suggest that these compounds could be very promising candidates for possible future applications both in the therapy and in the diagnosis of Alzheimer's disease (AD).

Glycofused tetracyclic compounds

Three new glycofused bicyclic scaffolds were synthesised. Bicycle **6a** was obtain in nine steps starting from methyl α-D-glucopyranoside in 10% overall yield. Bicyclic compounds **6b** and **10a** were obtain in thirteen and in ten steps respectively, in 10% and 5.2% overall yield. For the synthesis of tetracyclic compounds, bicyclic structures **6a** and **6b** reactivity was explored in a tandem Michael-Dieckmann reaction with *o*-toluates **139** and **143**. Structure **6a** revealed not to be a promising structure when reacted with compound **139**. The synthesis of a tetracyclic structure wasn't achieved possibly mainly due to the fact that the methyl ester present in the aromatic ring of compound **139** is not a good leaving group and also to the fact that compound **6a** has a hydroxyl group in *anti*-periplanar position to the proton in α to a carbonyl group which favors the elimination product. Structure **6b** which doesn't possess the problems of compound **6a**, demonstrated to be propitious as Michael acceptor, when reacted with compound **143**. Even if wasn't manageable to purify the product and do a more accurate characterization, this positive preliminary results encourage to continuing exploring this approach. The second method exploited to synthesize glycofused tetracyclic structures considered the Diels-Alder reaction of bicyclic compound **6a** with oQDM precursor **147**. This approach led to the synthesis of the first tetracyclic derivative **157** in 74% yield. Silyl ether cleavage revealed to be delicate and neutral conditions were tried, but unfortunately removal of TES group wasn't accomplished. Reactivity of bicyclic structure **10a** as well as **10b** will also be exploit in a near future.

In summary, this work generated a library of glucofused tricyclic structures able to interact with Aβ and led to the development of a promising lead structure. It was also established synthetic procedures to achieve a tetracyclic glycofused structure. This study did not allowed yet to draw definitive conclusions; however a synthesis of tetracyclic structure was accomplished. Since these linear fused tetracyclic structures have found wide application

in pharmaceutical field, we envisioned the synthesis of antitumor compounds taking advantage of the bicyclic structures synthesized before.

4.2. Future perspectives

4.2.1. Anthracyclines glycofused derivatives

Anthracyclines are an important class of antitumor agents with significant biological activities. Anthracyclines are DNA intercalating agents.[137] Anthracycline antibiotics are among the most potent antitumor agents, with proven clinical effectiveness against leukemias, lymphomas, breast carcinomas, and sarcomas. However, their therapeutic efficacy is limited due to a number of undesirable side effects. The toxic effects of therapy with anthracyclines include nausea and vomiting, alopecia totalis (especially for doxorubicin) and myelosuppression. The most serious effect of multiple anthracycline administration is myocardial degeneration, causing congestive cardiac failure which has limited the therapeutic potential of these drugs.[138] These side effects could be modulated by changing the aglycone moiety of the anthracycline by a tetracyclic glycofused structure (Figure 4.1).

Figure 4.1: Anthracyclines *vs* glycofused tetracyclic derivatives.

Among the strategies for assembling the tetracyclic skeleton of the aglycone, a particularly effective and versatile approach is based on the coupling of its AB and CD ring segments.[138] The retrosynthetic analysis is proposed in Scheme 4.1.

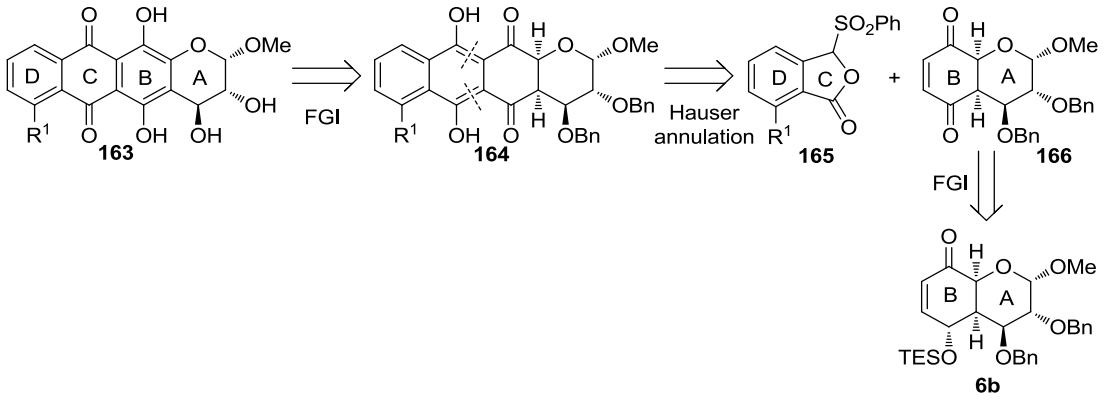

Scheme 4.1

The target molecule **164** could be made using a Hauser annulation between compound **165** and compound **166**. The originally proposed mechanism is depicted in Scheme 4.2,[139] being the first step deprotonation of phthalide **165**. The subsequent anion **167** undergoes Michael addition with acceptor **168**, forms carbanion **169** which undergoes intramolecular Dieckmann cyclization on the lactone carbonyl group to give **170**. Collapse of the intermediate **170** through expulsion of benzenesulfinate ion results in formation of annulated product **171**. Base-promoted tautomerization of **172** finally gives naphthoquinol **173**. The isobenzofuranone **165** is a synthetic equivalent of 1,4-dipolar synthon **174**.

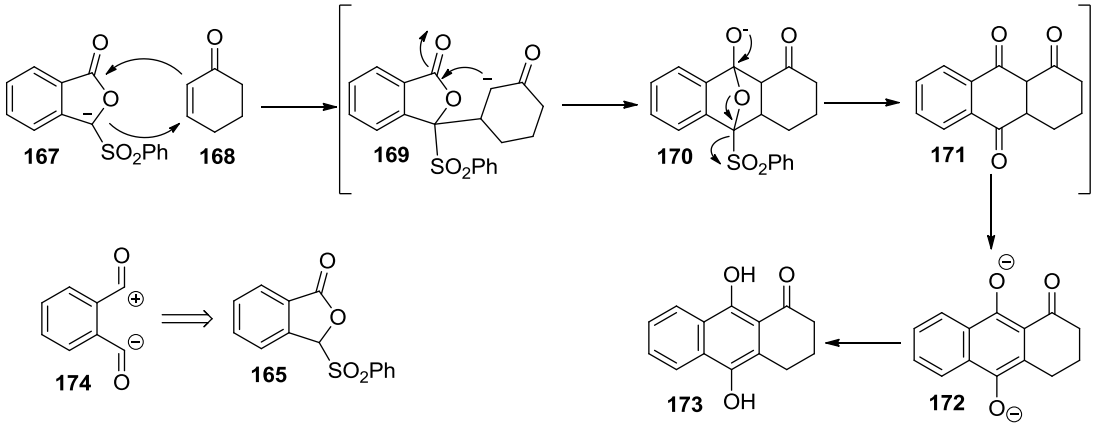

Scheme 4.2

4.2.2. Quinoxalines glycofused derivatives

Quinoxalines have shown a broad spectrum of biological activities such as antibacterial, antiviral, herbicidal and anti-inflammatory activity, thus they are an important class of nitrogen-containing heterocycles and useful intermediates in organic synthesis. Recently some of these types of molecules have been reported as candidates for the treatment of cancer and disorders associated with angiogenesis functions.[140-144]

Herein is described the synthesis of a possible antitumoral quinoxaline derivative with a glycofused tetracyclic structure that we developed in parallel with the previously described compounds. Starting from derivative **175** it's possible to obtain compound **181** (Scheme 4.3). Benzylation of the tertiary alcohol of compound **176** followed by dihydroxylation afforded compound **177** as mixture of diastereomers, which were oxidized to the corresponding 1,2-diketone **178**. Reaction of crude 1,2-diketone **178** with 1,2-diaminobenzene produce **179** in 71% (over 2 steps) and **180** in 10% yield.

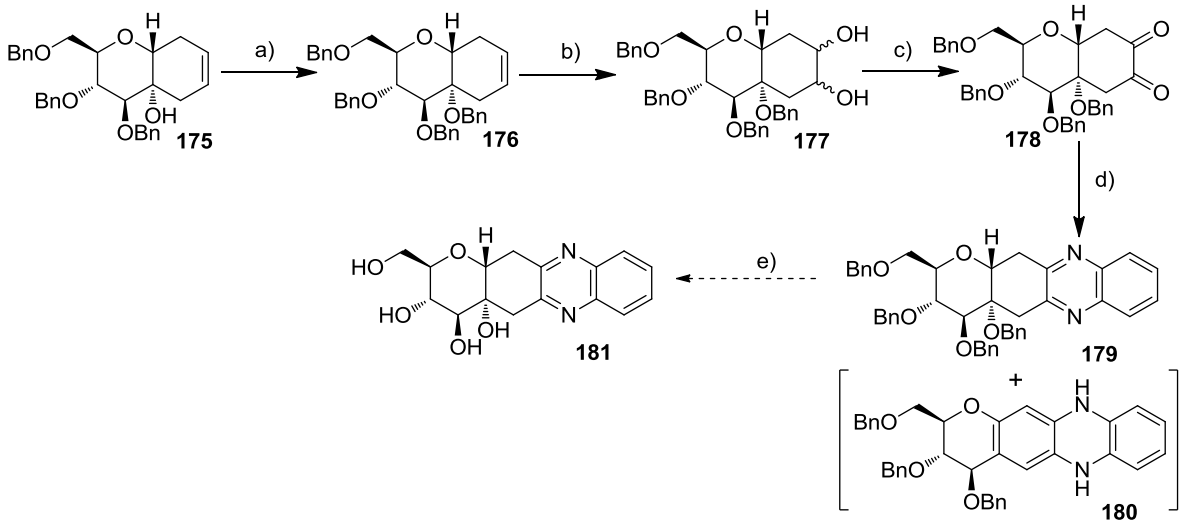

Scheme 4.3. *reagents and conditions:* a) NaH (1.2 equiv.), BnBr (1.2 equiv.), dry DMF, rt, 3 h, 94%; b) OsO_4 0.076M in *t*-BuOH (0.05 equiv.), NMO (2.1 equiv.), H_2O:acetone (1:1), rt, 2 h, 96%; c) triflic anhydride (2.0 equiv.), dry DMSO (4.0 equiv.), dry Et_3N (8.0 eq), dry CH_2Cl_2, -78ºC, 3 h; d) 1,2-diamino-benzene (1.2 equiv.), dry THF, rt, 3 h, 81% (overall yield over 2 steps), **179** in71%.

Chapter 5
Experimental section

5. Experimental section

5.1. General remarks

All solvents were dried with molecular sieves for at least 24 h prior to use. Thin layer chromatography (TLC) was performed on silica gel 60 F254 plates (Merck) with detection using UV light when possible, or by charring with a solution of concd. H_2SO_4/EtOH/H_2O (5:45:45) or a solution of $(NH_4)_6Mo_7O_{24}$ (21 g), $Ce(SO_4)_2$ (1 g), concd. H_2SO_4 (31 mL) in water (500 mL). Flash column chromatography was performed on silica gel 230-400 mesh (Merck). ^1H and ^{13}C NMR spectra were recorded at 25 °C unless otherwise stated, with a Varian Mercury 400 (400 MHz for ^1H and 100.1 MHz for ^{13}C) Bruker Avance 300 (300.13 MHz for ^1H and 75.47 MHz for ^{13}C) and Bruker Avance 500 (500.13 MHz for ^1H and 125.77 MHz for ^{13}C). Chemical shift assignments, reported in ppm, are referenced to the corresponding solvent peaks. HRMS were recorded on a QSTAR elite LC/MS/MS system with a nanospray ion source. Optical rotations were measured at room temperature using an Atago Polax-2L polarimeter and are reported in units of 10^{-1} deg·cm^2·g^{-1}.

5.2. Molecular mechanics and molecular dynamics calculations

Molecular mechanics (MM) and molecular dynamics (MD) studies were conducted with MacroModel 9.8.207[145] implemented in the 9.1.207 version of the Maestro suite,[146] using MM3* force field.[147] The starting coordinates for dynamics calculations were those obtained after energy minimization of the structures, followed by conformational search. In particular, a systematic variation of the torsional degrees of freedom of the molecules permitted different starting structures to be constructed that were further minimized to provide the corresponding local minima. For each compound the conformer with the lowest energy was considered. Simulations were carried out over 5 ns at 298 K with a 0.25 fs time step and a 20 ps equilibration step; 100 structures were sampled and minimized for further analysis. The continuum GB/SA solvent model[148] was employed and the general

PRCG (Polak–Ribiere Conjugate Gradient) method for energy minimization was used. An extended cut-off was applied and the SHAKE procedure for bonds was not selected.

5.3. Peptide synthesis and purification

Procedure

Aβ(1-42) was prepared by solid-phase peptide synthesis on a 433A synthesizer (Applied Biosystems) using Fmoc-protected L-amino acid derivatives, NOVASYN-TGA resin on a 0.1 mM scale [149]. Peptide was cleaved from the resin as previously described[150] and purified by reverse phase HPLC on a semi-preparative C4 column (Waters) using water:acetonitrile gradient elution. Peptide identity was confirmed by MALDI-TOF analysis (model Reflex III, Bruker). Peptide purity was always above 95%.

5.4. NMR spectroscopy binding studies

NMR experiments were recorded on a Varian 400 MHz Mercury. A batch of Aβ(1-42) was selected that contained pre-amyloidogenic seeds highly toxic to N2a cells. Immediately before use, lyophilized Aβ(1-42) was dissolved in 10 mM NaOD in D_2O at a concentration of 160 μM, then diluted 1:1 with 10 mM phosphate buffer saline (PBS), pH=7.4 containing 100 mM NaCl (PBS) and one of the tested compounds. Compounds **61-70**, **73** and **74** were dissolved in 10 mM NaOD in D_2O and then diluted in PBS, pH=7.4, sonicated for 1 h and added to the peptide solution. The pH of each sample was verified with a Microelectrode (Mettler Toledo) for 5 mm NMR tubes and adjusted with NaOD or DCl. All pH values were corrected for isotope effect. Basic sequences were employed for, 2D-NOESY and STD experiments. For STD, a train of Gaussian-shaped pulses each of 50 ms was employed to saturate selectively the protein envelope; the total saturation time of the protein envelope was adjusted by the number of shaped pulses and was varied between 3 s and 0.3 s.

5.4.1. Liposome binding studies

A batch of lyposomes functionalized with tricyclic derivative **97** [DPPC/Chol (1:1) + 4% peg-2000 + 20% lipid-N3 - Clicked (10% on surface)] was diluted 1:1 with H_2O and 10% D_2O, at pH=7.4. ^1H NMR (128 transients) and water-LOGSY (2048 transients, 1.2 s and 1.6 s mixing time) experiments were acquired at 298 K on a Bruker Advance 600 (600

MHz for ^{1}H and 150 MHz for ^{13}C) instrument, equipped with a triple resonance cryo-probe. The same experiments were acquired diluting the lyposome preparation with a solution of pre-dissolved Aβ(1-42), whose final concentration in the NMR tube was 80 μM.

5.5. Sections staining

Brain tissue from Tg CRND8 mice encoding a double mutant form of amyloid precursor protein 695 (KM670/671NL + V717F) under the control of the PrP gene promoter (Chishti et al., 2001) were dissected and were fixed in Carnoy's and embedded in paraffin.[151]

Procedures involving animals and their care were conducted in conformity with the institutional guidelines that are in compliance with italian (D.L. No. 116, G.U. Suppl. 40, Feb. 18, 1992, Circolare No. 8, G.U., 14 Luglio 1994) and international laws and policies (EEC Council Directive 86/609, OJ L 358, 1 Dec.12, 1987; NIH Guide for the Care and use of Laboratory Animals, U.S. National Research Council, 1996). All efforts were made to minimize the number of animals used and their suffering.

Seven-micrometer-thick serial sections of paraffin-embedded blocks from the temporal cortex were mounted on gelatin coated microscope slides and used for staining. Paraffin sections were subjected to two incubations of 5 min. in xylene, an incubation of 10 min. each in 100%, 96%, 70% EtOH for the complete dewaxing and two successive incubations of 5 min. in water. Tissue sections were covered with a solution of thioflavine T (ThT) (3 μM) or of compound **73** (6 μM) dissolved in water. After 30 min. of incubation, the sections were washed 3 times for 5 min. in water and 5 min. each in 70%, 96%, 100% EtOH. The sections were then incubated 5 min. in xylene before adding the coverslip. Sections were visualized by fluorescent fluoromicroscope M-3204CCCD (OlympusBX61) equipped with the filters FITC (Ex 488 nm) for detecting ThT and DAPI (Ex. 405 nm) for detecting the tested compounds.

5.6. Transport experiments

Trans-endothelial-electrical resistances (TEER) were measured by EVOMX meter, STX2 electrode (World Precision Instruments, Sarasota, Florida). Fluorescence measurements were done using a Cary Eclipse spectrofluorimeter (Varian Inc., Palo Alto, California). The radioactivity assay were achieved by means of a Tri-Carb 2200 CA Liquid Scintillation

Analyzer (Packard Instrument Co. Inc., Rockville, MD).The differences were evaluated for statistical significance using Student's t-test.

For transport experiments across a cell monolayer, hCMEC/D3 were seeded in a 12-well Transwell® inserts coated with type I collagen. Cell suspensions (0.5 mL) containing 2.0•105 cells were added to the upper (donor) chamber, which was inserted into the lower (acceptor) chamber containing the culture medium (1.0 mL). A cell monolayer was usually formed 14 days after seeding judged by three criteria: (1) the cells formed a confluent monolayer without visible spaces between cells under a light microscope; (2) the height of the culture medium in the upper chamber had to be at least 2 mm higher than that in the lower chamber for at least 24 h; and (3) a constant TEER (*trans*-endothelial-electrical resistance) value, measured using an EVOM Endohm chamber. Wells were used when TEER value was higher than 50 $\Omega \cdot cm^2$. *Trans*-endothelial permeability coefficient (PE) was calculated as reported by Bickel U.[152]

After adding the test substance to the donor compartment, repeated samples are taken from the donor compartment over the desired time course. The concentration measured in these samples and the known volumes of the compartments (V_{donor} and $V_{acceptor}$) are used to calculate the incremental clearance volumes ΔV_{Cl} for each time point:

$$\Delta V_{Cl} = C_{acceptor} \cdot V_{acceptor} / C_{donor}$$

As long as the concentration in the acceptor compartment is small and ΔV_{Cl} increases in linear manner, the slope of the line can be interpreted as the PS product for unidirectional transfer. With the known exchange surface, S, (filter area) the permeability may be obtained as P = PS/S. Finally, a correction needs to be made for the permeability of the cell-free filter:

$$1/P_{endothel} = 1/P_{totall} - 1(P_{filter})$$

With $P_{endothel}$ being equal to PE.

After adding the test substance to the upper compartment, samples were taken from the lower compartment at different times (0, 60, 180 min) for liquid scintillation counting (C14 sucrose) and for fluorescence assays (compound **73**). At the end of the experiments, TEER

and [^{14}C]sucrose PE were re-determined in order to prove no occurrence of adverse effects on tight junction function due to sample application.

5.7. Liposome

5.7.1. Nanoliposome preparation

Glycofused tricyclic-PEG-cyclooctyne derivative **95** was added to liposomes in presence of DMSO, and the reaction was gently stirred for 24 h at 25–27°C under continuous flow of N_2. Any aggregates that may have been formed during the reaction were disaggregated by gentle bath sonication (~2–5 min.) and the resulting mixture was placed in a 10.000 MW cutoff dialysis tubing (Servapore, Serva) and dialyzed against PBS buffer overnight. The vesicle dispersion was further purified by column chromatography (Sephadex G50). Quantification of **95** in final liposomal dispersion **98** after liposomal click reaction was achieved by HPLC analysis of a specific quantity of freeze-dried liposomal dispersion and integration of the corresponding peak HPLC was performed with a Lichrosphere 100 RP-18 (5 μm) column; eluted with a $CHCl_3$/MeOH (9:1) + 0.08% TFA mobile phase at a 1 mL/min flow rate, by a Shimatzu, LC-20AB Prominence Liquid Chromatography System.

5.7.2. Characterization of nanoliposome

5.7.2.1 Size, polydispersity and ζ-potential

The size, polydispersity and ζ-potential of the liposome were determined using a NanoZeta series particle sizer and ζ-potential analyzer (Malvern). The size and polydispersity measurements were performed at 25ºC. Liposomes, prepared in 10 mM PBS, 150 mM NaCl, 1 mM EDTA, pH=7.4, were diluted at 0.25 mM total lipid concentration. The particle size was assessed by dynamic laser light scattering with a 652 nm laser beam. Particle size and polydispersity index were obtained from the intensity autocorrelation function of the light scattered at a fixed angle of 173° (conditions which avoid errors due to back-scattering). The ζ-potential was measured at 25ºC. Each measurement was performed on freshly prepared liposome samples. For some of the liposome types prepared, vesicle stability was measured when the liposomes were dispersed in buffer (at various lipid concentrations) and stored at 4ºC, by following their size, polydispersity index and

ζ-potential (which were measured by dynamic laser light scattering as described above) for periods of 3–30 days.

5.7.2.2 Nanoliposome integrity studies

The integrity of vesicles with lipid membrane compositions similar to those used for surface decoration by the click chemistry methodology was evaluated in order to establish the optimum conditions for the reaction. Integrity of DPPC/Chol (1:1) liposomes were evaluated under the conditions and in the presence of the solutions required for the click reaction to take place. For this, the latency (%) of calcein in the vesicles was measured at various time points during incubation of liposomes at 25º or 37ºC, in presence of reaction media. Lipid/reaction compound ratios of 1:1 and 1:2 mol/mol were used. The lipid concentration in the incubated dispersions was always constant at 1 mM, and, calcein was initially encapsulated in the vesicles at a quenched concentration (100 mM). For % calcein latency calculation, samples from the liposomes (20 μL) were diluted with 4 mL buffer, pH=7.40, and fluorescence intensity (FI) was measured (EX 470 nm, EM 520 nm), before and after addition of triton X-100 at a final concentration of 1% v/v (that ensures liposome disruption and release of all encapsulated dye). Percent latency (% latency) was calculated from:

$$\%\ Latency = \frac{1.1 \cdot (F_{AT} - F_{BT})}{1.1\ \cdot F_{AT}} \cdot 100$$

Where: F_{BT} and F_{AT} are calcein fluorescence intensities before and after the addition of triton X-100, respectively.

After establishing the conditions at which the liposomes remain stable, and carrying out the click chemistry reaction for decoration of the vesicle surface as described above, the vesicles produced were studied for their integrity during incubation in absence and in presence of serum proteins. For this, liposomes that encapsulated calcein, were prepared as described above and subjected to the click reaction for glycofused tricyclic-PEG-cyclooctyne derivative **95** attached to their surface. They were subsequently incubated in absence or presence of serum proteins (80% v/v) and their integrity was evaluated during their incubation at 37ºC for 24 or 48 h.

5.8. Synthesis

5.8.1. General synthetic strategy for protected compounds 51-60

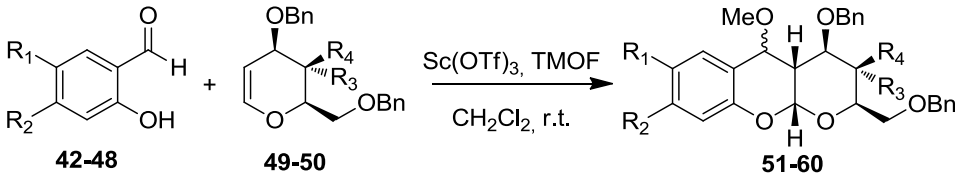

Scheme 5.1

A mixture containing the appropriate *o*-hydroxybenzaldehyde (**42-48**) (2.5 equiv.), trimethylorthoformate (2.5 equiv.) and scandium triflate (3% mol) in CH_2Cl_2 is stirred at rt for 20 min. The mixture is then cooled at 0°C and the appropriate tri-*O*-benzyl glycal (**49-50**) is added. The reaction is then left stirring at rt for 30 min. The reaction is then diluted with CH_2Cl_2, washed with water, dried over Na_2SO_4, filtrated and the solvent is removed under reduced pressure. The crude is purified by flash chromatography [(eluent toluene/AcOEt (9.75:0.25)] to afford pure compounds **51-60**.

Compound 51: yield 59%, C5 *R*/*S* 92/8

(5*R*)

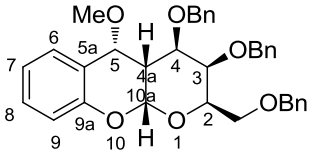

^{1}H NMR (400 MHz, $CDCl_3$) δ 7.55 (d, *J* = 7.6 Hz, 1H, H-6), 7.37 – 7.22 (m, 15H, Ar-*H*), 7.23 – 7.15 (m, 1H, H-8), 6.99 (t, *J* = 7.6 Hz, 1H, H-7), 6.83 (d, *J* = 8.1 Hz, 1H, H-9), 5.66 (d, *J* = 2.9 Hz, 1H, H-10a), 4.96 (d, *J* = 11.4 Hz, 1H, C*H*$_2$Ph), 4.77 (d, *J* = 4.3 Hz, 1H, H-5), 4.62 – 4.31 (m, 5H, C*H*$_2$Ph), 4.18 (t, *J* = 6.4 Hz, 1H, H-2), 3.79 (bs, 1H, H-3), 3.68 – 3.63 (m, 1H, H-4), 3.63 – 3.59 (m, 2H, C*H*$_2$O), 3.58 (s, 3H, OMe), 3.36 – 3.26 (m, 1H, H-4a); ^{13}C NMR (101 MHz, $CDCl_3$) δ 152.2, 139.0, 138.8, 138.2, 129.1, 128.6, 128.4, 128.4, 128.4, 128.1, 128.0, 127.9, 127.7, 127.5, 126.2, 122.4, 121.3, 115.5, 97.7, 76.2, 75.6, 75.1, 73.9, 73.7, 72.7, 71.71, 69.1, 57.1, 34.7. $[\alpha]_D^{20}$= +5.3 (c=1, $CHCl_3$). MS: m/z calcd for $[M + Na]^+$ = 575, $[M + K]^+$ = 591; found $[M + Na]^+$ = 575, $[M + K]^+$ = 591.

(5*S*)

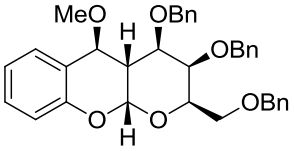

^{1}H NMR (400 MHz, $CDCl_3$) δ 7.39 – 7.24 (m, 13H, Ar-*H*), 7.24 – 7.20 (m, 1H, H-6), 7.18 (dd, *J* = 7.0, 2.2 Hz, 2H, Ar-*H*), 7.07 (d, *J* = 7.4 Hz, 1H, H-8), 6.95 – 6.79 (m, 2H, H-7, H-9), 5.71 (d, *J* = 3.2 Hz, 1H, H-10a), 4.92 (d, *J* = 11.5 Hz, 1H, C*H*$_2$Ph), 4.64 – 4.44 (m, 5H, C*H*$_2$Ph), 4.40 (d, *J* = 2.1 Hz, 1H, H-5), 4.23 – 4.19 (m, 1H, H-2), 3.98 (bs, 1H, H-3), 3.72 – 3.64 (m, 2H, C*H*$_2$O), 3.37 (s, 3H, OMe), 3.32 (dd, *J* = 11.8, 2.4 Hz, 1H, H-4), 3.06 – 2.98 (m, 1H, H-4a). ^{13}C NMR (101 MHz, $CDCl_3$) δ 153.8, 138.7, 138.0, 137.7, 131.2, 130.3, 128.6, 128.6, 128.5, 128.2, 128.2, 128.0, 128.0, 127.8, 127.8, 120.8, 118.5, 116.9, 95.0, 75.1, 74.7, 74.7, 73.7, 71.6, 71.5, 71.5, 68.9, 56.3, 37.7, 29.9. $[\alpha]_D^{20}$= +8.7 (c=1, $CHCl_3$). MS: m/z calcd for $[M + Na]^+$ = 575, $[M + K]^+$ = 591; found $[M + Na]^+$ = 575, $[M + K]^+$ = 591.

Compound 52: yield 40%, C5 *R*/*S* 100/0

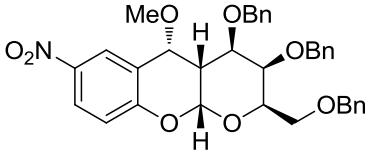

^{1}H NMR (400 MHz, $CDCl_3$) δ 8.43 (dd, *J* = 2.7, 1.1 Hz, 1H, H-6), 8.08 (dd, *J* = 9.0, 2.7 Hz, 1H, H-8), 7.43 – 7.17 (m, 15H, Ar-*H*), 6.87 (d, *J* = 9.0 Hz, 1H, H-9), 5.73 (d, *J* = 2.9 Hz, 1H, H-10a), 4.96 (d, *J* = 11.3 Hz, 1H, C*H*$_2$Ph), 4.74 (d, *J* = 4.3 Hz, 1H, H-5), 4.64 – 4.36 (m, 5H, C*H*$_2$Ph), 4.11 (t, *J* = 6.4 Hz, 1H, H-2), 3.86 (bs, 1H, H-3), 3.64 (dd, *J* = 9.2, 5.8 Hz, 2H, C*H*$_2$O), 3.59 (d, *J* = 7.4 Hz, 3H, OMe), 3.50 (dd, *J* = 11.1, 2.5 Hz, 1H, H-4), 3.41 – 3.32 (m, 1H, H-4a). ^{13}C NMR (101 MHz, $CDCl_3$) δ 157.5, 142.3, 138.7, 138.0, 137.9, 128.6, 128.5, 128.4, 128.4, 128.2, 128.1, 128.1, 127.9, 127.8, 125.3, 123.3, 123.2, 116.2, 98.8, 75.2, 75.2, 74.6, 73.8, 73.0, 72.3, 72.1, 68.9, 57.1, 33.9.$[\alpha]_D^{20}$= -4.5 (c=1, $CHCl_3$). MS: m/z calcd for $[M + H]^+$ = 598, $[M + Na]^+$ = 620, $[M + K]^+$ = 636; found $[M + H]^+$ = 598, $[M + Na]^+$ = 620, $[M + K]^+$ = 636.

Compound 53: yield 35%, C5 *R*/*S* 100/0

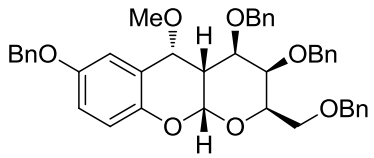

^{1}H NMR (400 MHz, $CDCl_3$) δ 7.52 – 7.25 (m, 20H, Ar-*H*), 7.23 (d, *J* = 2.6 Hz, 1H, H-6), 6.86 (dd, *J* = 8.8, 2.6 Hz, 1H, H-8), 6.78 (d, *J* = 8.8 Hz, 1H, H-9), 5.64 (d, *J* = 2.9 Hz, 1H, H-10a), 5.10 – 4.95 (m, 3H, C*H*$_2$Ph), 4.76 (d, *J* = 4.4 Hz, 1H, H-5), 4.64-4.34 (m, 5H, C*H*$_2$Ph), 4.20 (t, *J* = 6.5 Hz, 1H, H-2), 3.83 (bs, 1H, H-3), 3.67 (dd, *J* = 11.1, 2.6 Hz, 1H, H-4), 3.65 – 3.61 (m, 2H, C*H*$_2$O), 3.58 (s, 3H, OMe), 3.36 – 3.25 (m, 1H, H-4a). ^{13}C NMR (101 MHz, $CDCl_3$) δ 149.9, 139.0, 138.9, 138.1, 130.5, 129.6, 128.6, 128.4, 128.4, 128.3, 128.1, 127.9, 127.9, 127.7, 127.5, 126.5, 121.9, 115.3, 97.62, 76.3, 75.6, 75.1, 73.9, 73.7, 72.6, 71.6, 69.1, 57.1, 34.7, 20.9. $[\alpha]_D^{20}$= -5.5 (c=1, $CHCl_3$); MS: m/z calcd for $[M + Na]^+$ = 681 $[M + K]^+$ = 697; found $[M + Na]^+$ = 682, $[M + K]^+$ = 697

Compound 54: yield 73%, C5 *R*/*S* 85/15

(5*R*)

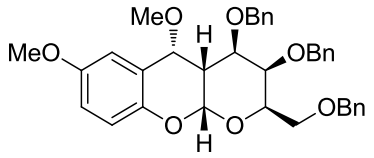

^{1}H NMR (400 MHz, $CDCl_3$) δ 7.37 – 7.21 (m, 15H, Ar-*H*), 7.11 (d, *J* = 0.9 Hz, 1H, H-6), 6.76 – 6.75 (AB, *J* = 8.6 Hz, 2H, H-8, H-9), 5.61 (d, *J* = 2.9 Hz, 1H, H-10a), 4.96 (d, *J* = 11.4 Hz, 1H, C*H*$_2$Ph), 4.74 (d, *J* = 4.4 Hz, 1H, H-5), 4.60-4.36 (m, 5H, C*H*$_2$Ph), 4.18 (t, *J* = 6.4 Hz, 1H, H-2), 3.83 – 3.78 (m, 4H, ArOMe and H-3), 3.66 (dd, *J* = 11.1, 2.6 Hz, 1H, H-4), 3.65 – 3.61 (m, 2H, C*H*$_2$O), 3.57 (s, 3H, OMe), 3.33 – 3.24 (m, 1H, H-4a). ^{13}C NMR (101 MHz, $CDCl_3$) δ 154.3, 146.1, 139.0, 138.9, 138.1, 128.6, 128.4, 128.4, 128.3, 128.1, 127.9, 127.9, 127.7, 127.5, 123.1, 116.3, 115.1, 110.8, 97.6, 76.2, 75.7, 75.1, 73.9, 73.7, 72.7, 71.6, 69.1, 57.0, 56.0, 34.7. $[\alpha]_D^{20}$= +7.1 (c=1, $CHCl_3$); MS: m/z calcd for $[M + K]^+$ = 621; found $[M + K]^+$ = 622.

(5*S*)

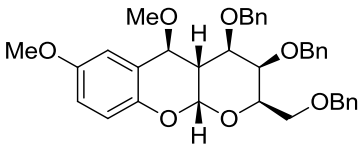

^{1}H NMR (400 MHz, $CDCl_3$) δ 7.39 – 7.15 (m, 15H, Ar-*H*), 6.84 – 6.76 (m, 2H, H-8 and H-9), 6.58 (bs, 1H, H-6), 5.64 (d, *J* = 3.1 Hz, 1H, H-10a), 4.91 (d, *J* = 11.5 Hz, 1H, C*H*$_2$Ph), 4.66 – 4.40 (m, 5H, C*H*$_2$Ph), 4.35 (d, *J* = 2.0 Hz, 1H, H-5), 4.26 – 4.17 (m, 1H, H-2), 4.00 (bs, 1H, H-3), 3.76 (s, 3H, ArOMe), 3.70 – 3.63 (m, 2H, C*H*$_2$O), 3.40 (s, 3H, OMe), 3.34 (dd, *J* = 11.8, 2.3 Hz, 1H, H-4), 3.03 – 2.94 (m, 1H, H-4a). ^{13}C NMR (101 MHz, $CDCl_3$) δ 153.6, 147.6, 138.7, 138.1, 137.7, 128.6, 128.5, 128.4, 128.4, 128.2, 128.2, 128.0, 128.03, 127.9, 127.8, 127.8, 127.7, 127.5, 119.0, 117.6, 116.6, 115.2, 99.1, 94.8, 74.9, 74.8, 73.7, 71.60, 71.4, 71.4, 70.6, 70.0, 69.8, 68.9, 56.5, 55.9, 37.6. $[\alpha]_D^{20}$= +6.6 (c=1, $CHCl_3$); MS: m/z calcd for $[M + K]^+$ = 621; found $[M + K]^+$ = 622

Compound 55: yield 91%, C5 *R*/*S* 95/5

(5*R*)

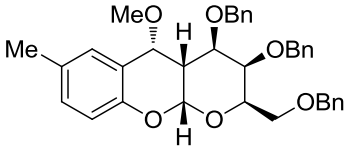

^{1}H NMR (400 MHz, $CDCl_3$) 7.31 – 7.21 (m, 16H, Ar-*H*, H-6), 6.99 (dd, *J* = 8.2, 0.9Hz, 1H, H-8), 6.72 (d, *J* = 8.2 Hz, 1H, H-9), 5.61 (d, *J* = 2.9 Hz, 1H, H-10a), 4.96 (d, *J* = 11.4 Hz, 1H, C*H*$_2$Ph), 4.74 (d, *J* = 4.5 Hz, 1H, H-5), 4.62 – 4.33 (m, 5H, C*H*$_2$Ph), 4.18 (t, *J* = 6.4 Hz, 1H, H-2), 3.80 (bs, 1H, H-3), 3.66 (dd, *J* = 11.2, 2.6 Hz, 1H, H-4), 3.61 (dd, *J* = 6.3, 4.1 Hz, 2H, C*H*$_2$O), 3.57 (s, 3H, OMe), 3.33 – 3.23 (m, 1H, H-4a), 2.31 (s, 3H, Me). ^{13}C NMR (101 MHz, $CDCl_3$) δ 149.9, 139.0, 138.9, 138.1, 130.5, 129.6, 128.6, 128.4, 128.4, 128.3, 128.1, 127.9, 127.7, 127.5, 126.5, 121.9, 115.3, 97.6, 76.9, 76.3, 75.6, 75.1, 73.9, 73.71, 72.69, 71.6, 69.1, 57.1, 34.7, 20.9. $[\alpha]_D^{20}$= -5.2 (c=1, $CHCl_3$); MS: m/z calcd for $[M + H]^+$ = 567, $[M + Na]^+$ = 589, $[M + K]^+$ = 605; found $[M + H]^+$ = 568, $[M + Na]^+$ = 590, $[M + K]^+$ = 606.

(5*S*)

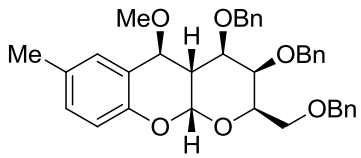

^{1}H NMR (400 MHz, $CDCl_3$) δ 7.40 – 7.13 (m, 15H, Ar-*H*), 7.01 (dd, *J* = 8.3, 1.7 Hz, 1H, H-8), 6.82 (s, 1H, H-6), 6.75 (d, *J* = 8.3 Hz, 1H, H-9), 5.66 (d, *J* = 3.2 Hz, 1H, H-10a), 4.92 (d, *J* = 11.5 Hz, 1H, C*H*$_2$Ph), 4.65 – 4.42 (m, 5H, C*H*$_2$Ph), 4.34 (d, *J* = 2.0 Hz, 1H, H-5), 4.26 – 4.17 (m, 1H, H-2), 3.98 (bs, 1H, H-3), 3.72 – 3.63 (m, 2H, C*H*$_2$O), 3.38 (s, 3H, ArOMe), 3.36 – 3.29 (dd, *J* = 11.8, 2.4 Hz, 1H, H-4), 3.06 – 2.93 (m, 1H, H-4a), 2.26 (s, 3H, Me). ^{13}C NMR (101 MHz, $CDCl_3$) δ 151.5, 138.8, 138.1, 137.7, 131.3, 131.0, 129.9, 128.6, 128.6, 128.5, 128.4, 128.2, 128.2, 128.0, 127.9, 127.8, 118.1, 116.6, 94.8, 75.0, 74.8, 74.8, 73.7, 71.5, 71.4, 71.3, 68.9, 56.4, 37.6, 29.9, 20.7. $[\alpha]_D^{20}$= -2.1 (c=1, $CHCl_3$); MS: m/z calcd for $[M + H]^+$ = 567, $[M + Na]^+$ = 589, $[M + K]^+$ = 605; found $[M + H]^+$ = 568, $[M + Na]^+$ = 590, $[M + K]^+$ = 601.

Compound 56: yield 64%, C5 *R*/*S* 53/47

(5*R*)

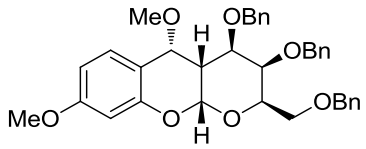

^{1}H NMR (400 MHz, $CDCl_3$) δ 7.42 (d, *J* = 8.6 Hz, 1H, H-6), 7.37 – 7.21 (m, 15H, Ar-*H*), 6.56 (dd, *J* = 8.6, 2.4 Hz, 1H, H-7), 6.39 (d, *J* = 2.4 Hz, 1H, H-9), 5.62 (d, *J* = 2.8 Hz, 1H, H-10a), 4.96 (d, *J* = 11.4 Hz, 1H, C*H*$_2$Ph), 4.71 (d, *J* = 4.4 Hz, 1H, H-5), 4.60-4.35 (m, 5H, C*H*$_2$Ph), 4.19 (t, *J* = 6.4 Hz, 1H, H-2), 3.80 (bs, 1H, H-3), 3.78 (s, 3H, ArOMe), 3.66 (dd, *J* = 11.1, 2.4 Hz, 1H, H-4), 3.60 (t, *J* = 6.3 Hz, 2H, C*H*$_2$O), 3.55 (s, 3H, OMe), 3.31 – 3.24 (m, 1H, H-4a). ^{13}C NMR (101 MHz, $CDCl_3$) δ 160.5, 153.1, 139.0, 138.9, 138.1, 128.6, 128.4, 128.4, 128.1, 127.9, 127.7, 127.5, 127.1, 114.7, 107.8, 100.7, 97.9, 76.0, 75.6, 75.2, 74.1, 73.7, 72.8, 71.8, 69.2, 56.9, 55.5, 34.9, 29.9. $[\alpha]_D^{20}$= -2.2 (c=1, $CHCl_3$); MS: m/z calcd for $[M + Na]^+$ = 605, $[M + K]^+$ = 621; found $[M + Na]^+$ = 606, $[M + K]^+$ = 621.

(5*S*)

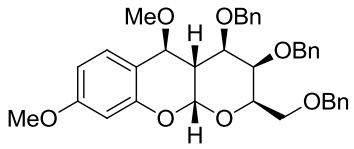

^{1}H NMR (400 MHz, $CDCl_3$) δ 7.39 – 7.16 (m, 15H, Ar-*H*), 6.97 (d, *J* = 8.4 Hz, 1H, H-6), 6.47 (dd, *J* = 8.4, 2.4 Hz, 1H, H-7), 6.43 (d, *J* = 2.4 Hz, 1H, H-9), 5.71 (d, *J* = 3.2 Hz, 1H, H-10a), 4.97 – 4.87 (d, *J* = 11.4 Hz, 1H, C*H*$_2$Ph), 4.65 – 4.43 (m, 5H, C*H*$_2$Ph), 4.37 (d, *J* = 2.1 Hz, 1H, H-5), 4.19 (t, *J* = 6.5 Hz, 1H, H-2), 3.98 (bs, 1H, H-3), 3.77 (s, 3H, ArOMe), 3.70 – 3.63 (m, 2H, C*H*$_2$O), 3.35 (s, 3H, OMe), 3.32 (d, *J* = 2.4 Hz, 1H, H-4), 3.05 – 2.95 (m, 1H, H-4a). ^{13}C NMR (101 MHz, $CDCl_3$) δ 161.4, 155.0, 138.8, 138.1, 137.8, 131.9, 128.6, 128.6, 128.5, 128.2, 128.2, 128.0, 128.0, 127.8, 111.1, 108.0, 101.4, 95.17, 75.3, 74.7, 74.3, 73.8, 71.7, 71.6, 71.6, 69.0, 56.1, 55.5, 37.8, 29.9. $[\alpha]_D^{20}$= -4.6 (c=1, $CHCl_3$). MS: m/z calcd for $[M + Na]^+$ = 605, $[M + K]^+$ = 621; found $[M + Na]^+$ = 606, $[M + K]^+$ = 622.

Compound 57: yield 45%, C5 *R*/*S* 100/0

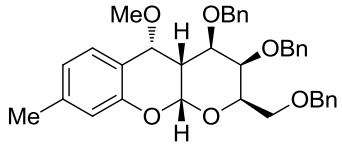

^{1}H NMR (400 MHz, $CDCl_3$) δ 7.42 (d, *J* = 7.8 Hz, 1H, H-6), 7.37 – 7.20 (m, 15H, Ar-*H*), 6.81 (d, *J* = 7.8 Hz, 1H, H-7), 6.66 (s, 1H, H-9), 5.63 (d, *J* = 2.8 Hz, 1H, H-10a), 4.97 (d, *J* = 11.4 Hz, 1H, C*H*$_2$Ph), 4.74 (bd, *J* = 4.2 Hz, 1H, H-5), 4.62 – 4.34 (m, 5H, C*H*$_2$Ph), 4.19 (t, *J* = 6.3 Hz, 1H, H-2), 3.81 (bs, 1H, H-3), 3.69 – 3.59 (m, 3H, H-4 and C*H*$_2$O), 3.56 (s, 3H, OMe), 3.34 – 3.21 (m, 1H, H-4a), 2.31 (s, 3H, Me). ^{13}C NMR (101 MHz, $CDCl_3$) δ 152.1, 139.2, 139.07, 139.0, 138.2, 128.6, 128.4, 128.4, 128.4, 128.1, 127.9, 127.9, 127.7, 127.5, 126.1, 122.3, 119.5, 116.0, 97.7, 76.2, 75.7, 75.2, 74.0, 73.7, 72.8, 71.7, 69.2, 57.0, 34.8, 21.4. $[\alpha]_D^{20}$= -6.2 (c=1, $CHCl_3$). MS: m/z calcd for $[M + K]^+$ = 605; found [$[M + K]^+$ = 605.

Compound 58: yield 66%, C5 *R*/*S* 100/0

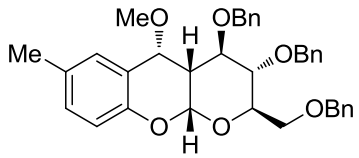

^{1}H NMR (400 MHz, $CDCl_3$) δ 7.43 – 7.18 (m, 14H, Ar-*H* and H-6), 7.09 (dd, *J* = 6.7, 2.7 Hz, 2H, Ar-*H*), 6.99 (d, *J* = 8.5 Hz, 1H, H-8), 6.72 (d, *J* = 8.5 Hz, 1H, H-9), 5.60 (d, *J* = 3.0 Hz, 1H, H-10a), 4.82 (d, *J* = 10.7 Hz, 1H, C*H*$_2$Ph), 4.74 (d, *J* = 4.4 Hz, 1H, H-5), 4.71 – 4.44 (m, 5H, C*H*$_2$Ph), 4.07 (bd, *J* = 9.9 Hz, 1H, H-2), 3.86 – 3.79 (m, 2H, C*H*$_2$O), 3.74 (bs, 1H, H-3), 3.72 – 3.65 (m, 1H, H-4), 3.55 (s, 3H, OMe), 2.83 (ddd, *J* = 10.5, 4.4, 3.2 Hz, 1H, H-4a), 2.30 (s, 3H, Me). ^{13}C NMR (101 MHz, $CDCl_3$) δ 149.8, 139.1, 138.4, 138.1, 130.7, 129.7, 128.6, 128.5, 128.4, 128.1, 128.0, 127.9, 127.8, 127.55, 126.48, 121.8, 115.5, 97.1, 78.5, 78.5, 76.4, 75.6, 74.9, 73.7, 72.5, 68.6, 57.3, 40.1, 20.9. $[\alpha]_D^{20}$= +3.7 (c=1, $CHCl_3$). MS: m/z calcd for $[M + Na]^+$ = 589, $[M + K]^+$ = 605; found $[M + Na]^+$ = 589, $[M + K]^+$ = 605.

Compound 59: yield 37%, C5 *R*/*S* 100/0

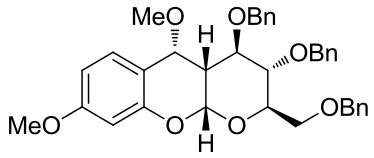

^{1}H NMR (400 MHz, $CDCl_3$) δ 7.43 (d, *J* = 8.6 Hz, 1H, H-6), 7.38 – 7.19 (m, 10H, Ar-*H*), 7.15 – 7.05 (m, 2H, Ar), 6.56 (dd, *J* = 8.6, 2.3 Hz, 1H, H-7), 6.40 (t, *J* = 2.3 Hz, 1H, H-9), 5.61 (d, *J* = 2.8 Hz, 1H, H-10a), 4.83 (d, *J* = 10.6 Hz, 1H, C*H*$_2$Ph), 4.72 (d, *J* = 4.4 Hz, 1H, H-5), 4.70-4.44 (m, 5H, C*H*$_2$Ph), 4.08 (d, *J* = 10.0 Hz, 1H, H-2), 3.88 – 3.73 (m, 3H, H-3 and C*H*$_2$O), 3.79 (s, 3H, OMe), 3.73 – 3.65 (m, 1H, H-4), 3.52 (s, 3H, OMe), 2.89 – 2.75 (m, 1H, H-4a). ^{13}C NMR (101 MHz, $CDCl_3$) δ 160.7, 152.9, 139.1, 138.4, 138.1, 128.6, 128.6, 128.4, 128.2, 128.2, 128.0, 127.9, 127.9, 127.6, 127.2, 114.6, 108.1, 100.8, 97.5, 78.5, 78.4, 76.1, 75.6, 74.9, 73.7, 72.7, 68.6, 57.2, 55.5, 40.2. $[\alpha]_D^{20}$= +11.6 (c=1, $CHCl_3$). MS: m/z calcd for $[M + Na]^+$ = 605, $[M + K]^+$ = 621; found $[M + Na]^+$ = 606, $[M + K]^+$ = 621.

Compound 60: yield 21%, C5 *R*/*S* 100/0

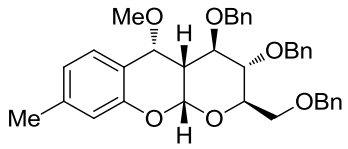

^{1}H NMR (400 MHz, $CDCl_3$) δ 7.41 (d, *J* = 7.8 Hz, 1H, H-6), 7.39 – 7.18 (m, 13H, Ar-*H*), 7.14 – 7.03 (m, 2H, Ar), 6.80 (d, *J* = 7.8 Hz, 1H, H-7), 6.65 (bs, 1H, H-9), 5.62 (d, *J* = 2.7 Hz, 1H, H-10a), 4.82 (d, *J* = 10.6 Hz, 1H, C*H*$_2$Ph), 4.74 (d, *J* = 3.8 Hz, 1H, H-5), 4.72 – 4.39 (m, 5H, C*H*$_2$Ph), 4.07 (d, *J* = 10.0 Hz, 1H, H-2), 3.89 – 3.72 (m, 3H, H-3 and C*H*$_2$O), 3.68 (t, *J* = 9.7 Hz, 1H, H-4), 3.53 (s, 3H, OMe), 2.87 – 2.78 (m, 1H, H-4a), 2.30 (s, 3H, Me). ^{13}C NMR (101 MHz, $CDCl_3$) δ 151.9, 139.7, 139.1, 138.4, 138.2, 128.6, 128.6, 128.4, 128.2, 128.0, 127.9, 127.9, 127.6, 126.1, 122.4, 119.3, 116.2, 97.2, 78.5, 76.9, 76.3, 75.6, 74.9, 73.8, 72.6, 68.7, 57.3, 40.2, 21.3. $[\alpha]_D^{20}$= +8.3 (c=1, $CHCl_3$). MS: m/z calcd for $[M + Na]^+$ = 589, $[M + K]^+$ = 605; found $[M + Na]^+$ = 590, $[M + K]^+$ = 605.

5.8.2. General synthetic strategy for compounds 61-70

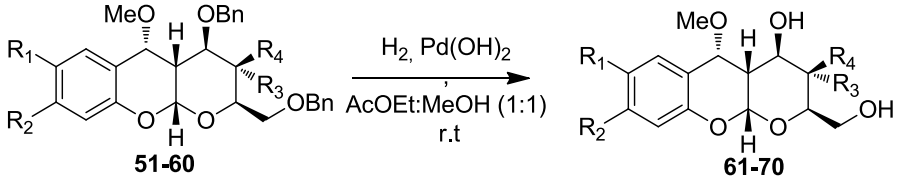

Scheme 5.2.

To a 6 mM solution of the protected compound in AcOEt/MeOH 1:1, previously degassed, $Pd(OH)_2$ 5% mol is added and the reaction mixture is stirred under H_2 atmosphere for 45 min.-1.5 h. Then the catalyst is removed by filtration and the solvent evaporated under reduced pressure to afford pure compounds **61-70.**

Compound 61: yield 97%

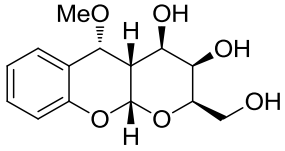

^{1}H NMR (400 MHz, CD_3OD) δ 7.45 (d, *J* = 7.7 Hz, 1H, H-6), 7.18 (t, *J* = 7.7 Hz, 1H, H-8), 6.95 (t, *J* = 7.7 Hz, 1H, H-7), 6.78 (d, *J* = 7.7 Hz, 1H, H-9), 5.62 (d, *J* = 3.1 Hz, 1H, H-10a), 4.91 (d, *J* = 2.4 Hz, 1H, H-5), 3.99 (t, *J* = 6.0 Hz, 1H, H-2), 3.83 – 3.78 (m, 2H, H-3

and H-4), 3.80 – 3.74 (m, 2H, C*H*$_2$O), 3.69 (s, 3H, OMe), 3.00 – 2.92 (m, 1H, H-4a). ^{13}C NMR (101 MHz, CD_3OD) δ 156.3, 132.9, 130.0, 125.3, 124.8, 119.2, 100.6, 81.5, 76.6, 71.5, 71.2, 65.5, 61.6, 38.4. $[\alpha]_D^{20}$= -7.6 (c=1, $CHCl_3$); MS: m/z calcd for $[M + Na]^+$ = 305, $[M + K]^+$ = 321; found $[M + Na]^+$ = 305, $[M + K]^+$ = 321.

Compound 62: yield 94%

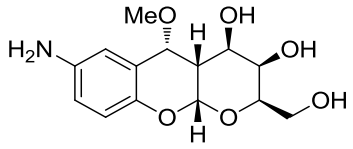

^{1}H NMR (400 MHz, CD_3OD) δ 6.89 (s, 1H, H-6), 6.65-6.55 (m, 2H, H-8 and H-9), 5.52 (d, *J* = 3.0 Hz, 1H, H-10a), 4.83 (d, *J* = 4.9 Hz, 1H, H-5), 3.98 (t, *J* = 5.8 Hz, 1H, H-2), 3.87 – 3.78 (m, 2H, H-3 and H-4), 3.79 – 3.73 (m, 1H, C*H*$_2$O), 3.67 (s, 3H, OMe), 2.96 – 2.85 (m, 1H, H4a). ^{13}C NMR (101 MHz, CD_3OD) δ 149.1, 144.7, 125.6, 121.0, 119.6, 118.6, 117.3, 114.5, 100.3, 81.7, 80.9, 76.5, 71.5, 71.4, 65.5, 61.7, 38.7. $[\alpha]_D^{20}$= +13.3 (c=1, $CHCl_3$). MS: m/z calcd for $[M + H]^+$ = 298 $[M + Na]^+$ = 320, $[M + K]^+$ = 336; found $[M + H]^+$ = 298, $[M + Na]^+$ = 320, $[M + K]^+$ = 336.

Compound 63: yield 100%

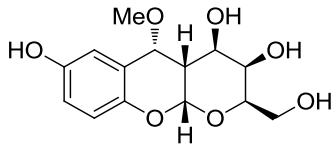

^{1}H NMR (400 MHz, CD_3OD) δ 6.88 (bs, 1H, H-6), 6.64 – 4.59 (m, 2H, H-8 and H-9), 5.54 (d, *J* = 2.8 Hz, 1H, H-10a), 4.84 (d, *J* = 4.8 Hz, 1H, H-5), 3.98 (t, *J* = 5.9 Hz, 1H, H-2), 3.84 (d, *J* = 2.7 Hz, 1H, H-4), 3.81 (bs, 1H, H-3), 3.76 (dd, *J* = 5.9, 2.3 Hz, 2H, C*H*$_2$O), 3.68 (s, 3H, OMe), 2.98 – 2.84 (m, 1H, H-4a). ^{13}C NMR (101 MHz, CD_3OD) δ 155.3, 149.1, 125.9, 119.8, 119.7, 116.1, 116.0, 100.4, 81.6, 76.5, 71.5, 71.3, 65.5, 61.6, 38.6. $[\alpha]_D^{20}$= +11.1 (c=1, $CHCl_3$); MS: m/z calcd for $[M + Na]^+$ = 321; found $[M + Na]^+$ = 321

Compound 64: yield 96%

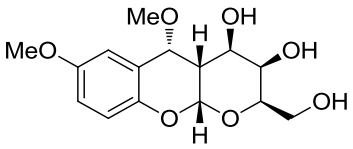

^{1}H NMR (400 MHz, CD_3OD) δ 7.00 (d, *J* = 2.2 Hz, 1H, H-6), 6.77 (dd, *J* = 8.9, 2.2 Hz, 1H, H-8), 6.71 (d, *J* = 8.9 Hz, 1H, H-9), 5.57 (d, *J* = 3.0 Hz, 1H, H-10a), 4.87 (bs, 1H, H-5), 3.98 (t, *J* = 6.0 Hz, 1H, H-2), 3.83 – 3.79 (m, 2H, H-3 and H-4), 3.76 (dd, *J* = 6.1, 3.0 Hz, 2H, C*H*$_2$O), 3.74 (s, 3H, OMe), 3.68 (s, 3H, OMe), 2.98 – 2.89 (m, 1H, H-4a). ^{13}C NMR (101 MHz, CD_3OD) δ 158.3, 150.1, 125.9, 119.9, 118.9, 114.6, 100.5, 81.5, 76.6, 71.6, 71.2, 65.5, 61.5, 58.8, 38.4. $[\alpha]_D^{20}$= +8.9 (c=1, $CHCl_3$); MS: m/z calcd for $[M + Na]^+$ = 335; found $[M + Na]^+$ = 335.

Compound 65: yield 95%

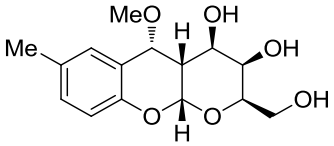

^{1}H NMR (400 MHz, CD_3OD) δ 7.24 (bs, 1H, H-6), 6.98 (d, *J* = 8.2 Hz, 1H, H-8), 6.66 (d, *J* = 8.2 Hz, 1H, H-9), 5.57 (d, *J* = 3.0 Hz, 1H, H-10a), 4.86 (1H, H-5, under the H_2O signal), 3.98 (t, *J* = 6.0 Hz, 1H, H-2), 3.83 – 3.78 (m, 2H, H-3 and H-4), 3.77 (dd, *J* = 6.0, 2.9 Hz, 2H, C*H*$_2$O), 3.68 (s, 3H, OMe), 2.96 – 2.89 (m, 1H, H-4a), 2.26 (s, 3H, Me). ^{13}C NMR (101 MHz, CD_3OD) δ 150.1, 130.2, 129.5, 126.3, 120.9, 115.1, 96.6, 77.6, 72.6, 67.6, 67.4, 61.6, 57.7, 34.59, 19.5. $[\alpha]_D^{20}$= +13.3 (c=1, $CHCl_3$); MS: m/z calcd for $[M + Na]^+$ = 319, $[M + K]^+$ = 335; found $[M + Na]^+$ = 319, $[M + K]^+$ = 335.

Compound 66: yield 97%

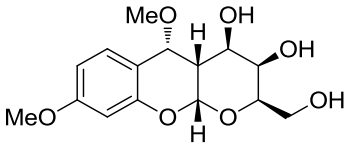

^{1}H NMR (400 MHz, CD_3OD) δ 7.32 (d, *J* = 8.6 Hz, 1H, H-6), 6.54 (dd, *J* = 8.6, 2.4 Hz, 1H, H-7), 6.35 (d, *J* = 2.4 Hz, 1H, H-9), 5.58 (d, *J* = 3.0 Hz, 1H, H-10a), 4.84 (d, *J* = 4.9 Hz, 1H, H-5), 4.00 (t, *J* = 6.0 Hz, 1H, H-2), 3.86 – 3.79 (m, 2H, H-3 and H-4), 3.77 (dd, *J* = 6.0, 3.3 Hz, 2H, C*H*$_2$O), 3.74 (s, 3H, OMe), 3.67 (s, 3H, OMe), 2.96-2.86 (m, 1H, H-4a). ^{13}C NMR (101 MHz, CD_3OD) δ 160.9, 153.2, 126.9, 113.5, 107.3, 100.4, 96.9, 77.5, 72.8,

67.6, 67.2, 61.6, 57.6, 54.5, 34.6. $[\alpha]_D^{20}$= -7.6 (c=1, $CHCl_3$); MS: m/z calcd for $[M + Na]^+$ = 335, $[M + K]^+$ = 351; found $[M + Na]^+$ = 335, $[M + K]^+$ = 351.

Compound 67: yield 97%

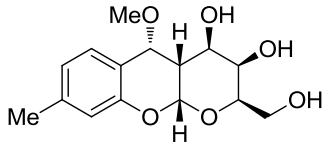

^{1}H NMR (400 MHz, CD_3OD) δ 7.29 (d, *J* = 7.8 Hz, 1H, H-6), 6.76 (d, *J* = 7.8 Hz, 1H, H-7), 6.60 (bs, 1H, H-9), 5.57 (d, *J* = 3.0 Hz, 1H, H-10a), 4.85 (d, *J* = 4.7 Hz, 1H, H-5), 3.98 (t, *J* = 5.9 Hz, 1H, H-3), 3.83 – 3.73 (m, 4H, C*H*$_2$O, H-2, H-4), 3.67 (s, 3H, OMe), 2.96 – 2.85 (m, 1H, H-4a), 2.25 (s, 3H, Me).^{13}C NMR (101 MHz, CD_3OD) δ 156.1, 143.2, 133.2, 129.6, 125.6, 122.2, 119.7, 100.6, 81.5, 76.6, 71.2, 65.6, 61.6, 38.5, 23.9. $[\alpha]_D^{20}$= +8.3 (c=1, $CHCl_3$); MS: m/z calcd for $[M + Na]^+$ = 319; found $[M + Na]^+$ = 319.

Compound 68: yield 98%

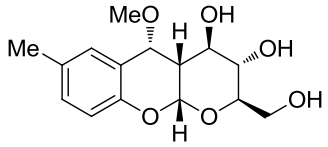

^{1}H NMR (400 MHz, CD_3OD) δ 7.12 (bs, 1H, H-6), 6.85 (d, *J* = 8.3 Hz, 1H, H-8), 6.54 (d, *J* = 8.3 Hz, 1H, H-9), 5.38 (d, *J* = 2.9 Hz, 1H, H-10a), 4.86 (1H, H-5, under the H_2O signal), 3.75 – 3.59 (m, 3H, C*H*$_2$O and H-2), 3.53 (bs, 4H, H-3 and OMe), 3.34 (t, *J* = 8.9 Hz, 1H, H-4), 2.50 – 2.40 (m, 1H, H-4a), 2.13 (s, 3H, Me). ^{13}C NMR (101 MHz, CD_3OD) δ 150.0, 130.3, 129.5, 126.4, 121.1, 115.1, 96.3, 77.5, 73.8, 70.3, 70.1, 61.2, 57.5, 40.0, 19.5. $[\alpha]_D^{20}$= +13,3 (c=1, $CHCl_3$); MS: m/z calcd for $[M + K]^+$ = 335.1; found $[M + K]^+$ = 335.3.

Compound 69: yield 97%

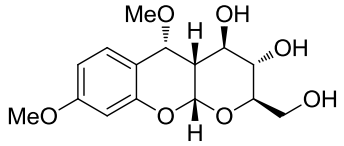

^{1}H NMR (400 MHz, CD_3OD) δ 7.33 (d, *J* = 8.6 Hz, 1H, H-6), 6.54 (dd, *J* = 8.6, 2.4 Hz, 1H, H-7), 6.36 (d, *J* = 2.4 Hz, 1H, H-9), 5.51 (d, *J* = 2.9 Hz, 1H, H-10a), 4.83 (d, *J* = 4.9 Hz, 1H, H-5), 4.00 (t, 1H, *J* = 6.0Hz, H-2), 3.87 – 3.66 (m, 6H, C*H*$_2$O and H-4 and

OMe), 3.66 (d, *J* = 6.3 Hz, 3H, OMe), 3.48 (t, *J* = 9.2 Hz, 1H, H-3), 2.57 (ddd, *J* = 10.3, 4.9, 3.1 Hz, 1H, H-4a). ^{13}C NMR (101 MHz, CD_3OD) δ 160.9, 153.1, 127.1, 113.7, 107.4, 100.4, 96.6, 77.4, 73.9, 70.2, 70.0, 61.2, 57.3, 54.5, 40.1. $[\alpha]_D^{20}$= +11.6 (c=1, $CHCl_3$); MS: m/z calcd for $[M + Na]^+$ = 335, $[M + K]^+$ = 351; found $[M + Na]^+$ = 336, $[M + K]^+$ = 352.

Compound 70: yield 98%

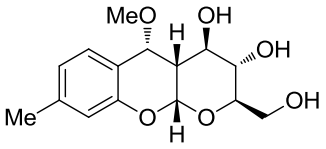

^{1}H NMR (400 MHz, CD_3OD) δ 7.31 (d, *J* = 7.8 Hz, 1H, H-6), 6.78 (d, *J* = 7.8 Hz, 1H, H-7), 6.62 (bs, 1H, H-9), 5.52 (d, *J* = 3.0 Hz, 1H, H-10a), 4.85 (d, *J* = 4.8 Hz, 1H, H-5), 3.85 (dd, *J* = 13.7, 4.4 Hz, 1H, C*H*$_2$O), 3.76 (m, 2H, C*H*$_2$O and H-2), 3.68 – 3.62 (m, 4H, H4 and OMe), 3.48 (t, *J* = 9.7 Hz, 1H, H-3), 2.58 (ddd, *J* = 9.7, 4.8, 3.0 Hz, 1H, H-4a), 2.27 (s, 3H, Me). ^{13}C NMR (101 MHz, CD_3OD) δ 152.1, 139.3, 126.1, 121.8, 118.5, 115.6, 96.4, 77.5, 73.8, 70.3, 70.0, 61.2, 57.4, 40.0, 19.9. $[\alpha]_D^{20}$= -7.8 (c=1, $CHCl_3$); MS: m/z calcd for $[M + Na]^+$ = 319, $[M + K]^+$ = 335; found $[M + Na]^+$ = 319.4, $[M + K]^+$ = 335.

5.8.3. Synthetic strategy for fluorescent compounds 71-74

Compound 78

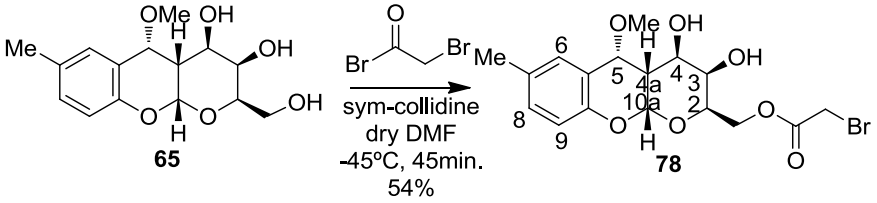

Scheme 5.3

To a solution of compound **65** (90 mg, 0.303 mmol) and 2,4,6-trimethylpyridine (0.424 mmol, 56 μL) in dry DMF (1.68 mL) with stirring at -45ºC a solution of bromoacetyl bromide (0.394 mmol, 34 μL) in dry toluene (200 μL) was added. Stirring was continued for 40 min. at -45ºC, and the mixture was allowed to warm to room temperature. Toluene (12 mL) was added, and the solid filtered off, and the filtrate concentrated. The residue was purified by flash chromatography [toluene/EtOAc (7:3) and EtOAc], affording 54% (68 mg) of a white solid. ^{1}H NMR (400 MHz, $CDCl_3$) δ 7.22 (bs, 1H, H-6), 7.02 (d, *J* = 8.2 Hz,

1H, H-8), 6.74 (d, *J* = 8.2 Hz, 1H, H-9), 5.55 (d, *J* = 3.0 Hz, 1H, H-10a), 4.81 (d, *J* = 4.7 Hz, 1H, H-5), 4.49 – 4.50 (m, 1H, C*H*$_2$O), 4.28 (t, *J* = 6.0 Hz, 1H, H-2), 4.04 – 3.95 (m, 1H, H-4), 3.95 – 3.84 (m, 3H, C*H*$_2$Br and H-3), 3.73 (s, 3H, OC*H*$_3$), 2.98 – 2.82 (m, 1H, H-4a), 2.30 (s, 3H, C*H*$_3$).^{13}C NMR (101 MHz, CD_3OD) δ 171.7, 153.7, 134.3, 133.5, 130.4, 125.0, 119.1, 100.2, 81.3, 75.2, 74.1, 73.9, 68.8, 61.41, 52.39, 52.2, 51.9, 51.7, 51.5, 51.3, 51.1, 43.8, 29.2, 23.5.

Compound 71

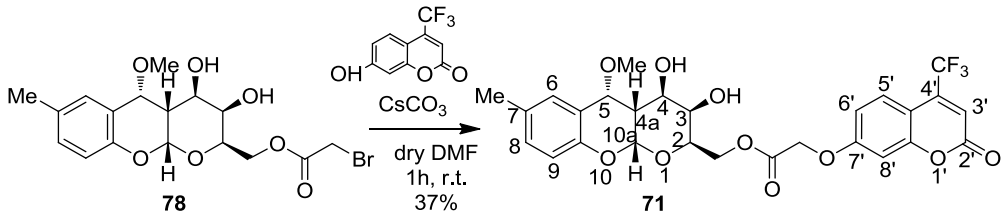

Scheme 5.4

A solution of 4-trifluoromethyl-7-hydroxycoumarin (41 mg, 0.18 mmol) in dry DMF (2 mL) was added to a stirred solution of compound **78** (50 mg, 0.12 mmol) in dry DMF (1 mL). To the reaction mixture was added $CsCO_3$ (43 mg, 0.13 mmol) and the resulting solution was stirred at rt for 1 h, after which was poured into a solution of CH_2Cl_2-H_2O. The organic phase was washed with 1 M NaOH solution (1 mL) and aqueous layer was washed with CH_2Cl_2 (5 mL). The combined organic layers were dried and concentrated under reduce pressure. The crude product was purified by flash chromatography [toluene/EtOAc (6:4)], affording 37% (25 mg) of a white powder. ^{1}H NMR (400 MHz, DMSO) δ 7.61 (d, *J* = 9.0 Hz, 1H, H-5´), 7.25 – 7.12 (m, 2H, H-8´,H-6), 7.09 (dd, *J* = 9.0, 2.3 Hz, 1H, H-6´), 6.95 (d, *J* = 8.4 Hz, 1H, H-8), 6.86 (s, 1H, H-3´), 6.63 (d, *J* = 8.4 Hz, 1H, H-9), 5.57 (d, *J* = 2.5 Hz, 1H, H-10a), 5.03 (s, 2H, -OCOC*H*$_2$-), 4.82 (d, *J* = 4.7 Hz, 1H, H-5), 4.39 – 4.26 (m, 1H, C*H*$_2$), 4.30 – 4.2 (m, 2H, C*H*$_2$, H-3), 4.10 – 3.98 (m, 1H, H-2), 3.62 – 3.54 (m, 1H, H-4), 3.53 (s, 3H, OC*H*$_3$), 2.90 – 2.76 (m, 1H, H-4a), 2.21 (s, 3H, C*H*$_3$).

Compound 79

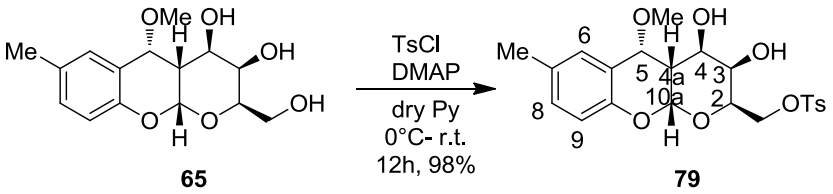

Scheme 5.5

A solution of compound **65** (482 mg, 1.63 mmol) in dry pyridine (3.3 mL) was cooled to 0ºC in an ice bath with stirring. A solution of *p*-toluenesulfonyl chloride (574 mg, 3 mmol) in dry pyridine (3.8 mL) was then added dropwise and stirring was continued at rt until the reaction seemed completed by TLC. After 12h, the solvent was then removed in vacuum to afford a crude product which was purified by flash chromatography, [petroleum ether/ EtOAc (5:5)], yielding 98% (719 mg) of a white powder. ^{1}H NMR (400 MHz, $CDCl_3$) δ 7.83 (d, *J* = 8.1 Hz, 2H, OTs), 7.34 (d, *J* = 8.1 Hz, 2H, OTs), 7.19 (bs, 1H, H-6), 7.01 (d, *J* = 8.3 Hz, 1H, H-8), 6.71 (d, *J* = 8.3 Hz, 1H, H-9), 5.46 (d, *J* = 2.8 Hz, 1H, H-10a), 4.76 (d, *J* = 5.0 Hz, 1H, H-5), 4.39 - 4.21 (m, 2H, C*H*$_2$O), 3.94 (m, 2H, H-4 and H-2), 3.83 (s, 1H, H-3), 3.69 (s, 3H, OMe), 2.82 (m, 1H, H-4a), 2.44 (s, 3H, Me), 2.29 (s, 3H, C*H*$_3$).^{13}C NMR (101 MHz, $CDCl_3$) δ 149.6, 145.1, 133.1, 131.1, 130.5, 130.1, 128.3, 126.7, 120.0, 116.1, 95.9, 78.5, 77.5, 77.2, 76.9, 69.5, 68.9, 66.9, 66.6, 59.6, 34.7, 21.8, 20.8. $[\alpha]_D^{20}$= +4,1 (c=1, CH_3CH_2OH); MS: m/z calcd for $[M + Na]^+$ = 474; found $[M + Na]^+$ = 473.

Compound 80

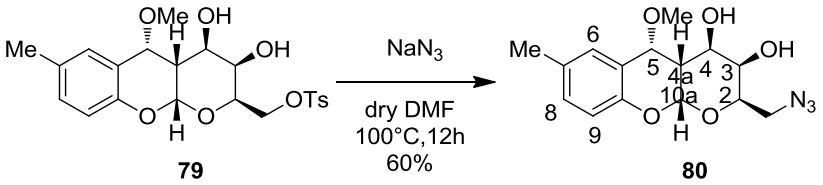

Scheme 5.6

To a solution of compound 7**9** (100 mg, 0.22 mmol) in dry DMF (1 mL), a solution of NaN_3 (101 mg, 1.55 mmol) in dry DMF (0.5 mL) was added and stirring was continued at 100ºC for 12 h. Upon cooling to rt, the colorless precipitate was filtrate ad the solvent was evaporated to dryness. The crude product was purified by flash chromatography, [petroleum ether/EtOAc (6:4)] affording 60% (42 mg) of a white powder. ^{1}H NMR (400 MHz, $CDCl_3$) δ 7.22 (bs, 1H, H-6), 7.02 (d, *J* = 8.1 Hz, 1H, H-8), 6.75 (d, *J* = 8.1 Hz, 1H, H-9), 5.56 (d, *J* = 2.7 Hz, 1H, H-10a), 4.80 (d, *J* = 5.0 Hz, 1H, H-5), 4.16 (t, *J* = 5.9 Hz,

1H, H-2), 3.98 (d, *J* = 2.9 Hz, 1H, H-4), 3.83 (s, 1H, H-3), 3.72 (s, 3H, OCH_3), 3.71 – 3.66 (m, 1H, CH_2O), 3.51 (dd, *J* = 12.7, 5.9 Hz, 1H, CH_2O), 2.93-2.84 (m, 1H, H-4a), 2.30 (s, 3H, CH_3). ^{13}C NMR (101 MHz, $CDCl_3$) δ 149.7, 131.1, 130.5, 126.7, 120.1, 116.1, 96.1, 78.5, 77.5, 77.2, 76.9, 70.6, 67.3, 67.2, 59.7, 51.5, 34.6, 20.9. $[\alpha]_D^{20}$= -10.3 (c=1, CH_3CH_2OH); MS: m/z calcd for $[M + Na]^+$ = 344; found $[M + Na]^+$ = 344.

Compound 81

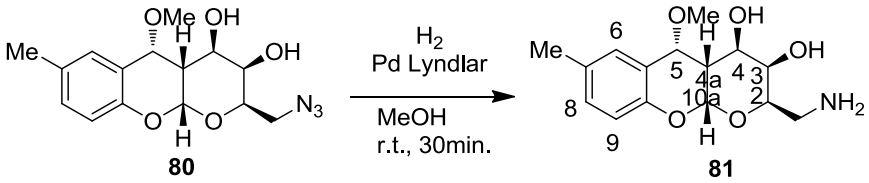

Scheme 5.7

To a solution of compound **80** (30 mg, 0.093 mmol) in MeOH (6 mL) was added Lindlar catalyst (5%), and the mixture was hydrogenated at 1 atm and rt for 30 min. Filtration and concentration gave amine **81** in a quantitative yield. ^{1}H NMR (400 MHz, CD_3OD) δ 7.23 (d, *J* = 2.4 Hz, 1H, H-6), 6.98 (d, *J* = 8.1 Hz, 1H, H-9), 6.64 (dd, *J* = 8.2, 2.4 Hz, 1H, H-8), 5.59 (d, *J* = 3.0 Hz, 1H, H-10a), 4.86 (d, *J* = 5.0 Hz, 1H, H-5), 3.97 – 3.90 (m, 1H, H-2), 3.88 – 3.77 (m, 1H, H-4), 3.74 (dd, *J* = 9.7, 5.3 Hz, 1H, H-3), 3.68 (s, 3H, OMe), 3.06 – 3.00 (m, 1H, CH_2O), 2.97 – 2.90 (m, 1H, H-4a), 2.87 (dd, *J* = 13.3, 4.7 Hz, 1H, CH_2O), 2.29 – 2.23 (m, 3H, CH_3).

Compound 82

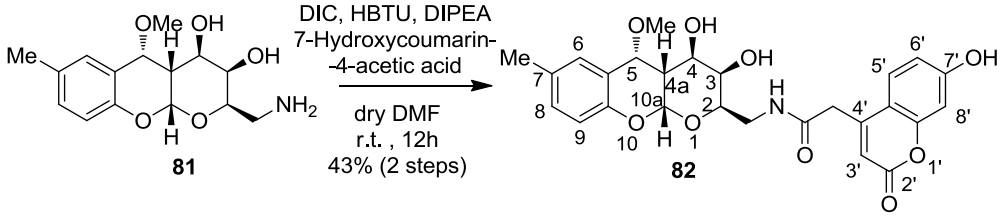

Scheme 5.8

Working in anhydrous conditions: Compound **81** (30 mg, 0.093 mmol), 7-hydroxycoumarin-4-acetic acid (24.6 mg, 0.112 mmol) and HBTU (53.1 mg, 0.14 mmol) were dissolved in dry DMF (1.3 mL). To this reaction mixture DIPEA (48 µL, 0.28 mmol) was added at rt and after 10 min. DIC (0.14 mmol, 22 µL) was added at 0ºC. The final reaction mixture was stirred at room temperature until the reaction seemed completed by TLC. After 12 h, the solvent was then removed in vacuum to afford a crude product, which

was purified by flash chromatography, [$CHCl_3$/MeOH (9.5:0.5)], yielding 43% (20 mg) of a white solid. ^{1}H NMR (400 MHz, CD_3OD) δ 7.59 (d, *J* = 8.8 Hz, 1H, H-5'), 7.23 (bs, 1H, H-6), 6.97 (d, *J* = 7.5 Hz, 1H, H-8), 6.76 (d, *J* = 8.8 Hz, 1H, H-6'), 6.68 – 6.58 (m, 2H, H-9 and H-8'), 6.16 (bs, 1H, H-3'), 5.54 (d, *J* = 2.8 Hz, 1H, H-10a), 4.85 (d, *J* = 4.9 Hz, 1H, H-5), 4.02 (m, 1H, H-2), 3.81-3.71 (m, 3H, H-4 and C*H*$_2$C=O), 3.67 (bs, 4H, OC*H*$_3$ and H-3), 3.57 (dd, *J* = 13.8, 4.5 Hz, 1H, C*H*$_2$O), 3.44 (dd, *J* = 13.5, 8.5 Hz, 1H, C*H*$_2$O), 2.90 – 2.84 (m, 1H, H-4a), 2.26 (s, 3H, C*H*$_3$).^{13}C NMR (101 MHz, CD_3OD) δ 170.4, 162.9, 156.0, 150.0, 130.2, 129.6, 126.3, 126.2, 120.9, 115.2, 114.7, 110.7, 110.4, 102.9, 96.6, 77.6, 70.5, 68.1, 67.1, 67.0, 57.6, 48.4, 48.2, 48.0, 47.8, 47.6, 47.4, 47.2, 40.7, 34.4, 29.6, 19.6. $[\alpha]_D^{20}$= +16.6 (c=1, CH_3CH_2OH); MS: m/z calcd for $[M + Na]^+$ = 521; found $[M + Na]^+$ = 520.

Compound 82

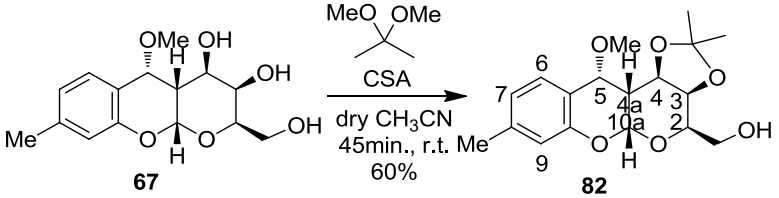

Scheme 5.9

To a solution of compound **67** (500 mg, 1.69 mmol) in dry CH_3CN (8.0 mL), acetone dimethylacetal (6.76 mmol, 0.4 mL) and CSA (1% mmol) were added under argon. The reaction mixture remained under magnetic stirring for 45 min. at room temperature, after which was added Et_3N to neutralize the CSA. The reaction was then concentrated under reduce pressure and the crude product purified by flash chromatography, [petroleum ether/EtOAc (6:4)] affording 60% (336 mg) of a yellow solid. ^{1}H NMR (400 MHz, CD_3OD) 7.30 (d, *J* = 7.9 Hz, 1H, H-6), 6.78 (d, *J* = 7.9 Hz, 1H, H-7), 6.63 (bs, 1H, H-9), 5.52 (d, *J* = 3.8 Hz, 1H, H-10), 4.68 (d, *J* = 5.2 Hz, 1H, H-5), 4.32 – 4.29 (m, 1H, H-2), 4.15 (dd, *J* = 5.6, 2.4 Hz, 1H, H-3), 4.12 – 4.06 (m, 1H, H-4), 3.80 (dd, *J* = 6.1, 3.5 Hz, 2H, C*H*$_2$O), 3.54 (s, 3H, OC*H*$_3$), 2.79 – 2.66 (m, 1H, H-4a), 2.26 (s, 3H, Ar C*H*$_3$), 1.53 (s, 3H, C*H*$_3$), 1.29 (s, 3H, C*H*$_3$). ^{13}C NMR (101 MHz, CD_3OD) δ 152.1, 139.1, 127.0, 121.8, 118.7, 115.8, 108.6, 95.5, 75.2, 71.4, 70.8, 69.4, 61.4, 55.9, 48.2, 48.0, 47.7, 47.5, 47.3, 47.1, 46.9, 37.6, 26.9, 24.8, 19.7. MS: m/z calcd for $[M + Na]^+$ = 359; found $[M + Na]^+$ = 359.

Compound 84

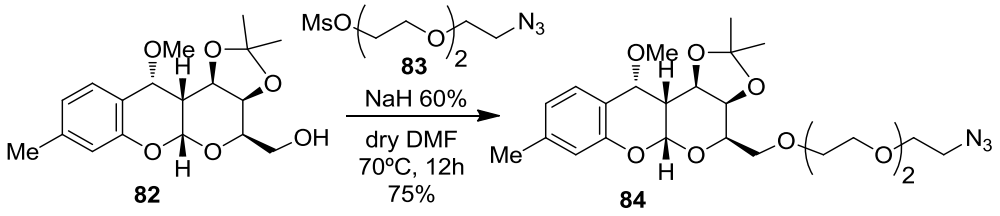

Scheme 5.10

To a 60 % suspension of sodium hydride in oil (75 mg, 2,67 mmol) an argon atmosphere dry DMF (10 mL) was added. The suspension was cooled to 0ºC with stirring and a solution of compound **83** (300 mg, 0.89 mmol) in dry DMF (3 ml) and compound **84** (570 mg, 1.79 mmol) in dry DMF (3 mL) were added. The mixture was stirred at 70ºC for 12 h. After cooling to 0ºC, the reaction was quenched by slowly addition of MeOH (4 mL) and stirred for more 20 min. The reaction mixture was diluted with EtOAc, and washed with water, dried (Na_2SO_4) and concentrated. The residue was purified by flash chromatography, [petroleum ether/EtOAc (3:7)], yielding 75% of a brownish oil. MS: m/z calcd for $[M + Na]^+ = 516$; found $[M + Na]^+ = 516$.

Compound 85

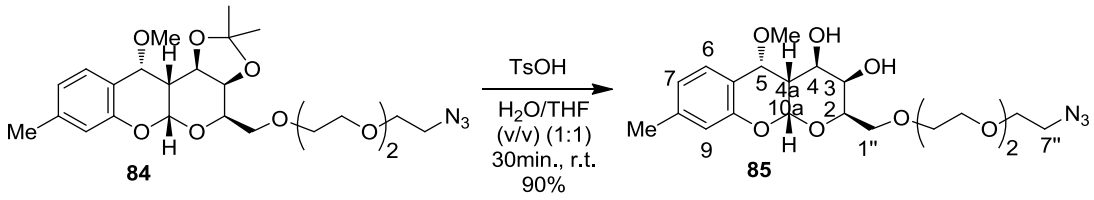

Scheme 5.11

To a solution of compoud **84** (100 mg, 0.22 mmol) in CH_3CN:H_2O (10:2) (10 mL), *p*-toluenesulfonic acid (0.42 mg, 0.002 mmol) was added. The final reaction mixture was stirred at room temperature until the reaction seemed completed by TLC. After 30 min., Et_3N is added and the solvent was then removed in vacuum to afford a crude product which was purified by flash chromatography, [petroleum ether/EtOAc (2:8)], yielding 90% of a brownish oil. ^{1}H NMR (400 MHz, $CDCl_3$) δ 7.29 (d, *J* = 7.7 Hz, 1H, H-6), 6.79 (d, *J* = 7.7 Hz, 1H, H-7), 6.65 (bs, 1H, H-9), 5.57 (d, *J* = 2.8 Hz, 1H, H-10a), 4.79 (s, 3H, OC*H*$_3$), 4.19 (t, *J* = 5.4 Hz, 1H, H-2), 4.01 – 3.90 (m, 2H, H-3, H-4), 3.83 (dd, *J* = 9.0, 5.7 Hz, 2H, H-1''), 3.77 – 3.57 (m, 13H, triethyleneglycol, C*H*$_3$O), 3.40 (t, *J* = 5.0 Hz, 2H, H-7''), 2.94 (dd, *J* = 11.5, 2.8 Hz, 2H, H-4a), 2.29 (s, 3H, C*H*$_3$). ^{13}C NMR (101 MHz, $CDCl_3$) δ 151.71,

139.79, 126.07, 122.23, 117.45, 116.30, 96.15, 78.29, 78.29, 77.33, 77.33, 77.01, 77.01, 76.69, 76.69, 70.63, 70.42, 70.02, 67.37, 67.12, 59.27, 50.66, 34.58, 29.69.

Compound 86

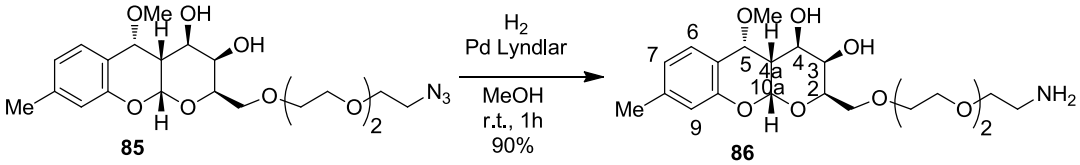

Scheme 5.12

To a solution of compound **85** (80 mg, 0.20 mmol) in $CHCl_3$:MeOH (1:1) (5 mL) was added Lindlar catalyst (5%), and the mixture was hydrogenated at 1 atm and rt for 1h. Filtration and concentration gave amine **86** in 90% yield as a yellow oil. ^{1}H NMR (400 MHz, $CDCl_3$) δ 7.29 (d, *J* = 7.8 Hz, 1H, H-6), 6.78 (d, *J* = 7.7 Hz, 1H, H-7), 6.64 (bs, 1H, H-9), 5.57 (d, *J* = 2.2 Hz, 1H, H-10a), 4.78 (d, *J* = 4.4 Hz, 1H, H-5), 4.17 (t, *J* = 5.6 Hz, 1H, CH_{2PEG}), 4.00 – 3.58 (m, 15H, H-2, H-3, H-4, CH_2O, 5 CH_{2PEG}, CH_3O), 3.54 (t, *J* = 4.7 Hz, 2H, CH_{2PEG}), 3.05 – 2.94 (m, 1H, H-4a), 2.88 (bs, 2H, CH_{2PEG}), 2.28 (s, 3H, CH_3). ^{13}C NMR (101 MHz, $CDCl_3$) δ 149.18, 137.10, 123.49, 119.60, 115.04, 113.67, 93.76, 75.59, 74.76, 74.45, 74.13, 69.93, 68.25, 67.99, 67.93, 67.92, 67.75, 67.57, 64.57, 64.28, 56.63, 38.73, 32.05, 18.59. MS: m/z calcd for $[M + H]^+$ = 429; found $[M + H]^+$ = 4289

Compound 73

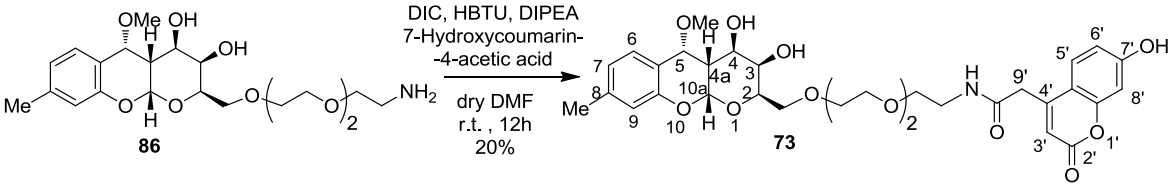

Scheme 5.13

Working in anhydrous conditions, compound **86** (50 mg, 0.13 mmol), 7-hydroxycoumarin-4-acetic acid (31 mg, 0.16 mmol) and HBTU (68.26 mg, 0.20 mmol) were dissolved in dry DMF (2 mL). To this reaction mixture DIPEA (0.39 mmol, 67 µL) was added at rt and after 10 min. DIC (0.20 mmol, 31 µL) was added at 0ºC. The final reaction mixture was stirred at room temperature until the reaction seemed completed by TLC. After 12 h, the solvent was then removed in vacuum to afford a crude product which was purified by flash chromatography, CH_2Cl_2/acetone (5:5), yielding 20% (15 mg) of a brown color solid. ^{1}H

NMR (400 MHz, CD_3OD) δ 7.61 (d, *J* = 9.0 Hz, 1H, H-5'), 7.28 (d, *J* = 8.0 Hz, 1H, H-6), 6.80 (dd, *J* = 9.0, 2.1 Hz, 1H, H-6'), 6.75 (d, *J* = 8.0 Hz, 1H, H-7), 6.70 (d, *J* = 2.1 Hz, 1H, H-8'), 6.56 (s, 1H, H-3'), 6.19 (bs, 1H, H-9), 5.54 (d, *J* = 3.0 Hz, 1H, H-10a), 4.10 (t, *J* = 5.7 Hz, 1H, CH_{2PEG}), 4.86 (1H, H-5, under H_2O signal), 3.85 – 3.48 (m, 18H, H-9', H-2. H-3, H-4, 4 CH_{2PEG}, OCH_3, CH_2O), 3.43 – 3.38 (m, 2H, CH_{2PEG}), 2.97 – 2.83 (m, 1H, H-4a), 2.24 (s, 3H, CH_3). ^{13}C NMR (101 MHz, CD_3OD) δ 169.56, 162.02, 161.61, 155.36, 151.85, 151.24, 139.06, 126.13, 125.72, 121.57, 118.06, 115.39, 112.97, 111.71, 111.59, 102.21, 96.44, 77.34, 70.81, 70.39, 70.30, 70.17, 70.09, 69.85, 68.94, 67.39, 66.91, 57.44, 48.21, 47.99, 47.78, 47.57, 47.35, 47.14, 46.93, 39.37, 38.78, 34.30, 19.77. MS: m/z calcd for $[M + H]^+$ = 629; found $[M + Na]^+$ = 629.

Compound 74

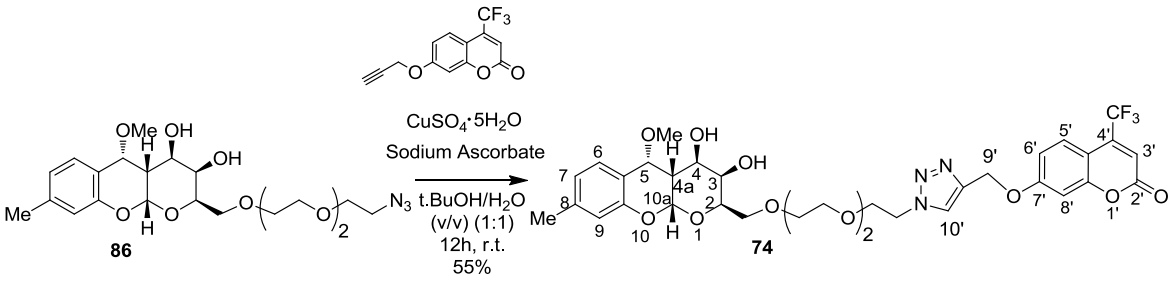

Scheme 5.14

To a vigorously stirring suspension of compound **86** (72 mg, 0.27 mmol) in 1:1 *t*-BuOH/H_2O, copper(II) sulfate pentahydrate (9 mg, 0.035 mmol) and sodium ascorbate (14 mg, 0.069 mmol) were added. The reaction mixture was stirred for 10 min at room temperture and then compound **76** (110 mg, 0.23 mmol) was added. The suspension was stirred vigorously at rt for 12 h. At this time TLC indicated completion of the reaction. Distilled water was added, and the aqueous layer was extracted with CH_2Cl_2. The combined extracts were dried, filtered and evaporated to afford a brownish oily solid. The product was then purified using column chromatography using $CHCl_3$ as eluant, which afforded the expected compound **74** as a brownish solid in 55% yield.^{1}H NMR (400 MHz, CD_3OD) δ 8.26 (s, 1H, H-10'), 7.65 (dd, *J* = 9.0, 1.8 Hz, 1H, H-5'), 7.25 (d, *J* = 7.8 Hz, 1H, H-6), 7.14 (d, *J* = 2.5 Hz, 1H, H-8'), 7.07 (dd, *J* = 9.0, 2.5 Hz, 1H, H-6'), 6.72 (d, *J* = 7.8 Hz, 1H, H-7), 6.68 (s, 1H, H-3'), 6.47 (bs, 1H, H-9), 5.52 (d, *J* = 3.0 Hz, 1H, H-10a), 5.32 (s, 2H, H-9'), 4.80 (d, *J* = 4.8 Hz, 1H, H-5), 4.67 – 4.57 (m, 2H, H-6''), 4.08 (t, *J* = 5.9 Hz, 1H, H-2''), 3.95 – 3.87 (m, 2H, H-7''), 3.79 – 3.52 (m, 15H, H-3'',H-4'', H-

5'', H-1'', H-2, H-3, H-4, OCH_3), 2.95 – 2.85 (m, 1H, H-4a), 2.22 (s, 3H, ArCH_3).^{13}C NMR (400 MHz, CD_3OD) δ 162.3, 156.2, 151.8, 142.2, 139.0, 125.9, 125.7, 125.5, 121.8, 112.2, 115.4, 113.6, 107.0, 102.2, 96.4, 76.3, 70.9, 70.5, 70.3, 70.4, 70.1, 70.0, 68.8, 67.4, 66.9, 66.9, 61.6, 61.6, 57.4, 50.1, 34.3, 19.7. ^{19}F NMR (400 MHz, CD_3OD) δ -62.2 MS: m/z calcd for $[M + H]^+$ = 722; found $[M + H]^+$ = 722

5.8.4. Synthetic strategy for tricyclic derivative 93 for the assembly of liposomes

Compound 88

Acording to literature procedure:[98]

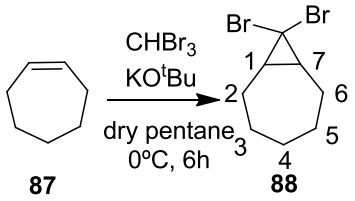

Scheme 5.15

A stirred suspension of *cis*-cycloheptene **87** (1.92 g, 20.0 mmol) and potassium *t*-butoxide (2.58 g, 23.0 mmol) in anhydrous pentane (50 mL) was cooled to 0 °C. A solution of bromoform (1.75 mL, 20.0 mmol) in anhydrous pentane (50 mL) was added dropwise over a period of 6 h at 0 °C under argon. After complete addition the resulting brown mixture was warmed to room temperature and stirred overnight. After addition of water (200 mL and neutralization with conc. HCl, the aqueous layer was extracted with pentane (3 x 30 mL). The combined organic layers were washed with water (3 x 30 mL) and dried over Na_2SO_4. Evaporation of the solvent under high vacuum gave crude product **88** as brown oil. ^{1}H NMR (400 MHz, $CDCl_3$) δ 2.33–2.21 (m, 2H, H-2a, H-6a), 1.94–1.78 (m, 3H, H-3a, H-4a, H-5a), 1.76–1.66 (m, 2H, H-1, H-7), 1.43–1.31 (m, 2H, H-3b, H-5b), 1.24–1.09 (m, 3H, H-2b, H-4b, H-6b).^{13}C NMR (101 MHz, $CDCl_3$) δ 40.9, 34.9, 32.4, 29.1, 28.2.

Compound 89

Acording to literature procedure:[98]

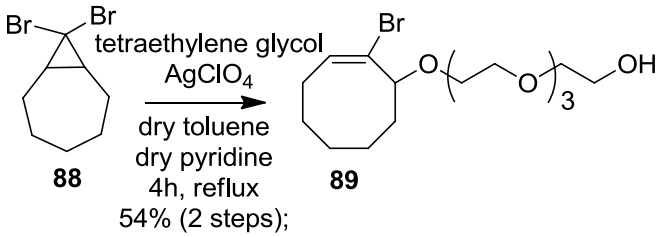

Scheme 5.16

Tetraethyleneglycol (24 mL, 139 mmol) and $AgClO_4$ (5.7 g, 139 mmol) dissolved in dry toluene (12 mL) were added to a solution of **88** (2.48 g, 9.25 mmol) in a mixture of dry toluene (5 mL) and dry pyridine (6.6 mL). The reaction was refluxed in the dark for 4 h and the solvent was evaporated. Then, brine (200 mL) was added, the insoluble silver salts were removed by filtration, and the aqueous phase was extracted with Et_2O (7x100 mL). The combined organic layer was washed with brine (140 mL) and H_2O (140 mL), dried (Na_2SO_4), and concentrated. The crude product was purified by flash chromatography [(petroleum ether/ EtOAc 3:7)] to give **89** in 54% yield (over two steps) as yellow pailed oil. ^{1}H NMR (400 MHz, $CDCl_3$) δ 6.18 (dd, *J* = 11.8, 4.1 Hz, 1H, C*H*=CBr), 3.92 (dd, *J* = 10.4, 4.9 Hz, 1H, C*H*O$_{propargyl}$), 3.79 – 3.64 (m, 13H, C*H*$_{2PEG}$), 3.64 – 3.57 (m, 2H, C*H*$_{2PEG}$), 3.57 – 3.40 (m, 1H, C*H*$_{2PEG}$), 2.73 (qd, *J* = 11.8, 5.5 Hz, 1H, C*H*$_{2ring}$), 2.35 – 2.14 (m, 2H, C*H*$_{2ring}$), 2.10 – 1.95 (m, H, C*H*$_{2ring}$), 1.96 – 1.80 (m, 2H, C*H*$_{2ring}$), 1.80 – 1.63 (m, 1H, C*H*$_{2ring}$), 1.48 (dq, *J* = 11.5, 5.0 Hz, 1H, C*H*$_{2ring}$), 1.36 – 1.19 (m, 1H, C*H*$_{2ring}$), 0.88 – 0.69 (m, 1H, C*H*$_{2ring}$). ^{13}C NMR (101 MHz, CDCl3) δ 131.8, 85.5, 76.9, 72.8, 70.8, 70.8, 70.6, 70.5, 68.2, 68.1, 61.9, 39.7, 28.3, 26.6.

Compound 90

Acording to literature procedure:[98]

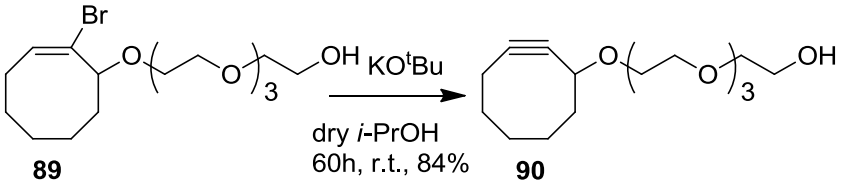

Scheme 5.17

KO^{t}Bu (1.066 g, 9.5 mmol) was added to a solution of **89** (1.45 g, 3.8 mmol) in a mixture of dry *i*-PrOH (29 mL)/ dry pyridine (4 mL). After 60 h of stirring at rt, the reaction was neutralized with 5% HCl and partitioned between CH_2Cl_2 and H_2O. Then, the aqueous layer was extracted with CH_2Cl_2 (7 x 30 mL), dried (Na_2SO_4), and concentrated under vacuum to give a crude product that was purified by column chromatography [gradient from petroleum ether/EtOAc 4:6 to EtOAc] to give **90** (1.337 g, 84%) as a yellow oil. ^{1}H NMR (400 MHz, $CDCl_3$) δ 4.26 – 4.11 (m, 1H, C*H*O$_{propargyl}$), 3.76 – 3.54 (m, 15H, C*H*$_{2PEG}$), 3.53 – 3.42 (m, 1H, C*H*$_{2PEG}$), 2.94 (br s, 1H, O*H*), 2.29 – 2.18 (m, 1H, C*H*$_{2ring}$), 2.19 – 2.04 (m, 2H, C*H*$_{2ring}$), 2.03 – 1.85 (m, 2H, C*H*$_{2ring}$), 1.85 – 1.73 (m, 2H, C*H*$_{2ring}$), 1.71 – 1.52 (m, 2H, C*H*$_{2ring}$), 1.46 –1.33 (m, 1H, C*H*$_{2ring}$). ^{13}C NMR (101 MHz, $CDCl_3$) δ 100.5, 92.8, 73.0, 73.0, 70.8, 70.7, 70.6, 70.5, 70.3, 68.6, 61.8, 42.3, 34.4, 29.9, 26.5, 20.9.

Compound 91

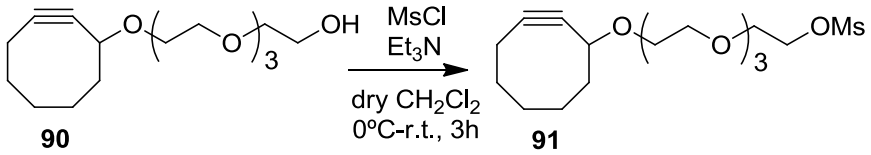

Scheme 5.18

To a solution of alcohol **90** (540 mg, 1.80 mmol) and dry triethylamine (0.376 mL, 2.70 mmol) in dry CH_2Cl_2 (8.5 mL), kept to 0ºC, was added mesyl chloride (0.167 mL, 2.16 mmol). The reaction was maintained at 0ºC during the first hour, followed by warming to room temperature, under vigorous stirring and argon atmosphere for 3 h. At the end of this time the solution was extracted with CH_2Cl_2 and the combined organic extracts were washed with a 10% aqueous HCl, brine, dried over sodium sulfate and evaporated. The obtained residue was used without further purification

Compound 92

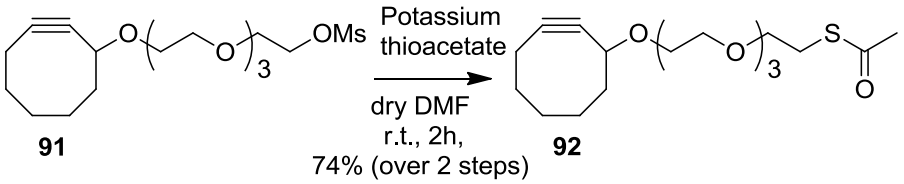

Scheme 5.19

Potassium thioacetate (393 mg, 3.44 mmol) was added to a stirred mixture of compound **91** (620 mg, 1.64 mmol) in dry DMF (8 mL). The resulting mixture was stirred at rt for

2 h. After removal of solvent under vacuum, the residue was purified by flash column chromatography on silica gel [(petroleum ether/ EtOAc 6:4)] to give compound **92** as an yellow oil (473 mg, 74% over 2 steps). ^{1}H NMR (400 MHz, $CDCl_3$) δ 4.20 (dd, *J* = 7.0, 5.3 Hz, 1H C*H*O$_{propargyl}$), 3.75 – 3.55 (m, 13H, C*H*$_{2PEG}$), 3.53 – 3.45 (m, 1H, C*H*$_{2PEG}$), 3.07 (t, *J* = 6.4 Hz, 2H, SC*H*$_{2PEG}$), 2.32 (s, 3H, C*H*$_3$), 2.30 – 2.05 (m, 3H C*H*$_{2ring}$), 2.00 – 1.86 (m, 2H, C*H*$_{2ring}$), 1.86 – 1.74 (m, 2H, C*H*$_{2ring}$), 1.72 – 1.51 (m, 2H, C*H*$_{2ring}$), 1.50 – 1.31 (m, 1H, C*H*$_{2ring}$).

Compound 93

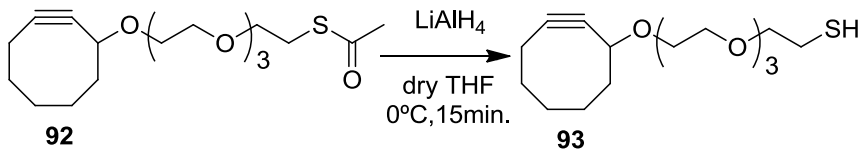

Scheme 5.20

To a stirred solution of the thioacetate **92** (50 mg, 0.14 mmol) in anhydrous THF (1.5 ml) at 0 °C was added $LiAlH_4$ (26 mg, 0.7 mmol) under an Ar atmosphere. The mixture was stirred at 0 °C for 15 min. Then, water was added and the aqueous phase was extracted with CH_2Cl_2. The combined organic layer was dried (Na_2SO_4), and concentrated under reduce pressure to give the crude thiol **93** as yellow oil. MS: m/z calcd for $[M + H]^+$ =317.46, $[M + Na]^+$ =339.46, $[M + K]^+$ =355; found $[M + H]^+$ = 318, $[M + Na]^+$ =339, $[M + K]^+$ =355.

Compound 94

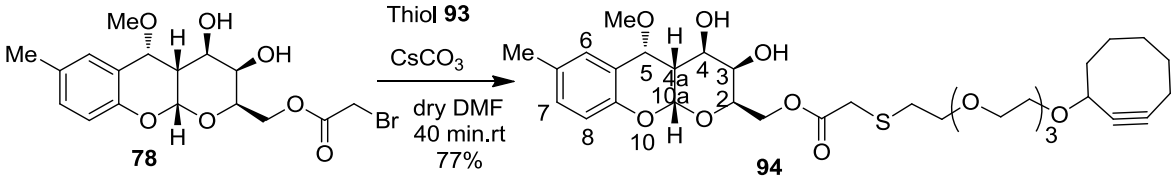

Scheme 5.21

A solution of the crude thiol **93** (74 mg, 0.24 mmol) in dry DMF (1 mL) was added to a solution of compound **78** (65 mg, 0.16 mmol) in dry DMF (1.0 mL). To the mixture was added $CsCO_3$ (57 mg, 0.176 mmol) and the resultant solution was stirred at room temperature for 40 min., after which was poured into CH_2Cl_2-H_2O mixture. The aqueous phase was extracted with CH_2Cl_2 (3 x 5 mL), and the combined organic layers were dried over Na_2SO_4 and concentrated under reduce pressure. The residue was purified by flash

chromatography [(toluene/EtOAc 7:3)] affording **94** (80 mg, 77%) as yellow pailed solid. ^{1}H NMR (400 MHz, $CDCl_3$) δ 7.21 (bs, 1H, H-6), 7.01 (dd, *J* = 7.9, 1.0 Hz, 1H, H-8), 6.72 (d, *J* = 7.9 Hz, 1H, H-9), 5.54 (d, *J* = 2.7 Hz, 1H, H-10a), 4.80 (d, *J* = 5.0 Hz, 1H, H-4a), 4.54 – 4.36 (m, 2H, H-1‘‘), 4.33 – 4.18 (m, 2H, H-2, C$H_{propargyl}$), 4.00 (d, *J* = 3.0 Hz, 1H, H-4), 3.88 (bs, 1H, H-3), 3.83 – 3.57 (m, 16H, CH_{2PEG}, OCH_3), 3.57 – 3.45 (m, 1H, CH_{2PEG}), 3.35 (s, 2H, SCH_2CO), 3.00 – 2.78 (m, 3H, H-5, SCH_{2PEG}), 2.31 (s, 3H, CH_3), 2.26 – 2.06 (m, 3H, CH_{2ring}), 2.04 – 1.88 (m, 2H, CH_{2ring}), 1.90 – 1.74 (m, 2H, CH_{2ring}), 1.74 – 1.53 (m, 2H, CH_{2ring}), 1.50 – 1.34 (m, 1H, CH_{2ring}).^{13}C NMR (101 MHz, $CDCl_3$) δ 170.6, 158.7, 149.7, 131.0, 130.5, 126.7, 120.1, 116.1, 100.2, 96.1, 93.1, 78.5, 72.9, 70.8, 70.6, 70.6, 69.7, 68.7, 67.1, 67.1, 64.6, 59.7, 46.3, 42.5, 34.7, 34.5, 34.1, 32.1, 29.1, 26.6, 20.1, 20.9.

5.8.5. Synthetic strategy for compound 6a

Compound 99

Acording to literature procedure:[153]

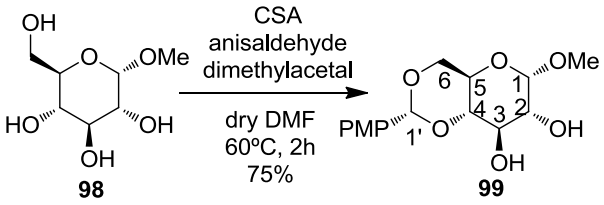

Scheme 5.22

Methyl *α*-D-glucopyranoside **98** (10 g, 51.5 mmol) and anisaldehyde dimethylacetal (9.63 mL, 56.6 mmol) are dissolved in dry DMF (40 mL). Camphorsulfonic acid (CSA) (0.01 equiv.) is added and the flask is attached to a rotary evaporator, rotated, evacuated, and lowered into a water bath at approximately 60ºC to remove the methanol, which is formed during the reaction. After 1 h, all the DMF is removed by evaporation. Then a solution of sodium hydrogen carbonate (1 g in 50 mL of water) is added to the residue, and the mixture is heated at 100ºC until the product is finely dispersed. The mixture is cooled to room temperature, and the product filtered off, washed thoroughly with water, and dried. ^{1}H NMR (400 MHz, DMSO) δ 7.34 (d, *J* = 8.4 Hz, 2H, Ar-*H*), 6.89 (d, *J* = 8.4 Hz, 2H, Ar-*H*), 5.48 (s, 1H, H-1’), 5.19 (s, 1H, OH), 5.03 (s, 1H, OH), 4.60 (d, *J* = 3.2 Hz, 1H, H-1),

4.12 (dd, *J* = 9.9, 4.4 Hz, 1H, H-6), 3.72 (s, 3H, OMe), 3.64 (t, *J* = 9.9 Hz, 1H, H-6), 3.59 – 3.50 (m, 2H, H-5, H-3), 3.37 – 3.26 (m, 5H, OC*H*$_3$, H-2, H-4). ^{13}C NMR (101 MHz, DMSO) δ 164.9, 135.6, 133.1, 118.7, 106.2, 105.9, 86.7, 77.8, 75.3, 73.6, 67.8, 60.5, 60.2, 45.6, 45.3, 45.1, 44.9, 44.7, 44.5, 44.3.

Compound 100

Acording to literature procedure:[153]

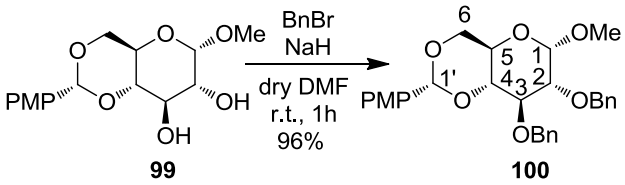

Scheme 5.23

A stirred solution of **99** (10 g, 0.032 mol) in anhydrous DMF (100 mL) under argon at 0 ºC was treated with of NaH (60% in mineral oil, 3.8 g, 0.096 mol). After 15 min. at room temperature, the mixture was treated dropwise and rapidly with BnBr (0.096 mol, 11 mL) and then allowed to stand for 1 h at rt. The mixture was diluted with EtOAc (40 mL), and washed with saturated $NaHCO_3$ solution (70 mL). The aqueous phase was back-extracted with EtOAc (3 x 30 mL), and all the organic fractions were combined, washed with brine, and dried over anhydrous Na_2SO_4. The residue was recrystallize from toluene to give **100** (15.2 g, 96% yield) as a white solid. ^{13}C NMR (101 MHz, $CDCl_3$) δ 159.4, 139.0, 138.2, 130.2, 129.5, 128.8, 128.7, 128.4, 128.2, 128.2, 128.1, 128.0, 113.9, 98.4, 81.6, 79.7, 77.5, 77.2, 76.9, 75.6, 73.4, 73.4, 71.0, 70.0, 69.3, 55.4.

Compound 101

Acording to literature procedure:[153]

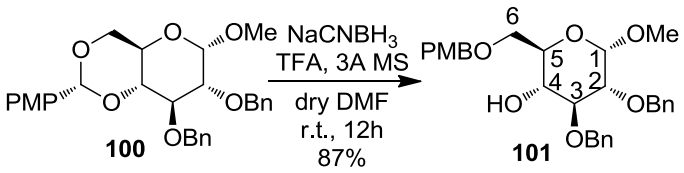

Scheme 5.24

A solution at 0ºC of trifluoroacetic acid (100 mmol, 7.40 mL) in dry DMF (40 mL) was added dropwise to a stirred solution containing compound **101** (5 g, 10 mol), $NaCNBH_3$ (3.142 g, 50 mmol) and 3Å MS in dry DMF (50 mL). After 12h at rt the mixture was

filtered through celite and powered into ice-cold saturated $NaHCO_3$. The aqueous phase was repeatedly extracted with EtOAc (3 x 30 mL). The combined extracts were washed with saturated aqueous $NaHCO_3$ (100 mL), dried over Na_2SO_4, filtered and concentrated under reduce pressure. The residue was purified by flash chromatography [(petroleum ether/ EtOAc 8:2)] do give 87% as green pale oil. ^{1}H NMR (400 MHz, $CDCl_3$) δ 7.42 – 7.19 (m, 12H, Ar-*H*), 6.85 (d, *J* = 8.7 Hz, 2H, Ar-*H*), 4.99 (d, *J* = 11.8 Hz, 1H, C*H*$_2$Ph), 4.77 (d, *J* = 12.3 Hz, 1H, C*H*$_2$Ph), 4.73 (d, *J* = 11.8 Hz, 1H, C*H*$_2$Ph), 4.65 (d, *J* = 12.3 Hz, 1H, C*H*$_2$Ph), 4.62 (d, *J* = 3.5 Hz, 1H, H-1), 4.51 (d, *J* = 11.8 Hz, 1H, C*H*$_2$Ph), 4.46 (d, *J* = 11.8 Hz, 1H, C*H*$_2$Ph), 3.83 – 3.74 (m, 4H, ArOMe, H-4), 3.73 – 3.66 (m, 1H, H-5), 3.66 – 3.60 (m, 2H, H-6), 3.62 – 3.56 (m, 1H, H-3), 3.52 (dd, *J* = 9.6, 3.5 Hz, 1H, H-2), 3.37 (s, 3H, OMe). ^{13}C NMR (101 MHz, $CDCl_3$) δ 159.4, 139.0, 138.2, 130.2, 129.5, 128.8, 128.6, 128.3, 128.2, 128.1, 128.0, 128.0, 113.9, 98.4, 81.6, 79.7, 77.5, 77.2, 76.9, 75.6, 73.4, 73.4, 71.0, 70.0, 69.3, 55.4.

Compound 102

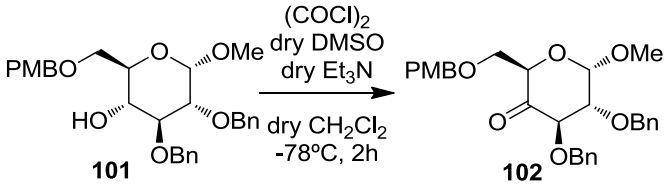

Scheme 5.25

To a solution of $(COCl)_2$ (46 mmol, 3.97 mL) in dry CH_2Cl_2 (92 mL) at -78ºC under argon atmosphere, a solution of anhydrous DMSO (92 mmol, 6.51 mL) in dry CH_2Cl_2 (20 mL) was added dropwise, and the resulting solution was stirred for 30 min. To the reaction flask, a solution of compound **101** (5.693 g, 11.5 mmol) in dry CH_2Cl_2 (20 mL) was added dropwise at -78ºC. This final reaction mixture stayed under magnetic stirring for 1 h at -78ºC. Then dry Et_3N (115 mmol, 13.91 mL) was added and the reaction stayed for more 30 min. under magnetic stirring, and then allowed to warm up until 0ºC. A saturated solution of NH_4Cl was added, and the reaction mixture was extracted with CH_2Cl_2 (x3). The organic extracts were dried over Na_2SO_4, filtered and concentrated under reduced pressure. The crude product was used without further purification.

Compound 103

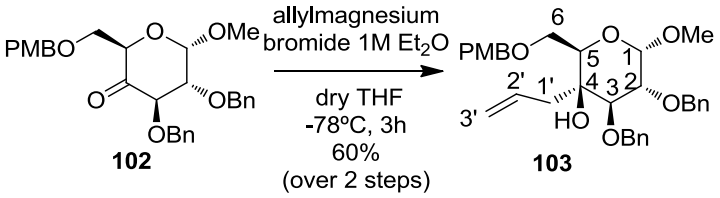

Scheme 5.26

To a solution of **102** (2.03 g, 4.12 mmol) in dry THF (20 mL) at -78ºC under argon atmosphere, a solution of allylmagnesium bromide (1 M in Et_2O) (8.24 mmol, 8.24 mL) was added dropwise. The resulting solution was stirred for 90 min. and then allowed to warm up until 0ºC. A saturated solution of NH_4Cl (60 mL) was added, and the reaction mixture was extracted with CH_2Cl_2 (3 x 20 mL). The organic extracts were dried over Na_2SO_4, filtered and concentrated under reduced pressure. The residue was purified by flash chromatography [(petroleum ether/ EtOAc 8.5:1.5)] do give 60% (over 2 steps) as green pale oil. ^{1}H NMR (400 MHz, benzene-d_6) δ 7.28 – 7.00 (m, 12H, Ar-*H*), 6.74 (d, *J* = 8.5 Hz, 2H, Ar-*H*), 5.84 – 5.57 (m, 1H, H-2'), 5.03 (d, *J* = 11.2 Hz, 1H, C*H*$_2$Ph), 4.97 – 4.86 (m, 2H, H-3), 4.75 (d, *J* = 3.4 Hz, 1H, H-1), 4.56 (d, *J* = 11.2 Hz, 1H, C*H*$_2$Ph), 4.46 – 4.29 (m, 4H, 2 C*H*$_2$Ph), 4.16 – 4.06 (m, 2H, H-5, H-2), 4.04 – 3.95 (m, 2H, H-3, H-6), 3.88 (dd, *J* = 10.6, 5.8 Hz, 1H, H-6), 3.23 (s, 3H, ArOMe), 3.20 (s, 3H, OMe), 2.66 (dd, *J* = 14.0, 7.7 Hz, 1H, H-1'), 2.34 (dd, *J* = 14.0, 7.4 Hz, 1H, H-1'). ^{13}C NMR (101 MHz, benzene-d_6) δ 159.5, 139.2, 139.0, 133.3, 130.7, 129.3, 128.4, 128.3, 128.2, 128.1, 127.89, 127.7, 127.6, 127.5, 118.5, 113.9, 98.0, 79.4, 77.1, 76.8, 75.3, 73.1, 72.3, 70.8, 69.4, 54.9, 54.5, 40.6.

Compound 104

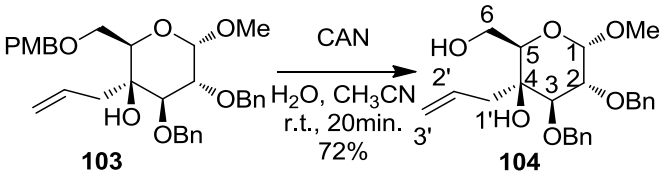

Scheme 5.27

To a solution of compound **103** (1.317 g, 2.46 mmol) in CH_3CN (100 mL) at 0ºC, a solution of CAN (6.743 g, 12.30 mmol) in water (30 mL) was added. The reaction mixture was stirred at room temperature for 20 min. and then diluted with CH_2Cl_2 (70 mL) and wash with water (2 x 100 mL). The combined organic phases were dried, concentrated and

purified by flash chromatography [(petroleum ether/ EtOAc 6:4)] do give 72% as green oil. ^{1}H NMR (400 MHz, $CDCl_3$) δ 7.44 – 7.23 (m, 10H, Ar-*H*), 5.66 (ddd, *J* = 18.2, 16.0, 7.5 Hz, 1H, H-2'), 5.15 – 5.08 (m, 2H, H-3'), 5.06 (d, *J* = 11.0 Hz, 1H, C*H*$_2$Ph), 4.76 (d, *J* = 11.9 Hz, 1H, C*H*$_2$Ph), 4.73 – 4.67 (m, 2H, H-1, C*H*$_2$Ph), 4.64 (d, *J* = 11.9 Hz, 1H, C*H*$_2$Ph), 4.03 (dd, *J* = 12.0, 5.8 Hz, 1H, H-6), 3.94 (dd, *J* = 9.4, 3.5 Hz, 1H, H-2), 3.87 – 3.78 (m, 2H, H-3, H-6), 3.74 – 3.68 (m, 1H, H-5), 3.39 (s, 3H, OC*H*$_3$), 2.65 (dd, *J* = 14.3, 7.2 Hz, 1H, H-1'), 2.30 (dd, *J* = 14.3, 7.7 Hz, 1H, H-1').^{13}C NMR (101 MHz, $CDCl_3$) δ 138.3, 138.2, 132.1, 128.7, 128.7, 128.4, 128.3, 128.2, 128.1, 119.6, 98.2, 78.7, 77.6, 77.2, 76.9, 76.9, 76.8, 75.8, 73.4, 70.0, 61.3, 55.6, 40.3.

Compound 105

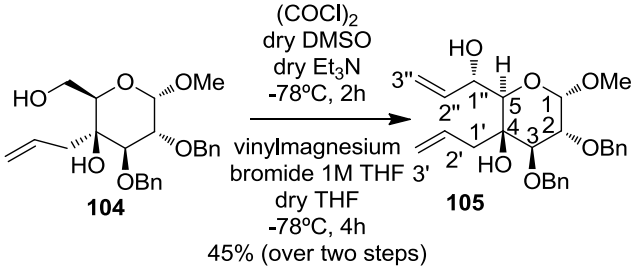

Scheme 5.28

To a solution of $(COCl)_2$ (0.48 mmol, 41 µL) in dry CH_2Cl_2 (92 mL) at -78ºC under argon atmosphere, a solution of anhydrous DMSO (0.96 mmol, 68 µL) in dry CH_2Cl_2 (0.75 mL) was added dropwise, and the resulting solution was stirred for 30 min. To the reaction flask, a solution of compound **104** (50 g, 0.12 mmol) in dry CH_2Cl_2 (0.75 mL) was added dropwise at -78ºC. This final reaction mixture stayed under magnetic stirring for 1 h at -78ºC. Then dry Et_3N (1.2 mmol, 167 µL) was added and the reaction stayed for more 30 min. under magnetic stirring, and then allowed to warm up until 0ºC. The solution was recooled to -78ºC and vinylmagnesium bromide 1 M in THF (1.44 mmol, 1.44 mL) was added dropwise and this final reaction mixture was stirred for 4h at -78ºC and then allowed to warm up until 0ºC. A saturated solution of NH_4Cl was added (80 mL), and the reaction mixture was extracted with CH_2Cl_2 (3 x 30 mL). The organic extracts were dried over Na_2SO_4, filtered and concentrated under reduced pressure. The residue was purified by flash chromatography [(petroleum ether/ EtOAc 8:2)] do give 45% as yellow pale oil. ^{1}H NMR (400 MHz, $CDCl_3$) δ 7.44 – 7.23 (m, 10H, Ar-*H*), 5.94 (ddd, *J* = 16.9, 10.4, 5.8 Hz, 1H, H-2''), 5.70-5.60 (m, H-2'), 5.32 (d, *J* = 16.9 Hz, 1H, H-3''$_{trans}$), 5.20 – 5.08 (m, 4H, H-3''$_{cis}$, H-3', C*H*$_2$Ph), 5.06 (d, *J* = 10.9 Hz, 1H, C*H*$_2$Ph), 4.75 (d, *J* = 12.0 Hz, 1H,

C*H*$_2$Ph), 4.72 – 4.66 (m, 3H, H-1, H-1'', C*H*$_2$Ph), 4.62 (d, *J* = 12.0 Hz, 1H, C*H*$_2$Ph), 3.94 (dd, *J* = 9.5, 3.6 Hz, 1H, H-2), 3.81 (d, *J* = 9.5 Hz, 1H, H-3), 3.57 (bs, 1H, H-5), 3.32 (s, 3H, OMe), 2.75 (dd, *J* = 14.3, 6.9 Hz, 1H, H-1'), 2.45 (dd, *J* = 14.4, 8.0 Hz, 1H, H-1'). ^{13}C NMR (101 MHz, $CDCl_3$) δ 138.2, 138.1, 132.0, 128.7, 128.7, 128.4, 128.3, 128.2, 128.1, 119.7, 115.9, 98.2, 78.3, 77.9, 77.5, 77.2, 76.9, 76.7, 75.9, 73.4, 71.5, 70.9, 55.6, 40.4, 32.1, 29.9, 29.9, 29.6, 14.3.

Compound 106

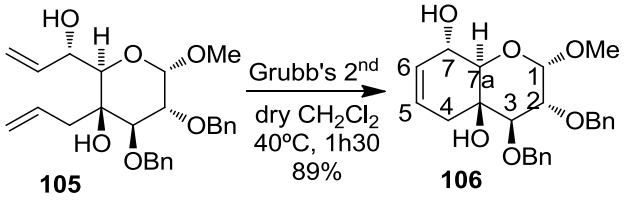

Scheme 5.29

To a solution of **105** (60 mg, 0.136 mmol) in dry CH_2Cl_2 (5 mL), Hoveyda-Grubbs catalyst 2nd generation (5% weight), was added. The reaction mixture was stirred at 40ºC for 90 min. The crude product was concentrated and purified by flash chromatography [(petroleum ether/ EtOAc 6:4)] to give 89% as brown pale oil. ^{1}H NMR (400 MHz, $CDCl_3$) δ 7.42 – 7.29 (m, 10H, Ar-*H*), 5.69 (d, *J* = 10.2 Hz, 1H, H-6), 5.64 – 5.57 (m, 1H, H-5), 5.00 (d, *J* = 11.0 Hz, 1H, C*H*$_2$Ph), 4.78 (d, *J* = 12.1 Hz, 1H, C*H*$_2$Ph), 4.73 (d, *J* = 3.5 Hz, 1H, H-1), 4.70 – 4.62 (m, 2H, C*H*$_2$Ph), 4.54 – 4.47 (m, 1H, H-7), 3.92 (dd, *J* = 9.5, 3.5 Hz, 1H, H-2), 3.71 (d, *J* = 9.5 Hz, 1H, H-3), 3.61 (d, *J* = 8.5 Hz, 1H, H-7a), 3.41 (s, 3H, OMe), 2.38 (dd, *J* = 18.4, 4.4 Hz, 1H, H-4), 2.12 – 2.03 (m, 1H, H-4).

Compound 6a

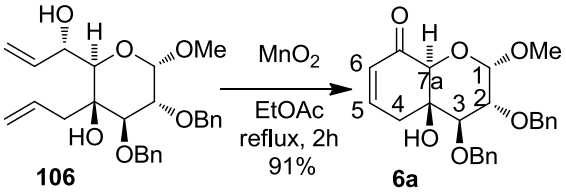

Scheme 5.30

Compound **106** (86 mg, 0.2 mmol) and activated MnO_2 (128 mg, 1.46 mmol) were slurried in EtOAc (2 mL), and the mixture was armed at reflux for 4 h. After consumption of the starting material, the reaction mixture was filtered hot though celite and the residual black solid was washed copiously with EtOAc (10 mL). The filtrate was concentrated in vacuum.

The crude product was purified by flash chromatography [(toulene/EtOAc 6:4)] to give 91% as brown pale oil. ^{1}H NMR (400 MHz, $CDCl_3$) δ 7.42 – 7.25 (m, 10H, Ar-*H*), 6.66 (ddd, *J* = 10.1, 5.6, 2.1 Hz, 1H, H-5), 6.07 (dd, *J* = 10.1, 2.8 Hz, 1H, H-6), 4.99 (d, *J* = 11.1 Hz, 1H, C*H*$_2$Ph), 4.79 (d, *J* = 3.4 Hz, 1H, H-1), 4.77 (d, *J* = 12.0 Hz, 1H, C*H*$_2$Ph), 4.69 (d, *J* = 11.1 Hz, 1H, C*H*$_2$Ph), 4.63 (d, *J* = 12 Hz, 1H, C*H*$_2$Ph), 4.37 (s, 1H, H-5), 3.91 (dd, *J* = 9.5, 3.4 Hz, 1H, H-2), 3.83 (d, *J* = 9.5 Hz, 1H, H-3), 3.40 (s, 3H, OMe), 2.67 (dd, *J* = 19.2, 5.7 Hz, 1H, H-4a), 2.33 – 2.26 (m, 1H, H-4b). ^{13}C NMR (101 MHz, $CDCl_3$) δ 193.6, 144.1, 138.0, 137.9, 128.7, 128.7, 128.5, 128.4, 128.3, 98.8, 98.7, 79.6, 77.6, 77.7, 77.3, 77.0, 76.4, 76.0, 74.6, 73.6, 56.3, 56.3, 37.4, 29.9.

5.8.6. Synthetic strategy for compound 6b

Compound 107

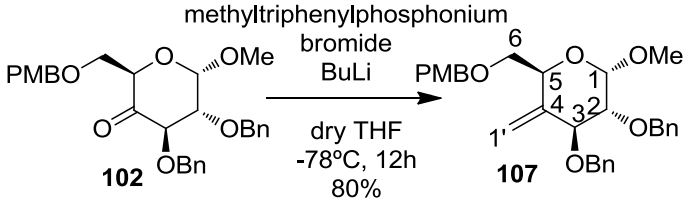

Scheme 5.31

To a suspension of methyltriphenylphosphonium bromide (10.6 g, 29.84 mmol) in dry THF (50 mL) was added *n*-BuLi 1.6 M solution in hexane (17.31 mL) at -78ºC with stirring under argon atmosphere. After being warmed to 0ºC for 30 min., the solution was recooled to -78ºC and treated with a solution of ketone **102** (2.1 g, 4.26 mmol) in dry THF (90 mL). The mixture was allowed to stir for 2 h until it warmed rt, poured in a saturated solution of NH_4Cl (100 mL) and extracted with Et_2O (3 x 30 mL). The organic extracts were dried over Na_2SO_4 and concentrated under reduced pressure. The residue was purified by flash chromatography [(petroleum ether/ EtOAc 8.5:1.5)] do give 80% as yellow oil. ^{1}H NMR (400 MHz, $CDCl_3$) δ 7.43 – 7.23 (m, 12H, Ar-*H*), 6.88 (d, *J* = 8.6 Hz, 2H, Ar-*H*), 5.35 (bs, 1H, H-1'), 4.96 (s, 1H, H-1'), 4.85 (d, *J* = 12.2 Hz, 1H, C*H*$_2$Ph), 4.80 (d, *J* = 11.3 Hz, 1H, C*H*$_2$Ph), 4.72 (d, *J* = 11.3 Hz, 1H, C*H*$_2$Ph), 4.71 – 4.63 (m, 2H, H-1, C*H*$_2$Ph), 4.58 – 4.48 (m, 2H, C*H*$_2$Ph), 4.35 – 4.27 (m, 2H, H-5, H-3), 3.80 (s, 3H, OMe), 3.76 (dd, *J* = 10.0, 4.9 Hz, 1H, H-6), 3.65 (dd, *J* = 10.0, 5.9 Hz, 1H, H-6), 3.48 (dd, *J* = 9.6, 3.6 Hz, 1H, H-2), 3.43 (s, 3H, OMe). ^{13}C NMR (101 MHz, $CDCl_3$) δ 159.2, 142.6, 138.4,

138.3, 129.9, 129.4, 128.3, 128.0, 127.7, 127.7, 127.5, 113.7, 107.7, 98.7, 81.5, 79.1, 77.3, 77.0, 76.7, 73.8, 73.6, 73.1, 69.2, 67.7, 55.3, 55.2.

Compound 108

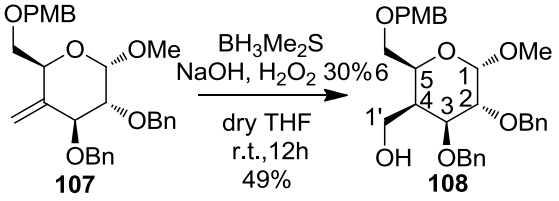

Scheme 5.32

A solution of BH_3•Me_2S (7.3 mmol, 0.7 mL) was added dropwise to a solution of **107** (2.9 g, 5.86 mmol) in dry THF (54 mL) at room temperature, under argon atmosphere and stirred for 90 min. The reaction mixture was cooled at 0ºC, aqueous NaOH 3 M (2.9 mL) and aqueous H_2O_2 (30%) (2.9 mL) were added dropwise subsequently. After 12 h, the reaction mixture was diluted with H_2O (200 mL) and extracted with EtOAc (3 x 70 mL), dried over Na_2SO_4, filtered and concentrated under vacuum. The resulting residue was purified by flash chromatography [(petroleum ether/ EtOAc 7.5:2.5)] to give 49% as brown pale oil. ^{1}H NMR (400 MHz, $CDCl_3$) δ 7.38 – 7.19 (m, 12H, Ar-*H*), 6.87 (d, *J* = 8.6 Hz, 2H, Ar-*H*), 4.82 (d, *J* = 12.1 Hz, 1H, C*H*$_2$Ph), 4.75 (d, *J* = 11.5 Hz, 1H, C*H*$_2$Ph), 4.70 (d, *J* = 11.5 Hz, 1H, C*H*$_2$Ph), 4.66 (d, *J* = 12.1 Hz, 1H, C*H*$_2$Ph), 4.64 (d, *J* = 3.9 Hz, 1H, H-1), 4.56 – 4.42 (m, 2H, C*H*$_2$Ph), 4.09 – 4.01 (m, 2H, H-5, H-3), 3.94 (dd, *J* = 11.5, 5.5 Hz, 1H, H-6), 3.83 – 3.75 (m, 4H, ArOMe, H-6), 3.68 (dd, *J* = 10.2, 3.9 Hz, 1H, H-2), 3.61 – 3.54 (m, 2H, H-1'), 3.37 (s, 3H, OMe), 2.34 (dd, *J* = 5.5, 1.9 Hz, 1H, H-4). ^{13}C NMR (101 MHz, $CDCl_3$) δ 159.4, 138.1, 129.5, 129.4, 128.4, 128.3, 128.0, 127.6, 113.7, 98.8, 78.5, 77.3, 77.0, 76.7, 76.5, 73.4, 73.0, 69.9, 67.9, 57.7, 55.2, 43.5.

Compound 109

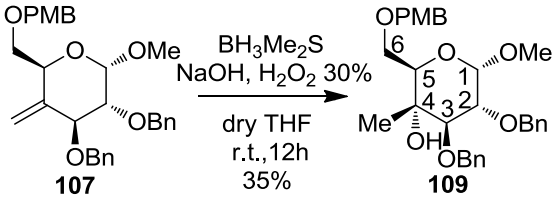

Scheme 5.33

Same experimental procedure used for compound **109**. ^{1}H NMR (400 MHz, $CDCl_3$) δ 7.46 – 7.17 (m, 12H, Ar-*H*), 6.87 (d, *J* = 8.6 Hz, 2H, Ar-*H*), 4.94 (d, *J* = 11.8 Hz, 1H, C*H*$_2$Ph),

4.81 (d, *J* = 11.9 Hz, 1H, C*H*$_2$Ph), 4.78 (d, *J* = 11.8 Hz, 1H, C*H*$_2$Ph), 4.62 (d, *J* = 11.9 Hz, 1H, C*H*$_2$Ph), 4.59 (d, *J* = 3.8 Hz, 1H, H-1), 4.51 (d, *J* = 11.7 Hz, 1H, C*H*$_2$Ph), 4.45 (d, *J* = 11.7 Hz, 1H, C*H*$_2$Ph), 3.88 (t, *J* = 6.1 Hz, 1H, H-5), 3.82 – 3.78 (m, 4H, H-3, ArOMe), 3.68 (dd, *J* = 9.8, 6.1 Hz, 1H, H-6), 3.55 (dd, *J* = 9.8, 6.1 Hz, 1H, H-6), 3.46 – 3.36 (m, 4H, H-2, OMe), 1.18 (s, 3H, C*H*$_3$). ^{13}C NMR (101 MHz, $CDCl_3$) δ 159.23, 139.17, 138.27, 129.79, 129.29, 128.41, 128.39, 128.03, 127.81, 127.76, 127.56, 113.78, 98.01, 83.49, 78.48, 77.37, 77.05, 76.73, 75.67, 74.32, 73.36, 73.23, 70.65, 68.61, 55.25, 55.10, 15.80.

Compound 110

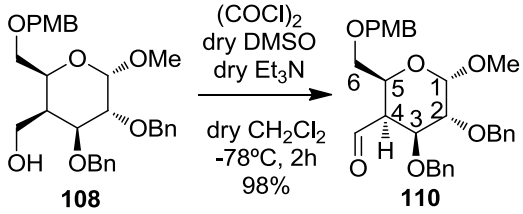

Scheme 5.34

To a solution of $(COCl)_2$ (7.86 mmol, 0.7 mL) in dry CH_2Cl_2 (16 mL) at -78ºC under argon atmosphere, a solution of anhydrous DMSO (15.76 mmol, 1.1 mL) in dry CH_2Cl_2 (6 mL) was added dropwise, and the resulting solution was stirred for 30 min. To the reaction flask, a solution of compound **108** (1 g, 1.97 mmol) in dry CH_2Cl_2 (10 mL) was added dropwise at -78ºC. This final reaction mixture stayed under magnetic stirring for 1 h at -78ºC. The dry Et_3N (19.7 mmol, 2.76 mL) was added and the reaction stayed for more 30 min. under magnetic stirring, and then allowed to warm up until 0ºC. A saturated solution of NH_4Cl (150 mL) was added, and the reaction mixture was extracted with CH_2Cl_2 (3 x 50 mL). The organic extracts were dried over Na_2SO_4, filtered and concentrated under reduced pressure. The residue was purified by flash chromatography [(petroleum ether/ EtOAc 7.5:2.5)] do give 98% as green pale oil. ^{1}H NMR (400 MHz, $CDCl_3$) δ 9.90 (d, *J* = 5.3 Hz, 1H, C*H*O), 7.43 – 7.14 (m, 12H, Ar-*H*), 6.86 (d, *J* = 8.6 Hz, 2H, Ar-*H*), 4.85 (d, *J* = 12.1 Hz, 1H, C*H*$_2$Ph), 4.78 (d, *J* = 3.8 Hz, 1H, H-1), 4.73 – 4.68 (m, 2H, C*H*$_2$Ph), 4.63 (d, *J* = 11.5 Hz, 1H, C*H*$_2$Ph), 4.47 – 4.35 (m, 2H, C*H*$_2$Ph), 4.17 – 4.05 (m, 2H, H-3, H-5), 3.98 (dd, *J* = 10.0, 3.8 Hz, 1H, H-2), 3.80 (s, 3H, OMe), 3.56 (dd, *J* = 10.4, 4.2 Hz, 1H, H-6), 3.47 (dd, *J* = 10.4, 5.0 Hz, 1H, H-6), 3.37 (s, 3H, OMe), 2.98 (ddd, *J* = 10.1, 5.3, 3.6 Hz, 1H, H-4). ^{13}C NMR (101 MHz, $CDCl_3$) δ 197.3, 155.3, 134.1, 133.9, 125.5, 125.5, 124.4, 124.4, 124.1, 123.9, 123.8, 123.7, 109.8, 95.1, 73.4, 73.0, 72.6, 72.5, 72.5, 69.6, 69.3, 68.1, 65.8, 63.7, 51.5, 51.3, 50.6, 25.7.

Compound 111

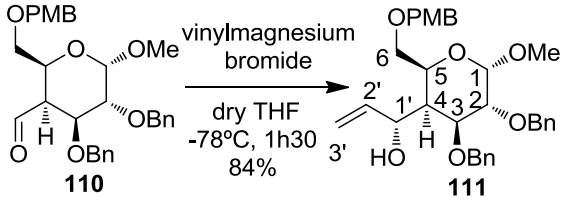

Scheme 5.35

To a solution of **110** (720 mg, 1.42 mmol) in dry THF (30 mL) at -78ºC under argon atmosphere, a solution of vinylmagnesium bromide (1M in THF) (3.55 mmol, 3.6 mL) was added dropwise. The resulting solution was stirred for 90 min. and then allowed to warm up until 0ºC. A saturated solution of NH_4Cl (100 mL) was added, and the reaction mixture was extracted with CH_2Cl_2 (3 x 35 mL). The organic extracts were dried over Na_2SO_4, filtered and concentrated under reduced pressure. The residue was purified by flash chromatography [(petroleum ether/ EtOAc 7:3)] do give 84% as brown pale oil. ^{1}H NMR (400 MHz, $CDCl_3$) δ 7.41 – 7.12 (m, 12H, Ar-*H*), 6.97 – 6.78 (m, 2H, Ar-*H*), 6.02 (ddd, *J* = 17.2, 10.1, 7.5 Hz, 1H, H-2'), 5.22 (d, *J* = 17.2 Hz, 1H, H-3'$_{trans}$), 5.08 – 5.02 (m, 1H, H-3'$_{cis}$), 4.79 (d, *J* = 12.1 Hz, 1H, C*H*$_2$Ph), 4.74 – 4.62 (m, 4H, H-1, 3 C*H*$_2$Ph), 4.53 – 4.48 (m, 1H, H-1'), 4.48 – 4.41 (m, 2H, C*H*$_2$Ph), 4.13 – 4.06 (m, 2H, H-3, H-5), 3.80 (s, 3H, OMe), 3.67 – 3.60 (m, 1H, H-6), 3.54 (dd, *J* = 10.2, 5.3 Hz, 1H, H-6), 3.38 (s, 3H, OMe), 2.45 – 2.39 (m, 1H, H-4). ^{13}C NMR (101 MHz, $CDCl_3$) δ 159.2, 141.1, 141.1, 138.3, 138.2, 137.9, 129.8, 129.7, 129.3, 129.3, 128.4, 128.4, 128.3, 128.1, 127.6, 127.5, 115.7, 113.8, 98.5, 79.6, 78.9, 77.3, 77.0, 76.7, 75.7, 73.5, 73.4, 73.3, 73.0, 71.2, 68.9, 55.2, 55.2, 45.3, 44.8.

Compound 112

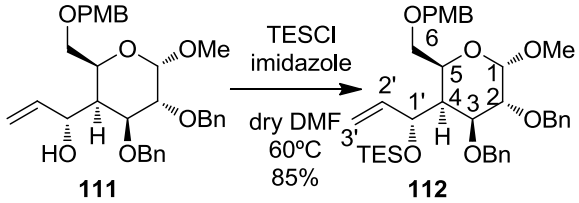

Scheme 5.36

To a solution of **111** (588 mg, 1.10 mmol) and imidazole (249 mg, 1.65 mmol) in dry DMF (7 mL) was added TESCl (1.65 mmol, 0.25 mL). The reaction mixture was heated at 60ºC for 90 min. and then allowed to cold until rt and a saturated aqueous solution of $NaHCO_3$ (40 mL) was added. The reaction mixture was extracted with EtOAc (3 x 15 mL) and the

organic extracts were dried over Na_2SO_4, filtered and concentrated under reduced pressure. The residue was purified by flash chromatography [petroleum ether/ EtOAc (8:2)] do give 85% as light green oil. ^{1}H NMR (400 MHz, $CDCl_3$) δ 7.46 – 7.16 (m, 12H, Ar-*H*), 6.86 (d, *J* = 8.6 Hz, 2H, Ar-*H*), 6.19 – 6.06 (m, 1H, H-2'), 5.08 (d, *J* = 17.2 Hz, 1H, H-3'$_{trans}$), 4.94 (d, *J* = 10.5 Hz, 1H, H-3'$_{cis}$), 4.77 – 4.49 (m, 7H, H-1', 5 C*H*$_2$Ph, H-1), 4.42 (d, *J* = 11.6 Hz, 1H, C*H*$_2$Ph), 4.14 (d, *J* = 9.0 Hz, 1H, H-5), 4.04 – 3.97 (m, 2H, H-2, H-3), 3.89 – 3.81 (m, 1H, H-6), 3.79 (s, 3H, ArOMe), 3.72 – 3.64 (m, 1H, H-6), 3.40 (s, 3H, OMe), 2.38 (bs, 1H, H-4), 0.88 (t, *J* = 7.8 Hz, 9H, C*H*$_3$CH$_2$Si), 0.51 (q, *J* = 7.8 Hz, 6H, CH$_3$C*H*$_2$Si). ^{13}C NMR (101 MHz, $CDCl_3$) δ 159.4, 141.5, 139.2, 138.9, 131.0, 129.5, 128.7, 128.6, 128.6, 128.3, 128.0, 127.8, 127.7, 127.4, 116.1, 114.0, 77.8, 77.4, 77.1, 73.4, 73.1, 73.1, 72.7, 55.6, 55.3, 7.3, 5.6, 5.3.

Compound 113

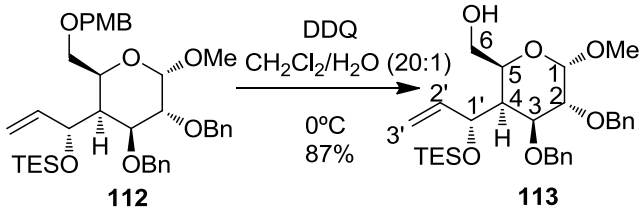

Scheme 5.37

DDQ (300 mg, 1.31mmol) was added to an ice-cooled solution of **112** (609 mg, 0.94 mmol) in H_2O/CH_2Cl_2 (1:20) (42 mL), and the mixture was stirred for 2 h. The reaction mixture was then diluted with saturated aqueous solution of $NaHCO_3$ (80 mL) and extracted with CH_2Cl_2 (3 x 15 mL). The extracts were washed with H_2O (50 mL) and brine (50 mL), dried and concentrated under reduce pressure. The residue was purified by flash chromatography [(petroleum ether/ EtOAc (8:2)] do give 87% as green oil.^{1}H NMR (400 MHz, $CDCl_3$) δ 7.45 – 7.21 (m, 10H, Ar-*H*), 6.26 – 6.06 (m, 1H, H-2'), 5.14 (d, *J* = 17.1 Hz, 1H, H-3'$_{trans}$), 4.98 (d, *J* = 8.7 Hz, 1H, H-3'$_{cis}$), 4.82 – 4.67 (m, 4H, 3 C*H*$_2$Ph, H-1'), 4.61 (d, *J* = 12.2 Hz, 1H, C*H*$_2$Ph), 4.55 (d, *J* = 3.4 Hz, 1H, H-1), 4.06 – 3.93 (m, 3H, H-2, H-3, H-5), 3.87 – 3.75 (m, 2H, H-6, H-6), 3.34 (s, 3H, OMe), 2.63 – 2.48 (m, 1H, H-4), 0.97 – 0.87 (m, 9H, C*H*$_3$CH$_2$Si), 0.63 – 0.55 (m, 6H, CH$_3$C*H*$_2$Si). ^{13}C NMR (101 MHz, $CDCl_3$) δ 140.4, 138.7, 138.4, 128.3, 128.1, 128.2, 128.1, 127.7, 127.4, 127.3, 127.2, 117.1, 98.7, 77.3, 77.1, 76.6, 74.2, 72.9, 72.93, 69.13, 62.7, 55.1, 55.1, 47.4, 29.6, 6.6, 4.6.

Compound 114

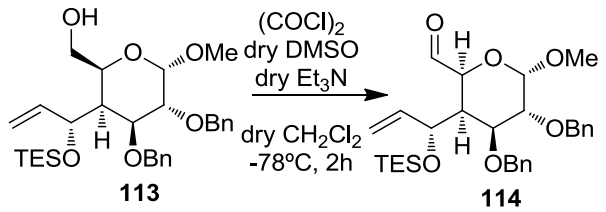

Scheme 5.38

To a solution of $(COCl)_2$ (1.51 mmol, 0.13 mL) in dry CH_2Cl_2 (2 mL) at -78ºC under argon atmosphere, a solution of anhydrous DMSO (2.96 mmol, 0.2 mL) in dry CH_2Cl_2 (3 mL) was added dropwise, and the resulting solution was stirred for 30 min. To the reaction flask, a solution of compound **114** (200 mg, 0.37 mmol) in dry CH_2Cl_2 (4 mL) was added dropwise at -78ºC. This final reaction mixture stayed under magnetic stirring for 1 h at -78ºC. Then dry Et_3N (3.7 mmol, 0.52 mL) was added and the reaction stayed for more 30 min. under magnetic stirring, and then allowed to warm up until 0ºC. A saturated solution of NH_4Cl (30 mL) was added, and the reaction mixture was extracted with CH_2Cl_2 (3 x 10mL). The organic extracts were dried over Na_2SO_4, filtered and concentrated under reduced pressure. The residue was used without further purification.

Compound 115

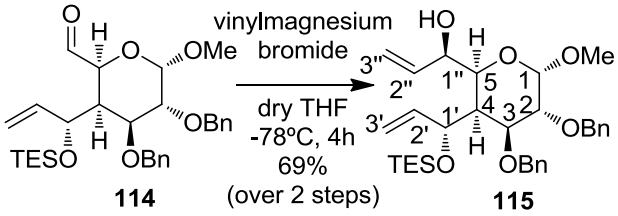

Scheme 5.39

To a solution of **114** (380 mg, 0.72 mmol) in dry THF (18 mL) at -78ºC under argon atmosphere, a solution of vinylmagnesium bromide (1 M in THF) (1.8 mmol, 1.8 mL) was added dropwise. The resulting solution was stirred for 90 min. and then allowed to warm up until 0ºC. A saturated solution of NH_4Cl (20 mL) was added, and the reaction mixture was extracted with CH_2Cl_2 (3 x 10 mL). The organic extracts were dried over Na_2SO_4, filtered and concentrated under reduced pressure. The residue was purified by flash chromatography [petroleum ether/ EtOAc (8.5:1.5)] to give 69% (over 2 steps) as green pale oil. ^{1}H NMR (400 MHz, $CDCl_3$) δ 7.40 – 7.24 (m, 10H, Ar-*H*), 6.39 – 6.25 (m, 1H, H-2'), 6.10 – 5.94 (m, 1H, H-2''), 5.40 (d, J = 17.5 Hz, 1H, H-3''$_{trans}$), 5.18 (d, J = 10.4 Hz,

1H, H-3''$_{cis}$), 5.11 (d, *J* = 17.0 Hz, 1H, H-3'$_{trans}$), 4.95 (d, *J* = 9.6 Hz, 1H, H-3'$_{cis}$), 4.85 – 4.68 (m, 4H, C*H*$_2$Ph, H-1, H-1'), 4.58 (bd, *J* = 12.4 Hz, 2H, C*H*$_2$Ph), 4.40 (s, 1H, H-1''), 4.13 – 4.03 (m, 1H, H-2), 4.03 – 3.93 (m, 1H, H-3), 3.79 (bs, 1H, H-5), 3.34 (s, 3H, OMe), 2.46 (bs, 1H, H-4), 0.92 (t, *J* = 7.9 Hz, 9H, C*H*$_3$CH$_2$Si), 0.65 – 0.53 (m, 6H, CH$_3$C*H*$_2$Si). ^{13}C NMR (101 MHz, $CDCl_3$) δ 141.1, 138.3, 138.0, 136.5, 128.4, 128.3, 128.1, 127.7, 127.7, 127.6, 117.5, 116.3, 99.1, 79.0, 77.3, 76.9, 76.6, 75.2, 73.4, 73.1, 72.8, 71.8, 71.7, 55.6, 55.5, 45.5, 29.6, 6.7, 6.4.

Compound 116

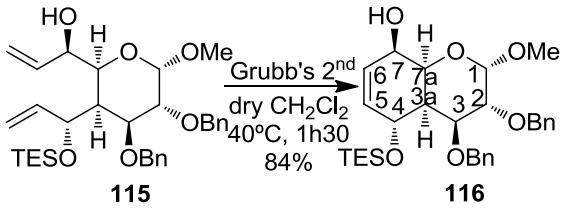

115 **116**

Scheme 5.40

To a solution of **115** (50 mg, 0.09 mmol) in dry CH_2Cl_2 (4 mL), Hoveyda-Grubbs catalyst 2nd generation (5% weight), was added. The reaction mixture was stirred at 40ºC for 2 h. The crude product was concentrated and purified by flash chromatography [(petroleum ether/ EtOAc 8:2)] to give 84% as brown pale oil. ^{1}H NMR (400 MHz, $CDCl_3$) δ 7.44 – 7.17 (m, 10H, Ar-*H*), 5.88 – 5.71 (m, 2H, H-6, H-5), 4.89 (d, *J* = 12.6 Hz, 1H, C*H*$_2$Ph), 4.80 (d, *J* = 12.6 Hz, 1H, C*H*$_2$Ph), 4.75 (d, *J* = 12.7 Hz, 1H, C*H*$_2$Ph), 4.65 – 4.56 (m, 2H, C*H*$_2$Ph, H-1), 4.39 (d, *J* = 6.3 Hz, 1H, H-4), 4.10 – 4.05 (m, 1H, H-7), 4.00 – 3.90 (m, 2H, H-7a, H-3), 3.71 (dd, *J* = 9.1, 3.7 Hz, 1H, H-2), 3.38 (s, 3H, OMe), 2.62 – 2.49 (m, 1H, H-3a), 0.98 – 0.84 (m, 9H, 3 C*H*$_3$CH$_2$Si), 0.64 – 0.52 (m, 6H, 2 CH$_3$C*H*$_2$Si).

Compound 6b

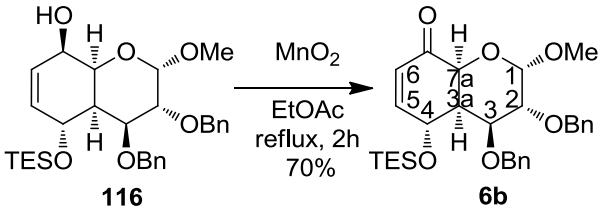

116 **6b**

Scheme 5.41

Compound **116** (10 mg, 0.019 mmol) and MnO_2 (12 mg, 0.132 mmol) were slurried in EtOAc (2 mL), and the mixture was armed at reflux for 2h. After consumption of the starting material, the reaction mixture was filtered hot though celite and the residual black

solid was washed copiously with EtOAc (10 mL). The filtrate was concentrated in vacuum. The crude product was purified by flash chromatography [(petroleum ether/ EtOAc 8.5:1.5)] to give 70% as brown pale oil. ^{1}H NMR (400 MHz, DMSO) δ 7.38 – 7.24 (m, 8H, Ar-*H*), 7.13 (d, *J* = 6.9 Hz, 2H, Ar-*H*), 6.62 (dd, *J* = 9.8, 3.0 Hz, 1H, H-5), 5.89 (d, *J* = 9.8 Hz, 1H, H-6), 4.72 (d, *J* = 11.6 Hz, 2H, C*H*$_2$Ph, H-1), 4.61 – 4.47 (m, 3H, 2 C*H*$_2$Ph, H-4), 4.33 (bd, *J* = 12.5 Hz, 1H, C*H*$_2$Ph), 3.80 – 3.74 (m, 1H, H-3), 3.72 – 3.67 (m, 1H, H-2), 3.43 (s, 3H, OMe), 2.66 (bs, 1H, H-3a), 0.85 (t, *J* = 7.9 Hz, 9H, C*H*$_3$CH$_2$Si), 0.51 (q, *J* = 7.9 Hz, 6H, CH$_3$C*H*$_2$Si). ^{13}C NMR (101 MHz, DMSO) δ 139.1, 138.3, 128.6, 128.5, 128.1, 127.9, 127.9, 127.7, 96.9, 76.0, 73.7, 73.1, 71.2, 56.9, 43.3, 40.5, 40.3, 40.1, 39.9, 39.7, 39.5, 39.2, 7.0, 4.5.

5.8.7. Synthetic strategy for compound 10a

Compound 117

Acording to literature procedure:[78]

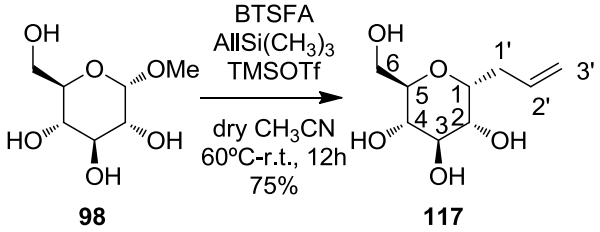

Scheme 5.42

To a suspension of methyl *α*-D-glucopyranoside **98** (2.00 g, 0.01 mol) in acetonitrile (2.0 mL), bis(trimethylsilyl)trifluoroacetamide (BTSFA) (8.20 mL, 0.031 mol) was added and the resulting mixture heated at reflux for 1 h (the mixture became clear and uniform). Allyltrimethylsilane (2.40 mL, 0.015 mol), followed by trimethylsilyl trifluoromethanesulfonate (0.92 mL, 5.00 mmol), was then added at 0 °C and the reaction mixture stirred for 18 h at room temp. After this time, the mixture was poured (CAUTION!) into ice-cold water and stirred for 3 h, prior to being neutralized (pH=7) with IRN78 resin, filtered through Celite and the filtrate concentrated under reduced pressure. The residue was purified by flash column chromatography over silica gel (EtOAc/MeOH, 15:1) affording 75 % of **117** as a powder solid. ^{1}H NMR (400 MHz, CD$_3$OD) δ 5.74 (ddt, *J* = 17.1, 10.1, 6.9, 1H, H-2'), 4.98 (dd, *J* = 17.1, 1.5, 1H, H-3'$_{trans}$), 4.91 (d, *J* = 10.1, 1H, H-3'$_{cis}$), 3.85 – 3.77 (m, 1H, H-1), 3.60 (dd, *J* = 11.7, 2.4, 1H, H-2), 3.48 (ddd, *J* = 15.1,

10.5, 5.4, 2H, H-6, H-4), 3.40 (t, *J* = 8.9, 1H, H-3), 3.35 – 3.28 (m, 1H, H-5), 3.19 – 3.12 (m, 1H, H-6), 2.41 – 2.22 (m, 2H, H-1').

Compound 118

Acording to literature procedure:[154]

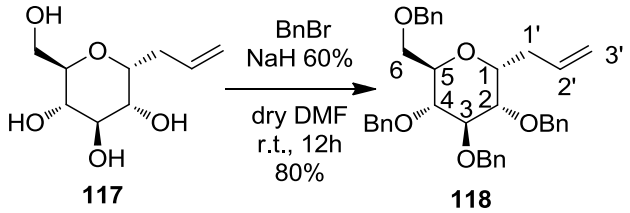

117 **118**

Scheme 5.43

A stirred solution of **117** (10 g, 0.032 mol) in anhydrous DMF (100 mL) under argon at 0 ºC was treated with NaH 60% in mineral oil (3.8 g, 0.096 mol). After 15 min. at room temperature, the mixture was treated dropwise and rapidly with BnBr (0.096 mol, 11 mL) and then allowed to stand for 1 h at rt. The mixture was diluted with EtOAc (80 mL), and washed with saturated $NaHCO_3$ solution (3 x 50mL). The aqueous phase was back-extracted with EtOAc (2 x 40 mL), and all the organic fractions were combined, washed with brine, and dried over anhydrous Na_2SO_4. The residue was purified by flash chromatography [petroleum ether/EtOAc (9:1)] affording **118** (80% yield) as colorless oil. NMR (300 MHz, $CDCl_3$) δ 7.27-7.39 (m, 18H, Ar-*H*), 7.14-7.18 (m, 2H, Ar-*H*), 5.86 (ddt, 1H, *J* = 6.6, 10.2, 17.1 Hz, H-2'), 5.08-5.18 (m, 2H, H-3'), 4.96 – 4.87 (m, 2H, C*H*$_2$Ph), 4.75 – 4.70 (m, 2H,C*H*$_2$Ph), 4.68 – 4.60 (m, 2H, C*H*$_2$Ph), 4.58 – 4.53 (m, 2H, C*H*$_2$Ph), 4.17 (m, 1H, H-1), 3.61-3.87 (m, 6H, H-2, H-3, H-4, H-4, H-6), 2.47-2.61 (m, 2H, H-1').

Compound 119

Acording to literature procedure: [154]

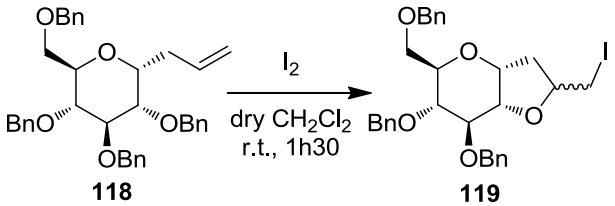

118 **119**

Scheme 5.44

To a solution of **118** (512 mg, 0.9 mmol) in dry CH_2Cl_2 (5 mL) was added iodine (2.3 g, 9 mmol) at rt. After 90 min. the reaction mixture was diluted with EtOAc, aqueous

$Na_2S_2O_3$ was added, and the mixture was stirred till the organic layer became colourless. Crude compound **119** was used without furder purification.

Compound 120

Acording to literature procedure: [154]

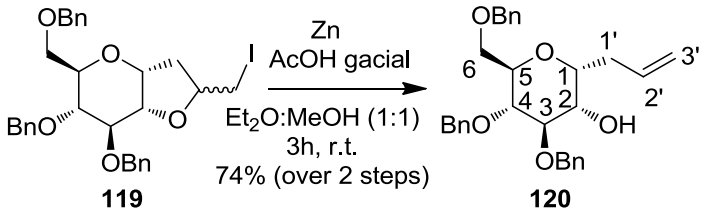

Scheme 5.45

Product **119** (477 mg, 0.79 mmol) was dissolved in a 1:1 mixture of Et_2O-MeOH (4 mL), and powdered zinc (519 mg, 7.9 mmol) and glacial acetic acid (90 μL, 1.58 mmol) were sequentially added. The suspension was stirred overnight and then filtered over a Celite pad. The filtrate was evaporated and then diluted with EtOAc (20 mL) and washed with HCl (5%) (10mL) and H_2O (10 mL), dried over Na_2SO_4, and purified by flash chromatography using [petroleum ether/EtOAc (8:2)] to give **120** (348mg, 74% yield over 2 steps) as colourless oil. ^{1}H NMR (400 MHz, $CDCl_3$) δ 7.46 – 7.10 (m, 15H, Ar-*H*), 5.98 – 5.66 (m, 1H, H-2'), 5.13 (broad dd, *J* = 16.8, 3.2 Hz, 1H, H-3'$_{trans}$), 5.07 (broad dd, *J* = 10.2, 3.2 Hz, 1H, H-3'$_{cis}$), 4.71 – 4.46 (m, 6H, 3 C*H*$_2$Ph), 4.08 – 4.02 (m, 1H, H-5), 3.97 – 3.90 (m, 1H, H-1), 3.82 (dd, *J* = 10.0, 5.7 Hz, 1H, H-4), 3.75 (t, *J* = 5.7 Hz, 1H, H-3), 3.72 – 3.60 (m, 3H, H-2, H-6a, H-6b), 2.91 (broad s, 1H, O*H*), 2.54 – 2.28 (m, 2H, H-1').

Compound 121

Acording to literature procedure: [154]

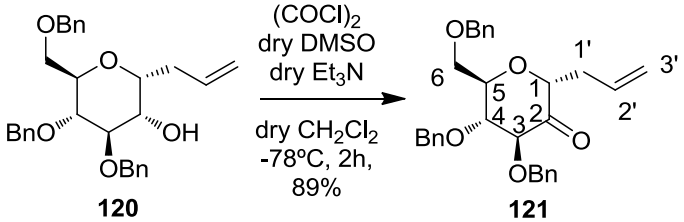

Scheme 5.46

To a solution of $(COCl)_2$ (364 mg, 2.87 mmol) of dry CH_2Cl_2 (6 mL) at -78ºC under argon atmosphere, anhydrous DMSO (0.4 mL) was added dropwise, and the resulting solution was stirred for 30 min. To the reaction flask, a solution of compound **120** (341 mg, 0.718 mmol) of dry CH_2Cl_2 (2.0 mL) was added dropwise at -78ºC. This final reaction mixture

stayed under magnetic stirring for 1 h at -78ºC. Then dry TEA (0.9 mL) was added and the reaction stayed for more 30 min under magnetic stirring at -78ºC, and then was allowed to warm up until 0ºC. It was carefully added NH_4Cl (10 mL), and the organic layer washed with H_2O (10 mL), dried over Na_2SO_4, and concentrated. The residue was purified by flash chromatography using [petroleum ether/EtOAc (9:1)] to give compound **121** (303 mg, 89% yield) as a white powder. ^{1}H NMR (400 MHz, $CDCl_3$) δ 7.49 – 7.13 (m, 15H, Ar-*H*), 5.86 – 5.64 (m, 1H, H-2'), 5.18 – 5.04 (m, 2H, H-3'), 4.95 (d, *J* = 11.5 Hz, 1H, C*H*$_2$Ph), 4.81 (d, *J* = 11.2 Hz, 1H, C*H*$_2$Ph), 4.61 (d, *J* = 11.5 Hz, 1H, C*H*$_2$Ph), 4.50 (bd, *J* = 11.5 Hz, 2H, C*H*$_2$Ph), 4.41 (d, *J* = 11.2 Hz, 1H, C*H*$_2$Ph), 4.39 (d, *J* = 8.9 Hz, 1H, H-3), 4.26 (t, *J* = 6.8 Hz, 1H, H-1), 4.10 – 3.99 (m, 1H, H-5), 3.90 (dd, *J* = 8.9, 7.7 Hz, 1H, H-4), 3.68 – 3.54 (m, 2H, H-6), 2.47 (t, *J* = 6.8 Hz, 2H, H-1').

Compound 122

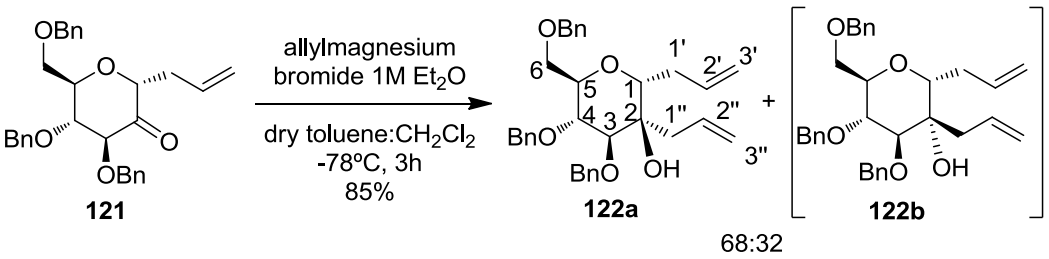

Scheme 5.47

Allylmagnesium bromide 1 M solution in THF (1.6 mmol, 1.6 mL) was added to a solution of **121** (293 mg, 0.62 mmol) in dry toluene:CH_2Cl_2 (2:1) (3 mL) at -78ºC. The reaction was stirred at -78ºC for 2 h. The reaction mixture was warm to 0 ºC, and was slowly added a solution of NH_4Cl (20 mL) and diluted with EtOAc (8 mL). The aqueous phase was back-extracted with EtOAc (3 x 8 mL) and all the organic fractions were combined and dried over anhydrous Na_2SO_4. The residue was purified by flash chromatography using [petroleum ether/EtOAc (9.5:0.5)] to give a mixture of diastereomers (68:32) **122** (0.271 g, 85% yield) as yellow oil. NMR characterization of the major isomer **122a**, ^{1}H NMR (400 MHz, $CDCl_3$) δ 7.45 – 7.14 (m, 15H), 6.12 – 5.68 (m, 2H, H-2', H-2''), 5.11 (m, 4H, H-3a', H-3', H-3''), 4.87 (d, *J* = 11.0 Hz, 1H, C*H*$_2$Ph), 4.73 (d, *J* = 11.4 Hz, 1H, C*H*$_2$Ph), 4.62 (d, 2H, C*H*$_2$Ph), 4.54 (d, *J* = 9.9 Hz, 1H, C*H*$_2$Ph), 4.52 (d, *J* = 11.4 Hz, 1H, C*H*$_2$Ph), 3.97 (t, *J* = 7.8 Hz, 1H, H-4), 3.83 – 3.72 (m, 3H, H-1, H-5, H-6a), 3.68 (d, *J* = 7.5 Hz, 1H, H-6), 3.60 (d, *J* = 7.8 Hz, 1H, H-3), 2.74 (dd, *J* = 14.6, 5.6 Hz, 1H, H-1''), 2.51 – 2.23 (m, 2H, H-1'), 2.02 (dd, *J* = 14.6, 8.4 Hz, 1H, H-1''). ^{13}C NMR (101 MHz, $CDCl_3$) δ 138.4,

138.2, 137.9, 134.8, 133.1, 128.7, 128.7, 128.5, 128.3, 128.2, 128.2, 128.0, 128.0, 127.8, 118.6, 117.0, 82.2, 77.7, 77.6, 77.3, 77.0, 76.7, 75.6, 75.4, 74.7, 73.6, 72.8, 69.2, 38.6, 31.2.

Compound 123

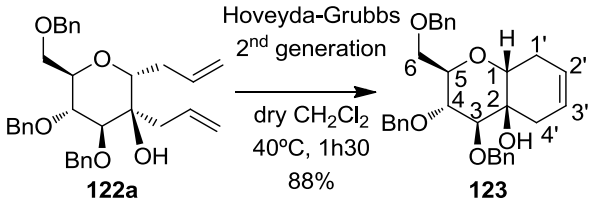

Scheme 5.48

To a solution of **122a** (768 mg 1.49 mmol) in dry CH_2Cl_2 (45 mL), Grubb's 2nd generation Hoveyda (5% weight) was added. The reaction mixture was stirred at 40ºC for 2 h. The crude product was concentrated and purified by flash chromatography [petroleum ether/EtOAc (9:1)] to give the corresponding ciclyzed product **123** (642 mg, 88% yield) as green oil. ^{1}H NMR (400 MHz, $CDCl_3$) δ 7.43 – 7.23 (m, 15H, Ar-*H*), 5.53 (bs, 1H, H-2'), 5.49 (bs, 1H, H-3'), 4.85 (d, *J* = 11.2 Hz, 1H, C*H*$_2$Ph), 4.73 (d, *J* = 10.9 Hz, 1H, C*H*$_2$Ph), 4.63 (d, *J* = 12.2 Hz, 1H, C*H*$_2$Ph), 4.60 – 4.55 (m, 2H, 2 C*H*$_2$Ph), 4.51 (d, *J* = 10.9 Hz, 1H, C*H*$_2$Ph), 4.08 (dd, *J* = 11.6, 9.1 Hz, 1H, H-1), 3.99 – 3.90 (m, 2H, H-4, H-5), 3.65 – 3.61 (m, 2H, H-6), 3.58 (dd, *J* = 11.8, 4.6 Hz, 1H, H-3), 2.62 (bd, *J* = 17.2 Hz, 1H, H-4'), 2.63 - 2.22 (m, 2H, H-1'), 1.85 (bd, 1H, H-4').

Compound 124

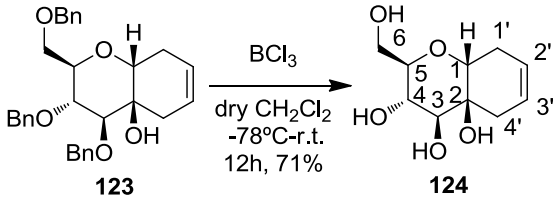

Scheme 5.49

To a solution of **123** (439 mg, 0.90 mmol) in dry CH_2Cl_2 (12 mL) was added BCl_3 (11 mmol, 11 mL) at -78 °C under argon. The reaction mixture was stirred 3 h at -78 °C, and overnight at room temperature. Then it was diluted by the addition of a solution MeOH/H_2O (20:1) (6 mL). The reaction mixture was then concentrated under reduced pressure. The crude product was purified by flash chromatography (EtOAc) to give the corresponding compound **124** (0.138 g, 71% yield) as colourless oil. ^{1}H NMR (400 MHz,

CD_3OD) δ 5.63 – 5.42 (m, 2H, H-2', H-3'), 4.13 (dd, *J* = 12.1, 8.6 Hz, 1H, H-6), 4.02 (dd, *J* = 9.5, 6.9 Hz, 1H, H-1), 3.92 (dd, *J* = 8.6, 4.2 Hz, 1H, H-5), 3.73 (d, *J* = 2.2 Hz, 1H, H-4), 3.59 (dd, *J* = 12.1, 4.2 Hz, 1H, H-6), 3.50 (d, *J* = 2.5 Hz, 1H, H-3), 2.61 (bd, *J* = 18.4, 1H, H-4'), 2.30 – 2.18 (m, 2H, H-1'), 1.87 (dd, *J* = 18.1, 3.7 Hz, 1H, H-4').

Compound 125

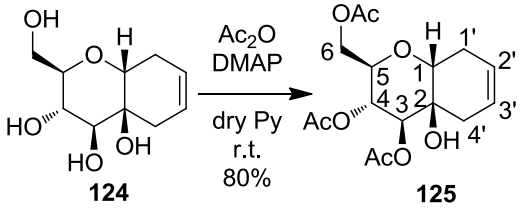

Scheme 5.50

To a solution of **124** (200 mg, 0.92 mmol) in dry Py (2 mL), Ac_2O (4.62 mmol, 0.5 mL) and a catalytic amount of 4-(*N*, *N*-dimethylamino)pyridine (DMAP) were added at rt. The reaction mixture was stirred overnight at rt. The reaction mixture was quenched by addition a solution of HCl (5%) (10 mL). The aqueous layer was extracted whit EtOAc (3 x 3 mL) and the combined organic extracts were wash with brine, dried over Na_2SO_4, and concentrated. The residue was purified by flash chromatography using [petroleum ether/EtOAc (3:7)] to give **125** (297 mg, 80% yield) as a yellow oil. NMR (500 MHz, $CDCl_3$) δ 5.69 – 5.62 (m, 1H, H-2'), 5.55 – 5.48 (m, H-3'), 5.33 (t, *J* = 9.3 Hz, 1H, H-4), 5.22 (d, *J* = 9.3 Hz, 1H, H-3), 4.24 (dd, *J* = 12.1, 5.0 Hz, 1H, H-6), 4.21 – 4.13 (m, 2H, H-1, H-6), 4.00 (ddd, *J* = 9.4, 5.0, 2.5 Hz, H-5), 2.67 – 2.58 (m, 1H, H-1'), 2.46 – 2.34 (m, 2H, H-1', H-4'), 2.19 – 2.13 (m, 1H, H-4'), 2.11 (s, 6H, Me), 2.02 (s, 3H, Me). NMR (75 MHz, $CDCl_3$) δ 170.8, 170.3, 169.8, 123.7, 123.4, 77.4, 77.0, 76.6, 75.7, 71.5, 71.4, 69.6, 68.2, 62.9, 34.1, 25.6, 20.8, 20.7.

Compound 10a

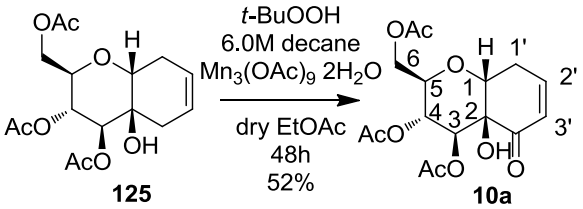

Scheme 5.51

To a solution of **126** (20 mg, 0.058 mmol) in dry EtOAc (1 mL) was added *tert*-butyl hydroperoxide in decane 5.5 M (0.304 mmol, 56 μL) and 3Å molecular sieves. The mixture was stirred for 30 min under argon at rt. Manganese (III) acetate dehydrate (0,006 mmol, 1.6 mg) was added and the mixture was stirred for 48h at rt. The solution was filtered through a pad o celite. Concentration of the filtrate followed by flash chromatography [petroleum ether/EtOAc] (6:4) gives **10a** (0.011 g, 52% yield) as colourless oil.^{1}H NMR (400 MHz, $CDCl_3$) δ 6.63 (bd, *J* = 10.0 Hz, 1H, H-2'), 6.10 (d, *J* = 10.0 Hz, 1H, H-3'), 5.20 (bs, 1H, H-4), 4.85 (d, *J* = 2.4 Hz, 1H, H-3), 4.66 (dt, *J* = 12.6, 6.3 Hz, 1H, H-5), 4.31 (dd, *J* = 12.1, 5.0 Hz, 1H, H-1), 4.25 – 4.13 (m, 2H, H-6), 2.86 (dd, *J* = 16.3, 12.1 Hz, 1H, H-1'), 2.59 (dd, *J* = 16.3, 5.0 Hz, 1H, H-1'), 2.17 (s, 3H, CH_3), 2.12 (s, 3H, CH_3), 2.09 (s, 3H, CH_3). NMR (75 MHz, $CDCl_3$) δ 196.4, 170.5, 168.7, 168.6, 145.1, 133.5, 77.4, 76.9, 76.5, 74.5, 68.7, 67.8, 66.3, 66.0, 59.6, 38.4, 20.8, 20.7, 20.6. MS: m/z calcd for $[M]^+$ =356, $[M + Na]^+$ =379; found $[M + Na]^+$ =379.

5.8.8. Synthetic strategy for compound 10b

Compound 126

Acording to literature procedure: [116]

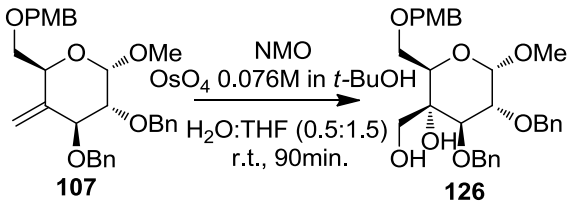

Scheme 5.52

A solution of compound **107** (981 mg, 1.99 mmol), *N*-methylmorpholine *N*-oxide (492 mg, 4.2 mmol) and osmium tetroxide (1.32 mL, 0.099 mmol) in H_2O/THF (0.5:1.5) (20 mL) is stirred at room temperature for 1.5 h and then diluted with CH_2Cl_2 (30 mL). The organic

layer is washed with 5 N hydrochloric acid (15 mL) and 45% of sodium hydrogen sulfite solution (15 mL), dried over sodium sulfate and concentrated under reduced pressure. The residue was used without further purification.

Compound 127

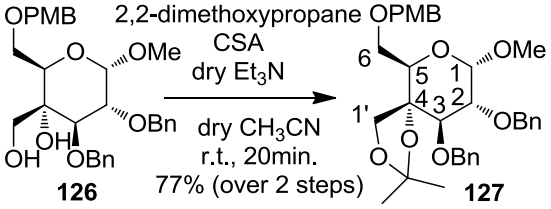

Scheme 5.53

To a solution of compound **127** (230 g, 0.44 mmol) in dry CH_3CN (3 mL) at rt, 2,2-dimethoxypropane (183 mg,1.76 mmol) and CSA (10 mg, 0.044 mmol) were added. The reaction mixture was stirred at room temperature for 20 min. After complete reaction dry Et_3N (178 mg, 1.76 mmol) was added to neutralize de CSA. The reaction mixture was then concentrated and purified by flash chromatography [(petroleum ether/ EtOAc 8:2)] to give 77% (over 2 steps) as green oil. ^{1}H NMR (400 MHz, $CDCl_3$) δ 7.36 – 7.22 (m, 12H, Ar-*H*), 6.85 (d, *J* = 8.3 Hz, 2H, Ar-*H*), 4.93 (d, *J* = 10.7 Hz, 1H, C*H*$_2$Ph), 4.79 (d, *J* = 10.7 Hz, 1H, C*H*$_2$Ph), 4.75 (d, *J* = 12.1 Hz, 1H, C*H*$_2$Ph), 4.62 – 4.54 (m, 3H, 2 C*H*$_2$Ph, H-1), 4.43 (d, *J* = 11.6 Hz, 1H, C*H*$_2$Ph), 4.12 (d, *J* = 8.8 Hz, 1H, H-1'), 4.01-3.95 (m, 2H, H-1', H-3), 3.89 (d, *J* = 7.9 Hz, 1H, H-5), 3.83 – 3.76 (m, 4H, H-6, ArOMe), 3.53 – 3.46 (m, 1H, H-6), 3.42 (s, 3H, OMe), 3.20 (dd, *J* = 10.2, 3.6 Hz, 1H, H-2), 1.56 (s, 6H, C*H*$_3$), 1.33 (s, 6H, C*H*$_3$). ^{13}C NMR (101 MHz, $CDCl_3$) δ 159.1, 138.5, 137.9, 130.3, 129.2, 128.4, 128.2, 128.1, 127.9, 127.7, 127.4, 113.7, 109.8, 97.3, 83.2, 79.5, 79.4, 77.3, 77.0, 76.7, 76.4, 73.4, 72.9, 71.4, 67.8, 63.6, 55.2, 55.1, 29.7, 26.2, 25.6.

Compound 128

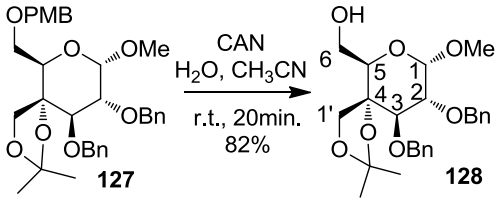

Scheme 5.54

To a solution of compound **127** (248 mg, 0.45 mmol) in CH_3CN (19 mL) at 0ºC, a solution of CAN (1.244 g, 2.27 mmol) in water (5.8 mL) was added. The reaction mixture was

stirred at room temperature for 20 min. and then diluted with CH_2Cl_2 (20 mL) and wash with water (2 x 15 mL). The combined organic phases were dried, concentrated and purified by flash chromatography using [petroleum ether/EtOAc (5:5)] to give 82% as orange pale oil. ^{1}H NMR (400 MHz, $CDCl_3$) δ 7.40 – 7.22 (m, 10H, Ar-*H*), 4.92 (d, *J* = 10.7 Hz, 1H, C*H*$_2$Ph), 4.81 (d, *J* = 10.7 Hz, 1H, C*H*$_2$Ph), 4.77 (d, *J* = 12.1 Hz, 1H, C*H*$_2$Ph), 4.61 (d, *J* = 12.1 Hz, 1H, C*H*$_2$Ph), 4.56 (d, *J* = 3.8 Hz, 1H, H-1), 4.21 – 4.05 (m, 2H, H-1'), 4.01 (d, *J* = 10.3 Hz, 1H, H-3), 3.93 – 3.74 (m, 1H, H-6), 3.76 – 3.63 (m, H-6), 3.40 (s, 3H, OMe), 3.20 (dd, *J* = 10.3, 3.8 Hz, 1H, H-2), 2.40 – 2.23 (m, 1H, H-5), 1.57 (s, 6H, 2 C*H*$_3$).

Compound 129

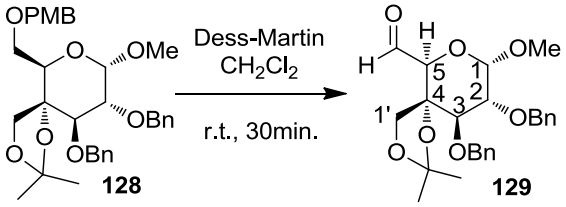

Scheme 5.55

Dess–Martin periodinane (236 mg, 0.577 mmol) was added to a mixture of compound **128** (165 mg, 0.371 mmol) in CH_2Cl_2 (3.5 ml) at rt. The reaction was stirred at rt for 30 min, before being quenched with saturated aqueous $Na_2S_2O_3$ (8 mL) and saturated with aqueous $NaHCO_3$ (8 mL). The mixture was extracted with ethyl acetate (3 x 8 mL) and the combined organic fraction was dried over Na_2SO_4. The solvent was removed under vacuum, and aldehyde **129** was used without further purification.

Compound 130

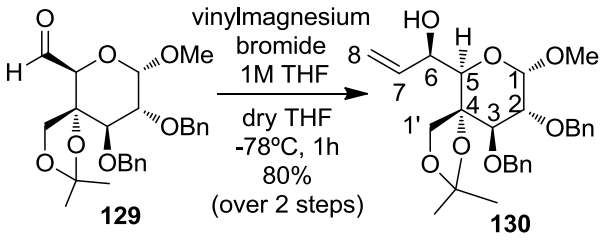

Scheme 5.56

To a solution of **129** (165 mg, 0.371 mmol) in dry THF (4 mL) at -78ºC under argon atmosphere, a solution of vinylmagnesium bromide (1 M in THF) (1.3 mmol, 1.3 mL) was added dropwise. The resulting solution was stirred for 2 h and then allowed to warm up until 0ºC. A saturated solution of NH_4Cl (15 mL) was added, and the reaction mixture was extracted with CH_2Cl_2 (3 x 6 mL). The organic extracts were dried over Na_2SO_4, filtered

and concentrated under reduced pressure. The residue was purified by flash chromatography [(petroleum ether/ EtOAc 8:2)] do give 80% as yellow pale oil (over 2 steps). ^{1}H NMR (400 MHz, $CDCl_3$) δ 7.43 – 7.20 (m, 10H, Ar-*H*), 6.02 – 5.83 (m, 1H, H-7), 5.39 (d, *J* = 17.3 Hz, 1H, H-8$_{trans}$), 5.19 (d, *J* = 10.5 Hz, 1H, H-8$_{cis}$), 4.92 (d, *J* = 10.7 Hz, 1H, C*H*$_2$Ph), 4.81 (d, *J* = 10.7 Hz, 1H, C*H*$_2$Ph), 4.76 (d, *J* = 12.1 Hz, 1H, C*H*$_2$Ph), 4.66 (bs, 1H, H-6), 4.58 (d, *J* = 12.1 Hz, 1H, C*H*$_2$Ph), 4.53 (d, *J* = 3.9 Hz, 1H, H-1), 4.42 (d, *J* = 8.7 Hz, 1H, H-1'), 4.18 (d, *J* = 8.7 Hz, 1H, H-1'), 3.96 (d, *J* = 10.3 Hz, 1H, H-3), 3.44 (d, *J* = 4.3 Hz, 1H, H-5), 3.35 (s, 3H, OMe), 3.18 (dd, *J* = 10.3, 3.9 Hz, 1H, H-2), 1.57 (s, 3H, C*H*$_3$), 1.55 (s, 3H, C*H*$_3$).

Compound 131

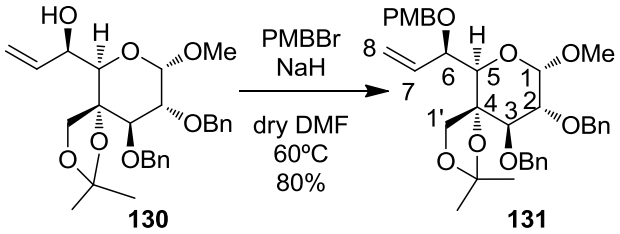

Scheme 5.57

A round-bottom flask was charged with a 60% dispersion of sodium hydride in mineral oil (2.6 mg, 0.106 mmol). Dry DMF (2 mL) was then added, and the resulting cloudy white suspension was cooled to 0 °C. A solution of alcohol **130** (30 mg, 0.064 mmol) in dry DMF (2 mL) was added via syringe, followed by *p*-methoxybenzyl bromide (15.4 mg, 0.076 mmol). The reaction mixture was stirred at 60ºC for 2 h. Upon cooling, the reaction was carefully quenched with saturated aqueous NH_4Cl (10 mL). The layers were separated, and the aqueous layer was extracted with EtOAc (1 x 10mL). The combined organic layers were dried ($MgSO_4$), filtered, and concentrated. Purification by flash chromatography [(petroleum ether/EtOAc 9:1)] afforded PMB ether **131** in 80% yield as a brown oil. ^{1}H NMR (400 MHz, $CDCl_3$) δ 7.45 – 7.18 (m, 12H, Ar-*H*), 6.83 (t, *J* = 12.1 Hz, 2H, Ar-*H*), 5.98 (ddd, *J* = 16.7, 9.5, 7.8 Hz, 1H, H-7), 5.31 (d, *J* = 16.7 Hz, 1H, H-8$_{trans}$), 5.28 (d, *J* = 9.5 Hz, 1H, H-8$_{cis}$), 4.95 (d, *J* = 10.9 Hz, 1H, C*H*$_2$Ph), 4.80 (d, *J* = 10.9 Hz, 1H, C*H*$_2$Ph), 4.72 (d, *J* = 12.3 Hz, 1H, C*H*$_2$Ph), 4.69 (d, *J* = 7.5 Hz, 1H, H-1'), 4.57 (d, *J* = 3.9 Hz, 1H, H-1), 4.55 (d, *J* = 12.3 Hz, 1H, C*H*$_2$Ph), 4.39 (s, 2H, C*H*$_2$Ph), 4.31 (d, *J* = 7.8 Hz, 1H, H-6), 4.14 (d, *J* = 7.5 Hz, 1H, H-1'), 3.96 (d, *J* = 10.5 Hz, 1H, H-3), 3.82 – 3.79 (m, 1H, H-5), 3.77 (s, 3H, ArOMe), 3.33 (s, 3H, OMe), 3.19 (dd, *J* = 10.5, 3.9 Hz, 1H, H-2), 1.54 (s,

3H, C*H*$_3$), 1.42 (s, 3H, C*H*$_3$).

Compound 132

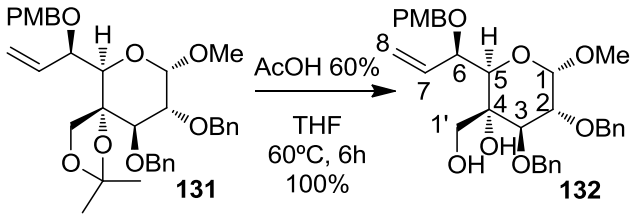

Scheme 5.58

A solution of AcOH 60% in water (4 mL) was added to a mixture of compound **131** (20 mg, 0.034 mmol) in THF (1 mL). The reaction was stirred at 60ºC for 6 h, before being quenched with saturated aqueous $NaHCO_3$ (8 mL). The mixture was extracted with ethyl acetate (3 x 5 mL) and the combined organic fraction was dried over Na_2SO_4. The solvent was removed under vacuum, and diol **132** was purified via flash column chromatography [(petroleum ether/EtOAc 8:2)] to give 100% as brown oil. ^{1}H NMR (400 MHz, $CDCl_3$) δ 7.46 – 7.18 (m, 12H, Ar-*H*), 6.86 (d, *J* = 8.6 Hz, 2H, Ar-*H*), 6.15 – 5.96 (m, 1H, H-7), 5.45 – 5.31 (m, 2H, H-8), 4.88 (d, *J* = 11.4 Hz, 1H, C*H*$_2$Ph), 4.81 (d, *J* = 11.4 Hz, 1H, C*H*$_2$Ph), 4.76 (d, *J* = 12.0 Hz, 1H, C*H*$_2$Ph), 4.60 – 4.53 (m, 3H, C*H*$_2$Ph, H-1, H-1'), 4.32 – 4.24 (m, 2H, H-6, H-1'), 3.89 (d, *J* = 13.1 Hz, 1H, C*H*$_2$Ph), 3.86 (d, *J* = 10.4 Hz, 1H, H-3), 3.79 (s, 4H, C*H*$_2$Ph, ArOMe), 3.65 – 3.61 (m, 1H, H-5), 3.55 (dd, *J* = 10.4, 3.9 Hz, 1H, H-2), 3.32 (s, 3H, OMe).

5.8.9. Synthetic strategy for Michael donor 139

C**ompound 134**

Acording to literature procedure:[122]

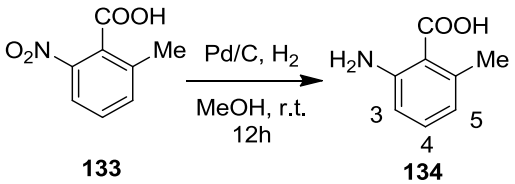

Scheme 5.59

To a stirred solution of 2-methyl-6-nitrobenzoic acid **133** (1.0 g, 5.52 mmol) in dry methanol (10 mL), 10% Pd on activated charcoal (20 mg) was added and then hydrogen

gas was purged to it. The reaction mixture was allowed to stir for overnight. The catalyst was filtered off and the filtrate was concentrated under reduced pressure. ^{1}H NMR (400 MHz, CD_3OD) δ 7.03 (t, *J* = 7.8 Hz, 1H, H-4), 6.60 (d, *J* = 7.8 Hz, 1H, H-3), 6.49 (d, *J* = 7.8 Hz, 1H, H-5), 2.41 (s, 3H, C*H*$_3$).

Compound 136

Acording to literature procedure:[122]

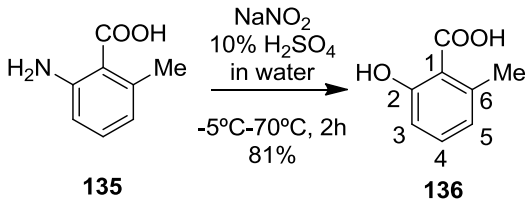

135 **136**

Scheme 5.60

The solid mass obtained was dissolved into 10% aqueous H_2SO_4 solution (10 mL). The resulting solution was cooled to -5 ºC and a cold saturated solution of $NaNO_2$ (419 mg, 6.07 mmol) was added slowly to it with hand shaking. Then, it was left for 20 min at room temperature and was heated until the temperature reached to 70 ºC. Heating was continued until evolution of N_2 ceases. The reaction mass was extracted with EtOAc (3 x 10 mL). The combined organic extract was washed successively with water (10 mL), brine (10 mL) and finally dried over Na_2SO_4. After removal of the solvent the crude product obtained was purified by flash chromatography [petroleum ether/EtOAc (8.5:1.5)] to furnish **136** (81%) as yellow solid. ^{1}H NMR (400 MHz, $CDCl_3$) δ 11.05 (s, 1H, COO*H*), 7.36 (dd, *J* = 8.3, 7.4 Hz, 1H, H-4), 6.88 (d, *J* = 8.3 Hz, 1H, H-3), 6.78 (d, *J* = 7.4 Hz, 1H, H-5), 2.67 (s, 3H, C*H*$_3$). ^{13}C NMR (101 MHz, $CDCl_3$) δ 176.4, 163.9, 143.2, 135.7, 123.5, 116.1, 111.1, 77.5, 77.2, 76.9, 24.4.

Compound 137

Acording to literature procedure:[122]

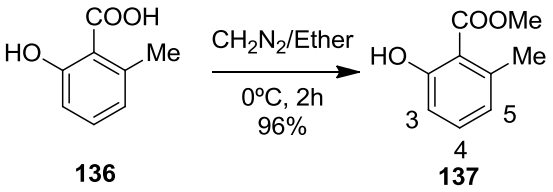

136 **137**

Scheme 5.61

To a solution of **136** (760 mg, 5.0 mmol) in diethyl ether (10 ml) at 0 ºC, diazomethane (15 mmol) in ether (10 mL) was added dropwise and stirred for 2 h. After removing the excess diazomethane the ether layer was washed with water, brine and finally dried over Na_2SO_4. After removal of the solvent under reduced pressure the residue obtained was purified by flash chromatography [petroleum ether/EtOAc (9:1)] to give the corresponding ester (96%) as colourless oil. ^{1}H NMR (300 MHz, $CDCl_3$): δ 7.25 (dd, *J* = 7.4, 8.3 Hz, 1H, H-4), 6.83 (d, *J* = 8.3 Hz, 1H, H-3), 6.69 (d, *J* = 7.4 Hz, 1H, H-5), 3.93 (s, 3H, OMe), 2.52 (s, 3H, C*H*$_3$), ^{13}C NMR (75 MHz, $CDCl_3$): δ 24.0, 52.1, 112.3, 115.6, 122.9, 134.2, 141.3, 162.9, 172.2

Compound 138

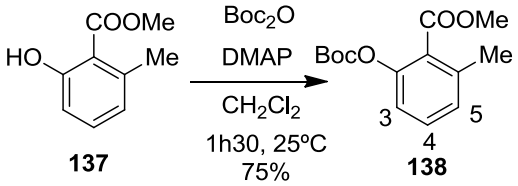

Scheme 5.62

Boc_2O (350 mg, 1.60 mmol) and DMAP (20 mg, 0.16 mmol) were added to compound **137** (243 mg, 1.46 mmol) in CH_2Cl_2 (8 mL). The reaction was stirred at 25°C for 90 min. and concentrated. Flash chromatography on silica gel [(9:1) petroleum ether/EtOAc] yielded the desired compound **138** (292 mg, 75%). ^{1}H NMR (400 MHz, $CDCl_3$) δ 7.33 (dd, *J* = 7.6, 8.1 Hz, 1H, H-4), 7.11 (d, *J* = 7.6 Hz, 1H, H-3), 7.02 (d, *J* = 8.1 Hz, 1H, H-5), 3.88 (s, 3H, OMe), 2.40 (s, 3H, C*H*$_3$), 1.52 (s, 9H, (C*H*$_3$)$_3$). ^{13}C NMR (101 MHz, $CDCl_3$) δ 151.9, 149.0, 138.8, 131.1, 128.5, 126.3, 120.6, 83.9, 77.6, 77.3, 76.9, 52.5, 27.9, 27.6, 20.4.

Compound 139

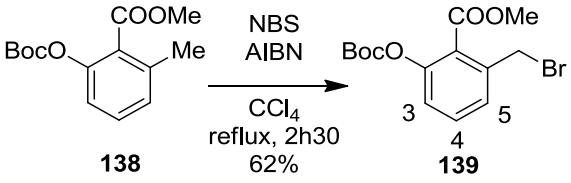

Scheme 5.63

N-Bromosuccinimide (99.6 mg, 0.56 mmol) was added to a solution of **138** (150 mg, 0.56 mmol) in carbon tetrachloride (2.8 mL) and was heated to reflux in the presence of visible light. Then, a catalytic amount of AIBN was added and the reflux was continued for 2 h.

After cooling to room temperature the precipitated solid was filtered off and the filtrate was concentrated under reduced pressure and the residue was extracted with CH_2Cl_2 (3 x 5 mL). The organic layer was washed successively with water (5 mL), brine (5 mL) and finally dried over Na_2SO_4. After removal of the solvent in vacuum the residue obtained was purified by flash chromatography [petroleum ether/EtOAc (9.5:0.5)] to furnish **139** (62%) as yellow oil. ^{1}H NMR (400 MHz, $CDCl_3$) δ 7.43 (dd, *J* = 7.7, 8.2 Hz, 1H, H-4), 7.32 (d, *J* = 7.7 Hz, 1H, H-3), 7.16 (d, *J* = 8.2 Hz, 1H, H-5), 4.67 (s, 2H, C*H*$_2$Br), 3.94 (s, 3H, OMe), 1.57 [s, 9H, (C*H*$_3$)$_3$]. ^{13}C NMR (101 MHz, $CDCl_3$) δ 165.8, 151.5, 149.4, 138.4, 131.7, 128.4, 126.1, 123.6, 84.3, 77.5, 77.2, 76.9, 52.9, 30.3, 29.9, 27.8.

5.8.1. Synthetic strategy for Michael donor 143

Compound 141

Acording to literature procedure:[124]

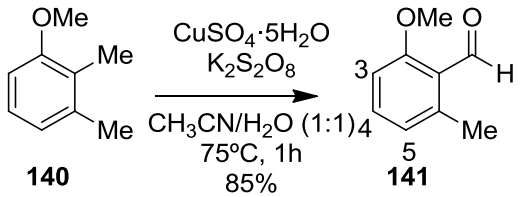

Scheme 5.64

A vigorously stirred mixture of 2,3-dimethylanisole **139** (4.12 g, 30.2 mmol), copper(II) sulfate pentahydrate (7.68 g, 30.7 mmol), and potassium peroxydisulfate (26.01 g, 96.2 mmol) in acetonitrile/water (1:1, 360 mL) was heated at 75°C. After no starting material was present shown by TLC analysis, the mixture was cooled to rt before adding CH_2Cl_2 (100 mL). The layers were separated, and the aqueous phase was further extracted with additional CH_2Cl_2 (2 x 40 mL). The combined organic solutions were dried over Na_2SO_4, filtered, and concentrated in vacuo. The residue was purified by flash chromatography [petroleum ether/ EtOAc (9.5:0.5)] to afford **141** (3.86 g, 85%) as a pale yellow powder. ^{1}H NMR (400 MHz, $CDCl_3$) δ 10.64 (s, 1H, C*H*O), 7.38 (t, *J* = 8.0 Hz, 1H, H-4), 6.87 – 6.77 (m, 2H, H-3, H-5), 3.90 (s, 3H, OMe), 2.57 (s, 3H, C*H*$_3$).

Compound 142

Acording to literature procedure:[124]

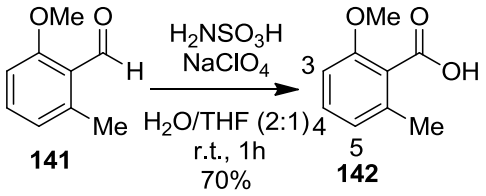

Scheme 5.65

A mixture of **141** (844 mg, 5.62 mmol) and sulfamic acid (731 mg, 7.53 mmol) in water (20 mL) and THF (10 mL) is stirred at rt for 5 min before sodium chlorite (661 mg, 7.31 mmol) dissolved in water (5 mL) is added. The mixture is stirred for 1 h followed by addition of ethyl acetate (10 mL). The layers are separated, and the aqueous phase is discarded. The ethyl acetate solution is extracted with aqueous 1 M NaOH (30 mL) by discarding the organic phase. The aqueous solution is acidified with concentrated HCl, and then extracted with CH_2Cl_2 (3 x 10 mL). The combined organic extracts are dried over Na_2SO_4, filtered, and evaporated at reduced pressure. Crystallization of the residue from petroleum ether/EtOAc gives the product **142** (645 mg, 70%) as white solid. ^{1}H NMR (400 MHz, $CDCl_3$) δ 7.31 (dd, *J* = 8.3, 7.6 Hz, 1H, H-4), 6.88 (d, *J* = 7.6 Hz, 1H, H-3), 6.83 (d, *J* = 8.3 Hz, 1H, H-5), 3.92 (s, 3H, OMe), 2.49 (s, 3H, C*H*$_3$).

Compound 143

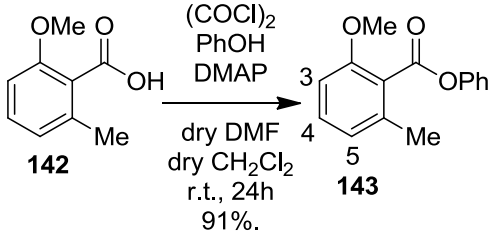

Scheme 5.66

Oxalyl chloride (0.208 mL, 2.41 mmol) and dry DMF (20 µL) were added to compound **142** (100 mg, 0.60 mmol) in dry CH_2Cl_2 (3.5 mL). The reaction was stirred at 25 °C for 1 h and concentrated. The resulting solid was redissolved in dry CH_2Cl_2 (3.5 mL). Phenol (113 mg, 1.20 mmol), DMAP (146 mg, 1.20 mmol), and dry triethylamine (0.59 mL, 4.2 mmol were added. The reaction was stirred at 25 °C for 12 h and concentrated. The residue was redissolved in EtOAc (10 mL). The solution was washed with aqueous 1 M NaOH (5 mL), water (5 mL), and brine (5 mL), dried over Na_2SO_4, and concentrated.

Flash chromatography on silica gel [(petroleum ether/toluene 3:7)] yielded the desired product (133mg, 91%) as green pale solid. ^{1}H NMR (400 MHz, $CDCl_3$) δ 7.44 (t, *J* = 7.9 Hz, 2H, H-3', H-5'), 7.36 – 7.21 (m, 4H, H-2', H-6', H-4', H-4), 6.92 – 6.78 (m, 2H, H-3, H-5), 3.89 (s, 3H, OMe), 2.46 (s, 3H, OMe). ^{13}C NMR (101 MHz, $CDCl_3$) δ 166.9, 156.7, 150.9, 136.7, 130.8, 129.5, 125.9, 122.9, 122.5, 121.7, 108.5, 77.3, 77.4, 76.7, 56.0, 19.3.

5.8.2. Synthetic strategy for diene 147

Compound 145

Acording to literature procedure:[130]

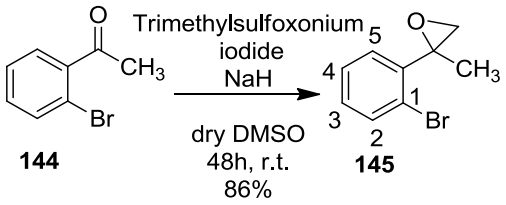

Scheme 5.67

Dry DMSO (40 mL) was added dropwise via syringe to a mixture of solid trimethylsulfoxonium iodide (2.9 g, 13.52 mmol) and solid sodium hydride (60% in oil, 325 mg, 13.52 mmol) at 23 °C. Vigorous gas evolution was observed upon addition. The resulting cloudy gray mixture was stirred at 23 °C for 40 min, then a solution of the 2'-bromoacetophenone **144** (2.0 g, 10.04 mmol) in dry DMSO (15 mL) was added dropwise via cannula. The transfer was quantitated with a portion of dry DMSO (2 mL). The resulting orange mixture was stirred at 23 °C for 48 h then was partitioned between brine (80 mL) and EtOAc (40 mL). The organic phase was separated and the aqueous phase was further extracted with one portion of EtOAc (40mL). The organic phases were combined and dried over anhydrous sodium sulfate. The dried solution was filtered and the filtrate was concentrated. The product was purified by flash column chromatography [petroleum ether/EtOAc (9.75:0.25)], affording the epoxide **145** as light yellow oil (1.84g, 86%). ^{1}H NMR (400 MHz, $CDCl_3$) δ 7.51 (dd, *J* = 8.0, 1.0 Hz, 1H, H-2), 7.47 (dd, *J* = 7.7, 1.7 Hz, 1H, H-5), 7.31 (td, *J* = 7.7, 1.0 Hz, 1H, H-4), 7.16 (td, *J* = 7.9, 1.7 Hz, 1H, H-3), 3.02 (d, *J* = 5.1 Hz, 1H, H-1'), 2.85 (d, *J* = 5.1 Hz, 1H, H-1'), 1.66 (s, 3H, C*H*$_3$).

Compound 146

Acording to literature procedure:[130]

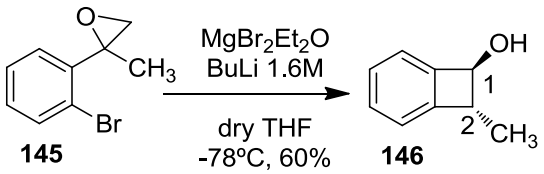

Scheme 5.68

A solution of *n*-butyllithium in hexanes (1.6 M, 6 mL, 9.5 mmol) was added dropwise via syringe down the side of a reaction vessel containing a solution of the epoxide **145** (1.84 g, 8.64 mmol) in dry THF (86 mL) at -78°C. The resulting solution was stirred at -78°C for 20 min whereupon a suspension of magnesium bromide ethyl etherate (4.46 g, 17.27 mmol) in dry THF (20 mL) was added dropwise via cannula. The transfer was quantitated with a portions of dry THF (2 mL). The resulting cloudy mixture was stirred at -78°C for 60 min, then the cooling bath was removed and the reaction mixture was allowed to warm to 23°C. The mixture became clear upon warming and was stirred at 23°C for 1 h. The reaction mixture was poured into aqueous Rochelle's salt solution (10% wt/wt) and the resulting mixture was extracted with EtOAc (3 x 10 mL). The organic phases were combined and dried over anhydrous sodium sulfate. The dried solution was filtered and the filtrate was concentrated. The product was purified by flash column chromatography [petroleum ether/EtOAc (9.5:0.5 to 9:1)], affording the *trans*-benzocyclobutene **146** as colorless oil (690mg, 60%). ^{1}H NMR (400 MHz, $CDCl_3$) δ 7.34 – 7.22 (m, 4H, Ar-*H*), 4.75 (s, 1H, H-1), 3.35 (q, *J* = 7.0 Hz, 1H, H-2), 1.42 (d, *J* = 7.0 Hz, 3H, C*H*$_3$).

Compound 147

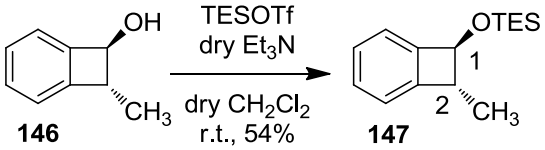

Scheme 5.69

Dry triethylamine (1.01 mL, 7.71 mmol) and triethylsilyl trifluoromethanesulfonate (1.51 mL, 6.69 mmol) were added in sequence to a solution of the benzocyclobutene **146** (690 mg, 5.14 mmol) in dry CH_2Cl_2 (10 mL) at 23°C. The solution was stirred at 23°C for 15 min. then was partitioned between water (20 mL) and CH_2Cl_2 (10 mL). The organic phase was separated and dried over anhydrous sodium sulfate. The dried solution was

filtered and the filtrate was concentrated. The product was purified by flash column chromatography [petroleum ether/toluene (9.5:0.5)], affording the triethyl-silyloxybenzocyclobutene **147** as clear oil (689 mg, 54%).[1]H NMR (400 MHz, $CDCl_3$) δ 7.33 – 7.16 (m, 3H, Ar-*H*), 7.12 (d, *J* = 6.4 Hz, 1H, Ar-*H*), 4.74 (d, *J* = 0.9 Hz, 1H, H-1), 3.37 (q, *J* = 7.0 Hz, 1H, H-2), 1.40 (d, *J* = 7.0 Hz, 3H, C*H*$_3$), 1.03 (t, *J* = 7.9 Hz, 9H, C*H*$_3$CH$_2$Si), 0.70 (q, *J* = 7.9 Hz, 6H, CH$_3$C*H*$_2$Si).[13]C NMR (101 MHz, $CDCl_3$) δ 146.9, 146.1, 129.3, 127.7, 122.8, 122.6, 77.7, 77.6, 77.3, 76.9, 50.4, 16.7, 6.8, 4.9.

5.8.3. Synthetic strategy for compound 148

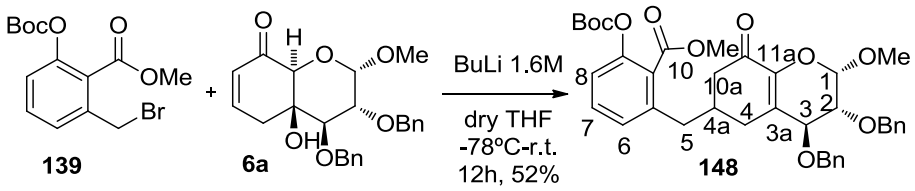

Scheme 5.70

A solution of *n*-butyllithium in hexanes (1.6 M, 120 μL, 0.1920 mmol) was added to a solution of compound **139** (33.6 mg, 0.097 mmol) and enone **6a** (10.0 mg, 0.024 mmol, in dry THF (2 mL) at –100 °C. The resulting yellow reaction mixture was allowed to warm to 0 °C overnight then was partitioned between aqueous potassium phosphate buffer solution (pH=7.0, 0.2 M, 2 mL) and CH_2Cl_2 (2 mL). The phases were separated and the aqueous phase was further extracted with dichloromethane. The organic extracts were combined and the combined solution was dried over anhydrous sodium sulfate. The dried solution was filtered and the filtrate was concentrated, affording a yellow solid. The product was purified by flash chromatography [petroleum ether/EtOAc (7:3)], affording the product **148** as a pale yellow oil (8 mg, 52%).[1]H NMR (400 MHz, $CDCl_3$) δ 7.42 – 7.21 (m, 11H, Ar-*H*, H-7), 7.10 (d, *J* = 8.0 Hz, 1H, H-8), 7.02 (d, *J* = 7.6 Hz, 1H, H-6), 4.86 (d, *J* = 2.3 Hz, 1H, H-1), 4.82 – 4.65 (m, 3H, 3 C*H*$_2$Ph), 4.55 (d, *J* = 11.0 Hz, 1H, C*H*$_2$Ph), 4.24 (d, *J* = 8.0 Hz, 1H, H-3), 3.86 (s, 3H, OMe), 3.82 (dd, *J* = 8.0, 2.3 Hz, 1H, H-2), 3.45 (s, 3H, OMe), 2.80 – 2.64 (m, 3H, 2 H-5, H-4), 2.55 (dd, *J* = 16.1, 2.6 Hz, 1H, H-10a), 2.45 – 2.35 (m, 1H, H-4), 2.26 (dd, *J* = 16.1, 11.4 Hz, 1H, H-10a), 1.97 (dd, *J* = 17.1, 9.4 Hz, 1H, H-4), 1.54 (s, 9H, 3 C*H*$_3$). [13]C NMR (101 MHz, $CDCl_3$) δ 192.9, 166.7, 151.6, 149.1, 141.5, 139.5, 137.8, 137.8, 131.1, 130.1, 128.8, 128.7, 128.5, 128.4, 128.4, 128.2, 128.1, 126.7, 121.4, 99.0, 84.1, 77.6, 77.3, 76.9, 75.5, 74.7, 73.4, 57.0, 52.6, 44.2, 39.0, 35.9, 29.9, 27.8.

5.8.4. Synthetic strategy for compound 149

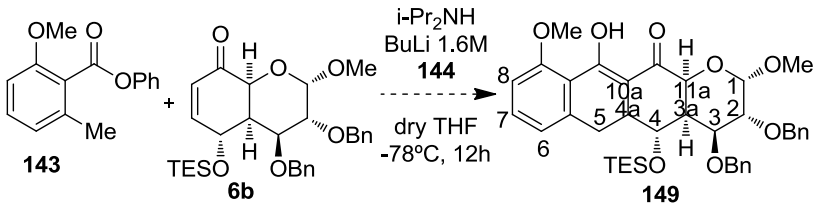

Scheme 5.71

To a solution of (*i*-Pr)$_2$NH (16 μL, 0.114 mmol) in dry THF (0.6 mL) at -78 °C was added n-BuLi (1.6 M in hexanes, 62 μL, 0.10 mmol) followed, after 20 min, by a solution of **143** (29 mg, 0.117 mmol) in dry THF (0.3 mL) that had been precooled to -78 °C. The resulting deep red solution was stirred for 15 min, after which a solution of **6b** (20 mg, 0.038 mmol) and LiBr (51mg, 0.38 mmol) in dry THF (0.7 mL) was added. The mixture was stirred at -78 °C for 2 h, during which the color changed from red to pale yellow. The mixture was allowed to warm to room temperature overnight and the reaction was quenched with satd. aqueous NH_4Cl (6 mL). The mixture was extracted with EtOAc (3 x 2 mL), and the extract was washed with H_2O (2 mL) and brine (2 mL) and was dried over Na_2SO_4. ^{1}H NMR (400 MHz, $CDCl_3$) δ 7.36 – 7.17 (m, 12H, Ar-*H*), 6.86 – 6.79 (m, 1H, Ar-*H*), 4.79 (d, *J* = 12.3 Hz, 1H, C*H*$_2$Ph), 4.69 – 4.66 (m, 2H, H-1, C*H*$_2$Ph), 4.62 (d, *J* = 13.3 Hz, 1H, C*H*$_2$Ph), 4.50 (d, *J* = 11.7 Hz, 1H, C*H*$_2$Ph), 4.21 (t, *J* = 6.2 Hz, 1H, H-4), 4.02 – 3.95 (m, 1H, H-3), 3.90 (s, 3H, ArOMe), 3.88 – 3.85 (m, 1H, H-2), 3.69 (s, 3H, OMe), 2.38 – 2.27 (m, 2H, H-5), 1.72 – 1.63 (m, 1H, H-4a), 1.62 – 1.52 (m, 1H, H-3a), 1.00 – 0.91 (m, C*H*$_3$CH$_2$Si, 9H), 0.81 – 0.69 (m, CH$_3$C*H*$_2$Si, 6H).

5.8.5. Synthetic strategy for compound 155

Compound 150

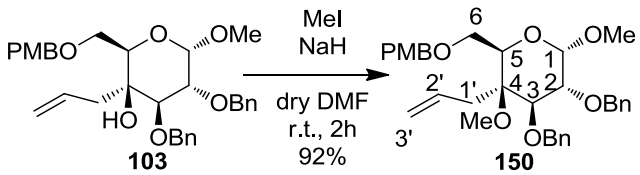

Scheme 5.72

To a solution of **103** (500 mg, 0.96 mmol) in dry DMF (2.5 mL), NaH (76 mg, 1.92 mmol) and MeI (70 μL, 1.15 mmol) were added. The reaction mixture stayed under magnetic

stirring for 2 h at room temperature, under argon atmosphere and then MeOH was added, and the reaction remained for more 10 min. This solution was partitioned between aqueous $NaHCO_3$ (8 mL) solution and EtOAc (4 mL). The phases were separated and the aqueous phase was further extracted with EtOAc (4 mL). The organic extracts were combined and the combined solution was dried over anhydrous sodium sulfate. The dried solution was filtered and the filtrate was concentrated. The product was purified by flash chromatography [petroleum ether/EtOAc (7:3)], affording the product **150** as a pale yellow oil (8 mg, 92%). ^{1}H NMR (400 MHz, $CDCl_3$) δ 7.41 – 7.17 (m, 12H, Ar-*H*), 6.86 (d, *J* = 8.6 Hz, 2H, Ar-*H*), 5.88 – 5.59 (m, 1H, H-2'), 5.14 – 4.94 (m, 3H, H-3', C*H*$_2$Ph), 4.79 – 4.70 (m, 2H, C*H*$_2$Ph, H-1), 4.67 – 4.60 (m, 2H, C*H*$_2$Ph), 4.55 (d, *J* = 11.7 Hz, 1H, C*H*$_2$Ph), 4.41 (d, *J* = 11.7 Hz, 1H, C*H*$_2$Ph), 4.00 (dd, *J* = 10.1, 3.5 Hz, 1H, H-2), 3.95 – 3.84 (m, 2H, H-3, H-5), 3.82 – 3.80 (m, 1H, H-6), 3.79 (s, 3H, ArOMe), 3.55 – 3.51 (m, 1H, H-6), 3.49 (s, 3H, OMe), 3.42 (s, 3H, OMe), 3.09 (dd, *J* = 13.6, 7.8 Hz, 1H, H-1'), 2.14 (dd, *J* = 13.6, 7.1 Hz, 1H, H-1'). ^{13}C NMR (101 MHz, $CDCl_3$) δ 159.3, 139.4, 138.4, 132.5, 130.7, 129.4, 128.6, 128.5, 128.4, 128.04, 127.54, 127.24, 119.55, 113.93, 98.28, 98.23, 79.73, 79.40, 78.52, 77.6, 77.3, 76.9, 76.1, 73.5, 73.3, 72.4, 68.8, 55.6, 55.5, 55.5, 53.2, 53.2, 34.1.

Compound 151

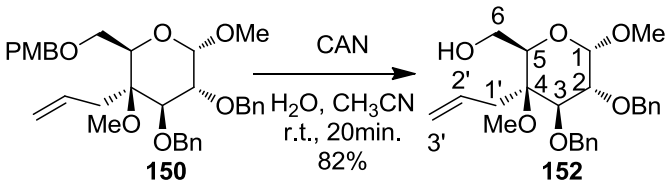

Scheme 5.73

To a solution of compound **150** (450 mg, 0.84 mmol) in CH_3CN (35 mL) at 0ºC, a solution of CAN (2.3 g, 4.21 mmol) in water (10 mL) was added. The reaction mixture was stirred at room temperature for 20 min. and then diluted with CH_2Cl_2 (20 mL) and wash with water (2 x 20 mL). The combined organic phases were dried, concentrated and purified by flash chromatography [petroleum ether/ EtOAc (6:4)] to give compound **151** in 82% as yellow pale oil.^{1}H NMR (400 MHz, $CDCl_3$) δ 7.43 – 7.20 (m, 10H, Ar-*H*), 5.67 (td, *J* = 17.1, 7.4 Hz, 1H, H-2'), 5.20 – 5.03 (m, 3H, H-3', C*H*$_2$Ph), 4.84 – 4.71 (m, 2H, H-1, C*H*$_2$Ph), 4.65 (d, *J* = 8.1 Hz, 1H, C*H*$_2$Ph), 4.62 (d, *J* = 7.6 Hz, 1H, C*H*$_2$Ph), 4.02 (dd, *J* = 10.0, 3.6 Hz, 1H, H-2), 3.98 – 3.84 (m, 2H, H-3, H-6), 3.80 – 3.64 (m, 2H, H-6, H-5), 3.53 (s, 3H, OMe), 3.39 (s, 3H, OMe), 3.13 (dd, *J* = 13.9, 7.2 Hz, 1H, H-1'), 2.21 (dd, *J* =

13.9, 7.6 Hz, 1H, H-1'). ^{13}C NMR (101 MHz, $CDCl_3$) δ 139.1, 138.3, 132.0, 128.7, 128.6, 128.4, 128.1, 127.7, 127.3, 119.9, 98.6, 80.6, 79.4, 78.2, 77.6, 77.3, 76.9, 76.3, 73.6, 71.9, 61.3, 55.7, 53.2, 34.0.

Compound 152

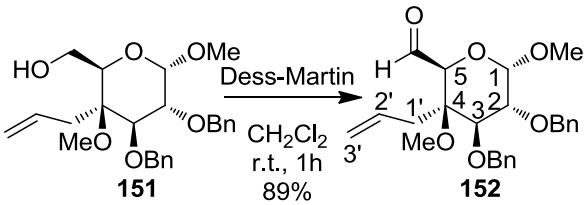

Scheme 5.74

Alcohol **151** (250 mg, 0.59 mmol) in CH_2Cl_2 (1 mL) was added to a stirred solution of Dess-Martin periodinane (371 mg, 0.88 mmol) in CH_2Cl_2 (5 mL) at 0ºC, and then the mixture was allowed to warm to rt. The reaction was completed after 2 h, the excess of oxidant was destroyed by addition of saturated solution of $Na_2S_2O_3$ (10 mL). After 5 min. of vigourous stirring, the mixture was diluted with CH_2Cl_2 (10 mL), the organic layer was sperated, and the aqueous layer extracted with CH_2Cl_2 (2 x 5 mL). The combined extracts were dried over Na_2SO_4, filtered and concentrated. The product was purified by flash chromatography [petroleum Ether/EtOAc (8.5:1.5)], affording the product **152** as yellow oil (221 mg, 89%). ^{1}H NMR (400 MHz, $CDCl_3$) δ 9.61 (d, *J* = 1.2 Hz, 1H, C*H*O), 7.44 – 7.23 (m, 10H, Ar-*H*), 5.90 – 5.71 (m, 1H, H-2'), 5.29 – 5.12 (m, 2H, H-3'), 5.07 (d, *J* = 11.4 Hz, 1H, C*H*$_2$Ph), 4.84 – 4.73 (m, 2H, H-1, C*H*$_2$Ph), 4.65 (m, 2H, C*H*$_2$Ph), 4.08 (dd, *J* = 10.0, 3.5 Hz, 1H, H-2), 4.03 (d, *J* = 1.2 Hz, 1H, H-5), 3.93 (d, *J* = 10.0 Hz, 1H, H-3), 3.45 (s, 3H, OMe), 3.39 (s, 3H, OMe), 3.07 (dd, *J* = 13.5, 7.9 Hz, 1H, H-1'), 2.46 (dd, *J* = 13.5, 7.2 Hz, 1H, H-1'). ^{13}C NMR (101 MHz, $CDCl_3$) δ 200.7, 139.0, 138.2, 132.3, 128.7, 128.6, 128.4, 128.2, 127.7, 127.4, 120.7, 98.9, 82.1, 78.4, 78.1, 77.6, 77.2, 76.9, 76.2, 75.7, 73.7, 56.2, 53.4, 32.9.

Compound 153

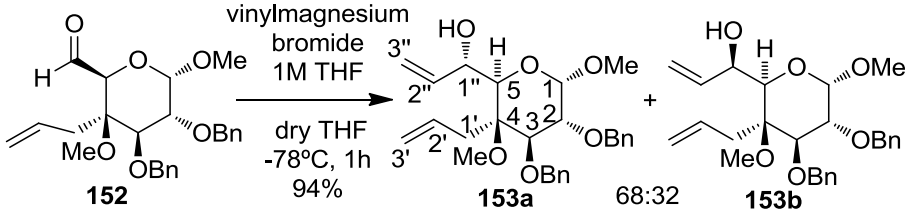

Scheme 5.75

Allylmagnesium bromide 1 M solution in THF (1.17 mmol, 1.17 mL) was added to a solution of **152** (200 mg, 0.47 mmol) in dry THF (3 mL) at -78ºC. The reaction was stirred at -78ºC for 2 h. The reaction mixture was warm to 0 ºC, and was slowly added a solution of NH_4Cl (15 mL) and diluted with EtOAc (10 mL). The aqueous phase was back-extracted with EtOAc (3 x 5 mL) and all the organic fractions were combined and dried over anhydrous Na_2SO_4. The residue was purified by flash chromatography using petroleum ether/EtOAc (9:1) to give a mixture of diastereoisomers (62:38) **153** (0.200 g, 94% yield) as yellow pale oil. NMR characterization of the major isomer: ^{1}H NMR (400 MHz, $CDCl_3$) δ 7.44 – 7.14 (m, 10H, Ar-*H*), 5.97 – 5.83 (m, 1H, H-2''), 5.74 – 5.57 (m, 1H, H-2'), 5.28 (d, *J* = 17.0 Hz, 1H, H-3''$_{trans}$), 5.22 – 5.03 (m, 4H, H-3', H-3''$_{cis}$, C*H*$_2$Ph), 4.77 – 4.70 (m, 2H, H-1, C*H*$_2$Ph), 4.67 – 4.51 (m, 3H, H-1'', C*H*$_2$Ph), 4.00 (dd, *J* = 10.1, 3.5 Hz, 1H, H-2), 3.86 (d, *J* = 10.1 Hz, 1H, H-3), 3.59 – 3.45 (m, 4H, H-5, OMe), 3.32 (s, 3H, OMe), 3.23 (dd, *J* = 13.8, 6.5 Hz, 1H, H-1'), 2.38 (dd, *J* = 13.8, 7.6 Hz, 1H, H-1').

Compound 154

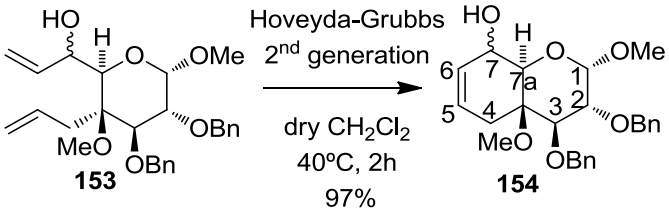

Scheme 5.76

To a solution of **153** (77 mg, 0.17 mmol) in dry CH_2Cl_2 (10 mL), Hoveyda-Grubbs catalyst 2nd generation (5% weight), was added. The reaction mixture was stirred at 40ºC for 90 min. The crude product was concentrated and purified by flash chromatography [petroleum ether/ EtOAc (6:4)] to give 97% as brown pale oil. NMR characterization of the major isomer, ^{1}H NMR (400 MHz, $CDCl_3$) δ 7.53 – 7.15 (m, 10H, Ar-*H*), 6.05 – 5.86 (m, 1H, H-5), 5.78 – 5.56 (m, 1H, H-6), 5.01 (d, *J* = 11.5 Hz, 1H, C*H*$_2$Ph), 4.88 (d, *J* = 3.4 Hz, 1H, H-1), 4.79 (d, *J* = 12.0 Hz, 1H, C*H*$_2$Ph), 4.67 (d, *J* = 12.0 Hz, 1H, C*H*$_2$Ph), 4.59 (d, *J* = 11.5 Hz, 1H, C*H*$_2$Ph), 4.17 – 3.96 (m, 2H, H-7, H-2), 3.74 (d, *J* = 9.5 Hz, 1H, H-3), 3.60 (d, *J* = 10.8 Hz, 1H, H-7a), 3.44 (s, 3H, OMe), 3.42 (s, 3H, OMe), 2.99 (dd, *J* = 19.0, 5.5 Hz, 1H, H-4), 1.79 (bd, *J* = 19.0 Hz, 1H, H-4).

Compound 155

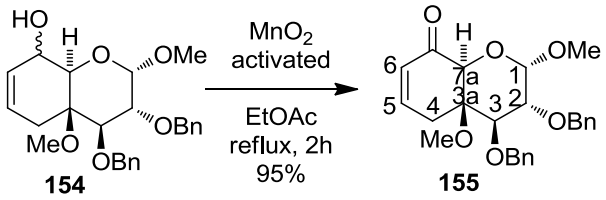

Scheme 5.77

Compound **154** (693 mg, 1.62 mmol) and activated MnO_2 (988 mg, 11.37 mmol) were slurried in EtOAc (20 mL), and the mixture was armed at reflux for 4 h. After consumption of the starting material, the reaction mixture was filtered hot though celite and the residual black solid was washed copiously with EtOAc (40 mL). The filtrate was concentrated in vacuum, to give **155** (656 mg, 95%yield) as brown pale oil. ^{1}H NMR (400 MHz, $CDCl_3$) δ 7.45 – 7.24 (m, 10H, Ar-*H*), 6.68 (ddd, *J* = 10.1, 5.9, 2.1 Hz, 1H, H-5), 6.06 (dd, *J* = 10.1, 3.1 Hz, 1H, H-6), 5.04 (d, *J* = 11.2 Hz, 1H, C*H*$_2$Ph), 4.84 (d, *J* = 3.4 Hz, 1H, H-1), 4.79 (d, *J* = 11.7 Hz, 1H, C*H*$_2$Ph), 4.65 (d, *J* = 11.2 Hz, 1H, C*H*$_2$Ph), 4.62 (d, *J* = 11.7 Hz, 1H, C*H*$_2$Ph), 4.35 (s, 1H, H-7a), 4.05 (dd, *J* = 10.0, 3.4 Hz, 1H, H-2), 3.90 (d, *J* = 10.0 Hz, 1H, H-3), 3.42 (s, 3H, OMe), 3.38 (s, 3H, OMe), 3.16 (dd, *J* = 19.6, 5.9 Hz, 1H, H-4), 2.20 – 2.11 (m, 1H, H-4). ^{13}C NMR (101 MHz, $CDCl_3$) δ 193.8, 142.2, 138.7, 138.2, 129.9, 129.7, 129.4, 128.7, 128.4, 128.3, 128.2, 128.0, 127.8, 99.2, 82.2, 80.5, 77.6, 77.5, 77.3, 76.9, 76.3, 76.2, 73.8, 56.3, 54.4, 30.2.

5.8.6. Synthetic strategy for compound 157

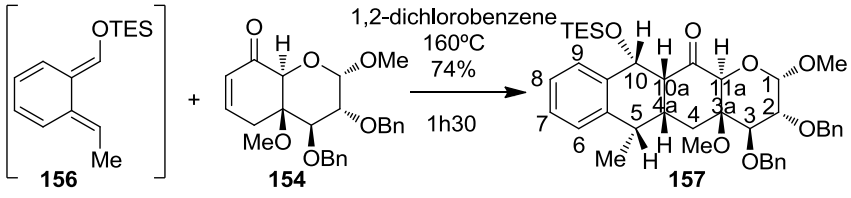

Scheme 5.78

To a solution of **154** (45 mg, 0.106 mmol) in 1,2-dichlorobenzene, benzocyclobutenol **156** (203 mg, 0.817 mmol) was added. The reaction mixture was stirred at 160ºC for 90min. The crude product was concentrated and purified by flash chromatography [petroleum ether/ EtOAc (8:2)] to give 74% as yellow pale oil. ^{1}H NMR (500 MHz, $CDCl_3$) δ 7.40 – 7.21 (m, 13H, Ar-*H*), 7.12 (d, *J* = 7.3 Hz, 1H, Ar-*H*), 4.91 – 4.83 (m, 2H, H-10, C*H*$_2$Ph),

4.78 (d, *J* = 3.5 Hz, H-1), 4.72 (d, *J* = 12.1 Hz, 1H, C*H*$_2$Ph), 4.61 (d, *J* = 12.1 Hz, C*H*$_2$Ph), 4.41 (d, *J* = 11.7 Hz, C*H*$_2$Ph), 3.95 (s, 1H, H-11a), 3.88 (dd, *J* = 10.1, 3.5 Hz, 1H, H-2), 3.50 (d, *J* = 10.1 Hz, 1H, H-3), 3.39 (s, 3H, OMe), 3.35 (s, 3H, OMe), 3.21 (t, *J* = 8.2 Hz, 1H, H-10a), 2.91 – 2.84 (m, 1H, H-5), 2.41 – 2.36 (m, 1H, H-4a), 2.23 (dd, *J* = 15.0, 5.4 Hz, 1H, H-4), 1.30 (d, *J* = 7.0 Hz, 3H, C*H*$_3$), 0.90 (t, *J* = 7.9 Hz, 9H, C*H*$_3$CH$_2$Si), 0.61 (m, 7H, H-4, CH$_3$C*H*$_2$Si). NMR (75 MHz, $CDCl_3$) δ 203.3, 140.2, 138.6, 138.3, 138.1, 130.2, 128.4, 128.4, 128.1, 127.8, 127.7, 127.6, 127.4, 126.1, 125.8, 124.9, 98.6, 81.8, 80.4, 78.0, 77.42, 77.00, 76.86, 76.57, 76.15, 73.32, 68.32, 55.46, 52.85, 34.86, 34.69, 26.3, 17.1, 6.8, 4.7.

5.8.7. Synthetic strategy for tetracyclic glycofused compound 163

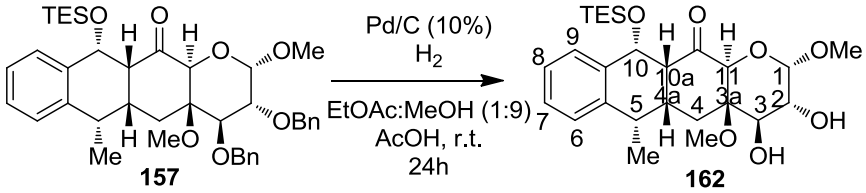

Scheme 5.79

A suspension containing **157** (50 mg, 0.0699 mmol) and Pd/C 10% in EtOAc:MeOH (1:1) (6 mL) was stirred at room temperature under H_2 (1 atm) for 18h. The suspension was filtered and the filtrate was concentrated to give **162** (12 mg, 45%) as a yellow oil. ^{1}H NMR (300 MHz,) δ 7.54 – 7.45 (m, 1H, Ar-*H*), 7.40 – 7.23 (m, 3H, Ar-*H*), 5.00 (d, *J* = 10.2 Hz, 1H, H-3), 4.75 (d, *J* = 3.8 Hz, 1H, H-1), 3.87 (s, 1H, H-10), 3.71 (dd, *J* = 10.2, 3.8 Hz, 1H, H-2), 3.45 (s, 3H, OMe), 3.43 – 3.36 (m, 1H, H-10a), 3.35 (s, 1H, H-11) 3.33 (s, 3H, OMe), 2.97 (dd, *J* = 7.0, 3.4 Hz, 1H, H-5), 2.60 – 2.39 (m, 2H, H-4a, H-4), 1.49 (s, *J* = 7.0 Hz, 3H, Me), 0.98 (dd, *J* = 9.6, 6.2 Hz, 9H, C*H*$_3$CH$_2$Si), 0.76 – 0.66 (m, 6H, CH$_3$C*H*$_2$Si), 0.56 – 0.45 (m, 1H, H-4).

5.8.8. Synthetic strategy for glucofused tetracyclic compound's 160 and 161

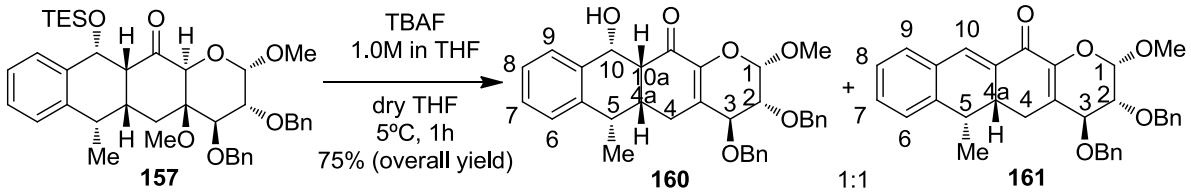

Scheme 5.80

A mixture of TES ether **157** (75 mg, 0.169 mmol) and TBAF (1.0M in THF, 56.41 μL, 0.056 mmol) in dry THF (2 mL) was stirred at 5ºC for 1h. After consumption of the starting material, was slowly added a solution of NH_4Cl (2 mL) and diluted with EtOAc (1 mL). The aqueous phase was back-extracted with EtOAc (3 x 1 mL) and all the organic fractions were combined and dried over anhydrous Na_2SO_4. The residue was purified by flash chromatography [petroleum ether/EtOAc (7:3) and (6:4)] to give a mixture (1:1) of tetracyclic compounds **160** and **161** in 75% overall yield. Compound **160** ^{1}H NMR (400 MHz, $CDCl_3$) δ 7.61 (d, *J* = 7.5 Hz, 1H, Ar-*H*), 7.43 – 7.20 (m, 12H, Ar-*H*), 7.07 (d, *J* = 7.3 Hz, 1H, Ar-*H*), 4.94 (d, *J* = 8.8 Hz, 1H, H-10), 4.90 (d, *J* = 2.3 Hz, 1H, H-1), 4.86 (d, *J* = 11.2 Hz, 1H, C*H*$_2$Ph), 4.79 (d, *J* = 12.2 Hz, 1H, C*H*$_2$Ph), 4.73 (d, *J* = 12.2 Hz, 1H, C*H*$_2$Ph), 4.65 (d, *J* = 11.2 Hz, 1H, C*H*$_2$Ph), 4.42 (broad s, 1H, OH), 4.30 (d, *J* = 8.0 Hz, 1H, H-3), 3.89 (dd, *J* = 8.0, 2.3 Hz, 1H, H-2), 3.49 (s, 3H, OMe), 2.95 – 2.86 (m, 1H, H-5), 2.72 – 2.64 (m, 1H, H-4), 2.55 (dd, *J* = 8.8, 4.4 Hz, 1H, H-10a), 2.49 – 2.38 (m, 1H, H-4), 2.31 – 2.19 (m, 1H, H-4a), 1.19 (d, *J* = 7.1 Hz, 3H, C*H*$_3$). Compound **161** ^{1}H NMR (400 MHz, $CDCl_3$) δ 7.66 (d, *J* = 2.9 Hz, 1H, H-10), 7.50 – 7.10 (m, 14H, Ar-*H*), 4.96 (d, *J* = 2.5 Hz, 1H, H-1), 4.88 (d, *J* = 11.3 Hz, 1H, C*H*$_2$Ph), 4.79 (d, *J* = 12.1 Hz, 1H, C*H*$_2$Ph), 4.73 (d, *J* = 12.1 Hz, 1H, C*H*$_2$Ph), 4.67 (d, *J* = 11.3 Hz, 1H, C*H*$_2$Ph), 4.37 (d, *J* = 8.0 Hz, 1H, H-3), 3.94 (dd, *J* = 8.0, 2.5 Hz, 1H, H-2), 3.52 (s, 3H, OMe), 3.07 – 2.93 (m, 1H, H-4a), 3.07 – 2.93 (m, 1H, H-5), 2.66 (dd, *J* = 16.8, 6.7 Hz, 1H, H-4), 2.36 (dd, *J* = 16.8, 10.1 Hz, 1H, H-4), 1.01 (d, *J* = 7.0 Hz, 3H, C*H*$_3$).

5.8.9. Synthetic strategy for glycofused quinoxaline derivative 179

Compound 176

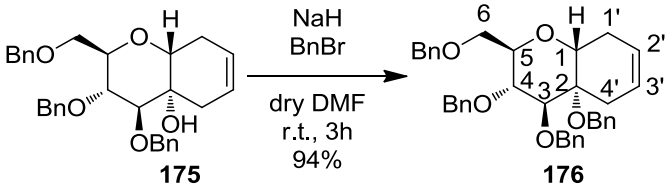

Scheme 5.81

A stirred solution of **175** (600 mg, 1.23 mmol) in anhydrous DMF (7 mL) under argon at 0 ºC was treated with of NaH (60% in mineral oil, 150 mg, 3.73 mmol). After 15 min. at room temperature, the mixture was treated dropwise and rapidly with BnBr (3.71 mmol, 0.44 mL) and then allowed to stand for 1 h at rt. The mixture was diluted with EtOAc (10 mL), and washed with saturated $NaHCO_3$ solution (20 mL). The aqueous phase was back-extracted with EtOAc (10 mL), and all the organic fractions were combined, washed with brine, and dried over anhydrous Na_2SO_4. The residue was purified by flash chromatography [petroleum ether/EtOAc (9.5:0.5)] affording **176** (669 mg, 94% yield) as powder solid. ^{1}H NMR (400 MHz, $CDCl_3$) δ 7.47 – 7.07 (m, 15H, Ar-*H*), 5.6 – 5.51 (m, 1H, H-2'), 5.41 – 5.30 (m, 1H, H-3'), 4.91 (d, *J* = 11.6 Hz, 1H, C*H*$_2$Ph), 4.76 (d, *J* = 10.6 Hz, 1H, C*H*$_2$Ph), 4.71 (d, *J* = 10.1 Hz, 1H, C*H*$_2$Ph), 4.68 – 4.54 (m, 4H, C*H*$_2$Ph), 4.49 (d, *J* = 11.6 Hz, 1H, C*H*$_2$Ph), 4.38 – 4.29 (m, 1H, H-1), 4.14 (t, *J* = 9.1 Hz, 1H, H-6), 3.97 – 3.85 (m, 1H, H-5), 3.80 – 3.68 (m, 3H, H-3, H-4, H-6), 2.75 (dd, *J* = 17.6, 4.9 Hz, 1H, H-4'), 2.64 – 2.32 (m, 2H, H-1'), 2.24 (d, *J* = 17.6 Hz, 1H, H-4').

Compound 177

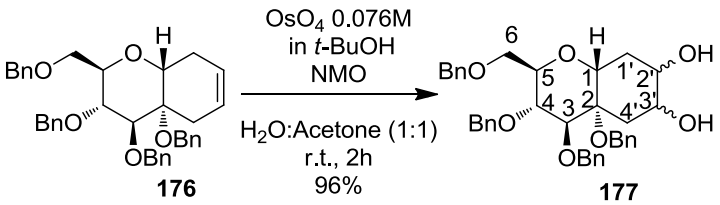

Scheme 5.82

A solution of compound **176** (260 mg, 0.451 mmol), *N*-methylmorpholine *N*-oxide (126 mg, 1.04 mmol) and osmium tetroxide (0.34 mL, 0.025 mmol) in H_2O/acetone (1:1) (4 mL) is stirred at room temperature for 1,5 h and then diluted with CH_2Cl_2 (15 mL). The organic layer is washed with 5 N hydrochloric acid (5 mL) and 45% of sodium hydrogen

sulfite solution (5 mL), dried over sodium sulfate and concentrated under reduced pressure. Flash chromatography using petroleum ether/EtOAc (6:4) of the residue affords a mixture of diasteoisomers (265 mg, 96%) as a yellow pale oil. ^{1}H NMR (400 MHz, $CDCl_3$) δ 7.51 – 7.15 (m, 20H, Ar-*H*), 4.98 – 4.70 (m, 1H, C*H*$_2$Ph), 4.70 – 4.44 (m, 7H, C*H*$_2$Ph), 4.42 – 4.19 (m, 1H, H-1), 4.17 – 4.00 (m, 1H, H-6), 4.00 – 3.90 (m, 1H, H-4'), 3.90 – 3.81 (m, 1H, H-5), 3.79 – 3.73 (m, 1H, H-3), 3.72 – 3.65 (m, 2H, H-6, H-4), 2.31 (bd, *J* = 12.0 Hz, 1H, H-1'), 2.02 – 1.88 (m, 2H, H-4', H-1').

Compound 178

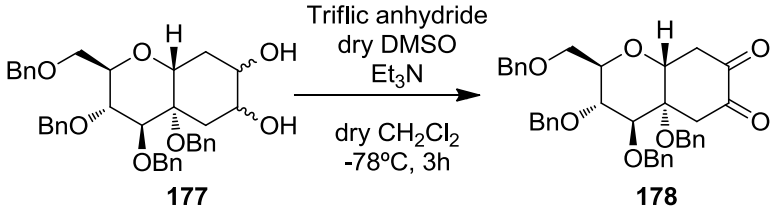

Scheme 5.83

To a solution of $(COCl)_2$ (364 mg, 2.87 mmol) in dry CH_2Cl_2 (6 mL) at -78ºC under argon atmosphere, anhydrous DMSO (0.4 mL) was added dropwise, and the resulting solution was stirred for 30 min. To the reaction flask, a solution of **177** (341 mg, 0.718 mmol) in dry CH_2Cl_2 (2.0 mL) was added dropwise at -78ºC. This final reaction mixture stayed under magnetic stirring for 1 h at -78ºC. Then dry TEA (0.9 mL) was added and the reaction stayed for more 30 min under magnetic stirring at -78ºC, and then was allowed to warm up until 0ºC. It was carefully added NH_4Cl (10 mL), and the organic layer was washed with H_2O (5 mL), dried over Na_2SO_4, and concentrated. The residue was used without further purification.

Compounds 179 and 180

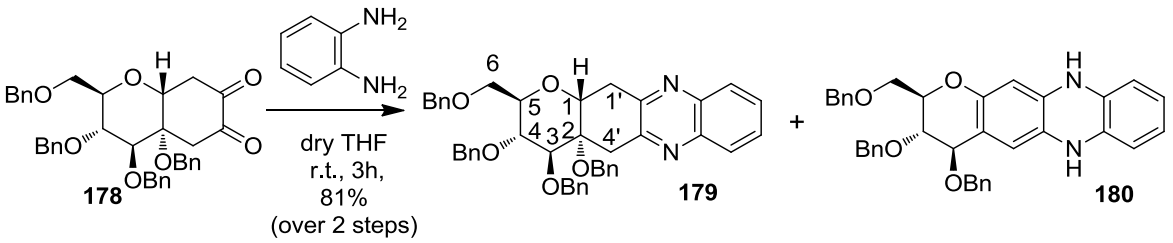

Scheme 5.84

To a solution of compound **178** (61 mg, 0.10 mmol) in dry THF (0.5 mL) 1,2-diaminobenzene (18 mg, 0.16 mmol) was added. The reaction mixture remained under magnetic stirring at reflux for 3 h. Then was allowed to cool to rt, and was concentrated. Flash chromatography [petroleum ether/EtOAc (7:3)] of the residue affords **179** (47 mg, 71%) as a yellow pale oil. ^{1}H NMR (400 MHz, $CDCl_3$) δ 8.05 – 7.90 (m, 2H, Ar-*H*), 7.73 – 7.59 (m, 2H, Ar-*H*), 7.41 – 6.94 (m, 20H, Ar-*H*), 4.66 (d, *J* = 12.0 Hz, 1H, C*H*$_2$Ph), 4.60 – 4.43 (m, 7H, H-1, C*H*$_2$Ph), 4.40 (d, *J* = 11.3 Hz, 1H, C*H*$_2$Ph), 4.27 – 4.17 (m, 2H, H-4', H-5), 4.05 – 4.00 (m, 1H, H-3), 3.93 – 3.79 (m, 3H, H-6, H-4), 3.66 (dd, *J* = 18.7, 5.6 Hz, 1H, H-1'), 3.37 (bd, *J* = 18.2 Hz, 1H, H-4'), 3.29 (dd, *J* = 18.7, 3.1 Hz, 1H, H-1'). ^{13}C NMR (101 MHz, $CDCl_3$) δ 151.88, 151.34, 141.71, 141.49, 138.43, 138.32, 137.87, 137.49, 129.21, 129.12, 128.75, 128.65, 128.61, 128.42, 128.34, 128.27, 128.21, 127.94, 127.91, 127.38, 127.25, 77.60, 77.28, 77.15, 76.96, 75.60, 75.38, 73.79, 73.48, 73.15, 72.52, 68.50, 67.92, 63.66, 35.25, 34.38. MS: m/z calcd for $[M]^+$ = 679, $[M + H]^+$ =680; found $[M]^+$ = 679, $[M + H]^+$ =681. Compound **180** ^{1}H NMR (400 MHz, $CDCl_3$) δ 8.28 (dd, *J* = 6.7, 3.5 Hz, 2H, Ar-*H*), 8.22 (d, *J* = 9.1 Hz, 2H, Ar-*H*), 7.99 (dd, *J* = 9.1, 1.7 Hz, 1H, Ar-*H*), 7.88 (dd, *J* = 6.7, 3.5 Hz, 2H, Ar-*H*), 7.47 – 7.22 (m, 10H, Ar-*H*), 7.11 – 7.07 (m, 2H, Ar-*H*), 7.01 – 6.95 (m, 2H, Ar-*H*), 5.01 (d, *J* = 3.0 Hz, 1H, H-3), 4.69 (d, *J* = 11.8 Hz, 1H, C*H*$_2$Ph), 4.50 (bs, 2H, C*H*$_2$Ph), 4.38 (d, *J* = 11.8 Hz, 1H, C*H*$_2$Ph), 4.26 (d, *J* = 11.1 Hz, 1H, C*H*$_2$Ph), 4.08 (m, 2H, C*H*$_2$Ph, H-5), 3.81 (dd, *J* = 7.4, 3.0 Hz, 1H, H-4), 3.68 – 3.57 (m, 2H, H-6), 2.60 (d, *J* = 6.0 Hz, 1H, N-*H*). ^{13}C NMR (101 MHz, $CDCl_3$) δ 143.69, 143.49, 143.41, 142.71, 137.56, 137.56, 130.83, 130.74, 129.88, 129.76, 128.73, 128.70, 128.59, 128.32, 128.22, 128.08, 127.83, 82.32, 79.87, 70.32, 30.06. MS: m/z calcd for $[M]^+$ = 571, $[M + H]^+$ =572; $[M + Na]^+$ =594, found $[M + H]^+$ = 572, $[M + Na]^+$ =594.

5.8.10. Synthetic strategy for pegylated derivative 83

Compound 182

According to literature procedure:[155]

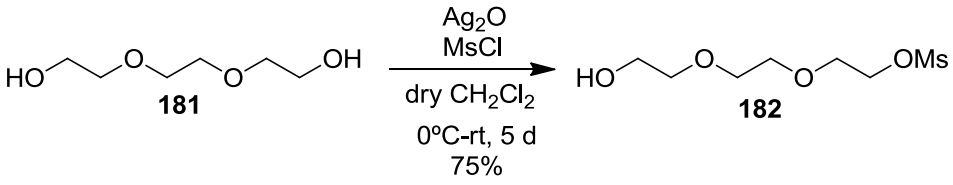

Scheme 5.85

Triethylene glycol **181** (4 g, 26.64 mmol, 3.6 mL) was dissolved in dry CH_2Cl_2 (62 mL). The solution was cooled to 0°C before adding silver(I)oxide (6.8 g, 29.3 mmol), followed by MsCl (2.5 ml, 31.97 mmol). The mixture was stirred at rt for 5 days. Progress of the reaction was followed by TLC. It was then filtered through celite and the solvent was evaporated. The crude product was purified by flash chromatography on silica gel [EtOAc/MeOH (95:5)]. The bis-mesylated product eluted first followed by the title compound **182** as a colorless oil (4.54 g, 75% yield): ^{1}H NMR (400 MHz, $CDCl_3$): δ 4.40 – 4.29 (m, 2H, C*H*$_2$), 3.78 – 3.72 (m, 2H, C*H*$_2$), 3.72 – 3.67 (m, 2H, C*H*$_2$), 3.65 (s, 4H, C*H*$_2$), 3.60 – 3.52 (m, 2H, C*H*$_2$), 3.05 (s, 3H, C*H*$_3$). ^{13}C NMR (101 MHz, $CDCl_3$): δ 72.5, 70.6, 70.3, 69.0, 61.7, 37.7.

Compound 183

According to literature procedure:[155]

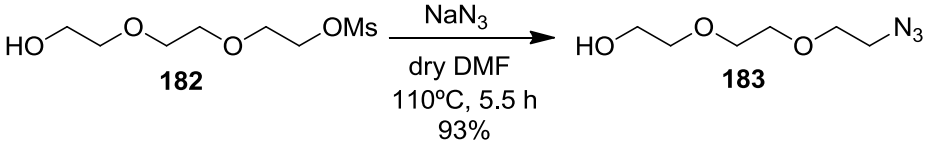

Scheme 5.86

To a solution of the alcohol **182** (1.8 g, 7.892 mmol) in dry DMF (25 mL) at rt was added NaN_3 (770 mg, 11.838 mmol). The reaction mixture was heated to 110 ºC, stirred at 110 ºC for 5.5 h, and cooled to 0 C. The resulting mixture was quenched with water (50 mL) and the mixture was extracted with EtOAc (3 × 25 mL). The extracts were washed with saturated NaCl solution, dried over Na_2SO_4, filtered, and concentrated. The concentrate was purified by flash column chromatography on silica gel [EtOAc/MeOH (98:2)] to give

1.285 g (93%) of azido alcohol **183**. ^{1}H NMR (400 MHz, $CDCl_3$): δ 3.74 – 3.70 (m, 2H, C*H*$_2$), 3.69 – 3.64 (m, 6H, C*H*$_2$), 3.62 – 3.57 (m, 2H, C*H*$_2$), 3.60 (t, *J* = 4.2 Hz, 2H, C*H*$_2$), 2.39 (bs, 1H, O*H*). ^{13}C NMR (101 MHz, $CDCl_3$): δ 72.5; 70.7; 70.5; 70.1; 61.8; 50.7.

Compound 83

According to literature procedure:[156]

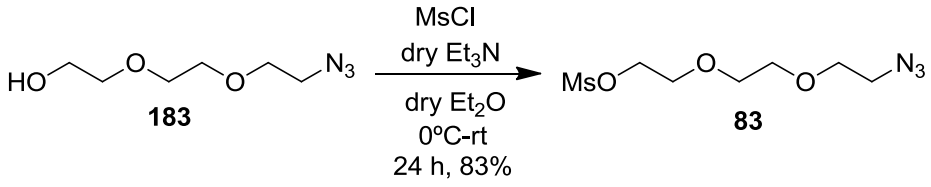

Scheme 5.87

To a 0 °C solution of **183** (0.500 g, 2.85 mmol) in dry Et_2O (10 mL) were added dry Et_3N (1.2 mL, 8.56 mmol) and, thereafter, MsCl (0.33 mL, 4.28 mmol). The resulting white slurry was quenched with water (30 mL) after 24 h and extracted with Et_2O (3×10 mL). The combined organic phases were dried ($MgSO_4$), filtered under suction, and purified via flash column chromatography [pentane/EtOAc (1:1)], yielding **83** (0.600 g, 2.37 mmol, 83%) as a clear oil. ^{1}H NMR (400 MHz, $CDCl_3$): δ 4.35−4.21 (m, 2H, C*H*$_2$), 3.73−3.65 (m, 2H, C*H*$_2$), 3.63−3.53 (m, 6H, C*H*$_2$), 3.31 (t, *J* = 5.2 Hz, 2H, C*H*$_2$), 2.99 (s, 3H, C*H*$_3$). ^{13}C NMR (101 MHz, $CDCl_3$): δ 70.4, 70.4, 69.8, 69.3, 68.9, 50.5, 37.4.

Chapter 6
Glossary of terms

6. Glossary of terms

Amyloid plaque: a largely insoluble deposit found in the space between nerve cells in the brain. Plaques are made of beta-amyloid peptide (Aβ), other molecules, and different kinds of nerve and non-nerve cells.

Amyloid precursor protein (APP): the larger protein from which beta-amyloid is formed.

Amyloidosis: A disease or disorder that results from a sequence of changes in protein folding that leads to the deposition of insoluble amyloid fibrils, mainly in the extracellular spaces of organs and tissues.

Amyloid fibrils: Structures formed by many disease-causing proteins when they aggregate. Amyloid fibrils share common biochemical characteristics such as detergent insolubility, high β-pleated sheet content and a cross β-structure, protease resistance and the ability to bind lipophilic dyes, such as Congo Red, Thioflavin S and Thioflavin T.

Amyloid plaques: Sites of Aβ accumulation and dystrophic neurites in the brains of mouse models and patients with Alzheimer's disease (AD).

Apolipoprotein E: a protein that carries cholesterol in blood and that appears to play some role in brain function. The gene that produces this protein comes in several forms, or alleles: ε2, ε3, and ε4. The APOE ε2 allele is relatively rare and may provide some protection against AD (but it may increase risk of early heart disease). APOE ε3 is the most common allele and appears to play a neutral role in AD. APOE ε4 occurs in about 40 percent of all people with AD who develop the disease in later life; it increases the risk of developing AD.

Axon: the long extension from a neuron that transmits outgoing signals to other cells.

Beta-amyloid peptide (Aβ): a part of the amyloid precursor protein found in plaques, the insoluble deposits outside neurons.

Brain stem: the portion of the brain that connects to the spinal cord and controls automatic body functions, such as breathing, heart rate, and blood pressure.

Blood–brain barrier (BBB): A protective wall of capillary epithelium separating the brain parenchyma from the bloodstream that is impenetrable to most circulating substances.

Calcein: also known as fluorexon, fluorescein complex, is a fluorescent dye with an excitation and emission wavelengths of 495/515nm, respectively.

Capillary: a tiny blood vessel. The brain has billions of capillaries that carry oxygen, glucose (the brain's principal source of energy), nutrients, and hormones to brain cells so they can do their work. Capillaries also carry away carbon dioxide and cell waste products.

Cerebellum: the part of the brain responsible for maintaining the body's balance and coordination.

Cerebral cortex: the outer layer of nerve cells surrounding the cerebral hemispheres.

Cerebral hemispheres: the largest portion of the brain composed of billions of nerve cells in two structures connected by the corpus callosum. The cerebral hemispheres control conscious thought, language, decision making, emotions, movement, and sensory functions.

Cerebrospinal fluid: the fluid found in and around the brain and spinal cord. It protects these organs by acting like a liquid cushion and by providing nutrients.

Chaperone: Proteins that reversibly bind unfolded segments of polypeptides susceptible to aggregation or diversion.

Chromosome: a threadlike structure in the nucleus of a cell that contains DNA. DNA sequences make up genes. Most human cells have 23 pairs of chromosomes containing approximately 30,000 genes.

Clinical trial: a research study involving humans that rigorously tests safety, side effects, and how well a medication or behavioral treatment works.

Cognitive functions: all aspects of conscious thought and mental activity, including learning, perceiving, making decisions, and remembering.

Dementia: a broad term referring to a decline in cognitive function to the extent that it interferes with daily life and activities.

Dendrite: a branch-like extension of a neuron that receives messages from other neurons.

Dystrophic neurites: Abnormal swelling that develops secondary to neuronal-cell stress in AD and other neurodegenerative diseases.

Early-onset Alzheimer's disease: a rare form of AD that usually affects people between ages 30 and 60. It is called familial Alzheimer's disease (FAD) if it runs in the family.

Entorhinal cortex: an area deep within the brain where damage from AD often begins.

Enzyme: a protein that causes or speeds up a biochemical reaction.

Free radical: a highly reactive molecule (typically oxygen or nitrogen) that combines easily with other molecules because it contains an unpaired electron. The combination with other molecules sometimes damages cells.

Gene: the biologic unit of heredity passed from parent to child. Genes are segments of DNA and contain instructions that tell a cell how to make specific proteins.

Genetic risk factor: a variant in a cell's DNA that does not cause a disease by itself but may increase the chance that a person will develop a disease.

Glial cell: a specialized cell that supports, protects, or nourishes nerve cells.

Hippocampus: a structure in the brain that plays a major role in learning and memory and is involved in converting short-term to long-term memory.

Hypothalamus: a structure in the brain under the thalamus that monitors activities such as body temperature and food intake.

Late-onset Alzheimer's disease: the most common form of AD. It occurs in people aged 60 and older.

Limbic system: a brain region that links the brain stem with the higher reasoning elements of the cerebral cortex. It controls emotions, instinctive behavior, and the sense of smell.

Magnetic resonance imaging (MRI): a diagnostic and research technique that uses magnetic fields to generate a computer image of internal structures in the body. MRIs are very clear and are particularly good for imaging the brain and soft tissues.

Metabolism: all of the chemical processes that take place inside the body. In some metabolic reactions, complex molecules are broken down to release energy. In others, the cells use energy to make complex compounds out of simpler ones (like making proteins from amino acids).

Microtubule: an internal support structure for a neuron that guides nutrients and molecules from the body of the cell to the end of the axon.

Microglia: Phagocytic immune cells in the brain that engulf and remove cells that have undergone apoptosis.

Mild cognitive impairment (MCI): a condition in which a person has memory problems greater than those expected for his or her age, but not the personality or cognitive problems that characterize AD.

Mutation: a permanent change in a cell's DNA that can cause a disease.

Myelin: a whitish, fatty layer surrounding an axon that helps the axon rapidly

transmits electrical messages from the cell body to the synapse.

Nerve growth factor (NGF): a substance that maintains the health of nerve cells. NGF also promotes the growth of axons and dendrites, the parts of the nerve cell that are essential to its ability to communicate with other nerve cells.

Neurodegenerative disease: a disease characterized by a progressive decline in the structure, activity, and function of brain tissue. These diseases include AD, Parkinson's disease, frontotemporal lobar degeneration, and dementia with Lewy bodies. They are usually more common in older people.

Neurofibrillary tangle: a filamentous collection of twisted and hyperphosphorylated tau found in the cell body of a neuron in AD.

Neuron: a nerve cell.

Neurotransmitter: a chemical messenger between neurons. These substances are released by the axon on one neuron and excite or inhibit activity in a neighboring neuron.

Nucleus: the structure within a cell that contains the chromosomes and controls many of its activities.

Oxidative damage: damage that can occur to cells when they are exposed to too many free radicals.

Oligomers: clusters of small numbers of protein or peptide molecules without a fibrillar appearance.

Passive immunization: The induction of immunity by the transfer of immune-globulins.

Positron emission tomography (PET): an imaging technique using radioisotopes that allows researchers to observe and measure activity in different parts of the brain by monitoring blood flow and concentrations of substances such as oxygen and glucose, as well as other specific constituents of brain tissues.

Protein misfolding: the conversion of a protein into a structure that differs from its native state.

Protofibrils: protein aggregates of isolated or clustered spherical beads 2–5 nm in diameter with β-sheet structure.

Protofilaments: the constituent units of amyloid fibrils. They should not be confused with protofibrils.

Synapse: the tiny gap between nerve cells across which neurotransmitters pass.

Tau: a protein that helps to maintain the structure of microtubules in normal nerve cells. Abnormal *tau* is a principal component of the paired helical filaments in neurofibrillary tangles.

Thalamus: a small structure in the front of the cerebral hemisphere that serves as a

way station that receives sensory information of all kinds and relays it to the cortex; it also receives information from the cortex.

Transgenic: an animal that has had a gene (like human APP) inserted into its chromosomes. Mice carrying the mutated human APP gene often develop plaques in their brains as they age.

Ventricle: a cavity within the brain that is filled with cerebrospinal fluid.

Vesicle: a small container for transporting neurotransmitters and other molecules from one part of the neuron to another.

Chapter 7
Bibliography

7. Bibliography

(1) Lit-Fui Lau, Michael A. Brodne, Topics in Medicinal Chemistry, Alzheimer's Disease; Springer-Verlag: Berlin, 2008; Vol. 2., p. 2..
(2) Soto, C. *FEBS Letters* **2001**, *498*, 204.
(3) Soto, C. *Nature Reviews Neuroscience* **2003**, *4*, 49.
(4) Dobson, C. M. *Trends in Biochemical Sciences* **1999**, *24*, 329.
(5) Aguzzi, A.; O'Connor, T. *Nature Reviews* **2010**, *9*, 237.
(6) Kepp, K. P. *Chemical Reviews* **2012**, *112*, 5193.
(7) Karran, E.; Mercken, M.; De Strooper, B. *Nature Reviews Drug Discovery* **2011**, *10*, 698.
(8) U.S. Department of Health and Human Services, National Institute of Anging http://www.nia.nih.gov/alzheimers/publication/part-2-what-happens-brain-ad/hallmarks-ad, 14/03/2013.
(9) Carlo, M. D. *European. Biophysics Journal* **2010**, *39*, 877.
(10) Huang, H. C.; Jiang, Z. F. *Journal of Alzheimer's Disease* **2009**, *16*, 15.
(11) Citron, M. *Nature Reviews* **2004**, *5*, 677.
(12) *Amyloid Proteins: The Beta Sheet Conformation and Disease*; Wiley-VCH Verlag: Weinheim, 2005; Vol. 2.
(13) Querfurth, H. W.; LaFerla, F. M. *The New England Journal of Medicine* **2010**, *362*, 329.
(14) Hamley, I. W. *Chemical Reviews* **2012**, *112*, 5147.
(15) Amijee, H.; Scopes, D. I. C. *Journal of Alzheimer's Disease* **2009**, *17*, 33.
(16) Walsh, D. M.; Thulin, E.; Minogue, A. M.; Gustavsson, N.; Pang, E.; Teplow, D. B.; Linse, S. *FEBS Journal* **2009**, *276*, 1266.
(17) Invernizzi, G.; Papaleo, E.; Sabate, R.; Ventura, S. *The International Journal of Biochemistry & Cell Biology* **2012**, *44*, 1541.
(18) Kozlowski, H.; Janicka-Klos, A.; Brasun, J.; Gaggelli, E.; Valensin, D.; Valensin, G. *Coordination Chemistry Reviews* **2009**, *253*, 2665.
(19) Budimir, A. *Acta Pharmaceutica* **2011**, *61*, 1.
(20) Perez, L. R.; Franz, K. J. *Dalton Transactions* **2010**, *39*, 2177.
(21) Bush, A. I.; Tanzi, R. E. *Neurotherapeutics* **2008**, *5*, 421.
(22) Gaeta, A.; Hider, R. C. *British Journal of Pharmacology* **2005**, *146*, 1041.
(23) Zatta, P.; Drago, D.; Bolognin, S.; Sensi, S. L. *Trends in Pharmacological Sciences* **2009**, *30*, 346.
(24) Nakamura, K.; Hori, T.; Sato, N.; Sugie, K.; Kawakami, T.; Yodoi, J. *Oncogene* **1993**, *8*, 3133.
(25) Butterfield, D. A.; Perluigi, M.; Sultana, R. *European Journal of Pharmacology* **2006**, *545*, 39.
(26) Dalle-Donne, I.; Scaloni, A.; Giustarini, D.; Cavarra, E.; Tell, G.; Lungarella, G.; Colombo, R.; Rossi, R.; Milzani, A. *Mass Spectrometry Reviews* **2005**, *24*, 55.

(27) Staal, F. J. T.; Anderson, M. T.; Staal, G. E. J.; Herzenberg, L. A.; Gitler, C.; Herzenberg, L. A. *Proceedings of the National Academy of Sciences of the United States of America* **1994**, *91*, 3619.
(28) Harman, D. *Age* **1995**, *18*, 97.
(29) Faraci, F. M. *Journal of Applied Physiology* **2006**, *100*, 739.
(30) Mantha, A. K.; Moorthy, K.; Cowsik, S. M.; Baquer, N. Z. *Biogerontology* **2006**, *7*, 1.
(31) Starke, D. W.; Chen, Y. G.; Bapna, C. P.; Lesnefsky, E. J.; Mieyal, J. J. *Free Radical Biology and Medicine* **1997**, *23*, 373.
(32) Ansari, M. A.; Scheff, S. W. *Journal of Neuropathology and Experimental Neurology* **2010**, *69*, 155.
(33) Heise, K.; Puntarulo, S.; Pörtner, H. O.; Abele, D. *Comparative Biochemistry and Physiology Part C: Toxicology & Pharmacology* **2003**, *134*, 79.
(34) Finkel, T.; Holbrook, N. J. *Nature* **2000**, *408*, 239.
(35) Squadrito, G. L.; Pryor, W. A. *Free Radical Biology and Medicine* **1998**, *25*, 392.
(36) Jomova, K.; Valko, M. *Current Pharmaceutical Design* **2011**, *17*, 3460.
(37) Tougu, V.; Karafin, A.; Zovo, K.; Chung, R. S.; Howells, C.; West, A. K.; Palumaa, P. *Journal of Neurochemistry* **2009**, *110*, 1784.
(38) Rivera-Mancia, S.; Perez-Neri, I.; Rios, C.; Tristan-Lopez, L.; Rivera-Espinosa, L.; Montes, S. *Chemico-Biological Interactions* **2010**, *186*, 184.
(39) Neugroschl, J.; Sano, M. *Current Neurology and Neuroscience Reports* **2009**, *9*, 368.
(40) Walsh, D. M.; Selkoe, D. J. *Journal of Neurochemistry* **2007**, 1172.
(41) Lemere, C. A.; Masliah, E. *Nature Reviews Neurology* **2010**, *6*.
(42) Schenk, D. *Nature Reviews* **2002**, *3*, 824.
(43) Jakob-Roetne, R.; acobsen, H. *Angewandte Chemie International Edition* **2009**, *48*, 2.
(44) Nerelius, C.; Johansson, J.; Sandegren, A. *Frontiers in Bioscience* **2009**, *14*, 1716.
(45) Golde, T. E.; Petrucelli, L.; Lewis, J. *Experimental Neurology* **2010**, *223*, 252.
(46) Pardridge, W. M. *Drug Discovery Today* **2002**, *7*, 5.
(47) Denora, N.; Trapani, A.; Laquintana, V.; Lopedota, A.; Trapani, G. *Current Topics in Medicinal Chemistry* **2009**, *2009*, 182.
(48) Wohlfart, S.; Gelperina, S.; Kreuter, J. *Journal of Controlled Release* **2012**, *161*, 264.
(49) Li, H.; Duan, X. *Nanoscience* **2006**, *11*, 207.
(50) Pauletti, G. M.; Okumu, F. W.; Borchardt, R. T. *Pharmaceutical Research* **1997**, *14*, 164.
(51) Wu, D. F.; Pardridge, W. M. *Drug Metabolism and Disposition* **1998**, *26*, 937.
(52) Pardridge, W. M. *Journal of Neurochemistry* **1998**, *70*, 1781.
(53) Chauhan, N. B. *Antisense & Nucleic Acid Drug Development* **2002**, *12*, 353.
(54) Illum, L. *Journal of Controlled Release* **2003**, *87*, 187.
(55) Roney, C.; Kulkarni, P.; Arora, V.; Antich, P.; Bonte, F.; Wu, A.; Mallikarjuana, N. N.; Manochar, S.; Liang, H.-F.; Kulkarni, A. R.; Sung, H.-W.; Sairam, M.; Aminabhavi, T. M. *Journal of Controlled Release* **2005**, *108*, 193.
(56) Wang, A. Z.; Langer, R.; Farokhzad, O. C. In *Annual Review of Medicine, Vol 63*; Caskey, C. T., Austin, C. P., Hoxie, J. A., Ed. 2012; Vol. 63, p 185.
(57) Gandhi, M.; Bohra, H.; Daniel, V.; Gupta, A. *International Journal of Pharmaceutical & Biological Archives* **2010**, *1*, 37.

(58) Malam, Y.; Loizidou, M.; Seifalian, A. M. *Trends in Pharmacological Sciences* **2009**, *30*, 592.
(59) Garcia-Garcia, E.; Andrieux, K.; Gil, S.; Couvreur, P. *International Journal of Pharmaceutics* **2005**, *298*, 274.
(60) Taylor, M.; Moore, S.; Mourtas, S.; Niarakis, A.; Re, F.; Zona, C.; Ferla, B. L.; Nicotra, F.; Masserini, M.; Antimisiaris, S. G.; Gregori, M.; Allsop, D. *Nanomedicine: Nanotechnology, Biology and Medicine* **2011**, *7*, 541.
(61) Mourtas, S.; Canovi, M.; Zona, C.; Aurilia, D.; Niarakis, A.; La Ferla, B.; Salmona, M.; Nicotra, F.; Gobbi, M.; Antimisiaris, S. G. *Biomaterials* **2011**, *32*, 1635.
(62) Fuoco, D. *Antibiotics* **2012**, *1*, 1.
(63) Chopra, I.; Roberts, M. *Microbiology and Molecular Biology Reviews* **2001**, *65*, 232.
(64) D'Agostino, P.; Ferlazzo, V.; Milano, S.; La Rosa, M.; Di Bella, G.; Caruso, R.; Barbera, C.; Grimaudo, S.; Tolomeo, M.; Feo, S.; Cillari, E. *International Immunopharmacology* **2001**, *1*, 1765.
(65) Cosentino, U.; Pitea, D.; Moro, G.; Saracino, G. A. A.; Caria, P.; Vari, R. M.; Colombo, L.; Forloni, G.; Tagliavini, F.; Salmona, M. *Journal of Molecular Modeling* **2008**, *14*, 987.
(66) De Luigi, A.; Colombo, L.; Diomede, L.; Capobianco, R.; Mangieri, M.; Miccolo, C.; Limido, L.; Forloni, G.; Tagliavini, F.; Salmona, M. *Plos One* **2008**, *3*.
(67) Airoldi, C.; Colombo, L.; Manzoni, C.; Sironi, E.; Natalello, A.; Doglia, S. M.; Forloni, G.; Tagliavini, F.; Del Favero, E.; Cantu, L.; Nicotra, F.; Salmona, M. *Organic Biomolecular Chemistry* **2011**, *9*, 463.
(68) Chen, M.; Ona, V. O.; Li, M. W.; Ferrante, R. J.; Fink, K. B.; Zhu, S.; Bian, J.; Guo, L.; Farrell, L. A.; Hersch, S. M.; Hobbs, W.; Vonsattel, J. P.; Cha, J. H. J.; Friedlander, R. M. *Nature Medicine* **2000**, *6*, 797.
(69) Thomas, M.; Le, W. D. *Current Pharmaceutical Design* **2004**, *10*, 679.
(70) Rubins, J. B.; Charboneau, D.; Alter, M. D.; Bitterman, P. B.; Kratzke, R. A. *Journal of Laboratory and Clinical Medicine* **2001**, *138*, 101.
(71) Forloni, G.; Salmona, M.; Marcon, G.; Tagliavini, F. *Infection Disorders - Drug Targets* **2009**, *2009*, 23.
(72) Forloni, G.; Colombo, L.; Girola, L.; Tagliavini, F.; Salmona, M. *FEBS Letters* **2001**, *487*, 404.
(73) Gammon, D. W.; Sels, B. F. *Handbook of Chemical Glycosylation: Advances in Stereoselectivity and Therapeutic Relevance*; Wiley-VCH: Weinheim, 2008.
(74) Dhawan, K. L.; Gowland, B. D.; Durst, T. *Journal of Organic Chemistry* **1980**, *45*, 922.
(75) Akgun, E.; Glinski, M. B.; Dhawan, K. L.; Durst, T. *Journal of Organic Chemistry* **1981**, *46*, 2730.
(76) Hollinshead, S. P.; Nichols, J. B.; Wilson, J. W. *Journal of Organic Chemistry* **1994**, *59*, 6703.
(77) Charest, M. G.; Siegel, D. R.; Myers, A. G. *Journal of the American Chemical Society* **2005**, *127*, 8292.
(78) Bennek, J. A.; Gray, G. R. *Journal of Organic Chemistry* **1987**, *52*, 892.
(79) Post, C. B. *Current Opinion in Structural Biology* **2003**, *13*, 581.
(80) Williamson, M. P. In *Annual Reports on NMR Spectroscopy*; Graham, A. W., Ed.; Academic Press: 2009; Vol. Volume 65, p 77.

(81) Calle, L. P.; Canada, F. J.; Jimenez-Barbero, J. *Natural Product Reports* **2011**, *28*, 1118.
(82) Domingo, L. R.; Sáez, J. A. *Organic Biomolecular Chemistry* **2009**, *7*, 3576.
(83) Yadav, J. S.; Reddy, B. V. S.; Chandraiah, L.; Jagannadh, B.; Kumar, S. K.; Kunwar, A. C. *Tetrahedron Letters* **2002**, *43*, 4527.
(84) Mayer, M.; Meyer, B. *Angewandte Chemie International Edition* **1999**, *38*, 1784.
(85) Meyer, B.; Peters, T. *Angewandte Chemie International Edition* **2003**, *42*, 864.
(86) Airoldi, C.; Zona, C.; Sironi, E.; Colombo, L.; Messa, M.; Aurilia, D.; Gregori, M.; Masserini, M.; Salmona, M.; Nicotra, F.; La Ferla, B. *Journal of Biotechnology* **2010**, *156*, 317.
(87) Airoldi, C.; Palmioli, A.; D'Urzo, A.; Colombo, S.; Vanoni, M.; Martegani, E.; Peri, F. *Chembiochem* **2007**, *8*, 1376.
(88) Airoldi, C.; Giovannardi, S.; La Ferla, B.; Jimenez-Barbero, J.; Nicotra, F. *Chemistry-A European Journal* **2011**, *17*, 13395.
(89) Cecchelli, R.; Dehouck, B.; Descamps, L.; Fenart, L.; Buee-Scherrer, V.; Duhem, C.; Lundquist, S.; Rentfel, M.; Torpier, G.; Dehouck, M. P. *Advanced Drug Delivery Reviews* **1999**, *36*, 165.
(90) Airoldi, C.; Cardona, F.; Sironi, E.; Colombo, L.; Salmona, M.; Silva, A.; Nicotra, F.; La Ferla, B. *Chemical Communications* **2011**, *47*, 10266.
(91) Meyer, B.; Peters, T. *Angewandte Chemie International Edition* **2003**, *42*, 864.
(92) Re, F.; Cambianica, I.; Zona, C.; Sesana, S.; Gregori, M.; Rigolio, R.; La Ferla, B.; Nicotra, F.; Forloni, G.; Cagnotto, A.; Salmona, M.; Masserini, M.; Sancini, G. *Nanomedicine-Nanotechnology Biology and Medicine* **2011**, *7*, 551.
(93) Poller, B.; Gutmann, H.; Kraehenbuehl, S.; Weksler, B.; Romero, I.; Couraud, P.-O.; Tuffin, G.; Drewe, J.; Huwyler, J. *Journal of Neurochemistry* **2008**, *107*, 1358.
(94) Baskin, J. M.; Bertozzi, C. R. *Qsar & Combinatorial Science* **2007**, *26*, 1211.
(95) Laughlin, S. T.; Baskin, J. M.; Amacher, S. L.; Bertozzi, C. R. *Science* **2008**, *320*, 664.
(96) Codelli, J. A.; Baskin, J. M.; Agard, N. J.; Berozzi, C. R. *Journal of the American Chemical Society* **2008**, *130*, 11486.
(97) Agard, N. J.; Prescher, J. A.; Bertozzi, C. R. *Journal of the American Chemical Society* **2004**, *126*, 15046.
(98) Lallana, E.; Fernandez-Megia, E.; Riguera, R. *Journal of the American Chemical Society* **2009**, *131*, 5748.
(99) Ziegler, T.; Eckhardt, E.; Keller, D. *Journal of Carbohydrate Chemistry* **1997**, *16*, 719.
(100) Dalvit, C.; Fogliatto, G.; Stewart, A.; Veronesi, M.; Stockman, B. *Journal of Biomolecular NMR* **2001**, *21*, 349.
(101) Dalvit, C.; Pevarello, P.; Tatò, M.; Veronesi, M.; Vulpetti, A.; Sundström, M. *Journal of Biomolecular NMR* **2000**, *18*, 65.
(102) Arcamone, F. M. In *Anticancer Agents from Natural Products* CRC Press: 2005, p 299.
(103) H.Laatsch; S.Fotso In *Anthracycline Chemistry and Biology I: Biological Occurence and Biosynthesis, Synthesis and Chemistry*; Springer-Verlag: 2008; Vol. 282, p 3.
(104) La Ferla, B.; Airoldi, C.; Zona, C.; Orsato, A.; Cardona, F.; Merlo, S.; Sironi, E.; D'Orazio, G.; Nicotra, F. *Natural Product Reports* **2011**, *28*, 630.

(105) Gruber, B. M.; Anuszewska, E. L.; Bubko, I.; Gozdzik, A.; Fokt, I.; Priebe, W. *Archivum Immunologiae Et Therapiae Experimentalis* **2007**, *55*, 193.
(106) Griffin, M. O.; Fricovsky, E.; Ceballos, G.; Villarreal, F. *American Journal of Physiology-Cell Physiology* **2010**, *299*, C539.
(107) Johansson, R.; Samuelsson, B. *Journal of the Chemical Society, Perkin Transactions 1* **1984**, 2371.
(108) Chang, C.-W. T.; Hui, Y.; Elchert, B. *Tetrahedron Letters* **2001**, *42*, 7019.
(109) Thoma, G.; Schwarzenbach, F.; Duthaler, R. O. *Journal of Organic Chemistry* **1996**, *61*, 514.
(110) Clausen, M. H.; Madsen, R. *Chemistry Euopean. Journal* **2003**, *9*, 3821.
(111) J., B.; A., G. G. *Journal of Organic Chemistry* **1987**, *52*, 892.
(112) Cipolla, L.; Lay, L.; Nicotra, F. *Journal of Organic Chemistry* **1997**, *62*, 6678.
(113) Cleator, E.; McCusker, C. F.; Steltzer, F.; Ley, S. V. *Tetrahedron Letters* **2004**, *45*, 3077.
(114) Shing, T. K. M.; Yeung; Su, P. L. *Organic Letters* **2006**, *8*, 3149.
(115) Borodkin, V. S.; Shpiro, N. A.; Azov, V. A.; Kochetkov, N. K. *Tetrahedron Letters* **1996**, *37*, 1489.
(116) Plewe, M.; Sandhoff, K.; Schmidt, R. R. *Liebigs Annalen der Chemie* **1992**, *1992*, 699.
(117) Hauser, F. M.; Rhee, R. P. *Journal of Organic Chemistry* **1978**, *43*, 178.
(118) Dodd, J. H.; Garigapati, R. S.; Weinreb, S. M. *Journal of Organic Chemistry* **1982**, *47*, 4045.
(119) Hill, B.; Rodrigo, R. *Organic Letters* **2005**, *7*, 5223.
(120) Mandal, S. K.; Roy, S. C. *Tetrahedron* **2008**, *64*, 11050.
(121) Vogel, A. *Vogel's Textbook of Practical Organic Chemistry* Third ed.; Longman Scientific and Technical, 1987.
(122) Mandal, S. K.; Roy, S. C. *Tetrahedron* **2008**, *64*, 11050.
(123) Hansen, M. M.; Riggs, J. R. *Tetrahedron Letters* **1998**, *39*, 2705.
(124) He, Q.-L.; Jia, X.-Y.; Tang, M.-C.; Tian, Z.-H.; Tang, G.-L.; Liu, W. *Chembiochem* **2009**, *10*, 813.
(125) Xiao, X.-Y.; Hunt, D. K.; Zhou, J.; Clark, R. B.; Dunwoody, N.; Fyfe, C.; Grossman, T. H.; O'Brien, W. J.; Plamondon, L.; Rönn, M.; Sun, C.; Zhang, W.-Y.; Sutcliffe, J. A. *Journal of Medicinal Chemistry* **2011**, *55*, 597.
(126) Segura, J. L.; Martin, N. *Chemical Reviews* **1999**, *99*, 3199.
(127) Collier, S. J.; Storr, R. C. *Progress in Heterocyclic Chemistry* **1999**, *10*, 25.
(128) Funk, R. L.; Vollhardt, K. P. C. *Chemical Society Reviews* **1980**, *9*, 41.
(129) Nicolaou, K. C.; Gray, D. L. F. *Journal of American Chemical Society* **2004**, *126*, 607.
(130) Akguen, E.; Glinski, M. B.; Dhawan, K. L.; Durst, T. *Journal of Organic Chemistry* **1981**, *46*, 2730.
(131) Nicolaou, K. C.; Snyder, S. A.; Montagnon, T.; Vassilikogiannakis, G. *Angewandte Chemie International Edition* **2002**, *41*, 1668.
(132) Nemoto, H.; Satoh, A.; Fukumoto, K. *Tetrahedron* **1995**, *51*, 10159.
(133) Sauer, J.; Sustman, R. *Angewandte Chemie International Edition* **1980**, *18*, 779.
(134) Corey, E. J.; Snider, B. B. *Journal of the American Chemical Society* **1972**, *94*, 2549.
(135) Greene, T. W.; Wuts, P. G. M. *Protective Groups in Organic Synthesis* 4th ed.; Wiley, 2006.

(136) Sajiki, H.; Ikawa, T.; Hattori, K.; Hirota, K. *Chemical Communications* **2003**, *5*, 654.
(137) Gewirtz, D. *Biochemical Pharmacology* **1999**, *57*, 727.
(138) Achmatowicz, O.; Szechner, B. *Journal of Organic Chemistry* **2003**, *68*, 2398.
(139) Mal, D.; Pahari, P. *Chemical Reviews* **2007**, *107*, 1892.
(140) Ghorab, M. M.; Ragab, F. A.; Hamed, M. M. *European Journal of Medicinal Chemistry* **2009**, *44*, 4211.
(141) Ghorab, M. M.; Ragab, F. A.; Heiba, H. I.; Arafa, R. K.; El-Hossary, E. M. *European Journal of Medicinal Chemistry* **2010**, *45*, 3677.
(142) Budakoti, A.; Bhat, A. R.; Azam, A. *European Journal of Medicinal Chemistry* **2009**, *44*, 1317.
(143) Giri, R. S.; Thaker, H. M.; Giordano, T.; Williams, J.; Rogers, D.; Sudersanam, V.; Vasu, K. K. *European Journal of Medicinal Chemistry* **2009**, *44*, 2184.
(144) Corona, P.; Carta, A.; Loriga, M.; Vitale, G.; Paglietti, G. *European Journal of Medicinal Chemistry* **2009**, *44*, 1579.
(145) MacroModel; 9.6 ed.; Schrödinger, LLC: New York, 2008.
(146) Maestro In *Schrödinger*; 9.1 ed.; LLC: New York, 2010.
(147) Allinger, N. L.; Yuh, Y. H.; Lii, J. H. *Journal of the American Chemical Society* **1989**, *111*, 8551.
(148) Still, W. C.; Tempczyk, A.; Hawley, R. C.; Hendrickson, T. *Journal of the American Chemical Society* **1990**, *112*, 6127.
(149) Di Fede, G.; Catania, M.; Morbin, M.; Rossi, G.; Suardi, S.; Mazzoleni, G.; Merlin, M.; Giovagnoli, A. R.; Prioni, S.; Erbetta, A.; Falcone, C.; Gobbi, M.; Colombo, L.; Bastone, A.; Beeg, M.; Manzoni, C.; Francescucci, B.; Spagnoli, A.; Cantu, L.; Del Favero, E.; Levy, E.; Salmona, M.; Tagliavini, F. *Science* **2009**, *323*, 1473.
(150) Salmona, M.; Morbin, M.; Massignan, T.; Colombo, L.; Mazzoleni, G.; Capobianco, R.; Diomede, L.; Thaler, F.; Mollica, L.; Musco, G.; Kourie, J. J.; Bugiani, O.; Sharma, D.; Inouye, H.; Kirschner, D. A.; Forloni, G.; Tagliavini, F. *Journal of Biological Chemistry* **2003**, *278*, 48146.
(151) Chishti, M. A.; Yang, D.-S.; Janus, C.; Phinney, A. L.; Horne, P.; Pearson, J.; Strome, R.; Zuker, N.; Loukides, J.; French, J.; Turner, S.; Lozza, G.; Grilli, M.; Kunicki, S.; Morissette, C.; Paquette, J.; Gervais, F.; Bergeron, C.; Fraser, P. E.; Carlson, G. A.; George-Hyslop, P. S.; Westaway, D. *Journal of Biological Chemistry* **2001**, *276*, 21562.
(152) Bickel, U. *NeuroRX* **2005**, *2*, 15.
(153) Johansson, R.; Samuelsson, B. *Journal of the Chemical Society, Perkin Transactions 1* **1984**, *0*, 2371.
(154) Cipolla, L.; Lay, L.; Nicotra, F. *Journal of Organic Chemistry* **1997**, *62*, 6678.
(155) Simonin, J.; Vernekar, S. K. V.; Thompson, A. J.; Hothersall, J. D.; Connolly, C. N.; Lummis, S. C. R.; Lochner, M. *Bioorganic & Medicinal Chemistry Letters* **2012**, *22*, 1151.
(156) Schneekloth, A. R.; Pucheault, M.; Tae, H. S.; Crews, C. M. *Bioorganic & Medicinal Chemistry Letters* **2008**, *18*, 5904.

Chapter 8
Appendix A

8. Appendix A: *Copyright permissions*